12-14-2017

USING DIFFERENT ANALYTICAL TECHNIQUES AND SYNTHETICALLY TAILORED SILICA NANOPARTICLES IN DRUG SEPARATIONS AND HYDROPHOBICITY-BASED DETECTION APPLICATIONS

Walid Abdelwahab

USING DIFFERENT ANALYTICAL TECHNIQUES AND SYNTHETICALLY TAILORED SILICA NANOPARTICLES IN DRUG SEPARATIONS AND HYDROPHOBICITY-BASED DETECTION APPLICATIONS

by

WALID ABDELWAHAB

Under the Direction of Professor Ramzia El-Bagary and Professor Gabor Patonay

ABSTRACT

The development and validation of accurate and reliable analytical methods using techniques such as capillary electrophoresis, liquid chromatography, UV-spectrophotometry, spectrofluorimetry and mass spectrometry for separation and determination of some selected drugs in different matrices are presented in the first three chapters. The developed methods were applied to the determination of these compounds in their dosage forms and/or in biological fluids such as human plasma. The stability indicating characteristics including the analysis and separation of certain drugs from their alkaline, acidic, oxidative, thermal or photolytic degradation products along with the study of the degradation kinetics were also investigated. The first chapter focuses on the liquid chromatographic methods and the second chapter covers the capillary electrophoretic methods whereas the third chapter includes the UV-spectrophotometric

and spectrofluorimetric methods. On the other hand, the fourth chapter shows how functionalized silica nanoparticles can be used in achieving enhanced electrophoretic separations of selected groups of acidic and basic drugs. Finally, the fifth chapter of this dissertation presents a library of fluorescently labeled-silica nanoparticles that can be used in certain hydrophobicity-based detection applications such as fingerprint detection.

INDEX WORDS: Separations, Liquid chromatography, Spectrometry, Capillary electrophoresis, Silica nanoparticles, Degradation kinetics, Pharmaceutical preparations, Fluorescent probes, Fingerprints detection, Haemocompatability studies

USING DIFFERENT ANALYTICAL TECHNIQUES AND SYNTHETICALLY TAILORED SILICA NANOPARTICLES IN DRUG SEPARATIONS AND HYDROPHOBICITY-BASED DETECTION APPLICATIONS

by

WALID ABDELWAHAB

A Dissertation Submitted in Partial Fulfillment of the Requirements for the Degree of

Doctor of Philosophy

in the College of Arts and Sciences

Georgia State University

2017

USING DIFFERENT ANALYTICAL TECHNIQUES AND SYNTHETICALLY TAILORED SILICA NANOPARTICLES IN DRUG SEPARATIONS AND HYDROPHOBICITY-BASED DETECTION APPLICATIONS

by

WALID ABDELWAHAB

Committee Chair: Professor Gabor Patonay

Committee: Professor Markus Germann

Professor Ning Fang

Electronic Version Approved:

Office of Graduate Studies

College of Arts and Sciences

Georgia State University

December 2017

DEDICATION

This dissertation is dedicated to my loving mother and father, to my wonderful wife Aya and my great son Adam, to my great aunt Magda, my brother Khaled and my two beloved sisters: Heidi and Hadeer.

ACKNOWLEDGEMENTS

All my praise, gratitude and thanks are due to ALLAH, who enabled me to complete this work.

I gratefully acknowledge the financial support received from the Cultural Affairs and Mission Sector (Egyptian Government) for the joint supervision award (JS 2756).

I really find it worthwhile to show how grateful I am to Prof. Dr. Ramzia El-Bagary, professor of Pharmaceutical chemistry, Faculty of Pharmacy, Cairo University; for her bighearted encouragement, continuous advice she kindly offered through all stages of the work; also, for her helpful comments thorough revising the dissertation.

I am also greatly indebted to Prof. Dr. Asmaa El-Zaher, professor of Pharmaceutical Chemistry, Faculty of Pharmacy, Cairo University; for her incessant supervision, inexorable support and endless encouragement throughout the course of the work.

I want to express my gratefulness to Associate prof. Ehab ElKady, associate professor of Pharmaceutical Chemistry, Faculty of Pharmacy, Cairo University; for his valuable suggestions and remarks.

I am cordially indebted to Prof. Dr. Gabor Patonay, professor of Analytical Chemistry, Georgia State University, USA, for providing all the facilities during this work, his valuable instructions, kind supervision and sincere help that he presented to me in his group.

Deep thanks to my sincere colleague in Georgia State University, Dr. Mohamed Salim, doctor of Analytical Chemistry, Mansoura University, for his help, support, and valuable advice.

Thanks to all of the staff members and to my colleagues, technicians, and employees in both Cairo University and Georgia State University for their ultimate support and fruitful discussions that made this work possible.

I owe a special gratitude to my Mother and my Father, whose continual encouragement and unlimited assistance support throughout all of the stages of my life

Finally, my deepest thanks and grateful appreciation to my Wife, who offered her encouragement, kindness, help and loving support that made this dissertation a reality. Also, I would like to thank, my kid, Adam, all my Brothers and my Sisters for bearing with me during this study.

TABLE OF CONTENTS

LIST OF TABLES

LIST OF FIGURES

LIST OF SCHEMES

1 SEPARATION AND DETERMINATION OF SELECTED PHARMACEUTICAL COMPOUNDS USING LIQUID CHROMATOGRAPHY

1.1 Introduction

Mechanism of action for the majority of the approved drugs in the market are mediated in one way or another through affecting the normal biological function of some endogenous peptides such as angiotensinogen, angiotensin I, angiotensin II, renin or biogenic amines such as noradrenaline, serotonin, histamine…etc. Some examples of these drug classes include protease inhibitors, angiotensin II receptor blockers, angiotensin converting enzyme inhibitors, renin inhibitors, dipeptidyl peptidase-4 (DPP-4) inhibitors, signal transduction inhibitors (protein tyrosine kinase inhibitors), incretin hormone glucagon-like peptide-1 (GLP-1) agonists, α agonists, α blockers, β agonists, β blockers, some antidepressants, some antipsychotics, some anti-parkinsonism, antihistaminics and H1 receptor antagonists [1]. Therefore, it is important to develop and apply precise, accurate and advanced analytical techniques including capillary electrophoresis, liquid chromatography, spectrophotometry, spectrofluorimetry and mass spectrometry for determination of drugs such as valsartan, azilsartan moexipril and aliskiren hemifumarate that affect endogenous peptides as well as drugs affecting biogenic amines such as atenolol in different matrices including dosage forms and biological fluids.

It proved useful for elucidating the stability indicating characteristics of some of these methods. In addition, these developed methods were validated according to the proper validation guidelines.

High-pressure (high-performance) liquid chromatography (HPLC) is a separation technique based on a liquid or solid stationary phase and a liquid mobile phase. Depending upon the type of stationary phase used, separations are achieved by adsorption, partitioning, or ion-

exchange processes. The elution time of a compound is better to be described by the capacity factor K', which depends on the nature of the analyte, the mobile phase composition, and the surface area and structure of the stationary phase. Only compounds holding different capacity factors can be separated by HPLC. Column length is also an important determinant of resolution. [2].

Based on sales volumes and the scientific importance of HPLC, this is the most popular analytical method. Its present popularity results from its effective separation of a wide range of samples, ease of use, speed, and nanomolar detection levels [3].

Five major types of HPLC can be mentioned based on its purposes: normal phase chromatography, reversed phase chromatography, size exclusion chromatography, ion exchange chromatography and bioaffinity chromatography. Reversed phase HPLC (RP-HPLC) consists of an aqueous, moderately polar mobile phase and a non-polar stationary phase. Silica is a common stationary phase which was treated with RMe_2SiCl, where R is a straight chain alkyl group such as C8H17 or $C_{18}H_{37}$. The retention time is therefore longer for non-polar molecules, allowing polar molecules to elute faster. Retention time is decreased by the addition of a hydrophobic solvent to the mobile phase and increased by the addition of a more polar solvent [4].

Structural features of the analyte molecule play a crucial role in its retention behavior. In general, an analyte with a more hydrophobic nature results in a longer retention time as it increases the molecule's non-polar surface area, which interacts less with the polar component of the mobile phase. On the other hand, polar groups result in a shorter retention time as they interact well with water. Very large molecules, however, can result in a poor interaction between the ligands alkyl chains and the large analyte surface, and can have problems accessing the pores

of the stationary phase. Branched chain compounds elute faster than their corresponding linear isomers because the overall surface area is lower [3].

Different applications of HPLC on the analysis of drugs in dosage forms and biological matrices have been investigated extensively. The applications of HPLC in the field of pharmaceutical analysis are expected to continue to grow mainly supported by the recent advances in instrumentations. Improvements made in HPLC include changes in packing material, hyphenated detection systems, automation, and computer-assisted optimization. These improvements facilitate its introduction into high assay volume situations such as clinical laboratories and quality control [5-9].

1.2 Stability-Indicating RP-LC Method for Determination of Azilsartan medoxomil and Chlorthalidone in Pharmaceutical Dosage Forms: Application to Degradation Kinetics

Analytical and Bioanalytical Chemistry (2014) 406:6701–6712

DOI 10.1007/s00216-014-8085-0

A RP-LC method was developed and validated for simultaneous determination of the active components, azilsartan medoxomil (AZL) and chlorthalidone (CLT), in their antihypertensive combined recipe. The chromatographic separation was achieved on Eclipse XDB-C18 (4.6 x 150 mm, 5 µm) column using a mobile phase consisting of methanol: potassium hydrogen phosphate buffer (pH 8, 0.05 M) (40:60, *v/v*) in isocratic mode. The flow rate was maintained at 0.8 mL min^{-1} at ambient temperature. Detection was carried out at 210 nm. The method was validated according to ICH guidelines. Linearity, accuracy and precision were satisfactory over the concentration range of 5.0–50.0 and 2.5-25.0 µg mL^{-1} for AZL and CLT, respectively (r^2 = 0.9999). LODs for AZL and CLT were 0.90 and 0.32 µg mL^{-1} whereas LOQs were 2.72 and 0.98 µg mL^{-1}, respectively. Both drugs were subjected to forced degradation studies under hydrolysis (neutral, acidic and alkaline), oxidative and photolytic extensive stress conditions. The proposed method is stability-indicating by the resolution of the investigated drugs from their degradation products. Moreover, the kinetics of the acidic degradation of AZL as well as the kinetics of the alkaline degradation of CLT were investigated. Arrhenius plots were constructed and the apparent first-order rate constants, half-life times, shelf-life times and the activation energies of the degradation processes were calculated. The

method was successfully applied for the determination of the studied drugs simultaneously in their co-formulated tablet. The developed method is specific and stability indicating for the quality control and routine analysis of the cited medications in their pharmaceutical preparations.

1.2.1 Introduction

Azilsartan medoxomil (AZL), is chemically designated as ((5-Methyl-2-oxo-1,3-dioxol-4yl) methyl 2-ethoxy-1-((2`-(5-oxo-4,5-dihydro-1,2,4-oxadiazol-3-yl) biphenyl-4-yl) methyl)-1H-benzimidazole-7-carboxylate), (Fig. 1.2.1a). Azilsartan, the active metabolite of AZL, is a novel non-peptide angiotensin II type 1 (AT_1) receptor blocker (ARB), was recently approved for treatment of hypertension [10]. It has a superior ability to control systolic blood pressure relative to other widely used ARBs. Greater antihypertensive effects of AZL might be due in part to its unusually potent and persistent ability to inhibit binding of angiotensin II to AT_1 receptors [11]. Preclinical studies have indicated that AZL may also benefit cellular mechanisms of cardio-metabolic disease and insulin sensitizing activity [12]. There is only one reported method [13] for determination of AZL alone and it was applied to its analysis in plasma. Chlorthalidone (CLT), (2-chloro-5- (1-hydroxy-3-oxoiso-indolin-1-yl) benzenesulfonamide), (Fig. 1.2.1b), is an orally taken thiazide-like diuretic for controlling hypertension and edema, including that associated with heart failure [14]. CLT has been determined in different matrices either alone or in combination with other medications using LC [15, 16], LC-MS/MS [17], HPTLC [18, 19], chemiluminometry [20], spectrophotometry [21] and CE [22] techniques. Binary combination therapies of AZL and CLT proved to induce significant reductions in systolic and diastolic blood pressure in patients with mild to severe hypertension [23]. Regarding simultaneous determination of CLT and AZL, there is only one LC reported method [24], done on a symmetry C18 column with a mobile phase consisting of methanol: Water: Acetonitrile: 0.1% *o*-phosphoric acid (30:35:15:5,

v/v/v/v) at λ of 251 nm. To the best of our knowledge, the present study is the first reported stability-indicating LC method for the determination of AZL and CLT in tablets. The parent drug stability test guideline Q1A (R2) issued by International Conference of Harmonization (ICH) [25] suggests that, stress studies should be carried out on a drug to establish its inherent stability characteristics. Accordingly, the aim of the present study was to establish the inherent stability of AZL and CLT through stress studies under a variety of ICH recommended test conditions, and to develop the first stability-indicating assay method for their determination in their commercially available tablets. In the present work, AZL and CLT were subjected to forced degradation studies under an extensive stress testing. These studies included the effects of hydrolysis (neutral, acidic and alkaline), oxidation and photolysis. The currently developed LC method effectively separated the two investigated drugs from their degradation products (DPs). Furthermore, the proposed LC method was applied to study the degradation kinetics of AZL and CLT under acidic and alkaline degradation stress conditions, respectively. Arrhenius plots were constructed and the apparent first-order rate constants, half-life times, shelf-life times and the activation energies of the degradation processes were calculated. The described method demonstrates its novelty and pros by combining several advantages in one method: the limit of detections for AZL and CLT were as low as 0.9 and 0.3 µg mL^{-1}, respectively. The method was able to simultaneously determine the two drugs in their pharmaceutical preparation. Moreover, the present work was designed to detect and analyze AZL and CLT in presence of their potential DPs using a stability indicating accurate, inexpensive and simple procedure. Another added advantage of the current method resides in its ability to study the kinetics of degradation processes of AZL and CLT which were obtained by subjecting them to acidic and alkaline stress conditions, respectively.

1.2.2 Experimental

1.2.2.1 Instruments

Separations were performed using Agilent HPLC system 1200 chromatograph (USA) equipped with a quaternary pump G1311A and a Rheodyne injector valve with a 20 µL loop and a G1315D MWD detector. Mobile phases were degassed using a G1322A solvent degasser. Agilent Chemstation for LC systems [Rev.B.03.01-SR1 (317)] PC program was used for the instrument control, data analysis and acquisition. A SympHonly (SB20) pH-meter (Thermo Orion, MA, USA) was used for pH adjustment. Nano pure water was prepared using a Barnstead NANO pure DIamond Analytical ultrapure water system (Fischer Scientific, NJ, USA). Fisher Biotech UV fluorescent lamp, model FBUVLS-80 dual wavelength (254/366) was used in the photo-stability studies (Fisher Scientific, PA, USA). The LC–MS studies was performed using an Agilent 1200 ultra-high pressure liquid chromatography system (USA) consisting of a binary pump (G1312A) with a degasser, autosampler (G1329A) and a DAD (Agilent 1100, G1315B) using a mobile phase composed of water and methanol (20: 80, v/v) coupled to a 3200 Q TRAP mass spectrometer (AB Sciex; CA, USA) fitted with a TurboV ion source operating in negative and positive electrospray ionization (ESI) mode. The data were acquired and processed using Analyst® 1.6.1 Software (AB Sciex; Ontario, Canada). MS source parameters were set at: desolvation temperature (TEM): 200 °C, high voltage: -4500 V (ESI -), 4500 V (ESI +), curtain (CUR) and nebuliser (GS1 and GS2) gases: nitrogen; 20, 40, and 50 psi; respectively, nitrogen collision gas pressure: 5 mTorr.

1.2.2.2 Materials and reagents

All the chemicals used were of Analytical Reagent grade, and the solvents were of HPLC grade. AZL (certified to contain 98%) was supplied by D-L Chiral Chemicals, LLC., NJ 08540

USA. CLT (certified to contain 98%) was supplied by Ark Pharm. Inc., IL 60048 USA. Edarbcyclor® 40-25 mg tablets; batch # NDC 64764-0994-30 (Takeda Pharmaceutical Company Limited, Tokyo, Japan) each labeled to contain 42.68 mg of azilsartan kamedoxomil (equivalent to 40 mg AZL) and 25 mg CLT were purchased from commercial sources in the local market. Sodium hydroxide, potassium hydroxide, acetic acid and dipotassium hydrogen orthophosphate were obtained from J.T. Baker, NJ, USA. Orthophosphoric acid 85%, hydrochloric acid and ammonium acetate (Fisher Scientific, NJ, USA) were also used. Methanol and hydrogen peroxide (30% w/v) (Sigma-Aldrich, MO, USA).

1.2.2.3 Chromatographic conditions

A mixture of methanol: dipotassium hydrogen phosphate buffer (PBS) (pH 8±0.1, 0.05M) (40:60, v/v) was prepared. Flow rate was maintained at 0.8 mL min^{-1}. All analyses were performed at ambient temperature. The system was equilibrated and saturated with the mobile phase for 30 min before the injection of the solutions. Quantification was achieved with UV detection at 210 nm based on peak area. Twenty μL of the solutions were injected with a 50 μl Agilent analytical syringe in triplicates.

1.2.2.4 Standard solutions

Ten mg of each of AZL and CLT were accurately weighed and transferred in to 10 mL volumetric flasks separately. Then, they were dissolved and made up to volume with methanol to give final concentrations of 1000 μg mL^{-1} for each. The solutions were stable for at least 14 days without alteration when kept in the refrigerator at 4 ˚C and protected from light.

1.2.2.5 Procedures

1.2.2.5.1 Construction of the calibration graphs

Accurate aliquots from the standard solutions were transferred separately into a series of 10 mL Fisherbrand disposable tubes. Then, the volumes were completed to the mark with the mobile phase so that the final concentrations were in the range of 5.0-50.0 and 2.5-25.0 µg mL^{-1} for AZL and CLT, respectively. Aliquots of 20 µL were injected (triplicate) and eluted with the mobile phase under the optimum chromatographic conditions using UV detection at 210 nm. The average peak area versus the final concentration of the drug in µg mL^{-1} was plotted. Alternatively, the corresponding regression equations were derived.

1.2.2.5.2 Preparation of the laboratory prepared mixtures

Accurate aliquots of AZL and CLT standard solutions were transferred into a series of 10 mL Fisherbrand disposable tubes keeping the medicinally recommended ratio of 1.6:1 for AZL/CLT mixture to give final concentrations of 8, 16, 24 µg mL^{-1} for AZL and 5, 10, 15 µg mL^{-1} for CLT. The above procedure described under "section 2.5.1" was then applied. The recovery percentage was calculated using the corresponding regression equation.

1.2.2.5.3 Analysis of the studied drugs in their pharmaceutical preparation

Ten tablets of Edarbcyclor® 40-25mg were weighed, finely pulverized and thoroughly mixed. After calculating the average tablet weight, amounts of powder equivalent to 40 and 25 mg of AZL and CLT, respectively, were accurately weighed and transferred into a 25 mL measuring flask. Twenty milliliters of methanol were added and the solution was sonicated for 30 min then completed to volume with the same solvent. The solution was filtered through a Whatman filter paper and then filtered again using 0.2µm a Whatman inorganic membrane filter. For analyses, different aliquots from the prepared sample solutions were chromatographed using

the same procedure described under “section 2.5.1”. The recovery percentage was calculated by referring to the corresponding regression equations.

1.2.2.5.4 Procedures for the extensive stress stability studies

1.2.2.5.4.1 Stress degradation by hydrolysis under acidic and alkaline conditions

Aliquots of AZL and CLT standard solutions equivalent to 500 and 400 µg, respectively, were transferred separately into Fischerbrand disposable tubes; treated with 2 mL of 0.1 M NaOH or 0.1M HCl and heated at 80 and 100 ^{o}C for 1 h, respectively. After the specified time, the contents of each tube were cooled and neutralized to pH 7.0 with 0.1 M HCl or 0.1 M NaOH, respectively. The solutions were then transferred into 10-mL volumetric flasks. Five milliliters methanol were added to each flask and completed to the volume with Nano pure water. Two milliliters of the resulting solutions were then transferred into Fischerbrand disposable tubes and diluted to 4 mL with the mobile phase (final concentrations were 25 and 20 µg mL^{-1} as equivalent to AZL and CLT, respectively, before degradation) and filtered before injection into the column. The above procedure described under “section 2.5.1” was then applied.

1.2.2.5.4.2 Procedure for oxidative and wet heat induced degradations

Aliquots of AZL and CLT standard solutions equivalent to 500 and 400 µg, respectively, were transferred separately into Fischerbrand disposable tubes; 2 mL aliquots of 6% H_2O_2 or Nano pure water were added and heated at 80 and 100 ^{o}C for 1 h for AZL and CLT, respectively. After the specified time, the resulting solution was cooled and transferred into 10-mL volumetric flasks. Five milliliters methanol were added to each flask and completed to the volume with Nano pure water. Two milliliters of the resulting solutions were then transferred into Fischerbrand disposable tubes and diluted to 4 mL with the mobile phase (final concentrations were 25 and 20 µg mL^{-1} as equivalent to AZL and CLT, respectively, before degradation) and

filtered before injection into the column. The above procedure described under “section 2.5.1” was then applied.

1.2.2.5.4.3 Procedure for photolytic degradation

The photo degradation study was performed by subjecting 4 mL from each of AZL (100 μg mL^{-1}) and CLT (80 μg mL^{-1}), prepared in methanol and placed in 1-cm stoppered quartz cells to direct UV radiation (UV lamp set at 254 nm) at room temperature for 24 h at a distance of 10 cm. Protected samples, wrapped in aluminum foil in order to protect them from light, were submitted to identical conditions and used as control. One milliliter of the resulting solutions were then transferred into Fischerbrand disposable tubes and diluted to 4 mL with the mobile phase (final concentrations 25 and 20 μg mL^{-1} as equivalent to AZL and CLT, respectively, before degradation) and filtered before injection into the column. The above procedure described under “section 2.5.1” was then applied.

1.2.2.5.5 Kinetics investigation

1.2.2.5.5.1 Study of the acidic induced degradation of AZL at different temperatures

Aliquots of AZL standard solution (equivalent to 500 μg) were transferred into Fischerbrand disposable tubes. Two milliliters of 0.1 M HCl were added for each tube. The tubes were heated at different temperatures (50, 60, 70, 80 ºC) for different time intervals (15–60 min). At the specified time interval, the contents of each tube were cooled and neutralized to pH 7.0 with 0.1 M NaOH. The solutions were then transferred into 10-mL volumetric flasks. Five milliliters methanol were added to each flask and completed to the volume with Nano pure water. Two milliliters of the resulting solutions were then transferred into Fischerbrand disposable tubes and diluted to 4 mL with the mobile phase (final concentration was 25 μg mL^{-1} as equivalent to AZL before degradation) and filtered before injection into the column. The

above procedure described under “section 2.5.1” was then applied. The concentration of the remaining drug was calculated for each temperature and time interval. Data were further processed and degradation constants were calculated for each temperature to construct the Arrhenius plot. An Arrhenius plot was constructed and the apparent first-order rate constants, half-life times, shelf-life times and the activation energy of the degradation process were then calculated. All solutions were filtered through 0.2 µm membrane filters and degassed for 5 min before injection to the LC system.

1.2.2.5.5.2 Study of the alkaline induced degradation of CLT at different temperatures

Aliquots of CLT stock solutions (equivalent to 400 µg) were transferred into Fischerbrand disposable tubes. Two milliliters of 0.1 M NaOH were added for each tube. The tubes were heated at different temperatures (70, 80, 90, 100 ^{o}C) for different time intervals (30–120 min). At the specified time interval, the contents of each tube were cooled and neutralized to pH 7.0 with 0.1 M HCl. The solutions were then transferred into 10-mL volumetric flasks. Five milliliters methanol were added to each flask and completed to the volume with Nano pure water. Two milliliters of the resulting solutions were then transferred into Fischerbrand disposable tubes and diluted to 4 mL with the mobile phase (final concentration was 20 µg mL^{-1} as equivalent to CLT before degradation) and filtered before injection into the column. The above procedure described under “section 2.5.1” was then applied. The concentration of the remaining drug was calculated for each temperature and time interval. Data were further processed and degradation constants were calculated for each temperature to construct the Arrhenius plot. An Arrhenius plot was constructed and the apparent first-order rate constants, half-life times, shelf-life times and the activation energy of the degradation process were then

calculated. All solutions were filtered through 0.2 µm membrane filters and degassed for 5 min before injection to the LC system.

1.2.3 Results and discussion

The proposed method permitted the separation and quantitation of the studied drugs in a short time <9 min. Furthermore, the suggested procedure was applied for the quality control of commercial dosage form (Fig. 1.2.2). The proposed LC method allows the separation of AZL and CLT from all possible degradation products. Fig. (1.2.3b-f) as well as (1.2.4b-f) show good resolution of AZL and CLT from each of its alkaline, acidic, oxidative, thermal (wet heat) and photolytic degradation products, respectively. The stability studies for the acidic degradation kinetics of AZL as well as the alkaline degradation kinetics of CLT were successfully conducted.

1.2.3.1 Optimization of experimental conditions

Several trials were carried out to achieve the best chromatographic conditions for the simultaneous determination of AZL and CLT as well as their separation from their degradation products. Three columns were tested for performance investigation, including: Ultrasphere ODS column (4.6 mm ×250 mm, 5 µm particle size), Beckman, Fullerton, CA, USA, Eclipse XDB-C18 column (4.6 x 150mm, 5 µm) Agilent, East Windsor, NJ, USA and Spherex 10 phenyl column (250 mm x 2.0 mm i.d.), Phenomenex, CA, USA. The experimental studies revealed that, the second column was the most suitable one since it produced symmetrical peaks with high resolution and within a reasonable analytical run time. AZL is practically insoluble in water, freely soluble in methanol, dimethylsulfoxide, soluble in acetic acid, slightly soluble in acetone, and acetonitrile and sparingly soluble in tetrahydrofuran and 1-octanol [13]. Methanol and acetonitrile were examined as the organic modifiers and acetonitrile was found to cause splitting

for the peak of AZL due to its poor solubility in that solvent so methanol was chosen as the organic modifier in this study. Water, 1% acetic acid, ammonium acetate buffer (pH 5.5; 0.05 M) and PBS (pH 8; 0.05 M) were tested as the aqueous component in the mobile phase. The use of buffer is necessary in this method in order to enhance the ionization of the analytes, obtain proper separation and increase the sharpness of peaks. Both ammonium acetate buffer and PBS are able to achieve proper separation. PBS was selected as it was able to produce sharper and more symmetric peaks than ammonium acetate buffer. Then, effect of pH on the separation of the analytes was studied. The higher the pH of the used buffer the lower the retention time with sharp and symmetric peak for AZL so pH 8 was selected as it achieved satisfactory separation at a reasonable run time (<9 min) and with satisfactory resolution between all of the analytes, (Fig. 1.2.2). Ratio of aqueous to organic component in the mobile phase system was also studied and a ratio of (60:40, *v/v*) was selected. Increasing the ratio of the aqueous component will produce significant delay and broadening of peaks meanwhile increasing the ratio of the organic component will cause overlap between the studied analytes. Different flow rates were studied as it affects both resolution and shape of peaks and flow rate of 0.8 mL min^{-1} was selected. Proper choice of the detection wavelength is crucial for sensitivity of the method. Quantitation was achieved with UV-detection at 210 nm based on good peak area for each of the analyzed drugs. System suitability tests were used to verify that the conditions of the chromatographic system were adequate for the separation and hence for the analysis [26], (Table 1.2.1).

1.2.3.2 Method validation

The validity of the proposed LC method was assessed according to ICH guidelines in terms of linearity, range, limit of detection, limit of quantification, accuracy, precision, robustness, specificity and stability [26].

1.2.3.2.1 Linearity and range

Under the above described experimental conditions, linear relationships were established by plotting the peak area versus the corresponding concentration in μg mL^{-1}. The graphs were found to be rectilinear over the concentration ranges cited in table 1.2.2. Statistical analysis of the data gave high value of the correlation coefficient (r) of the regression equation, small values of the standard deviation of residuals ($S_{y/x}$), of intercept (S_a), and of slope (S_b), and small value of the percentage relative standard deviation and the percentage relative error, (Table 1.2.2). These data indicated the linearity of the calibration graphs.

1.2.3.2.2 Limit of quantitation (LOQ) and limit of detection (LOD)

LOQs and LODs were calculated according to ICH Q2 (R1) recommendations using the following equation [26]: LOQ = 10 S_a /b and LOD = 3.3 S_a /b, where S_a = standard deviation of the intercept and b = slope of the calibration curve. Results are given in (Table 1.2.2).

1.2.3.2.3 Accuracy and precision

The satisfactory recovery results for the assay of AZL and CLT in their laboratory prepared mixtures indicate the accuracy of the method, (Table 1.2.3). Repeatability (intraday) and intermediate precision (inter-day) were assessed using three concentrations and three replicates of each concentration. The relative standard deviations were found to be very small indicating reasonable repeatability and intermediate precision of the proposed method (Table 1.2.4).

1.2.3.2.4 Stability of standard solutions and mobile phase

Stability of the standard solutions of AZL and CLT stored at 4 °C, were evaluated at various time points over one month. The concentrations of freshly prepared solutions and those aged for one month were calculated by the method developed and the difference between them

was found to be non-significant (% RSD <2%). Similarly, the stability of the mobile phase was checked for two weeks. The results obtained in both cases proved that the samples solutions and mobile phase used during the assay were stable for the specified durations, when kept in the refrigerator at 4 ˚C.

1.2.3.2.5 Robustness of the method

Minor deliberate changes in different experimental parameters such as flow rate (±0.1 mL min^{-1}), pH (±0.1) and ratio of mobile phase components (±2%) did not significantly affect resolution of the analyzed compounds indicating that the proposed method is robust, (Table 1.2.5).

1.2.3.2.6 Specificity

The specificity is the ability of the analytical method to assess unequivocally the analyte in the presence of components which may be expected to be present. The specificity of the method was investigated by observing any interference encountered from common tablet excipients and it was confirmed that the signals measured was caused only by the analytes. The inactive ingredients in Edarbcylor® are: mannitol, microcrystalline cellulose, fumaric acid, sodium hydroxide, hydroxypropyl cellulose, crospovidone, magnesium stearate, hypromellose 2910, talc, titanium dioxide, ferric oxide red, polyethylene glycol 8000, and printing ink gray F1. It was found that the excipients did not interfere with the results of the proposed method. As shown in (Fig. 1.2.2) the chromatograms of the combined formulations did not show any additional peaks when compared with the chromatograms of the laboratory prepared mixtures which confirm the specificity of the developed method. Specificity of the method was also confirmed by its ability to measure AZL and CLT in the presence of all of their degradation products, as revealed by the results of the stability study (Fig. 1.2.3b–3f and 1.2.4b-4e).

1.2.3.3 Application of the proposed method for quality control of AZL and CLT in their combined commercial dosage form

The proposed method was applied to determine AZL and CLT in their commercially available tablets. Satisfactory recoveries were obtained and the results are given in (Table 1.2.3).

1.2.3.4 Forced degradation studies

AZL and CLT were subjected to forced decomposition by alkali, acidic, wet heat, light and oxidation, as suggested in the International Conference on Harmonization (ICH) Q1A (R2) and (Q1B) guideline [25], (Fig. 1.2.4).

1.2.3.4.1 Alkaline Induced Degradation

AZL showed high stability to alkaline degradation. Only 3.1 % degradation was observed as evidenced by the decrease in the parent drug peak area upon the addition of 2 mL 0.1 M NaOH to the drug and boiling at 80 ^{o}C for 1 h, (Fig. 1.2.3b). On the contrary, CLT was found to undergo alkaline degradation very readily after addition of 2 mL 0.1 M NaOH to the drug and boiling at 100 ^{o}C for 1 h. 69.0 % degradation was observed as evidenced by the decrease in the parent drug peak area, and the appearance of two major DPs with peaks at 3.8 min and 4.9 min, (Fig. 1.2.4b).

1.2.3.4.2 Acid induced degradation

AZL was found to undergo acid degradation very readily upon the addition of 2 mL 0.1 M HCl to the drug and boiling at 80 ^{o}C for 1 h. 94.7 % degradation was observed as evidenced by the decrease in the parent drug peak area, (Fig. 1.2.4c) and the appearance of one major DP peak at 2.7 min, (Fig. 1.2.3c). On the contrary, CLT was found to show high stability to acidic degradation upon the addition of 2 mL 0.1 M HCl to the drug and boiling at 100 ^{o}C for 1 h. Only 3.6 % degradation was observed as evidenced by the decrease in the parent drug peak area, (Fig.

1.2.4c).

1.2.3.4.3 Hydrogen Peroxide and thermal (wet heat) induced degradation:

Oxidative and thermal (wet heat) degradation of AZL and CLT were also studied. AZL was found to show certain stability to oxidative and thermal (wet heat) degradation upon the addition of 2 mL of 6% H_2O_2 or water, respectively, to the drug and boiling at 80 ^oC for 1 h. Only 19.2 and 2.6 % degradation was observed as evidenced by the decrease in the parent drug peak area, (Fig. 1.2.3d, 3e). Also, CLT showed certain stability to oxidative and thermal (wet heat) degradation upon the addition of 2 mL of 6% H_2O_2 or water, respectively, to the drug and boiling at 100 ^oC for 1 h. Only 7.7 and 0.7 % degradation was observed as evidenced by the decrease in the parent drug peak area, (Fig. 1.2.4d, 4e).

1.2.3.4.4 Photolytic degradation

The effect of UV-light on the stability of AZL and CLT were studied. It was found that 99.1% and 96.1% degradation was observed after exposure of the drug to 254 nm light for 1 day at room temperature, respectively, (Fig. 1.2.3f, 4f).

1.2.3.5 Identification of the potential acid degradation product for AZL

As shown in scheme 1.2.1, the LC-MS total ion chromatograms (negative mode) for the intact AZL and its acidic induced degradation after 1 h boiling at 80 °C, a predominant DP was found to be present with a molecular ion at m/z 539. It is postulated that the drug degraded through cleavage of the ether linkage attached to the benzodiazole moiety. This DP showed a fragment at m/z 427 due to cleavage of the ester bond. Then, further fragmentation occurred through opening of the oxadiazole ring and losing CO_2 molecule to give a fragment at m/z 383. This anticipation was supported by the disappearance of the peaks at δ= 1.3 and 4.6 of the ethyl group in the ^1H NMR spectrum (400 MHz, DMSO) of AZL DP and by the appearance of new

peaks at δ= 5.5 and 11.4 of the resonating iminol group in the benzdiazole ring.

1.2.3.6 Identification of the potential alkaline degradation product for CLT

The LC-MS total ion chromatogram (negative mode) for the intact CLT and its alkaline degradation after 1 h boiling at 100 °C revealed some distinguishable molecular ion peaks at m/z 375, 339, 356, 294 and 258 from that of the ion chromatogram of the intact drug. Also, it showed many peaks for dimer adducts. As demonstrated in scheme 1.2.2, we have two anticipated pathways for the alkaline induced degradation of CLT. The first one is through hydrolytic cleavage of the amide bond in the isoindole ring with a molecular ion at m/z 356 followed by removal of the ammonia group to form a stable benzophenone derivative with m/z at 339. Further fragmentation of that DP was proposed to be via decarboxylation to give a fragment at m/z 294. The second pathway is through direct opening of the isoindole ring to form amido benzophenone derivative at m/z 339. Further fragmentation of that DP was through removal of sulphonamide moiety to form a fragment at m/z 258. The second anticipated pathway was supported by the disappearance of the peaks at δ= 8.1 and 9.4 of the hydroxyl and the secondary amino groups in the ^{1}H NMR spectrum (400 MHz, DMSO) of CLT DP and by the appearance of a new peak at δ= 6.1 of the amide group.

1.2.3.7 Degradation kinetics for AZL and CLT

The experimental investigation of the possible breakdown of the drugs is usually studied to produce more stable preparations and to assist the pharmacists and physicians regarding the proper storage and handling of the medicinal agents. Degradation reaction rates are affected by temperature, as suggested by the Arrhenius equation [27]:

$$Log\ K = Log\ A - \frac{E_a}{2.303}\ \frac{1}{RT}$$

Where: K = specific reaction rate at temperature T, A = Arrhenius factor (collision factor) constant, E_a = energy of activation (the minimum kinetic energy a molecule must possess in order to undergo reaction), R = gas constant, and T = absolute temperature in Kelvin.

In this study, the constant A and E_a were evaluated by determining K for the acid degradation of 25 µg mL^{-1} of AZL in 0.1 M HCl at different temperatures (50, 60, 70, and 80 ^oC) as well as for the alkaline degradation of 20 µg mL^{-1} of CLT in 0.1 M NaOH at different temperatures (70, 80, 90, and 100 ^oC). As shown in Fig. 1.2.5 the degradation was found to be temperature dependent.

The apparent first order degradation rate constant, half-life time (**$t_{1/2}$**), shelf-life (**t_{90}**) and the activation energy E_a were calculated (Table 1.2.6). By plotting log K_{obs} values versus 1/T, Arrhenius plot was obtained (Fig. 1.2.6) and the resulting lines were extrapolated at room temperature to obtain K_{25}^{o}, which is used as a measure of the stability of the drug under ordinary shelf conditions. Arrhenius equations [27] were found to be: (*Log K = 11.482 + 4.5441 x 103/T*) for AZL as well as (*Log K = 10.235 + 4.4562 x* $10^3/T$) for CLT. Where; K is the specific reaction rate, T is the absolute temperature.

Table 1.2.1 System Suitability data for the RP-LC Method

Item	AZL	CLT
N	4422	4185
K`	2.63	1.89
T	1.19	1.22
R	3.88	
α	1.26	

(N: number of theoretical plates; K`: capacity factor; R: resolution factor; T: tailing factor; α: relative retention time)

Table 1.2.2 Characteristics and Results of the Proposed RP-LC Method

Item	**AZL**	**CLT**
Limit of detection, LOD (µg mL^{-1})	0.90	0.32
Limit of quantitation, LOQ (µg mL^{-1})	2.72	0.98
Intercept (a)	-189.71	-72.54
Slope (b)	175.78	193.75
Correlation coefficient (r)	0.9999	0.9999
S.D. of residuals (Sy/x)	61.09	24.24
S.D. of intercept (Sa)	47.84	18.99
S.D. of slope (Sb)	1.71	1.36
% Error	1.02	0.83
% RSD	2.27	1.86
Linearity range (µg/mL)	5.00-50.00	2.50-25.00
Mean %recovery ± S.D.	100.83 ± 2.29	99.48 ± 1.85

Table 1.2.3 Assay results for the determination of the studied drugs in their laboratory prepared mixtures and dosage forms

Ratio	Compound	Laboratory prepared mixtures			Dosage form		
		Amount taken ($\mu g\ mL^{-1}$)	Amount found ($\mu g\ mL^{-1}$)	% Found	Amount taken ($\mu g\ mL^{-1}$)	Amount found ($\mu g\ mL^{-1}$)	% Found
(AZL:CLT) (1.6:1.0)	AZL	8.00	8.10	101.25	8.00	8.22	102.75
		16.00	15.98	99.88	16.00	16.19	101.19
		24.00	23.93	99.71	24.00	24.10	100.42
	Mean recovery%			100.28			101.45
	± %RSD			0.84			1.17
	CLT	5.00	5.04	100.80	5.00	5.06	101.20
		10.00	10.03	100.30	10.00	9.99	99.90
		15.00	14.60	97.33	15.00	15.28	101.87
	Mean recovery%			99.48			100.99
	± %RSD			1.88			0.99

Each result is the average of three separate determinations.

Table 1.2.4 Assay results for the determination of the studied drugs in their laboratory prepared mixtures and dosage forms

AZL			CLT		
Conc. of AZL (μg mL^{-1})	Intra-day assay Recovery % ± %RSD [a]	Inter-day assay Recovery % ± %RSD [a]	Conc. of CLT (μg mL^{-1})	Intra-day assay Recovery % ± %RSD [a]	Inter-day assay Recovery % ± %RSD [a]
12.50	100.48 ± 0.96	101.50 ± 1.25	7.50	100.65 ± 0.75	101.59 ± 0.88
25.00	98.87 ± 1.22	100.17 ± 1.25	12.50	98.67 ± 1.08	99.61 ± 1.75
40.00	100.32 ± 0.94	101.55 ± 1.05	20.00	98.12 ± 0.61	99.03 ± 0.96
Mean recovery% ± %RSD	99.89 ± 0.89	101.07± 0.77	Mean recovery% ± %RSD	99.15 ± 1.34	100.08± 1.34

[a] Mean and relative standard deviation of three determinations

Table 1.2.5 Results of the robustness study

Parameter	Drug	Standard Method	Flow rate (mL min^{-1})		pH		Mobile phase Composition	
			0.7	0.9	7.9	8.1	PBS : Methanol (62:38)	PBS : Methanol (58:42)
Retention time	AZL	7.0	8.1	6.4	7.3	6.8	5.7	8.8
(min)	CLT	5.6	6.4	5.0	5.7	5.5	4.8	6.5
Resolution	CLT/AZL	3.7	3.8	3.7	3.9	3.7	2.7	4.9

Table 1.2.6 Kinetics data of AZL and CLT degradation

Drug	Temperature (°C)	K x 10^{-4} (min^{-1})	$t_{1/2}$ (min)	t_{90} (min)	Ea (k cal mol^{-1})
AZL in 0.1N HCl	50	27.64	250.8		
	60	89.82	77.2		
	70	158.91	43.6		
	80	476.72	14.5		
	Value at 25 °C	1.96	-	537.8	35.34
CLT in 0.1N NaOH	70	16.12	429.9		
	80	55.27	125.4		
	90	115.15	60.2		
	100	177.33	39.1		
	Value at 25 °C	0.22	-	4834.9	20.39

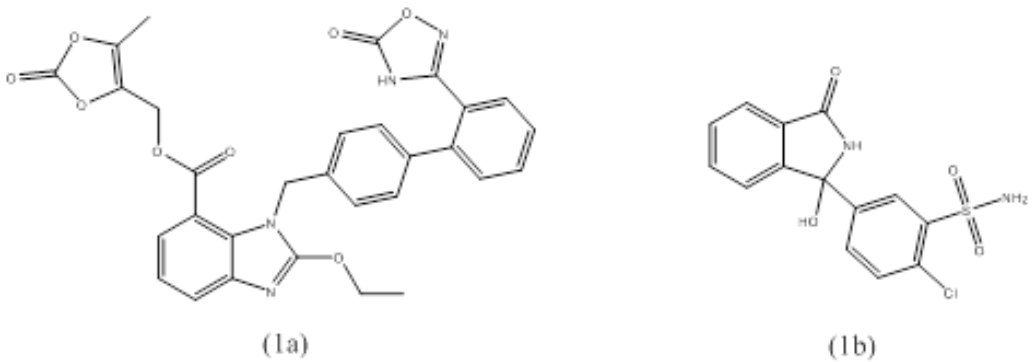

Figure 1.2.1 The structural formulae of the studied drugs; (a) azilsartan medoxomil (AZL), and (b) chlorthalidone (CLT)

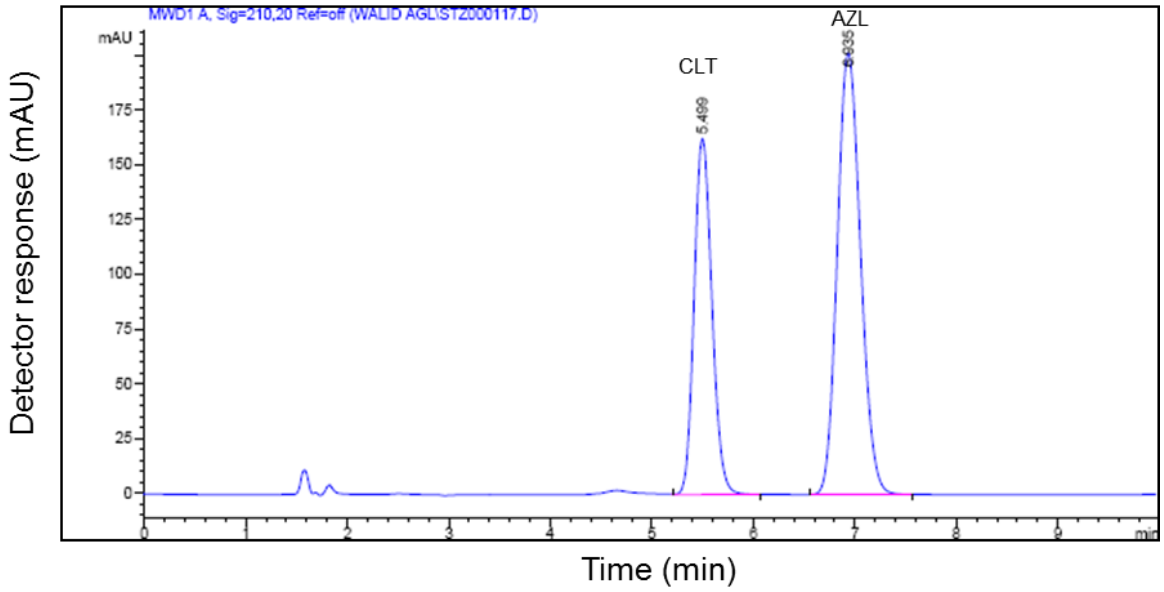

Figure 1.2.2 A typical LC chromatogram for Edarbcyclor® tablets: 24 µg mL^{-1} AZL (6.9 min), and 15 µg mL^{-1} of CLT (5.5 min) under the descried chromatographic conditions

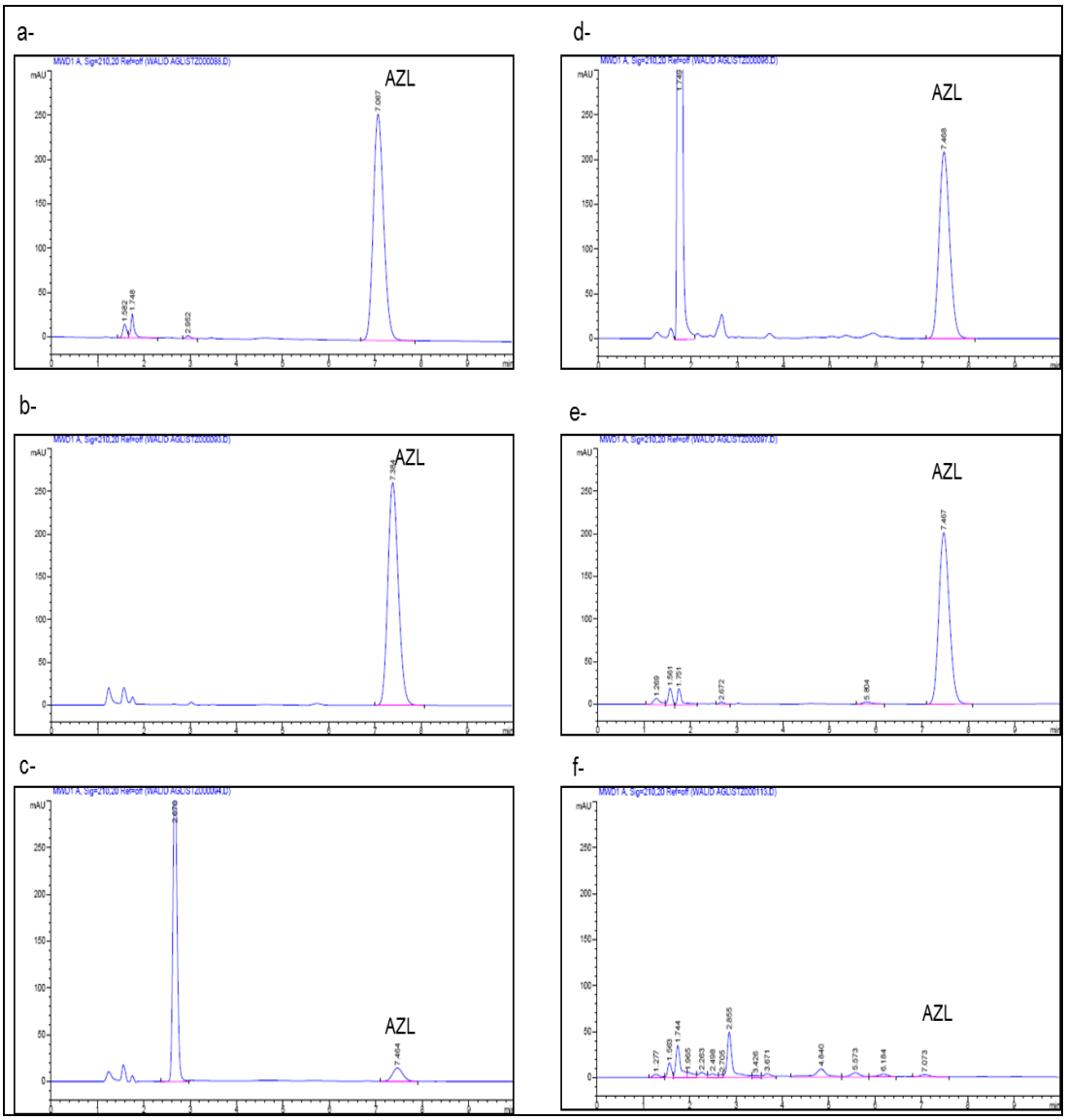

Figure 1.2.3 LC chromatograms of 25 µg mL^{-1} AZL under different stress degradation conditions: (a) control, (b) alkaline (0.1N NaOH), (c) acidic (0.1N HCl), (d) oxidative (6% H_2O_2, w/v), (e) thermal (wet heat) and (f) photolytic (254 nm) using the described degradation and chromatographic conditions

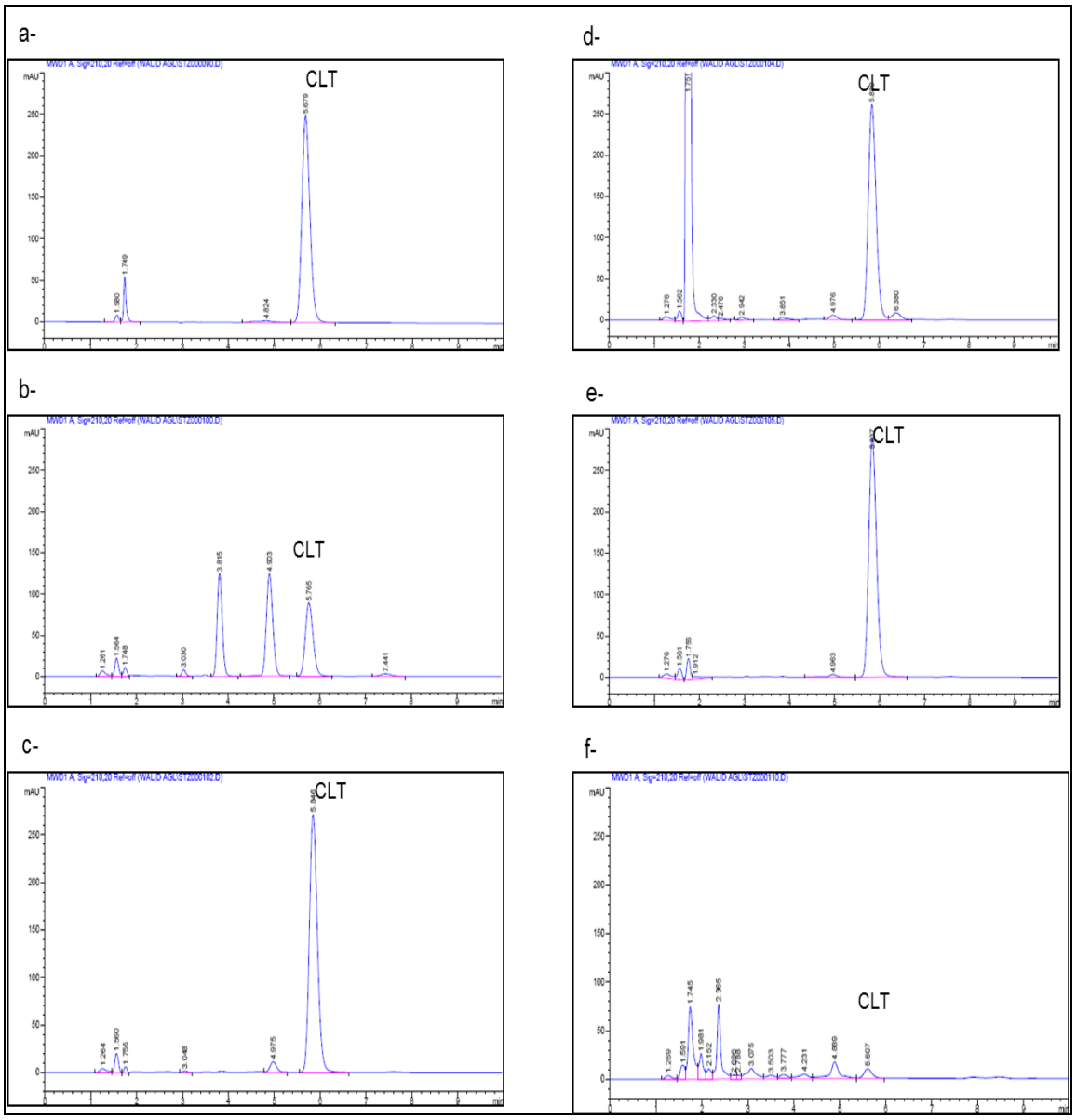

Figure 1.2.4 LC chromatograms of 20 µg mL^{-1} CLT under different stress degradation conditions: (a) control, (b) alkaline (0.1N NaOH), (c) acidic (0.1N HCl), (d) oxidative (6% H_2O_2, w/v), (e) thermal (wet heat) and (f) photolytic (254 nm) using the described degradation and chromatographic conditions

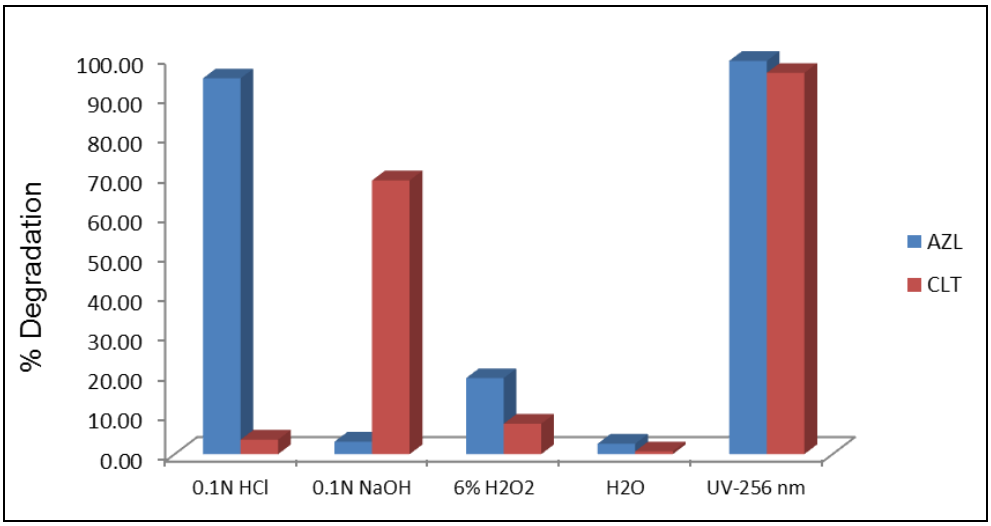

Figure 1.2.5 Percentage of degradation of 25 µg mL^{-1} of AZL and 20 µg mL^{-1} of CLT under different stress degradation conditions

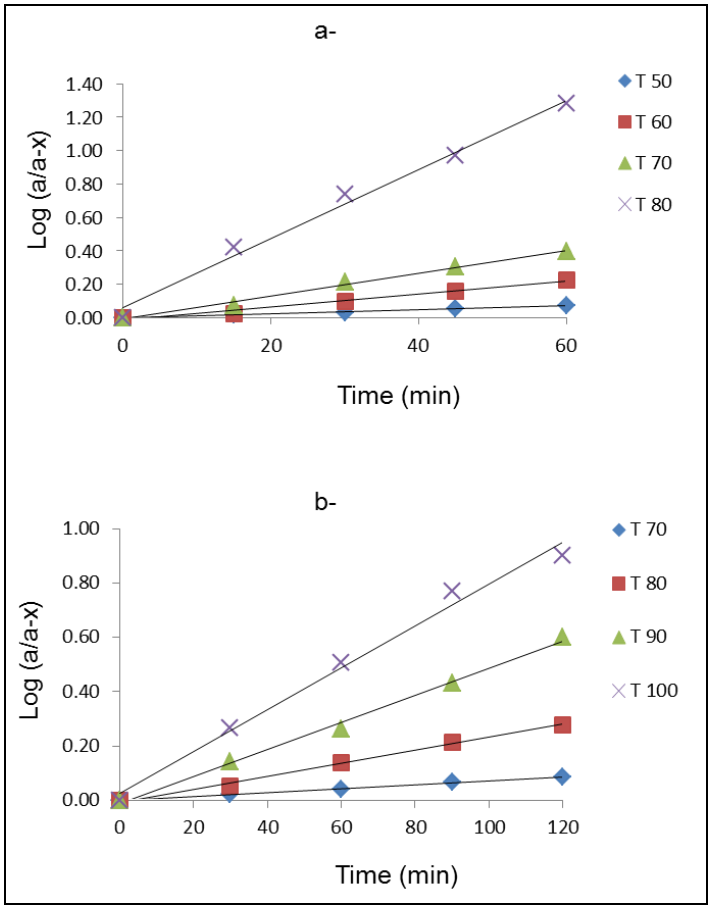

Figure 1.2.6 Effect of different heating times with 0.1 M HCL and 0.1 M NaOH on the rate of degradation of (a) AZL (25 µg mL^{-1}) and (b) CLT (20 µg mL^{-1}), respectively

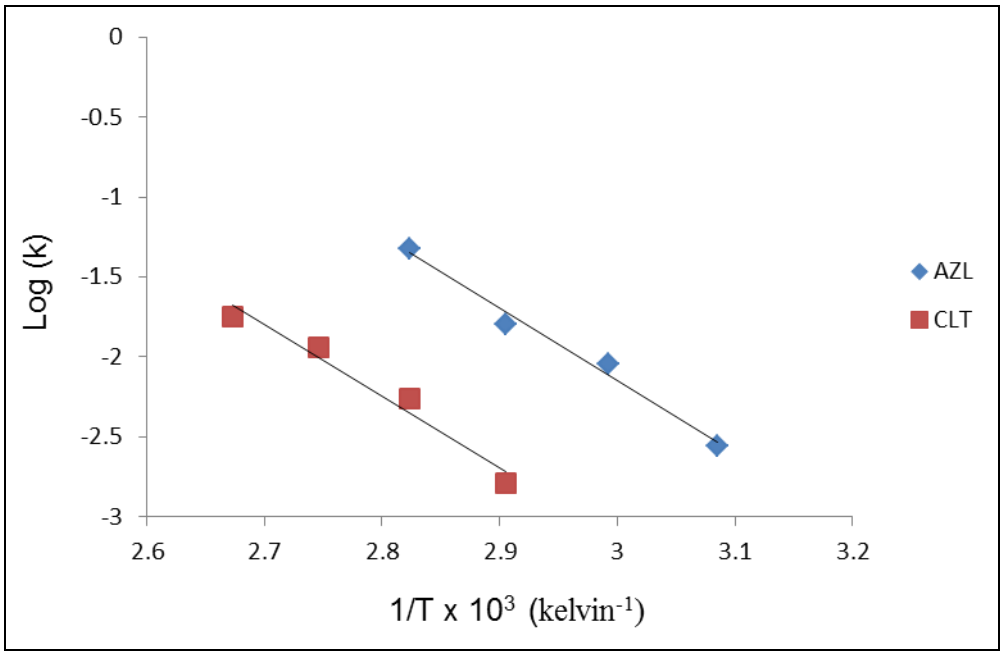

Figure 1.2.7 Arrhenius plots for AZL (25 µg mL^{-1}) and CLT (20 µg mL^{-1})

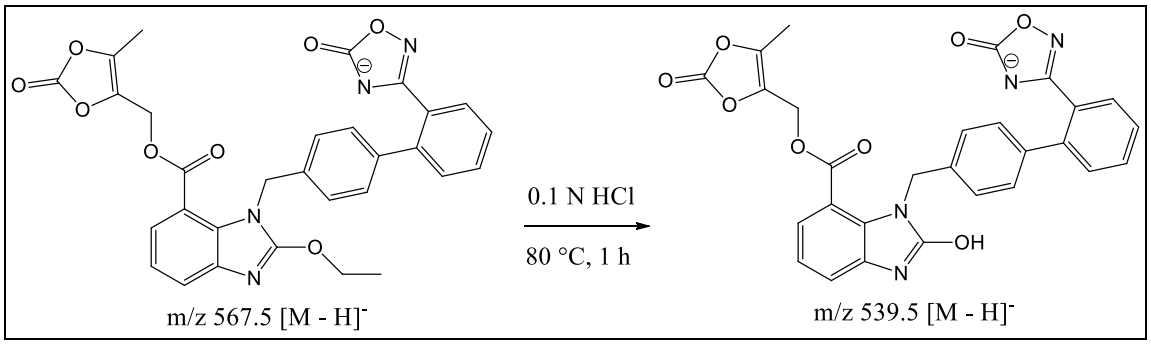

Scheme 1.2.1 Proposed structure for the acid induced degradation product of AZL

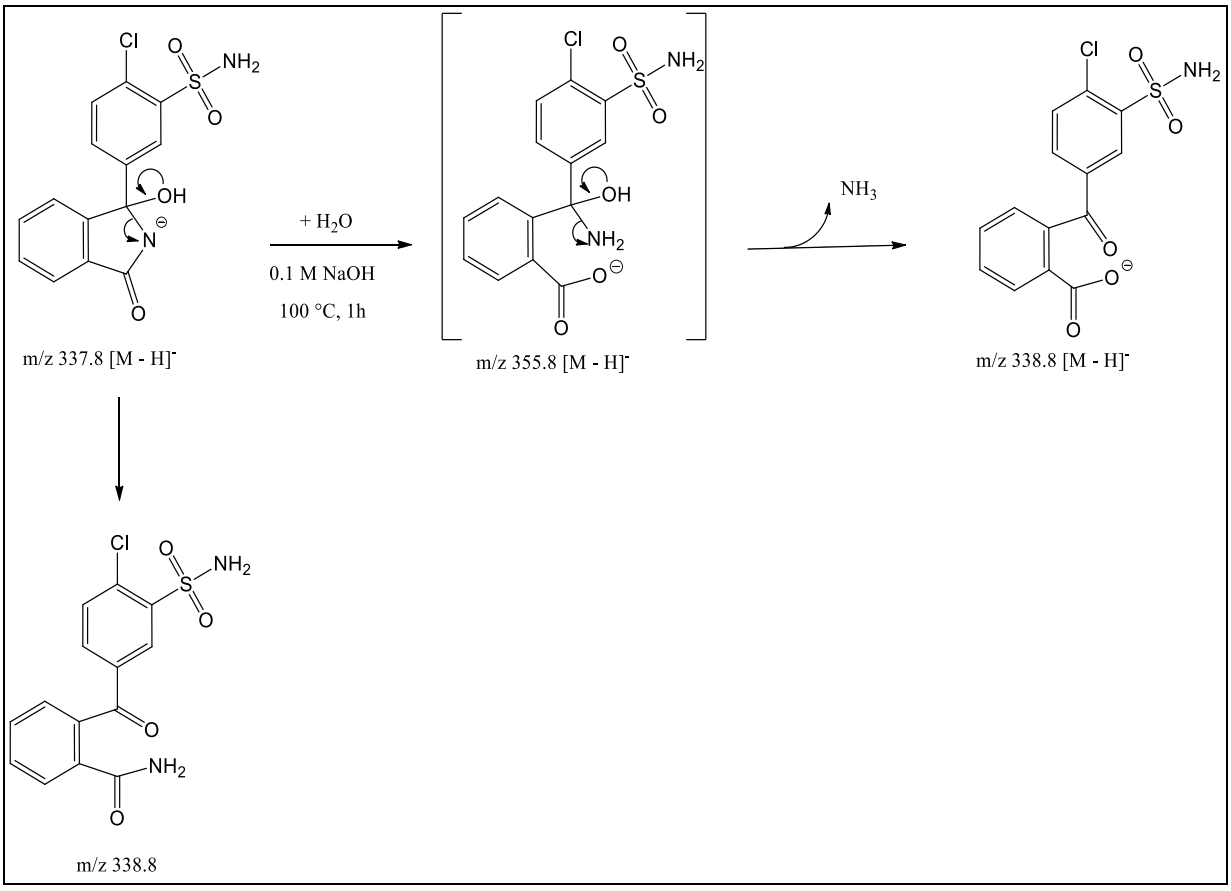

Scheme 1.2.2 Proposed structures for the alkaline induced degradation products of CLT

1.3 Synchronized Separation of Seven Medications Representing Most Commonly Prescribed Antihypertensive Classes using RP-LC: Applied to Analysis in Their Combined Formulations

Journal of Separation Science (2014) 37:748–757

DOI 10.1002/jssc.201301298

A reversed phase high performance liquid chromatography method was developed for simultaneous determination of the diuretic, hydrochlorothiazide, along with six drugs representing most commonly prescribed antihypertensive pharmacological classes such as atenolol, a selective β_1 blocker, amlodipine besylate, a calcium channel blocker, moexipril hydrochloride, an ACE inhibitor, valsartan and candesartan cilexetil which are angiotensin II receptor blockers and aliskiren hemifumarate, a renin inhibitor, using irbesartan as an internal standard. The chromatographic separation was achieved using acetonitrile: sodium phosphate dibasic buffer (0.02 M, pH 5.5) at a flow rate of 1 mL min^{-1} in gradient elution mode at ambient temperature on a stationary phase composed of Eclipse XDB-C18 (4.6 x 150 mm, 5 µm) column. UV detection was carried out at 220 nm. The method was validated according to ICH guidelines. Linearity, accuracy and precision were satisfactory over the concentration ranges of 2-40 µg mL^{-1} for hydrochlorothiazide and candesartan cilexetil, 20-200, 10-160, 5-40, 20-250 and 5-50 µg mL^{-1} for atenolol, valsartan, moexipril hydrochloride, aliskiren hemifumarate and amlodipine besylate, respectively. The method was successfully applied for the determination of each of the studied medications in their combined formulations with hydrochlorothiazide. The developed

method is suitable for the quality control and routine analysis of the cited drugs in their pharmaceutical dosage forms.

1.3.1 Introduction

Hydrochlorothiazide (HCZ) is an orally potent diuretic which inhibits active chloride reabsorption and thus increases the excretion of sodium chloride and water [28]. It is chemically 6-chloro-1, 1-dichloro-3, 4, dihydro-2H-1, 2, 4-benzoliadiazine-7-sulphanomide1, 1-dioxide (Fig.1.3.1a). Atenolol (ATN), (2-[4-[(2RS)-2-hydroxy-3-[(1-methylethyl) amino] propoxy] phenyl] acetamide (Fig. 1.3.1b), is a cardioselective β_1 blocker used in the management of hypertension, angina pectoris, cardiac arrhythmias, and myocardial infarction [29]. It may also be used in the prophylactic treatment of migraine [30]. Valsartan (VAL), (S)-N-valeryl-N-([2'-(1H-tetrazol-5-yl)biphenyl-4-yl]-methyl)-valine (Fig. 1.3.1c), and candesartan cilexetil (CND), ± (1-cyclohexyloxycarbonyloxy) ethyl-2-ethoxyl ([20-(1H-tetrazol-5-yl) biphenyl-4-yl]-methyl)-1H-benzimidazole-7-carboxylate (Fig. 1.3.1d), are potent, highly selective, and orally active non peptide antagonist on AT_1-receptor subtype [31]. Angiotensin receptor blockers (ARBs) are a major class of antihypertensive therapies due to their powerful lowering effects on blood pressure and excellent tolerability. Recent clinical trials have shown the added benefits of ARBs in hypertensive patients (reduction in left ventricular hypertrophy, improvement in diastolic function, decrease in ventricular arrhythmias, reduction in microalbuminuria, and improvement in renal function), and cardioprotective effect in patients with heart failure [32]. Moexipril hydrochloride (MXP), (3S)-2-[(2S)-2-{[(1S)-1-(ethoxycarbonyl)-3-phenyl-propyl]amino}-1-oxopropyl]-6,7-dimethoxy-1,2,3,4-tetrahydroisoquinoline-3-carboxylic acid hydrochloride (Fig. 1.3.1e), is a new potent orally active non-sulfhydryl angiotensin-converting enzyme (ACE) inhibitor for the treatment of hypertension and congestive heart failure [33]. Aliskiren

hemifumarate (ALS), (2(S), 4(S), 5(S), 7(S)-*N*-(2-carbamoyl- 2- methylpropyl) -5-amino-4-hydroxy 2,7 diisopropyl-8-[4-methoxy-3-(3-methoxypropoxy) phenyl] octanamide hemifumarate) (Fig 1.3.1f) is the first direct renin inhibitor suitable for oral administration. By achieving more complete renin–angiotensin system inhibition, direct renin inhibitors may afford greater protection from hypertensive complications [34]. Present evidence indicates that ALS reduces baseline systolic and diastolic blood pressure and that it is as effective as other first-line antihypertensive agents. Extra advantages can be reached when it is used in combination therapy [34]. Amlodipine besylate (AML), (3-Ethyl 5-methyl (4RS)-2-[(2-aminoethoxy)methyl]-4-(2-chlorophenyl)-6-methyl-1,4-dihydropyridine-3,5-dicarboxylate benzenesulphonate) (Fig. 1.3.1g) is a long acting dihydropyridine calcium channel blocker that prevents the transmembrane influx of calcium ions into vascular smooth muscles and cardiac muscles [35]. Also, it is a direct peripheral arterial vasodilator that reduces peripheral vascular resistance and hence lowers blood pressure [36]. Binary combination therapies of HCZ with each of ATN [37], MXP [38] and CND [39] induce significant reductions in systolic and diastolic BP from in patients with mild to severe hypertension. Also, triple combination therapies of ALS, AML and HCZ [40] as well as VAL, AML and HCZ [41] proved to be effective and well tolerated in treatment of hypertensive high-risk patients. So, it is necessary to develop a validated analytical method for assay of the cited drugs in combination with HCZ in their pharmaceutical preparations. Literature review revealed some published methods for simultaneous determination of one or more of the studied drugs in combination with HCZ using different analytical techniques such as LC-UV: ATN [42-44], VAL [45-52], MXP [53, 54], ALS [51, 55-58], AML [48, 50, 52, 55, 56, 58], CND [49, 59-62], LC/MS/MS: ATN [63], VAL [63, 64], CND [65], UV-spectrometry: ATN [44, 66, 67], VAL [44, 68, 69], MXP [70], ALS [71], AML [66, 68, 69], CND [72, 73] and CE: ATN [74], VAL [75], ALS [76], CND [75]. To the best of our knowledge there is no method was

developed to separate the cited seven drugs. Thus, the aim of this method was to develop and validate an analytical method using the most preferable RP-LC technique for the simultaneous determination of the well-known diuretic HCZ, along with commonly prescribed antihypertensive drugs from different pharmacological classes as mentioned before, namely; ATN, VAL, MXP, ALS, AML and CND. Irbesartan (Fig. 1.3.1h) was used as an internal standard in this method. This method is characterized by simplicity, accuracy, preciseness besides its wide range of applications as it can be used for routine analysis and quality control of the cited drugs separately or in combinations in more than 17 combined therapies, (Table 1.3.1). Also, this method is able to separate the seven analytes along with IS in a short run time of about 12 minutes in agreement with system suitability parameters.

1.3.2 Experimental

1.3.2.1 Materials and reagents

All the chemicals used were of analytical reagent grade, and the solvents were of HPLC grade. HCZ (certified to contain 99.93%) and CND ((certified to contain 99.95%) were supplied by AstraZeneca - Cairo - Egypt. Pharmaceutical grade VAL USP was supplied by Zydus, batch No.: VSK1MK A02B (certified to contain 99.40%). ALS (certified to contain 99.51%) was supplied by Novartis Pharmaceuticals Corporation East, New Jersey, USA, 07936. AML (certified to contain 99.75%) was kindly supplied by Global Nabi Co., (Giza -Egypt). ATN (certified to contain >98%), MXP (certified to contain >98%), sodium 1-heptanesulphonate and acetonitrile were obtained from (Sigma-Aldrich, MO, U.S.A). Amturnide® 300-10-25 mg tablets; batch # NDC 0078-0614-15 (Novartis Pharmaceuticals Corporation East, New Jersey, USA 07936) each labeled to contain 332 mg ALS, 13.9 mg AML and 25 mg HCZ, Exforge

HCT® 160/10/12.5 mg tablets; batch # NDC 0078-0614-15 (Novartis Pharmaceuticals Corporation, East Hanover, NJ, 07936 USA) each labeled to contain 160 mg VAL, 13.9 mg AML and 12.5 mg HCZ, Uniretic® 15/12.5 mg tablets; batch # NDC 68462-0206-01 (SCHWARZ PHARMA, LLC a subsidiary of UCB, Inc. Smyrna, GA 30080, USA) each labeled to contain 15 mg MXP and 12.5 mg HCZ, and Atacand HCT® 16/12.5 mg tablets; batch # NDC 60505-3758-09 (AstraZeneca - Cairo, - Egypt) each labeled to contain 16 mg CND and 12.5 mg HCZ were purchased from commercial sources in the local market. Sodium hydroxide, sodium phosphate dibasic and *o*-phosphoric acid 85% (Fisher Scientific, NJ, USA) were used.

1.3.2.2 Instrumentation

Separations were performed using Agilent HPLC system 1200 chromatograph (USA) equipped quaternary pump G1311A and with a Rheodyne injector valve with a 20 µL loop and a G1315D MWD detector. Mobile phases were degassed using G1322A solvent degasser. Agilent chemstation for LC systems [Rev.B.03.01-SR1 (317)] PC program was used for the instrument control, data analysis and acquisition. Separation and quantitation were made on Agilent Eclipse XDB-C18 (4.6 x 150mm, 5 µm) column. A SympHonly (SB20) pH-meter (Thermo Orion Beverly, MA, U.S.A) was used for pH measurements. Deionized water was prepared using a Barnstead NANO pure DIamond Analytical (USA) ultrapure water system. The mobile phase was filtered through 0.2 µm Anatop 25 Whatman inorganic membrane filter (Maidstone, England) and degassed using Branson Ultrasonic 5510 degasser (Danbury, CT, U.S.A).

1.3.2.3 Chromatographic conditions

A mixture of sol-A: sodium phosphate dibasic buffer (pH 5±0.1, 0.02M): sol-B: acetonitrile in gradient elution mode (0-3 min. sol-A: 95-65; 3-6 min. sol-A: 65-65; 6-10 min. sol-A: 65-20; 10-15 min. sol-A: 20-95) was used. Flow rate was maintained at 1 mL min^{-1}. All

determinations were performed at ambient temperature. The system was equilibrated and saturated with the mobile phase for 30 min before the injection of the solutions. Quantification was achieved with UV detection at 220 nm based on peak area. Twenty μL of the solutions were injected with a 50 μl Agilent analytical syringe in triplicates.

1.3.2.4 Standard stock solutions preparation

10 mg of each of MXP and IS as well as 20 mg of each of HCZ, ATN, VAL, ALS, AML and CND were accurately weighed and transferred in to 10 mL volumetric flasks separately. Then, they were dissolved in a solvent composed of acetonitrile and water (50:50, v/v) and the solutions were made up to volume with the same solvent to give final concentrations of 1000 μg mL^{-1} of MXP and IS as well as 2000 μg mL^{-1} for HCZ, ATN, VAL, ALS, AML and CND. Further dilutions were made to prepare 200 μg mL^{-1} of HCZ, AML and CND in the same diluent.

1.3.2.5 Procedure

1.3.2.5.1 Construction of calibration graphs

Accurate aliquots of HCZ, ATN, VAL, MXP, ALS, AML and CND from the suitable stock solutions were transferred into a series of 10 mL Fisherbrand disposable tubes so that the final concentrations were in the range of 2–40 μg mL^{-1} for HCZ and CND as well as 20–200, 10-160, 5-40, 20-250 and 5-50 μg mL^{-1} for ATN, VAL, MXP, ALS and AML, respectively. A constant 80 μL IS stock solution was added and the volume was diluted to 4 mL with a solvent composed of acetonitrile and phosphate buffer (50:50, v/v). Each solution (n=5) was injected in triplicates and chromatographed under the described chromatographic conditions. The peak area ratio (peak area of the studied drug/ peak area of IS) was plotted versus the concentration of each drug in μg mL^{-1} to get the calibration graphs and the corresponding regression equations were derived.

1.3.2.5.2 Preparation of the laboratory prepared mixtures

Accurate aliquots of ATN, VAL, MXP and ALS stock solutions as well as HCZ, AML and CND working solutions were transferred into a series of 10 mL Fisherbrand disposable tubes keeping the pharmaceutical ratios of 1:1.8:23.9 for AML/HCZ/ALS, 1:1.1:12.8 for HCZ/AML/VAL, 1:1.2 for HCZ/MXP, 1:4 for HCZ/ATN and 1:1.28 for HCZ/CND mixtures, diluted to 4 mL with a solvent composed of acetonitrile and phosphate buffer (50:50, v/v) after addition of 80µL IS and mixed well. The percentage recoveries were calculated using the corresponding regression equations.

1.3.2.5.3 Samples preparation

A composite of ten tablets of Amturnide®, Exforge HCT®, Uniretic®, and Atacand HCT® tablets were ground to fine and uniform size powder (after removing the coat from the first three dosage forms by rubbing with a tissue moistened with methanol). Then, they were triturated using mortar and pestle. After calculating the average tablet weight, amounts of powder equivalent to (5.00, 64.00, 6.00, 66.40 and 6.40 mg) for HCZ, VAL, MXP, ALS and CND, respectively, as well as 2.78 and 5.50 mg for AML in Amturnide® and Exforge HCT®, respectively, of each type of tablets were accurately weighed and transferred separately in to 25 ml volumetric flasks and completed to volume with a solvent composed of acetonitrile and water (50:50, v/v). The solutions were sonicated for 30 min then filtered through a Whatman filter paper and then filtered again using 0.2µm Whatman inorganic membrane filter. For analysis, different aliquots from the prepared sample solution, spiked with 80 µL IS stock solution, were diluted to 4 mL using a solvent composed of acetonitrile and phosphate buffer (50:50, v/v). The percentage recoveries were calculated by referring to the corresponding regression equations.

1.3.3 Results and discussion

The aim of this method was to develop and validate a simple and fast RP-LC method for the simultaneous determination of HCZ, along with commonly prescribed antihypertensive drugs from different pharmacological classes as mentioned before. The proposed method permitted the separation of the seven drugs in a reasonable run time less than 12 min. (Fig. 1.3.2), shows a typical chromatogram for a synthetic mixture of the seven drugs under the described chromatographic conditions. It also permitted the quantification of the drugs in their laboratory prepared mixtures and co-formulated tablets.

1.3.3.1 Optimization of chromatographic conditions

Several trials were carried out to obtain a simple, rapid, accurate, precise and reliable LC method for the simultaneous determination of the seven antihypertensive drugs with low cost and available accessories such as column and detector used. Different columns with different length and internal diameter were tried and a satisfactory separation was obtained on Agilent Eclipse XDB-C18 (4.6 x 150 mm, 5 µm) column. Isocratic mode of elution was tried and it was found that it is difficult to be used with such number of analytes as many compounds will overlap together so gradient elution mode was attempted. Methanol and acetonitrile were examined as organic modifiers and acetonitrile was found to be more suitable as it allowed appropriate separation of the seven analytes. The use of buffer was necessary in this method in order to keep the pH constant as ATN elution is affected by the mobile phase composition, pH and by the properties of the combined analytes, (Fig. 1.3.3 and 1.3.4). Different gradient elution modes were tested in order to achieve proper separation of the cited analytes in a reasonable run time, (Fig. 1.3.5). The described gradient elution mode (0-3 min. sol-A: 95-65; 3-6 min. sol-A: 65-65; 6-10 min. sol-A: 65-20; 10-15 min. sol-A: 20-95) was selected. Then, the effect of pH on the

separation of the analytes was studied. It was found that pH lower than 5.5 and higher than 7.5 were not suitable as shown in (Fig. 1.3.3) as it results in poor separation of the analyzed compounds. pH 5.5 was finally selected as it achieved the best separation between the seven analytes in a reasonable run time (<12min) and with good resolution between all peaks especially between HCZ and VAL, (Fig. 1.3.3). Different flow rates were studied and flow rate of 1 mL min^{-1} was found to be the optimum. Proper choice of the detection wavelength is crucial for sensitivity of the method. Quantitation was achieved with UV-detection at 220 nm based on satisfactory peak area for each of the analyzed drugs especially for HCZ, (Fig. 1.3.6). Many trials were done to enhance symmetry and sharpness of peaks and hence improve the resolution of the cited drugs. Increasing the ionic strength of phosphate buffer up to 60mM as well as addition of 0.25mM heptane 1-sulphonate, as ion pairing agent, did not produce significant improvement. The analytes were first dissolved in a solvent composed of acetonitrile and water (50:50, v/v). This solvent allowed proper dissolution for the analyzed compounds as ALS and ATN are sparingly soluble in acetonitrile while VAL and HCZ are sparingly soluble in water. Then aliquots withdrawn were completed to volumes with a solvent composed of acetonitrile and phosphate buffer (50:50, v/v) which successfully achieved significant enhancement in peaks symmetry as well as sharpness of peaks and hence improved the resolution between the studied analytes, (Fig. 1.3.2). The use of IS is recommended to compensate for injection errors, minor fluctuations effect of the retention time and to improve the quantitative analysis. Irbesartan was chosen as the IS in this study IS and itself is another antihypertensive drug belonging to ARBs so it can be determined selectively using this developed method. The retention times for ATN, HCZ, VAL, MXP, ALS, AML, CND and IS were 3.37, 4.62, 5.36, 6.49, 7.33, 8.59, 11.25 and 7.79 min, respectively.

1.3.3.2 Validation of the method

Validation of the proposed CZE method was performed according to ICH guidelines [http://www.ich.org/fileadmin/Public_Web_Site/ICH_Products/Guidelines/Quality/Q2_R1/Step4/Q2_R1__Guideline.pdf] with respect to stability, linearity, range, specificity, limit of detection (LOD), limit of quantitation (LOQ), accuracy, precision and robustness.

1.3.3.2.1 Linearity

A linear relationship was established by plotting the peak area ratio (the studied drug peak area/IS peak area) against the corresponding drug concentration in the range of 2–40 µg mL^{-1} for HCZ and CND as well as 20–200, 10-160, 5-40, 20-250 and 5-50 µg mL^{-1} for ATN, VAL, MXP, ALS and AML, respectively. Statistical analysis of the data gave high value for the correlation coefficient (R^2) of the regression equation, small values of the standard deviation of residuals ($S_{y/x}$), of intercept (S_a), and of slope (S_b), as well as small value of the percentage relative standard deviation and % Error, (Table 1.3.2). These data indicate the linearity of the calibration graphs.

1.3.3.2.2 Limit of quantitation (LOQ) and limit of detection (LOD)

LOD was considered as the minimum concentration with a signal to noise ratio of at least three (S/N˜3), while LOQ was taken as a minimum concentration with a signal to noise ratio of at least ten (S/N˜10). Results are given in (Table 1.3.2).

1.3.3.2.3 Accuracy and precision

The good recovery results obtained from the assay of HCZ, ATN, VAL, MXP, ALS, AML and CND indicate the accuracy of the proposed method, (Table 1.3.3 and 1.3.4). Repeatability (intra-day) and intermediate precision (inter-day) were assessed using three concentrations and three replicates of each concentration. The good relative standard

deviations indicate good precision of the proposed method, (Table 1.3.3).

1.3.3.2.4 Stability

Stability of the standard stock solutions of HCZ, ATN, VAL, MXP, ALS, AML and CND, stored at 2-8 ˚C, were evaluated at various time points over 2 months. The concentrations of freshly prepared solutions and those aged for 2 months were calculated by the method developed and the difference between them was found to be less than 1% for HCZ, AML, VAL and less than 2% for MXP, CND, ALS and ATN. Also, the solutions prepared for analysis were found to be stable for at least 3 days at 2-8 °C and for a day at room temperature. These solutions can therefore be used during this interval of time without the results being affected.

1.3.3.2.5 Specificity

The specificity of the method was investigated by observing any interference encountered from common tablet excipients and it was confirmed that the signals measured was caused only by the analytes. The inactive ingredients in the four analyzed dosage forms were: colloidal anhydrous silicon dioxide, crospovidone, hypromellose, magnesium stearate, carboxymethylcellulose calcium, hydroxypropyl cellulose, corn starch, povidone, talc, titanium dioxide, hypromellose, macrogol 4000, polyethylene glycol 6000, lactose, magnesium oxide, gelatin, iron oxide red, iron oxide yellow and iron oxide black. Also, ATN and HCZ were analyzed in their in-house prepared formulation with some of the common excipients such as anhydrous silica, magnesium stearate, microcrystalline cellulose, lactose, polyethylene glycol and talc, (Fig. 1.3.8). It was found that the excipients did not interfere with the results of the proposed method, (Table 1.3.5). As shown in (Fig. 1.3.8) the chromatograms of the combined formulations did not show any additional peaks when compared to the chromatograms of their laboratory prepared mixtures which confirms the specificity of the developed method, (Fig.

1.3.7).

1.3.3.2.6 Robustness

Minor deliberate changes in different experimental parameters such as flow rate (±0.2 mL min^{-1}) and pH (±0.1) did not significantly affect resolution of the analyzed compounds indicating that the proposed method is robust, (Table 1.3.6).

1.3.3.2.7 System suitability testing

The results of the system suitability tests assure the adequacy of the proposed RP-LC method for routine analysis of the seven investigated analytes, (Table 1.3.7). The values of the capacity factor (k) indicate that all peaks are well resolved with respect to the void volume. The values of % RSD of six consecutive injections performed for each analyte show good injection repeatability. The tailing factors (T) reflect good peak symmetry. The values for resolution (Rs) indicate good separation of the investigated analytes. The theoretical plate numbers (N) demonstrate good column efficiency.

1.3.3.3 Application of the proposed method for the analysis of HCZ in combination with one or more of either ATN, VAL, MXP, ALS, AML and CND in their laboratory prepared mixtures and combined formulations

The proposed RP-LC method was applied to the simultaneous determination of HCZ with one or more of the other antihypertensive drugs in their laboratory prepared mixtures in the medicinally recommended ratios of 1:1.8:23.9 for AML/HCZ/ALS, 1:1.1:12.8 for HCZ/AML/VAL, 1:1.2 for HCZ/MXP, 1:4 for HCZ/ATN and 1:1.28 for HCZ/CND mixtures, (Fig. 1.3.7). Furthermore, the proposed method was successfully applied for their determination in co-formulated tablets, (Fig. 1.3.8).

1.3.3.4 Comparison methods and statistical analysis

The results shown in Table 1.3.5 for the analysis of the cited medications in their combined formulations are in good agreement with those obtained using the reported methods for each combination. The reported method for simultaneous determination of HCZ, AML and ALS ternary mixture was based on an ion pairing RP-LC-UV technique using acetonitrile: 25 mM octane sulphonic acid sodium salt monohydrate in water (60: 40, v/v) as the mobile phase [58], whereas the proposed method is more conventional for analysis of that mixture. Regarding the reported method for simultaneous determination of HCZ, AML and VAL, it was based also on a RP-LC technique using acetonitrile, methanol and 50 mM phosphate buffer adjusted to pH 3 with orthophosphoric acid as the mobile phase in the ratio of (20: 50: 30, v/v) and the eluents were monitored at 239 nm [52]. On the other hand, Erturk et al. reported a RP-LC method for simultaneous determination of HCZ and MXP in tablets which was performed using a mobile phase consisting of acetonitrile and phosphate buffer (pH 4) (50: 50, v/v) [53]. Also for HCZ and ATN simultaneous determination in tablets, Zaveri et al. reported a RP-LC method for analysis of that mixture using a mobile phase consisting of water: phosphate buffer: methanol (50:35:15, v/v) [42]. Finally, Qutab et al. reported a RP-LC method for simultaneous determination of HCZ and CND in their combined formulation and they used phosphate buffer (pH 6), methanol and triethylamine (25:75:0.2, v/v) as the mobile phase [62]. The newly developed method is reliable, simple, rapid and selective in comparison to all of the reported methods for determination of the selected drug combinations in their pharmaceutical dosage forms. Statistical analysis of the results obtained using Student's t-test and variance ratio F-test revealed no significant difference between the performance of the methods regarding the accuracy and precision, respectively.

Table 1.3.1 Examples for some prescribed antihypertensive dosage forms available in the market

Dosage form	Active ingredients
Amturnide® tablets	ALS, AML and HCZ
Exforge HCT® tablets	VAL, AML and HCZ
Ziblok-H® tablets	ATN and HCZ
Diovan HCT® tablets	VAL and HCT
Uniretic® tablets	MXP and HCZ
TeKturna® tablets	ALS and HCZ
Atacand HCT® tablets	CND and HCZ
Amlokind-AT® tablets	ATN and AML
Exforge® tablets	VAL and AML
Tekamlo® tablets	ALS and AML
Tenormin® tablets	ATN
Aquazide® tablets	HCZ
Diovan® tablets	VAL
Univasc® tablets	MXP
Tekturna® tablets	ALS
Norvasc® tablets	AML
Atacand® tablets	CND

Table 1.3.2 Characteristics and results of the proposed RP-LC method

Item	**HCZ**	**ATN**	**VAL**	**MXP**	**ALS**	**AML**	**CND**
Linearity range (µg mL^{-1})	2-40	20-120	10-160	5-40	20-250	5-50	2-40
LOD (µg mL^{-1})	0.34	4.86	3.22	0.41	4.06	1.35	0.23
LOQ (µg mL^{-1})	1.02	14.72	9.75	1.26	12.31	4.09	0.71
Intercept (a)	0.0552	-0.0139	0.6631	0.0094	0.0628	-0.0038	0.0077
Slope (b)	0.0614	0.0043	0.0395	0.0315	0.0101	0.0201	0.0509
Correlation coefficient (R^2)	0.9999	0.9996	0.9998	0.9999	0.9999	0.9997	1.000
S.D. of residuals (Sy/x)	0.0093	0.0067	0.0545	0.0046	0.0161	0.0105	0.0053
S.D. of intercept (Sa)	0.0063	0.0063	0.0385	0.0040	0.0124	0.0082	0.0036
S.D. of slope (Sb)	0.0003	0.0001	0.0004	0.0002	0.0001	0.0003	0.0002
% Error	1.33	1.57	1.01	0.73	0.69	1.19	2.18
%RSD	2.99	3.54	2.24	1.63	1.55	2.64	0.97
Accuracy	99.39	99.28	100.41	99.70	99.64	100.92	99.53

Table 1.3.3 Accuracy and precision results for the proposed RP-LC method

Conc. of HCZ (μg mL^{-1})	Intra-day assay Recovery % ± %RSD[a]	Inter-day assay Recovery % ± %RSD[a]	Conc. of ALS (μg mL^{-1})	Intra-day assay Recovery % ± %RSD[a]	Inter-day assay Recovery % ± %RSD[a]
15.00	99.37 ± 1.79	101.63 ± 1.96	143.00	100.62 ± 0.66	100.41 ± 0.25
20.00	98.51 ± 1.48	100.15 ± 1.68	191.00	101.58 ± 0.95	100.80 ± 0.77
25.00	100.60 ± 0.92	100.77 ± 0.58	215.00	100.26 ± 1.23	99.56 ± 0.66
Mean	99.49 ± 1.06	100.85 ± 0.74	Mean	100.82 ± 0.68	100.26 ± 0.63
Conc. of ATN (μg mL^{-1})	Intra-day assay Recovery % ± %RSD[a]	Inter-day assay Recovery % ± %RSD[a]	Conc. of AML (μg mL^{-1})	Intra-day assay Recovery % ± %RSD[a]	Inter-day assay Recovery % ± %RSD[a]
60.00	99.32 ± 1.19	99.44 ± 0.81	8.25	101.13 ± 1.79	100.53 ± 2.16
80.00	99.00 ± 1.62	98.71 ± 0.45	11.00	100.72 ± 0.45	100.72 ± 1.80
100.00	98.50 ± 1.92	99.90 ± 1.40	13.75	99.88 ± 0.42	100.36 ± 2.05
Mean	98.94 ± 0.42	99.35 ± 0.60	Mean	100.58 ± 0.63	100.54 ± 0.18
Conc. of VAL (μg mL^{-1})	Intra-day assay Recovery % ± %RSD[a]	Inter-day assay Recovery % ± %RSD[a]	Conc. of CND (μg mL^{-1})	Intra-day assay Recovery % ± %RSD[a]	Inter-day assay Recovery % ± %RSD[a]
96.00	99.33 ± 1.29	99.33 ± 2.72	6.40	100.68 ± 1.23	99.45 ± 1.17
128.00	100.72 ± 1.21	100.42 ± 1.58	19.20	100.89 ± 0.86	100.31 ± 0.67
160.00	101.01 ± 1.12	101.39 ± 0.59	32.00	101.22 ± 0.14	100.75 ± 0.43
Mean	100.35 ± 0.89	100.38 ± 1.03	Mean	100.93 ± 0.27	100.17 ± 0.66
Conc. of MXP (μg mL^{-1})	Intra-day assay Recovery % ± %RSD[a]	Inter-day assay Recovery % ± %RSD[a]			
18.00	98.82 ± 1.41	97.18 ± 1.53			
24.00	97.45 ± 1.56	99.40 ± 1.96			
30.00	97.56 ± 1.51	98.86 ± 1.10			
Mean	97.94 ± 0.78	98.48 ± 1.18			

[a] Mean and relative standard deviation of three determinations

Table 1.3.4 Assay and statistical results for the determination of the studied drugs in their laboratory prepared mixtures by the proposed method and comparison methods

(HCZ:AML:ALS) (1.8:1:23.9)	HCZ		AML		ALS	
	The developed RP-LC method	Comparison method [31]	The developed RP-LC method	Comparison method [31]	The developed RP-LC method	Comparison method [31]
Mean recovery% ± S.D.	100.45±2.15	100.23±1.49	99.54±2.12	98.41± 0.88	101.05±1.45	100.09±1.99
Student *t* test (2.78)*	0.14		1.36		0.68	
F value (19)*	1.01		5.82		1.88	

(HCZ:AML:VAL) (1:1.1:12.8)	HCZ		AML		VAL	
	The developed RP-LC method	Comparison method [25]	The developed RP-LC method	Comparison method [25]	The developed RP-LC method	Comparison method [25]
Mean recovery% ± S.D.	99.94±1.67	99.52±1.91	99.66±0.53	100.66± 0.74	98.47±1.21	99.74± 1.53
Student *t* test (2.78)*	0.38		1.20		0.34	
F value (19)*	3.38		6.45		1.26	

(HCZ:MXP) (1:1.2)	HCZ		MXP	
	The developed RP-LC method	Comparison method [26]	The developed RP-LC method	Comparison method [26]
Mean recovery% ± S.D.	98.47±0.84	100.43±0.66	100.21±2.00	100.13 ± 1.72
Student *t* test (2.78)*	3.18		0.05	
F value (19)*	1.64		1.36	

(HCZ:ATN) (1:4)	HCZ		ATN	
	The developed RP-LC method	Comparison method [15]	The developed RP-LC method	Comparison method [15]
Mean recovery% ± S.D.	99.89±1.48	98.94±2.26	98.76±1.48	100.27± 1.14
Student *t* test (2.78)*	0.61		1.41	
F value (19)*	2.35		1.69	

(HCZ:CND) (1:1.28)	HCZ		CND	
	The developed RP-LC method	Comparison method [35]	The developed RP-LC method	Comparison method [35]
Mean recovery% ± S.D.	100.45±1.19	99.49±1.31	100.31±0.67	99.80± 0.40
Student *t* test (2.78)*	0.94		1.13	
F value (19)*	1.21		2.70	

Each result is the average of three separate determinations.
The values between parentheses are the tabulated t and F values at $P = 0.05$.

Table 1.3.5 Assay results for the determination of the studied drugs in their co-formulations

Amturnide® 300-10-25mg tablets (HCZ:AML:ALS) (1.8:1:23.9)	HCZ		AML		ALS	
	Proposed method	Comparison method [31]	Proposed method	Comparison method [31]	Proposed method	Comparison method [31]
Mean recovery% ± S.D.	97.70 ± 1.42	99.43 ± 1.58	101.37 ± 1.21	99.50 ± 1.99	100.89±1.34	99.78 ± 1.83
Student *t* test (2.78)*	1.42		1.39		0.85	
F value (19)*	1.24		2.71		1.86	
Exforge HCT® 160/10/12.5mg tablets (HCZ:AML:VAL) (1:1.1:12.8)	HCZ		AML		VAL	
	Proposed method	Comparison method [25]	Proposed method	Comparison method [25]	Proposed method	Comparison method [25]
Mean recovery% ± S.D.	98.59 ± 0.7	99.75 ± 2.00	101.80 ± 1.64	99.82 ± 1.38	98.80±1.08	99.78 ± 1.01
Student *t* test (2.78)*	1.85		1.19		1.32	
F value (19)*	1.06		1.79		1.44	
Uniretic® 100/25mg tablets (HCZ:MXP) (1:1.2)	HCZ		MXP			
	Proposed method	Comparison method [26]	Proposed method	Comparison method [26]		
Mean recovery% ± S.D.	97.59 ± 1.15	101.60 ± 1.07	98.01 ± 2.25	99.20 ± 1.06		
Student *t* test (2.78)*	1.55		0.82			
F value (19)*	1.09		4.09			
In house formulation (HCZ:ATN) (1:4)	HCZ		ATN			
	Proposed method	Comparison method [15]	Proposed method	Comparison method [15]		
Mean recovery% ± S.D.	98.82 ± 1.11	100.51 ± 1.11	98.42 ± 0.67	98.88 ± 1.56		
Student *t* test (2.78)*	1.86		0.47			
F value (19)*	2.79		5.51			
Atacand HCT® 16/12.5mg tablets (HCZ:CND) (1:1.28)	HCZ		CND			
	Proposed method	Comparison method [35]	Proposed method	Comparison method [35]		
Mean recovery% ± S.D.	98.17±1.74	101.39 ± 0.76	100.54±1.99	100.63 ± 1.12		
Student *t* test (2.78)*	1.79		021			
F value (19)*	1.75		6.82			

Each result is the average of three determinations and values between parentheses are the tabulated t and F values at $P = 0.05$.

Table 1.3.6 Results of the robustness Study for the proposed RP-LC method

Parameter	Drug	Standard Method	Flow rate (mL min^{-1})		pH	
			0.8	1.2	5.4	5.6
Retention time (min)	ATN	3.4	4.1	2.9	3.3	3.4
	HCZ	4.6	5.5	4.0	4.6	4.6
	VAL	5.4	6	4.8	5.6	5.3
	MXP	6.5	7.3	5.7	6.5	6.5
	ALS	7.3	8.0	6.2	7.2	7.4
	IS	7.9	8.9	6.8	8.0	7.8
	AML	8.6	9.3	7.2	8.6	8.7
	CND	11.2	12.0	10.7	11.3	11.1
Resolution	ATN/HCZ	10.2	11.3	9.1	10.9	10.0
	HCZ/VAL	5.4	4.3	5.9	5.5	5.2
	VAL/MXP	7.0	7.5	6.6	6.5	6.7
	MXP/ALS	4.5	5.4	4.9	4.2	4.6
	ALS/IS	2.5	2.9	2.3	3.1	2.0
	IS/AML	4.9	5.2	3.9	4.6	5.4
	AML/CND	22.0	23.5	24	22.3	20.9

Table 1.3.7 System suitability data for the proposed RP-LC method

Item	ATN	HCZ	VAL	MXP	ALS	IS	AML	CND
N	18133	16751	27039	18151	24906	28634	58809	194583
K`	0.94	1.56	1.98	2.60	3.06	3.33	3.77	4.45
Tailing factor (T)	1.56	0.86	1.08	1.05	1.45	1.22	1.44	1.19
%RSD of 6 injections	2.27	2.95	0.25	1.92	1.29	2.32	2.25	2.56
R	10.24	5.38	6.99	4.45	2.47	4.89	21.80	
α	1.37	1.16	1.21	1.13	1.06	1.10	1.31	

(N: number of theoretical plates; K`: capacity factor; R: resolution factor; T: tailing factor; selectivity factor)

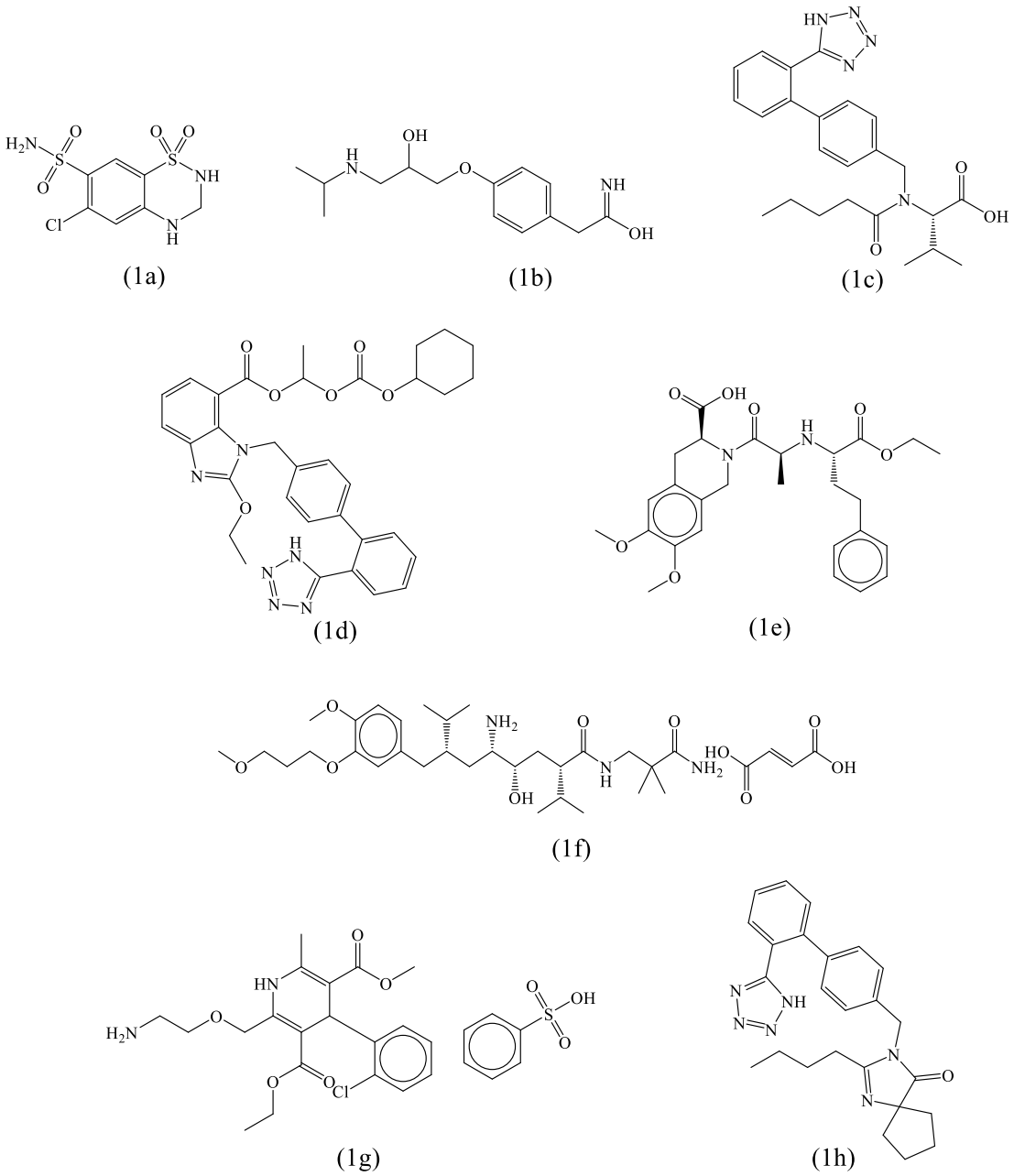

Figure 1.3.1 The structural formulae of the studied medications; (a) hydrochlorothiazide (HCZ), (b) atenolol (ATN), (c) valsartan (VAL), (d) candesartan cilexetil (CND), (e) Moexipril HCl (MXP), (f) aliskiren hemifumarate (ALS), (g) amlodipine besylate (AML), and (h) Irbesartan (IS)

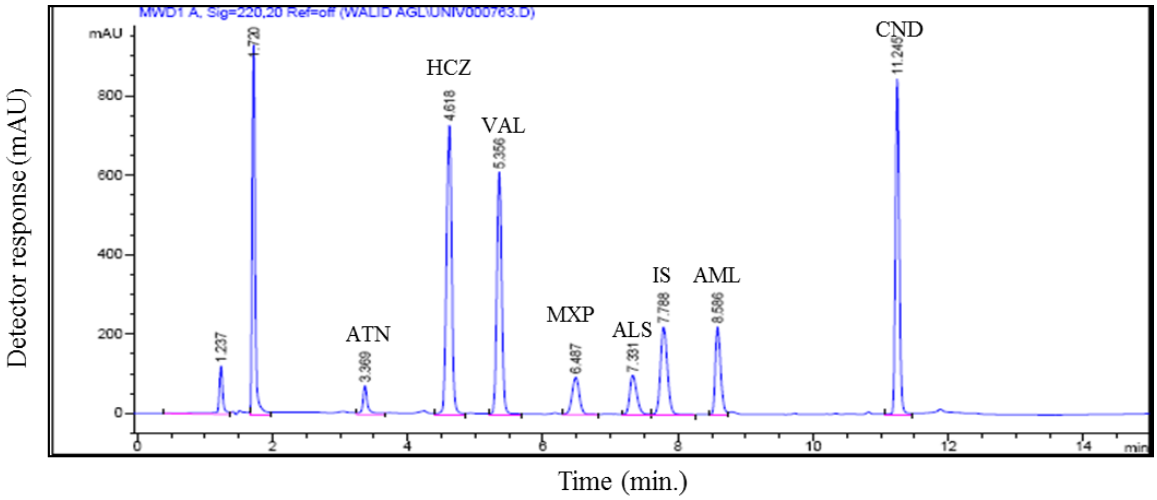

Figure 1.3.2 Typical chromatogram of 80 µg mL^{-1} ATN (3.37 min), 40 µg mL^{-1} for each of HCZ (4.62 min), VAL (5.36 min), MXP (6.49 min), ALS (7.30 min), AML (8.59 min), CND (11.25 min) and IS 20 µg mL^{-1} (7.79 min) under the described chromatographic conditions

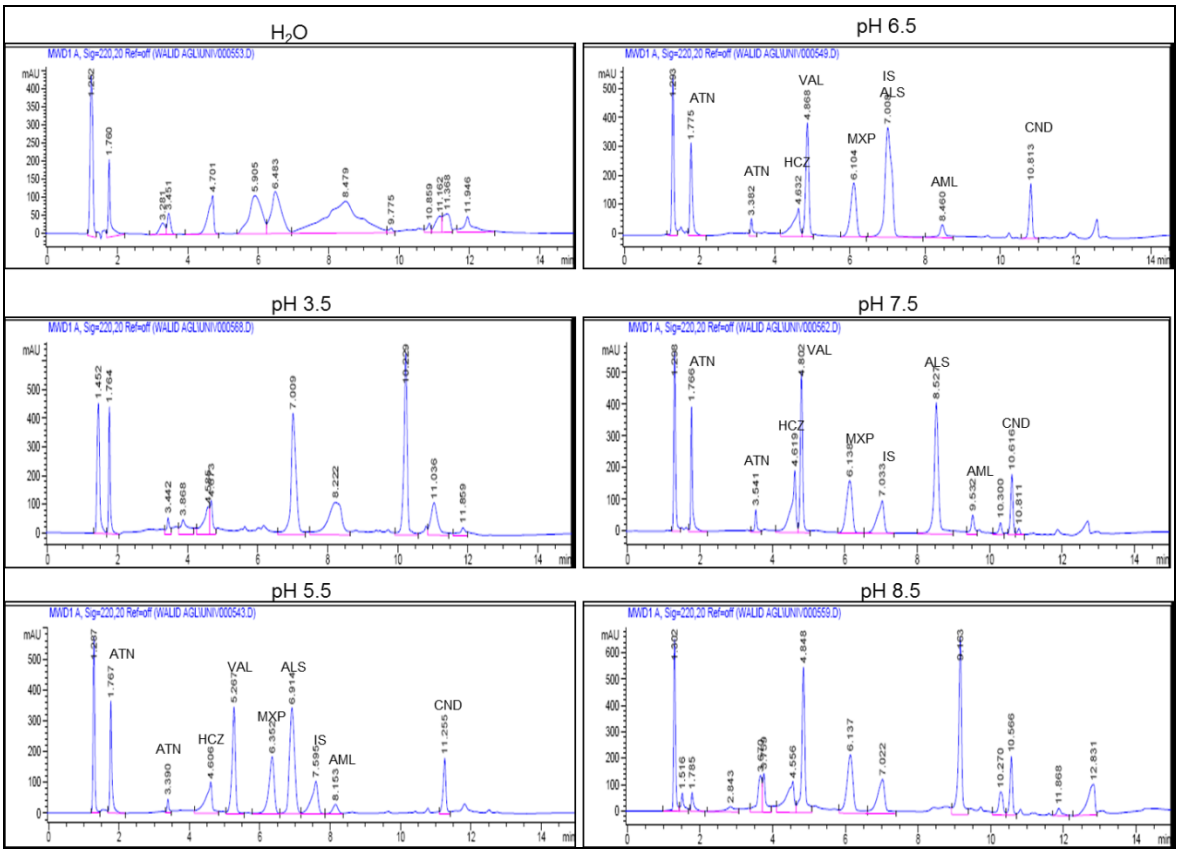

Figure 1.3.3 LC chromatograms of 10.0, 40.0, 128.0, 60.0, 239.0, 11.0, 12.8 and 20.0 µg mL^{-1} of HCZ, ATN, VAL, MXP, ALS, AML, CND and IS, respectively, dissolved in a solvent composed of acetonitrile and water (50:50, v/v) at different pH values of the phosphate buffer using the described chromatographic conditions

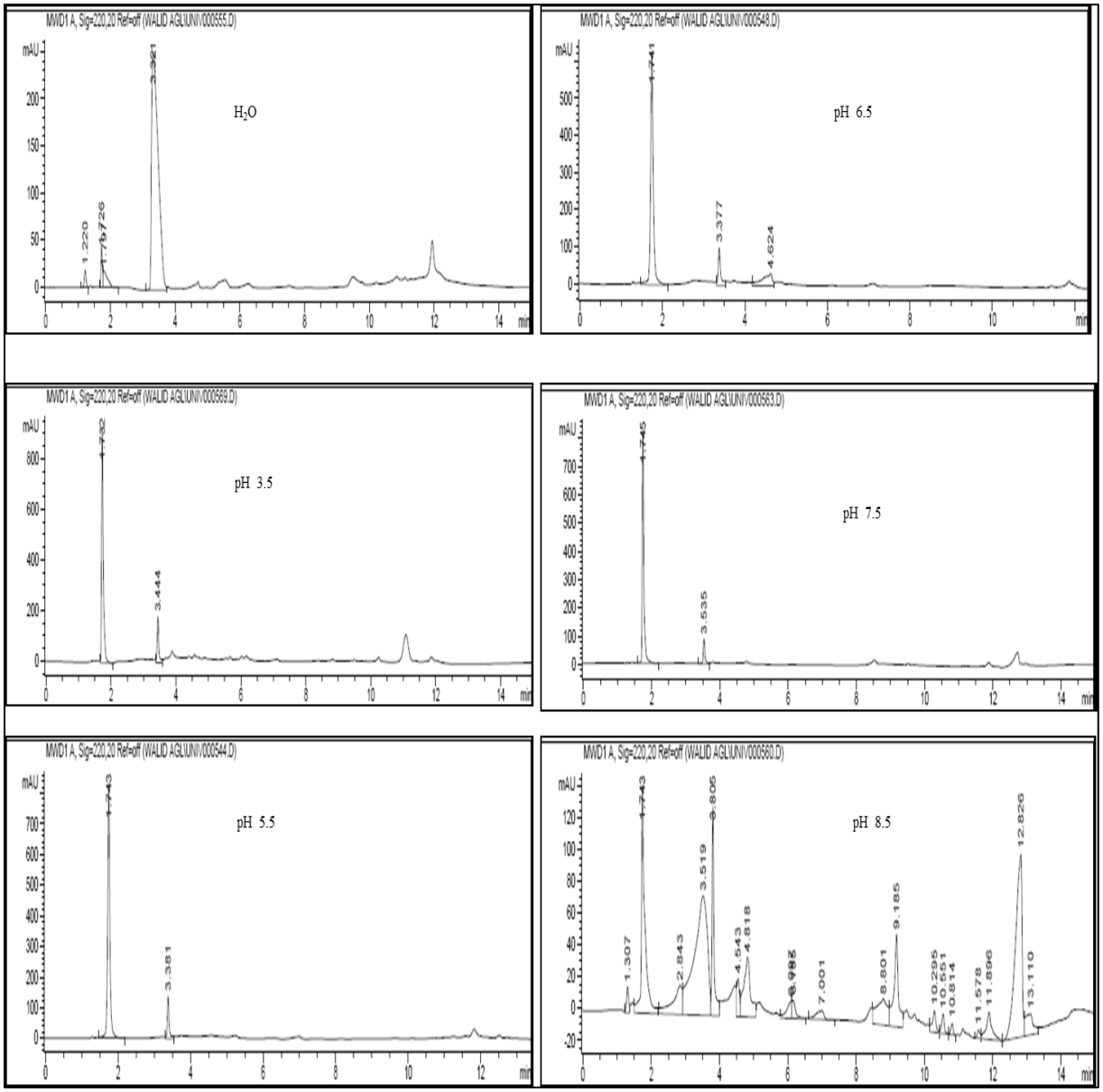

Figure 1.3.4 LC chromatograms of 200µg mL^{-1} ATN dissolved in a solvent composed of acetonitrile and water (50:50 v/v) at different pH values of the phosphate buffer using the described chromatographic conditions

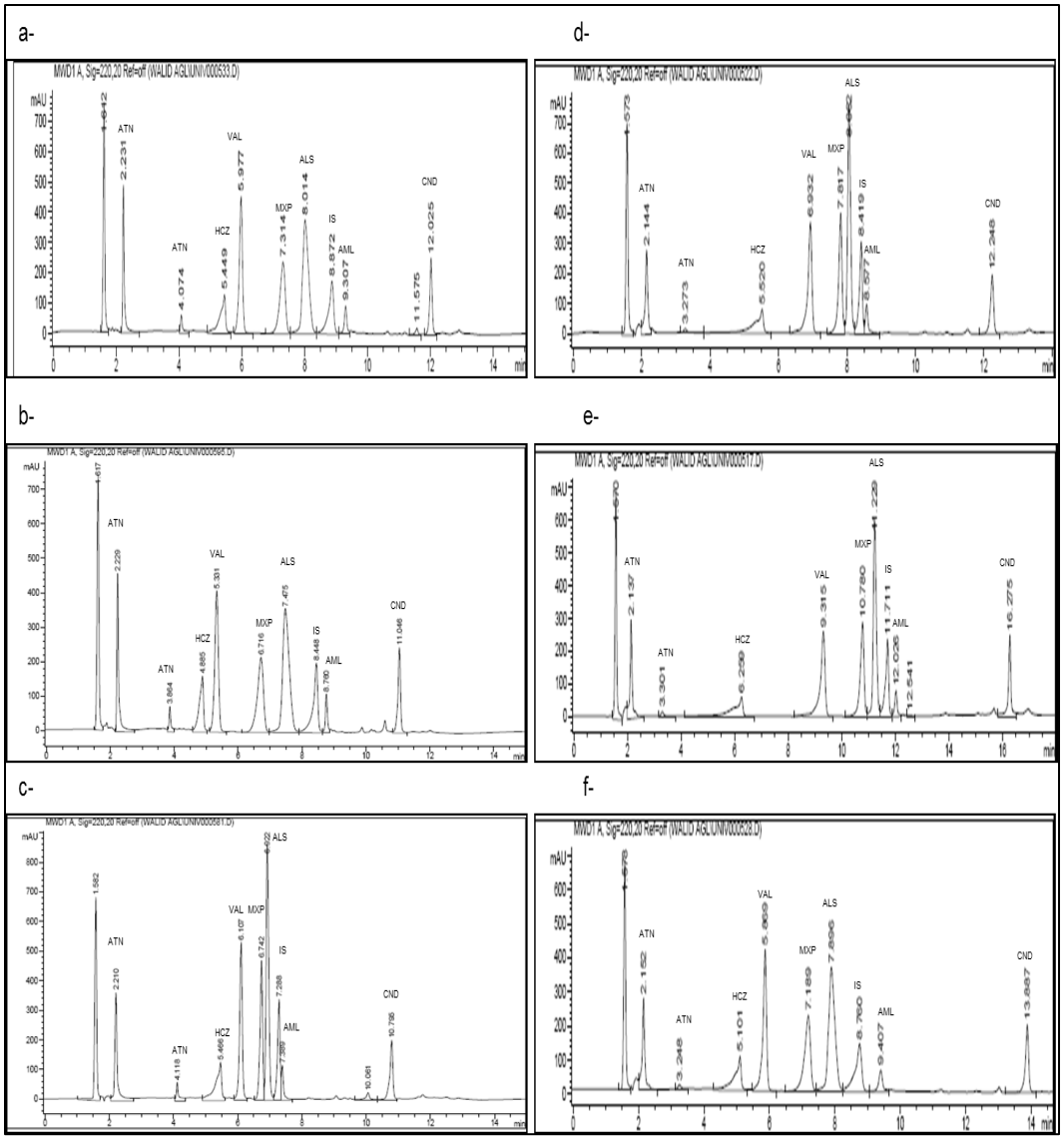

Figure 1.3.5 LC chromatograms using mobile phase consisting of sol-A: phosphate buffer (pH 5.5) and sol-B: acetonitrile at flow rate of 0.8 ml min^{-1} and at λ=220 nm in different gradient modes where (a)- 0-3 min. sol-A: 95-65; 3-6 min. sol-A: 65-65; 6-10 min. sol-A: 65-20; 10-15 min. sol-A: 20-95. (b)- 0-2 min. sol-A: 95-65; 2-5.5 min. sol-A: 65-65; 5.5-8.5 min. sol-A: 65-20; 8.5-15 min. sol-A: 20-95. (c)- 0-3 min. sol-A: 95-65; 3-10 min. sol-A: 65-20; 10-15 min. sol-A: 20-95. (d)- 0-12 min. sol-A: 90-60; 12-16 min. sol-A: 20-90. (e)- 0-12 min. sol-A: 90-50; 12-14 min sol-A: 50-20; 12-18 min. sol-A: 20-90. (f)- 0-3 min. sol-A: 90-65; 3-6 min. sol-A: 65-65; 6-12 min. sol-A: 65-30; 12-16 min. sol-A: 30-90

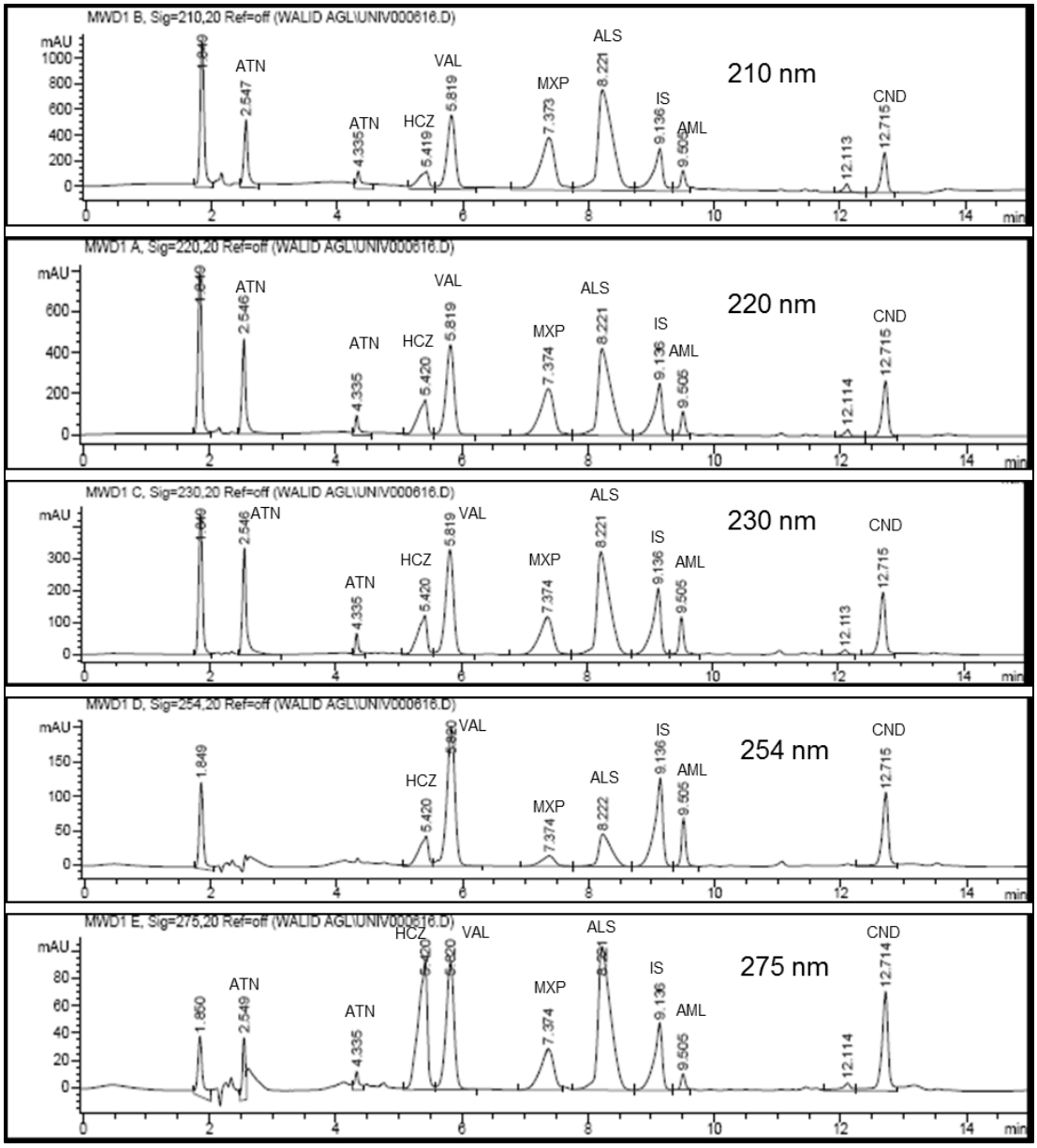

Figure 1.3.6 LC chromatograms of 10.0, 40.0, 128.0, 60.0, 239.0, 11.0, 12.8 and 20.0 µg mL^{-1} of HCZ, ATN, VAL, MXP, ALS, AML, CND and IS, respectively, dissolved in a solvent composed of acetonitrile and water (50:50 v/v) using mobile phase consisting of sol-A: phosphate buffer (pH 5.5) and sol-B: acetonitrile, flow rate of 0.7 ml min^{-1} at variable detection wavelengths where the gradient elution mode was as follow: 0-2 min. sol-A: 95-65; 2-5.5 min. sol-A:65-65; 5.5-10.5 min. sol-A: 65-20; 10.5-15 min. sol-A: 20-95

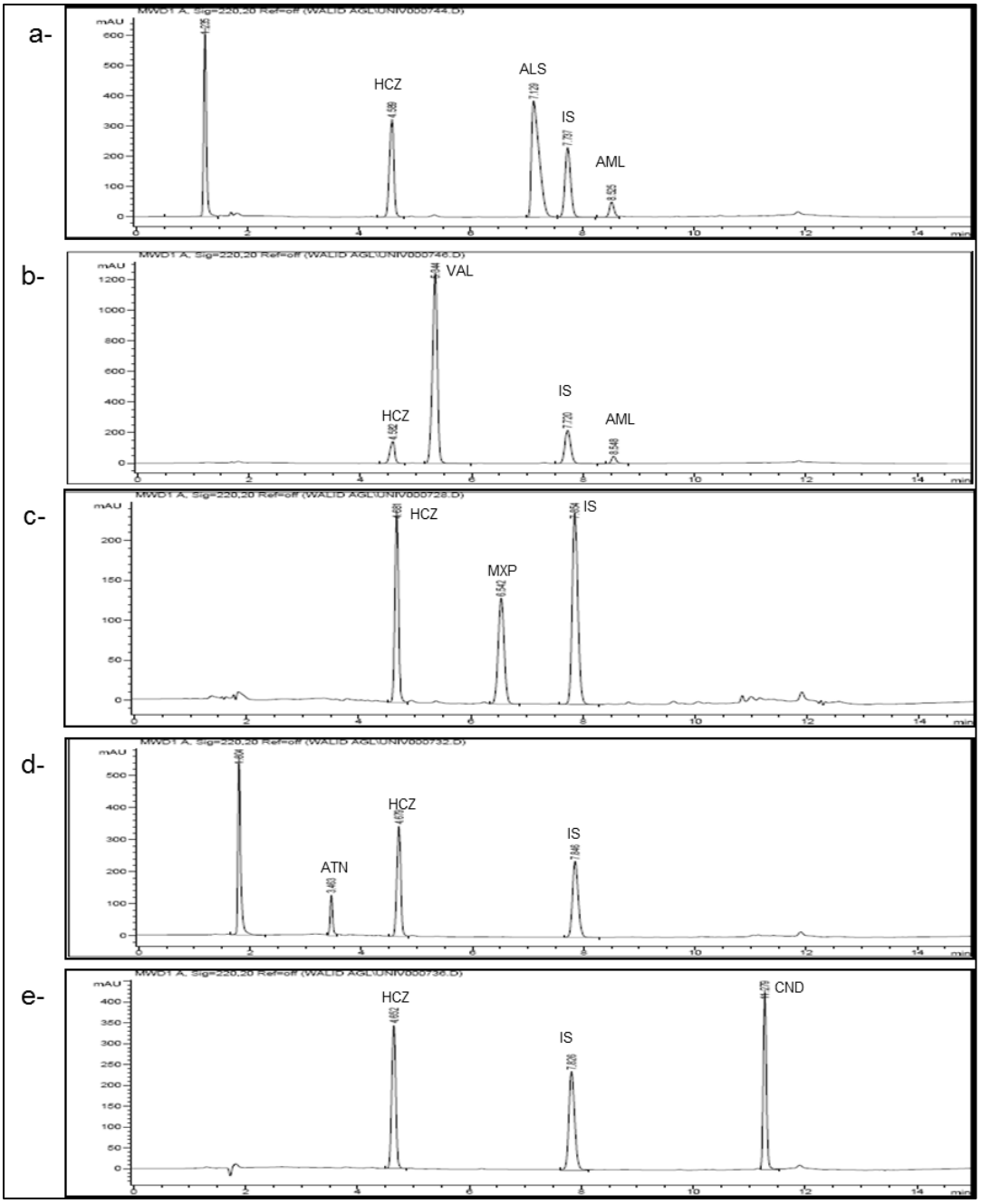

Figure 1.3.7 LC chromatograms of different laboratory prepared mixtures using the described chromatographic conditions where; (a)- 16.2, 215, 9, 20 µg mL^{-1} of HCZ, ALS, AML and IS, respectively, (b)- 7.5, 96, 8.25, 20 µg mL^{-1} of HCZ, VAL, AML and IS, respectively, (c)- 20, 24, 20 µg mL^{-1} of HCZ, MXP and IS, (d)- 15, 60, 20 µg mL^{-1} of HCZ, ATN and IS, respectively, and (e)- 15, 19.2, 20 µg mL^{-1} of HCZ, CND and IS, respectively

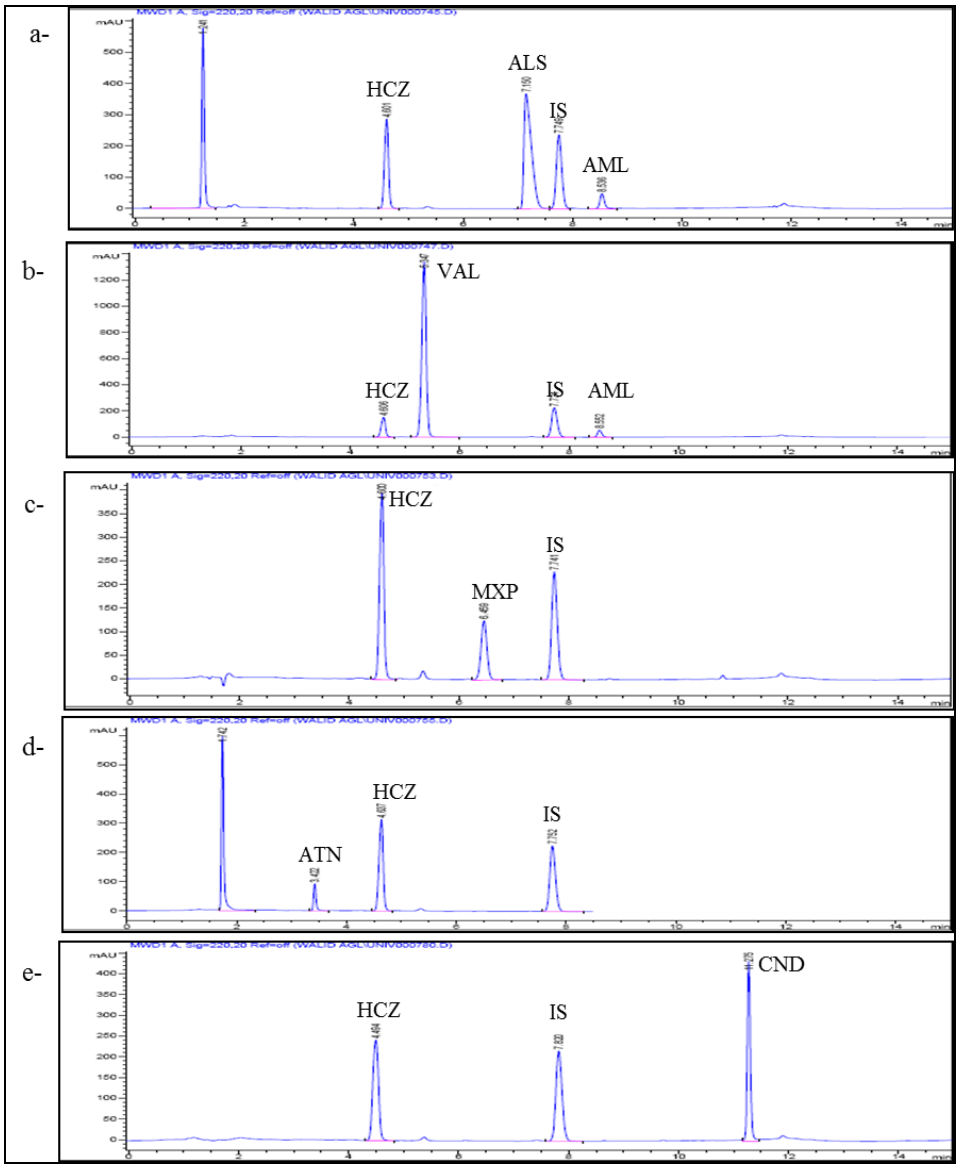

Figure 1.3.8 LC chromatograms of the analyzed combined formulations using the described chromatographic conditions where; (a)- Amturnide® tablets: 16.2, 215, 9, 20 µg mL^{-1} of HCZ, ALS, AML and IS, respectively, (b)- Exforge HCT® tablets: 7.5, 96, 8.25, 20 µg mL^{-1} of HCZ, VAL, AML and IS, respectively, (c)- Uniretic® tablets: 20, 24, 20 µg mL^{-1} of HCZ, MXP and IS, (d)- In house formulation: 15, 60, 20 µg mL^{-1} of HCZ, ATN and IS, respectively, and (e)- Atacand HCT® tablets: 15, 19.2, 20 µg mL^{-1} of HCZ, CND and IS, respectively

1.4 Validated Ion-Pair LC Method for Simultaneous Determination of Aliskiren hemifumarate, Amlodipine besylate and Hydrochlorothiazide in Pharmaceuticals

Chromatographia (2014) 77: 257

DOI 10.1007/s10337-013-2592-6

A rapid and precise LC method was developed for the simultaneous determination of aliskiren hemifumarate (ALS), amlodipine besylate (AML) and hydrochlorothiazide (HCZ) using acetonitrile: 25 mM octane sulphonic acid sodium salt monohydrate in water (60: 40 *v/v*) as the mobile phase. The flow rate was maintained at 1.2 mL min^{-1} on a stationary phase composed of Supelco, discovery® HS (C18) column (25cm x 4.6mm, 5μm). Isocratic elution was applied throughout the analysis. Detection was carried out at λ max (232 nm) at ambient temperature. The method was validated according to ICH guidelines. Linearity, accuracy and precision were satisfactory over the concentration ranges of 32 – 320, 2 – 44 and 4 – 64 μg mL^{-1} for ALS, AML and HCZ, respectively. LOD and LOQ were estimated and found to be 0.855 and 2.951 μg mL^{-1}, respectively, for ALS, 0.061 and 0.202 μg mL^{-1}, respectively, for AML as well as 0.052 and 0.174 μg mL^{-1}, respectively, for HCZ. The method was successfully applied for the determination of the three drugs in their co-formulated tablets. The results were compared statistically with reference methods and no significant difference was found. The developed method is specific and accurate for the quality control and routine analysis of the cited drugs in pharmaceutical preparations.

1.4.1 Introduction

Aliskiren hemifumarate, (2(S), 4(S), 5(S), 7(S)-*N*-(2-carbamoyl- 2- methylpropyl) -5-amino-4-hydroxy2,7 diisopropyl-8-[4-methoxy-3-(3-methoxypropoxy) phenyl] octanamide hemifumarate) (Fig 1.4.1a), is the first direct renin inhibitor suitable for oral administration. By achieving more complete renin–angiotensin system inhibition, direct renin inhibitors may afford greater protection from hypertensive complications [77]. Present evidence indicates that ALS reduces baseline systolic and diastolic blood pressure and that it is as effective as other first-line antihypertensive agents. Extra advantages can be reached when it is used in combination therapy [77]. Amlodipine besylate (AML), (3-Ethyl 5-methyl (4RS)-2-[(2-aminoethoxy)methyl]-4-(2-chlorophenyl)-6-methyl-1,4-dihydropyridine-3,5-dicarboxylate benzenesulphonate) (Fig 1.4.1b) is a dihydropyridine long-acting calcium channel blocker that inhibits the transmembrane influx of calcium ions into vascular smooth muscle and cardiac muscle [78]. AML is a peripheral arterial vasodilator that acts directly on vascular smooth muscle to cause a reduction in peripheral vascular resistance and reduction in blood pressure [79]. Hydrochlorothiazide is a potent orally diuretic and antihypertensive agent which inhibits active chloride reabsorption and thus increases the excretion of sodium chloride and water [80]. It is chemically 6-chloro-1, 1-dichloro-3, 4, dihydro-2H-1, 2, 4-benzoliadiazine-7-sulphanomide1, 1-dioxide (Fig 1.4.1c). Triple combination therapy of ALS, AML and HCZ proved to be effective and well tolerated in treating hypertensive high-risk patients [81]. Literature survey revealed LC [82-85], CE [86], UV-spectrophotometric [87, 88] and spectroflourimetric [89, 90] methods reported for the estimation of aliskiren hemifumarate alone or in combination with other anti-hypertensive agents. Methods such as LC [91-93], LC/MS/MS [78], CE [94], UV-spectrophotometric [95-97] and spectroflourimetric [98, 99] are reported for estimation of amlodipine alone or in combination with other agents. Methods such as LC [100-105], LC-MS [106-109],

UPLC [110] and UV- spectrophotometric methods [111] are reported for the estimation of HCZ alone or in combination with other anti-hypertensive agents. The aim of the present study was to develop a reliable and validated chromatographic procedure for analysis of ALS, AML and HCZ in bulk drug samples and in combined dosage formulation. The developed RP-LC method has the advantages of being simpler, more sensitive and faster for quality control and routine analysis of ALS, HCZ and AML triple mixture in comparison with the reported methods [112, 113].

1.4.2 Experimental

1.4.2.1 Materials and reagents

Working standards of ALS (certified to contain 99.51%) was supplied by Novartis Pharmaceuticals Corporation East, New Jersey, USA 07936, AML (certified to contain 99.75%) was kindly supplied by Global Nabi Co., (Giza -Egypt). HCZ (certified to contain 99.93%) was supplied by AstraZeneca - Cairo, - Egypt (Under license of AstraZeneca, Sweden). Amturnide® 300-10-25 mg tablets; batch # NDC 0078-0614-15 (Novartis Pharmaceuticals Corporation East, New Jersey, USA 07936) were purchased from commercial sources in the USA market. Each labeled to contain 331 mg ALS (equivalent to 300 mg aliskiren as a free base), 13.9 mg AML (equivalent to 10 mg amlodipine as a free base) and 25 mg HCZ. Acetonitrile (HPLC grade) and octane sulphonic acid sodium salt monohydrate were obtained from Sigma-Aldrich, MO, USA.

1.4.2.2 Instrument and conditions

The LC system consisted of a (Younglin instrument Acme 9000, Korea) equipped with vacuum degasser, mixer, gradient pump and UV/Vis detector. Separation and quantitation were made on Supelco, Discovery® HS (C18) column (25cm x 4.6mm, 5μm). A Soniclean120T ultrasonic processor was also used.

The mobile phase was filtered through 0.45 μm membrane filter and degassed using ultrasonic bath. The flow rate was 1.2 mL min-1. The solutions were injected (30 μl) with a 100 μl Agilent analytical syringe. All determinations were performed at ambient temperature. The system was equilibrated and saturated with the mobile phase for 30 min before the injection of the solutions. Quantification was achieved with UV detection at 232 nm based on peak area. Data acquisition was performed on Autochrome 3000 LC younglin software.

1.4.2.3 Preparation of mobile phase

A mixture of acetonitrile: 25 mM octane sulphonic acid sodium salt monohydrate in water (60: 40 *v/v*) was prepared.

1.4.2.4 Standard stock solutions preparation

40 mg of ALS, 10 mg of AML and HCZ were accurately weighed and transferred in to 50 mL volumetric flasks separately. Then, they were dissolved in a solvent composed of acetonitrile and water (60:40 *v/v*) and the solutions were made up to volume with the same solvent to give final concentrations of 800 μg mL^{-1} of ALS and 200 μg mL^{-1} of both AML and HCZ.

1.4.2.5 Procedure

1.4.2.5.1 Construction of calibration graphs

Different solutions containing 32 – 320, 2-44 and 4 – 64 μg mL^{-1} of ALS, AML and HCZ, respectively, were prepared in 10 mL volumetric flasks and completed to volume with the mobile phase. A volume of 30μL of each solution was injected in triplicates into the chromatogram. The chromatographic conditions were adjusted. The resulting chromatograms, retention times (t_r) of the peaks and the areas under the peaks (AUPs) were recorded. The

recorded AUPs of ALS, AML and HCZ were plotted versus the concentrations of ALS, AML and HCZ (µg mL^{-1}) to obtain the calibration curves.

1.4.2.5.2 Application of the proposed methods to dosage form

Twenty tablets of Amturnide® 300-10-25 mg tablets were weighed and finely powdered. A portion of the powder equivalent to ALS (166.5 mg), AML (6.95 mg) and HCZ (12.5 mg) was introduced into a 100 mL beaker and sonicated with 50 mL acetonitrile for 15 min. The extract was filtered. Further dilutions of the filtrate were carried out with acetonitrile. The general procedure for LC method was followed and the concentrations of the examined drugs were calculated using the corresponding regression equation.

1.4.2.6 Validation

The suggested analytical method was validated according to ICH guidelines [114] with respect to certain parameters such as linearity, accuracy, LOD and LOQ, precision, specificity, stability and robustness.

1.4.2.6.1 Linearity

The linearity of the method was established by spiking a series of standard mixtures in the range 32 – 320, 2-44 and 4 – 64 µg mL^{-1} of ALS, AML and HCZ, respectively. Above solutions were injected onto the LC system. Calibration curves were constructed for standard solutions by plotting their response ratios (ratios of the peak area of the analytes) against their respective concentrations. Linear regression was applied and standard deviation of slope (Sb), standard deviation of intercept (Sa), correlation coefficient (r) and standard error (Es) were determined.

1.4.2.6.2 Limit of detection and limit of quantification

Detection and quantification limits were determined through dilution method using S/N approach by injecting a 30 µl sample. LOD was considered as the minimum concentration with a signal to noise ratio of at least three (S/N˜3), while LOQ was taken as a minimum concentration with a signal to noise ratio of at least ten (S/N˜10) [114].

1.4.2.6.3 Accuracy

Accuracy was determined in terms of percent recovery. A set of standard mixtures at six different concentration levels 48, 96, 144, 176, 224, 288 µg mL^{-1} of ALS, 4, 12, 20, 28, 36, 40 µg mL^{-1} of AML and 12, 20, 32, 48, 56, 60 µg mL^{-1} of HCZ were prepared and injected onto the LC system in triplicate. The general procedure for LC method was followed and the percentage recoveries of ALS, AML and HCZ were calculated.

1.4.2.6.4 Precision

Method precision was determined both in terms of repeatability (intra-day reproducibility) and intermediate precision (inter-days reproducibility) using three different concentration levels 72, 176, 224 µg mL^{-1} of ALS, 12, 28, 36 µg mL^{-1} of AML and 12, 32, 48 µg mL^{-1} of HCZ.

1.4.2.6.5 Specificity

Specificity was examined by analyzing ALS, AML and HCZ in laboratory prepared mixtures and pharmaceutical dosage form to detect any interference caused by the combined drugs present in dosage formulations or the co-formulated excipients.

1.4.2.6.6 Robustness

The robustness of the developed method was investigated by evaluating the influence of small deliberate variations in procedure variables like flow rate (±0.1 mL min^{-1}) and mobile phase components` ratio (±2%). Retention time, peak area and resolution between fumaric acid/HCZ, HCZ/ALS and ALS/AML were recorded.

1.4.2.6.7 Stability

The stability studies of ALS, AML and HCZ samples were carried out over a period of 72h at 2–8 ^{0}C (refrigerator) and standard stock solutions for one month at 2–8 ^{0}C.

1.4.3 Results and discussion

The goal of the present investigation was to develop a well validated, sensitive, simple and quick analytical method for the simultaneous determination and quantification of ALS, AML and HCZ in pharmaceutical preparations. Concerning ALS, AML and HCZ simultaneous analysis, only two LC methods to the best of our knowledge have been reported for the simultaneous determination of the triple mixture. Rao et al [112] described a LC method for determination of the drugs in their dosage form using C18 column and a mobile phase consisting of acetonitrile: methanol: 50mM phosphate buffer (pH 3) in the ratio of 20:50:30% v/v. The linearity range of ALS practically will not allow proper simultaneous determination of the three drugs in their co-formulated tablets. Also, Selvakumar et al [113] reported a LC method using 20 mM potassium dihydrogen phosphate buffer (pH 6.5): methanol: acetonitrile (55:10:35 v/v) as the mobile phase for determination of the triple mixture in their pure form only. The samples were separated with poor sensitivity on C8 column within a long run time of 18 min. The newly

developed method has distinct advantages regarding simplicity, reliability and suitability to be applied for the simultaneous analysis of the cited drugs either in pure form or in their co-formulated tablets.

1.4.3.1 Method development

Various reversed phase chromatographic columns and a series of aqueous mobile phases containing different organic modifiers were tested to adjust the optimum conditions. Mobile phase systems such as phosphate and acetate buffers were tried at different pH values along with different organic modifiers such as methanol and acetonitrile in different ratios and flow rates. None of them achieved proper resolution and symmetric peaks. Since the analyzed compounds are ionic, the use of conventional RP-HPLC is somewhat restricted. Ionic suppression approach based on pH adjustment was examined to separate these charged analytes but it couldn`t achieve proper resolution with sharp and symmetric peaks. Ion Pair Chromatography is a more reliable approach that allows the separation of complex mixtures of ionic compounds. The separation pattern is determined by the mobile phase composition where an organic modifier is combined with a specific ion-pairing reagent in a certain ratio. The ion-pairing reagents are large ionic molecules having a charge opposite to the analytes of interest, as well as a hydrophobic region to interact with the stationary phase. The counter-ion combines with the ions of the eluent, becoming ion pairs in the stationary phase. This results in enhanced symmetry and sharpness of the peaks and hence increasing the reliability and reproducibility of the method. Using of ion pairing agents to achieve such goals and reduce tailing was examined. Triethylamine made the separation worse as it is basic ion pairing agent and the analyzed compounds need oppositely charged anionic alkyl sulphonate ion pairing agent. Also, the concentrations of both the ion pair agent and the organic modifier in the mobile phase are crucial for proper elution. It is worth

noting that the separation was improved with the relative increase of the percentage of the aqueous to organic phases. A satisfactory separation was obtained on a Supelco, Dicovery® HS (C18) column (25cm x 4.6mm, 5μm) with a mobile phase consisting of acetonitrile: 25 mM octane sulphonic acid sodium salt monohydrate in water (60: 40 v/v). Good separation of the cited compounds with good peaks' shape and minimum retention times (< 5 min) were obtained with that mobile phase at a flow rate 1.2 mL min^{-1}. Proper choice of the detection wavelength is crucial for sensitivity of the method. Quantitation was achieved with UV detection at 232 nm based on good peak area for each of the analyzed drugs. The retention times were 2.25, 3.13 and 3.92 min for HCZ, ALS and AML, respectively, (Fig 1.4.2). In the course of optimizing the conditions of the proposed method, different parameters affecting the chromatographic separation were studied. The system suitability tests were used to verify that the conditions of the chromatographic system were adequate for the resolution and hence for the analysis [114] (Table 1.4.1).

1.4.3.2 LC method validation

1.4.3.2.1 Linearity and range

Linear relationships between the recorded AUPs of ALS, AML and HCZ versus their concentrations were obtained. The regression equation $y = bC \pm a$ for each drug was also computed. In this study, 6 concentrations for each compound were used. The linearity of the calibration curves was validated by the high value of correlation coefficients. The analytical data of the calibration curves including standard deviations for the slope and intercept (S_b, S_a) are summarized in (Table 1.4.2). The calibration ranges were established within protocol range necessary, according to the intact drugs' concentrations in pharmaceutical product to give

accurate and precise results. The calibration ranges of the proposed procedure are given in (Table 1.4.2).

1.4.3.2.2 Limit of detection and limit of quantification

Lower limit of detection (LOD) and lower limit of quantification (LOQ) for each drug were calculated. Results are given in (Table 1.4.2).

1.4.3.2.3 Accuracy

Accuracy of the results was calculated by % recovery of 6 different concentrations of the three drugs analyzed by the proposed LC method. The results obtained including the mean of the recovery and standard deviation were displayed in (Table 1.4.2).

1.4.3.2.4 Precision

Repeatability (intra-day, n=3) and intermediate precision (inter-day, n=3) were checked using three different concentrations at low, medium and high level of the standard curve. The relative standard deviation and SE were calculated to check the precision of the method, (Table 1.4.3).

1.4.3.2.5 Specificity

Specificity was checked by analyzing ALS, AML and HCZ in laboratory prepared mixtures. Good resolution and absence of interference between drugs being analyzed and fumarate were shown in (Fig. 1.4.2, 1.4.3). Moreover, there was no interference observed from other materials in the pharmaceutical formulations (Fig. 1.4.2) confirming the specificity of the

method. Good recoveries were obtained in the sample indicating specificity of the proposed method, (Table 1.4.2).

1.4.3.2.6 Robustness

Minor deliberate changes in different experimental parameters such as flow rate (±0.1 mL min^{-1}) and mobile phase components` ratio (±2%) did not significantly affect resolution, peak area and retention time of the three drugs indicating that the proposed method is robust, (Table 1.4.4).

1.4.3.2.7 Stability

Results from the stability studies of working and stock solutions indicated that working solutions were stable for 72 h when stored at refrigerator (2–8 ^{0}C) while the stock solutions were stable for one month at 2–8 ^{0}C with satisfactory recovery % of about 98%.

1.4.3.3 Statistics

Statistical analysis of the results obtained using Student`s t-test and variance ratio F-test revealed no significant difference between the performance of the proposed methods and reported methods [83, 115, 116] regarding accuracy and precision (Table 1.4.5).

Table 1.4.1 System Suitability Tests for the LC Method Applied for the Determination of ALS, AML and HCZ

Item	Fumaric acid	HCZ	ALS	AML
N	2870	4043	4000	3781
R	5.769	5.212		3.466
α	1.484	1.393		1.250
T	1.17	1.00	1.08	1.19
%RSD of 6 injections	-----	1.695	1.899	1.798

(N: number of theoretical plates; R: resolution factor; T: tailing factor; α: selectivity factor)

Table 1.4.2 Characteristics and Results of the Proposed LC Method for Simultaneous Determination of ALS, AML and HCZ

Item	ALS	AML	HCZ
Linearity range (μg/mL)	32 – 320	2 – 44	4 – 64
LOD (μg mL^{-1})	0.885	0.061	0.052
LOQ (μg mL^{-1})	2.951	0.202	0.174
Regression equation (Y) [a]: Slope (b)	10.986	23.740	44.965
Standard deviation of slope (S_b)	0.127	0.151	0.609
Confidence limit of the slope [b]	10.986 ± 0.353	23.740 ± 0.148	44.965 ± 1.691
Intercept (a)	+ 0.2838	+ 9.3369	- 0.0094
Standard deviation of intercept (S_a)	27.064	3.823	23.972
Confidence limit of the intercept [b]	0.2838 ± 75.147	9.3369 ± 10.615	0.0094 ± 66.557
Regression coefficient (r^2)	0.9995	0.9993	0.9993
Standard error of estimation	29.492	5.252	32.023
Accuracy ± S.D.			
Drug in bulk	100.26 ± 1.29	99.79 ± 1.13	99.10 ± 1.58
Amturnide® 300-10-25 mg tablets	100.06± 1.32	99.86± 0.99	99.98± 0.17

[a] Y=a+bC, where C is the concentration in μg mL^{-1} and Y is the peak area.

[b] 95% confidence limit.

Table 1.4.3 Intra-and Inter-day Validation for the Determination of ALS, AML and HCZ

Concentration of **ALS** (μg mL^{-1})	**Intra-day assay**		**Inter-day assay**	
	Found ± R.S.D [a]	**SE**	**Found ± R.S.D** [a]	**SE**
72.000	72.438 ± 0.51	0.21	72.822 ± 1.00	0.42
176.000	173.255 ± 0.33	0.18	171.637 ± 0.43	0.43
224.000	221.172 ± 0.96	1.22	217.782 ± 1.58	1.98
Concentration of **AML** (μg mL^{-1})	**Intra-day assay**		**Inter-day assay**	
	Found ± R.S.D [a]	**SE**	**Found ± R.S.D** [a]	**SE**
12.000	11.431 ± 1.60	0.11	11.798 ± 2.00	0.14
28.000	27.960 ± 1.16	0.19	28.482 ± 1.60	0.26
36.000	34.934 ± 1.24	0.25	36.035 ± 1.74	0.36
Concentration of **HCZ** (μg mL^{-1})	**Intra-day assay**		**Inter-day assay**	
	Found ± R.S.D [a]	**SE**	**Found ± R.S.D** [a]	**SE**
12.000	12.210 ± 0.66	0.05	12.443 ± 1.57	0.11
32.000	31.019 ± 0.48	0.09	31.258 ± 0.98	0.18
48.000	46.414 ± 1.69	0.45	46.047 ± 1.81	0.48

[a] Mean and standard deviation of three determinations

Table 1.4.4 Robustness Study for the Determination of ALS, AML and HCZ

Parameters		Retention time (min.)			Area under the peak			Resolution		
		ALS	AML	HCZ	ALS	AML	HCZ	HCZ/ALS	ALS/AML	Fumaric acid/HCZ
Standard		3.13	3.92	2.25	1921	175	712	5.21	3.47	5.77
Flow rate (mL min^{-1})	1.1	3.35	4.23	2.46	1915	174	705	4.80	3.54	5.61
	1.3	2.82	3.57	2.06	1867	167	686	4.80	3.50	5.80
Mobile phase composition (acetonitrile: 25mM sodium	62:38	2.90	3.60	3.21	1993	182	728	4.40	3.20	5.45
	58:42	3.25	4.23	2.28	2046	182	754	5.70	3.80	5.96

Table 1.4.5 Statistical Comparison between Analysis Results of Pure Samples of the Studied Drugs using HPLC Method and those of the Reference Methods

Statistical Term	**ALS**		**AML**		**HCZ**	
	Reference method [7]	HPLC method	Reference method [39]	HPLC method	Reference method [40]	HPLC method
Mean	101.10	100.26	99.90	99.79	100.64	99.10
±S.D.	1.64	1.29	1.59	1.13	1.22	1.58
±S.E.	0.73	0.53	0.71	0.46	0.55	0.65
%RSD	1.62	1.29	1.59	1.13	1.21	1.59
n	5.00	6.00	5.00	6.00	5.00	6.00
V	2.69	1.66	2.53	1.27	1.49	2.44
Student`s t test	0.93 (1.83*)		0.11 (1.83*)		1.81 (1.83*)	
F-test	1.62 (6.26*)		1.99 (6.26*)		1.68 (6.26*)	

* Figures in parentheses are the theoretical t and F values at (p= 0.05) and n is the number of experiments.

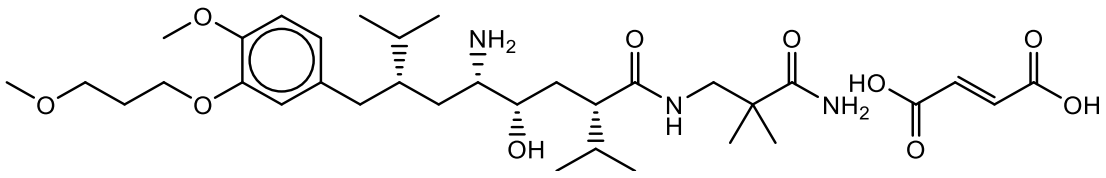

(a)

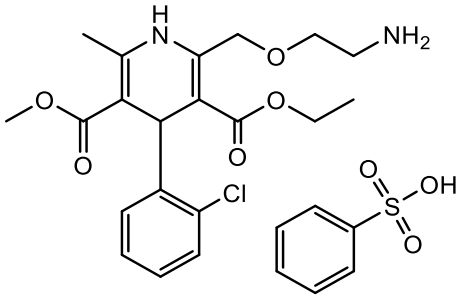

(b)

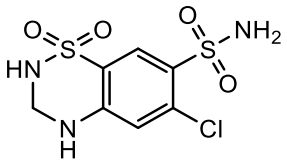

(c)

Figure 1.4.1 Chemical structures of aliskiren hemifumarate (a), amlodipine besylate (b) and hydrochlorothiazide (c)

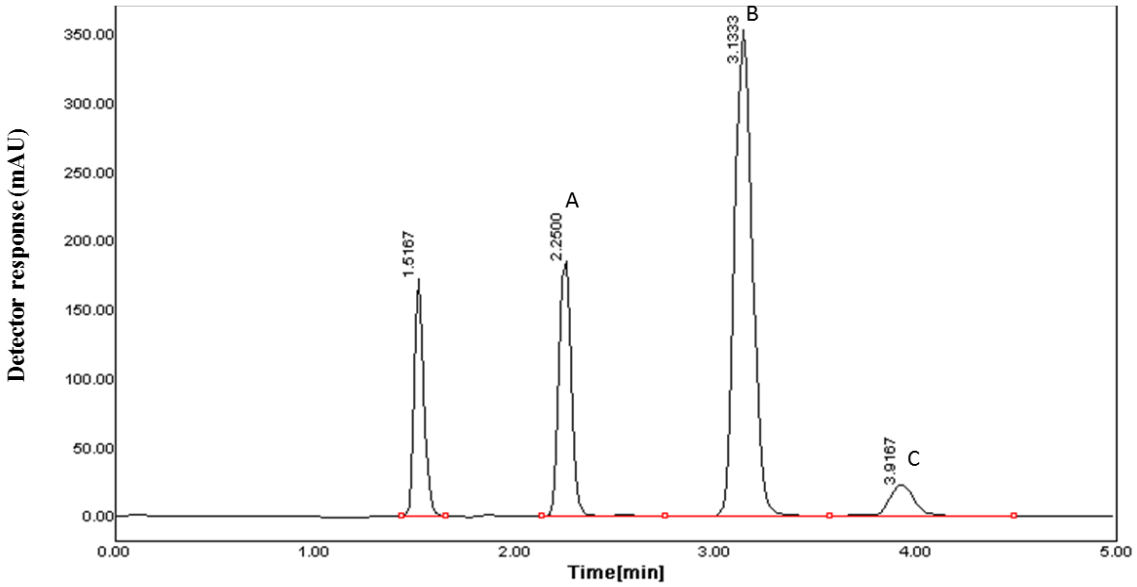

Figure 1.4.2 A typical LC chromatogram of 30 µL injector for a tablet sample of the triple mixture: HCZ 15 µg mL^{-1} (tr= 2.25 min) (A), ALS 199.8 µg mL^{-1} (tr= 3.13 min) (B) and AML 8.4 µg mL^{-1} (tr= 3.92 min) (C)

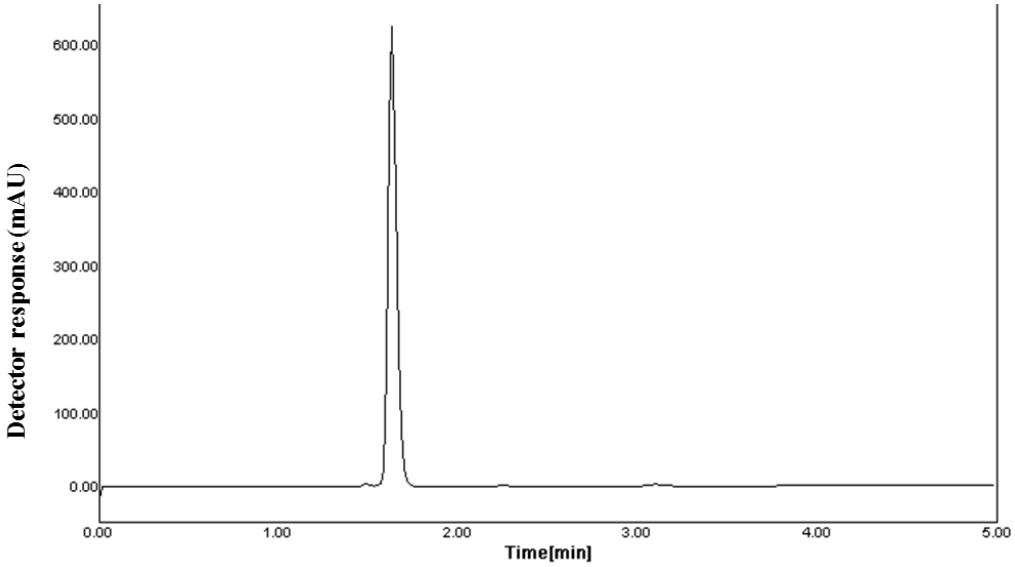

Figure 1.4.3 A typical LC chromatogram of 30 µL injector of fumaric acid 8 µg mL^{-1} (tr =1.81 min)

1.5 Simultaneous determination of aliskiren hemifumarate, amlodipine besylate and hydrochlorothiazide in spiked human plasma using UPLC-MS/MS

Journal of Chromatographic Science (2015) 53(7):1178-84

DOI 10.1093/chromsci/bmu213

A sensitive UPLC-MS/MS method was developed and validated for simultaneous estimation of aliskiren hemifumarate (ALS), amlodipine besylate (AML) and hydrochlorothiazide (HCZ) in spiked human plasma using valsartan as an internal standard (IS). Liquid-liquid extraction was used for purification and pre-concentration of analytes. The mobile phase consisted of 0.1% formic acid in ammonium acetate buffer (0.02 M, pH=3.5) and methanol (25: 75, v/v), flowing through XBridge BEH (50 mm x 2.1 mm ID, 5 µm) C18 column, at a flow rate of 0.6 mL min^{-1}. Multiple reaction monitoring (MRM) transitions were measured using an electrospray source in the positive ion mode for ALS and AML, while HCZ and IS were measured in negative ion mode. Validation of the method was performed as per US-FDA guidelines with linearity in the range of 2.0 – 400.0, 0.3 – 25.0 and 5.0 – 400.0 ng mL^{-1} for ALS, AML and HCZ, respectively. In human plasma, ALS, AML and HCZ were stable for at least one month at -70 ± 5 °C and for at least 6 hours at ambient temperature. After extraction from plasma, the reconstituted samples of ALS, AML and HCZ were stable in auto sampler at ambient temperature for 6 hours. The LC-MS/MS method is suitable for bioequivalence and pharmacokinetic studies of this combination.

1.5.1 Introduction

Aliskiren hemifumarate, (2(S), 4(S), 5(S), 7(S)-N-(2-carbamoyl- 2- methylpropyl) -5-amino-4-hydroxy2,7 diisopropyl-8-[4-methoxy-3-(3-methoxypropoxy) phenyl] octanamide hemifumarate) (Fig. 1.5.1a). Aliskiren is the first orally taken direct renin inhibitor simulating endogenous peptides approved for clinical use. By achieving more complete renin–angiotensin system inhibition, direct renin inhibitors may afford greater protection from hypertensive complications [117]. Present evidence indicates that aliskiren reduces baseline systolic and diastolic blood pressure and that it is as effective as other first-line antihypertensive agents. Extra advantages can be reached when it is used in combination therapy [117]. Amlodipine besylate (AML), (3-Ethyl 5-methyl (4RS)-2-[(2-aminoethoxy)methyl]-4-(2-chlorophenyl)-6-methyl-1,4-dihydropyridine-3,5-dicarboxylate benzenesulphonate) (Fig. 1.5.1b) is a dihydropyridine long-acting calcium channel blocker that inhibits the transmembrane influx of calcium ions into vascular smooth muscle and cardiac muscle [118]. Amlodipine is a peripheral arterial vasodilator that acts directly on vascular smooth muscle to cause a reduction in peripheral vascular resistance and reduction in blood pressure [119]. Hydrochlorothiazide (HCZ) is a potent diuretic and antihypertensive agent which inhibits active chloride reabsorption and thus increases the excretion of sodium chloride and water [80]. It is chemically 6-chloro-1, 1-dichloro-3, 4, dihydro -2H-1, 2, 4-benzoliadiazine-7-sulphanomide1, 1-dioxide (Fig. 1.5.1c). Triple combination therapy of ALS, AML and HCZ proved to be effective and well tolerated in treating hypertensive high-risk patients [120]. Literature survey revealed some LC [83, 121-126], CE [127], UV-spectrophotometric [128, 129] and spectroflourimetric [130-132] methods for estimation of ALS alone or in combination with other anti-hypertensive agents. Methods such as LC [126, 133-135], LC-MS/MS [118], CE [136], UV-spectrophotometry [137-139] and spectroflourimetry [140, 141] were reported for estimation of AML

only or in combination with other agents. Moreover, methods such as LC [142-147], LC-MS/MS [148-151], UPLC [152] and UV- spectrophotometry [153] were reported for the estimation of HCZ alone or in combination with other anti-hypertensive agents. Regarding the simultaneous determination of ALS, HCZ and AML triple mixture, there are four reported LC methods [125, 154-156] with UV detection and one reported CE method [157] for their determination in pharmaceutical dosage forms. LC methods with UV detection are not sensitive enough to measure ALS, AML or HCZ in human plasma, while the use of GC-MS/MS requires derivatization steps prior to analysis. Amongst the reported LC-MS/MS methods, there was no developed one for simultaneous determination of ALS, AML and HCZ in biological fluids. Thus, the aim of the present work was to develop a highly selective and sensitive LC-MS/MS method with good precision and accuracy, besides a simple sample treatment procedure, for simultaneous estimation of ALS, AML and HCZ in human plasma, using valsartan as the internal standard (IS). A detailed validation of the proposed method was performed in accordance with US-FDA guidelines [158] to yield reliable results. Moreover, the developed method can be successfully applied for further research to assess for instance the pharmacokinetics of ALS, AML and HCZ in combination.

1.5.2 Experimental

1.5.2.1 Materials and reagents

Working standards of ALS (certified to contain 99.51%) was supplied by (Novartis Pharmaceuticals Co., NJ, USA), AML (certified to contain 99.75%) was kindly supplied by (Global Nabi Co., Giza, Egypt). HCZ (certified to contain 99.93%) was supplied by (AstraZeneca, Cairo, Egypt). Pharmaceutical grade valsartan USP (certified to contain 99.40%) was supplied by (Zydus Pharmaceuticals, NJ, USA). Methanol HPLC grade, Methyl tert-butyl

ether and ammonium acetate were obtained from Sigma-Aldrich, USA. Formic acid was obtained from El-Nasr Pharmaceutical Chemicals Co., Egypt. Human plasma was obtained from VACSERA Blood Bank, Egypt. Deionized and purified water produced in-house from Millipore's Milli-Q System (USA) was used throughout the analysis.

1.5.2.2 Instrument and conditions

Quantitation was performed via MS/MS detection using Waters ACQUITY triple quadrupole LC-MS/MS mass spectrometer (Waters Corp., Milford, MA, USA). A Waters series UPLC system (Waters Corp., Milford, MA, USA) equipped with degasser, electrospray interface (ESI) and a solvent delivery unit along with an auto-sampler were used to inject 10 µL aliquots of the processed samples. The chromatographic separation was carried out on XBridge BEH (50 mm x 2.1 mm ID, 5 µm) C18 column obtained from Waters. Soniclean120T ultrasonic processor (Australia), Eppendorf Vacufuge 5301 Vacuum Centrifuge Concentrator (Germany) and Vortex-2 G-560 Lab Shaker Mixer (USA) were used as well.

Chromatographic elution was performed with a mobile phase consisted of 0.1% formic acid in 20 mM ammonium acetate and methanol, pH 3.5 (25: 75, v/v) pumped through the column at a flow rate of 0.6 mL min^{-1}. The column temperature was maintained at 30 °C. Under these conditions, the retention times for the HCZ, AML, ALS and IS were at 1.20, 2.91, 3.21 and 2.04 min, respectively (Fig. 1.5.2). The injection volume was 10 µL. The LC-MS/MS system allowed using the positive ion mode for monitoring ALS and AML as well as the negative ion mode for monitoring HCZ and IS simultaneously in each run. Multiple reaction monitoring (MRM) is a highly sensitive method of targeted mass spectrometry that can be used to selectively detect and quantify specific molecules in a complex mixtures based on the screening of specified precursor molecule-to-fragment ion transitions [159]. MRM transitions were measured

at positive mode at *m/z* 552.7 → 117.1, CV=35V, CE=40eV for ALS and at *m/z* 409.4 → 238.2, CV=15V, CE=10eV for AML, while HCZ was measured at negative mode at *m/z* 296.2 → 269.1, CV=35V, CE=20eV and at *m/z* 434.3 → 179.2, CV=40V, CE=30eV for the IS, where; CV is the cone voltage and CE is the value of collision energy for MRM acquisition, with a 20 ms dwell time of all analytes. The capillary voltage was set at +4000 V for both of ALS and AML, while it was set at -4000V for HCZ and IS. The cone gas flow was set at 40 L h^{-1} at 4 psi, and temperature at 350 °C with nozzle voltage of 2900 V. Nitrogen (99.99% purity) was used in the ion source and the collision cell. Quantitation of the analytes in spiked human plasma was based on the peak area ratio of cited drugs to IS. Data acquisition and processing were performed using Empower2 software (Waters Corp., MA, USA).

1.5.2.3 Standard stock solutions preparation

Standard stock solutions of 200 µg mL^{-1} of ALS and HCZ as well as 100 µg mL^{-1} of AML and IS were prepared separately in methanol. Appropriate further dilutions were prepared in the same solvent. All solutions were stored under refrigeration (2-8 ˚C) when not in use.

1.5.2.4 Procedure

1.5.2.4.1 Calibration and quality control samples preparation

Seven non-zero calibration standard solutions ranging from 20-4000 ng mL^{-1} for ALS, 3-250 ng mL^{-1} for AML and 50-4000 ng mL^{-1} of HCZ were prepared in 10 ml volumetric flasks where 100 µL of IS stock solution was added to each flask and completed to the mark with methanol. 50 µL of each working solution was added to 450 µL of drug free human plasma containing EDTA as anticoagulant. The quality control samples (QC) were prepared in the same manner similar to the calibration standards at three concentration levels; low, medium and high

(60, 1600 and 3200 ng mL^{-1}), (9, 100 and 200 ng mL^{-1}), (150, 1600 and 3200 ng mL^{-1}) for ALS, AML and HCZ, respectively. All samples were vortexed to ensure complete mixing. During each run, five replicates of the QC samples were used along with the calibration standards to verify the repeatability and integrity of the method.

1.5.2.4.2 Sample preparation

To 500 µL of each spiked calibration plasma standard or QC sample, 4 mL of methyl tert-butyl ether was added. It was then vortexed for 30 sec. and centrifuged at 4000 rpm, at 4 °C for 5 min. 1350 µL of the supernatant was collected and evaporated using an Eppendorff concentrator. The residue was reconstituted in 150 µL of the mobile phase and transferred to a glass vial for LC-MS/MS analysis.

1.5.3 Discussion and Method development

To the best of our knowledge there is no reported method for simultaneous determination of ALS, AML and HCZ in human plasma using LC-MS/MS, so the aim of the present work was to simultaneously determine ALS, AML and HCZ using UPLC system interfaced with tandem mass spectrometry to attain higher sensitivity and selectivity for detection and quantitation of the cited drugs in human plasma with a rapid and affordable extraction procedure. Moreover, the proposed method should be suitable for human clinical pharmacology, bioavailability and bioequivalence studies requiring simultaneous pharmacokinetic evaluation of ALS, AML and HCZ either separately or in combination in human plasma. Peak plasma concentrations for ALS reach 186±91 ng mL^{-1} following oral administration of a single oral dose (300 mg) of ALS [160]. Also, peak plasma concentrations for AML and HCZ reach 6.7±1.2 ng mL^{-1} and 131±4 ng mL^{-1}

following oral administration of single oral doses (10 mg and 25 mg) of AML [161] and HCZ [162], respectively. Based on the C_{max} value of each drug, suitable linearity ranges of 2.0 – 400.0 ng mL^{-1}, 0.3 – 25.0 ng mL^{-1} and 5.0 – 400.0 ng mL^{-1} for ALS, AML and HCZ, respectively, were selected. For sample preparation, extraction methods including direct precipitation and liquid-liquid extraction were studied. Liquid-liquid extraction using 4 mL methyl tert-butyl ether as the extraction solvent has the advantage of better deproteinization of the plasma samples, lower cost and good recovery results for the cited drugs, (Table 1.5.1). The use of C18 column was suitable for optimum separation of ALS, AML and HCZ. During the optimization cycle, various mobile phase compositions of ammonium acetate buffer, 0.1% formic acid in water, 0.1% formic acid in 20 mM ammonium acetate buffer, methanol and acetonitrile, in different proportions were tried in an isocratic mode. It was found that methanol allowed good elution of the analytes with better responses. The use of 0.1% formic acid in 20 mM ammonium acetate buffer was to obtain higher detection response through assisting the ionization of the cited drug molecules especially AML. Thus, the optimized conditions allowed the proposed method to be selective, sensitive, rapid and suitable for human clinical pharmacology, bioavailability and bioequivalence studies requiring pharmacokinetic simultaneous evaluation of ALS, AML and HCZ combination in human plasma.

1.5.4 Results and Bio-analytical method validation

1.5.4.1 Calibration, linearity and limit of quantitation

Blank samples (matrix samples processed without internal standard) and zero samples (matrix samples processed with internal standard) were analyzed. To establish the linearity, seven non-zero samples covering the expected range of each drug were prepared and added to

drug free human plasma then analyzed. Calibration curves were constructed by plotting peak area ratio of cited drug to the IS versus the corresponding concentration of each cited drug. Satisfactory linearity was obtained in the concentration range of 2.0 – 400.0, 0.3 – 25.0 and 5.0 – 400.0 ng mL^{-1} for ALS, AML and HCZ, respectively. The lowest standard on the calibration curve was to be accepted as the lower limit of quantitation (LLOQ) if the analytes response in the standard was at least five times more than that of drug free (blank) plasma [158]. In addition, the analyte peak in LLOQ sample was identifiable, discrete, and reproducible with satisfactory precision and accuracy (Table 1.5.2). A correlation coefficient of more than 0.998 for each of the analytes was obtained (Table 1.5.3). The regression equation for each of the cited drugs was also computed (Table 1.5.3).

1.5.4.2 Specificity

Six randomly selected drug free human plasma samples were processed by the similar liquid-liquid extraction procedure and analyzed. No endogenous plasma components showed interference at retention time of any analyte or of the IS.

1.5.4.3 Recovery (extraction efficiency) from human plasma matrix

Recovery of ALS, AML and HCZ were evaluated by comparing the mean peak responses of five extracted quality control (QC) samples of low, medium and high concentrations to mean peak responses of five plain standards of equivalent concentration. Similarly, the recovery of IS was also evaluated at the concentration of 100 ng mL^{-1}. The recovery of the analytes was consistent, precise and reproducible. The mean recovery results for the cited drugs in human

plasma are listed in table 1.5.1. The recovery for the IS from plasma was found to be 88.54 ± 1.91 (mean recovery % ± S.D.).

1.5.4.4 Accuracy and precision (inter- and intra-day)

The satisfactory recovery percentage results obtained from the assay of ALS, AML and HCZ indicate the accuracy of the proposed method, (Table 1.5.4). Repeatability (intra-day) and intermediate precision (inter-day) were assessed using three concentrations and three replicates of each concentration. The intermediate precision it was performed over three different days. The acceptable values for the coefficient of variation indicate good precision of the proposed method, (Table 1.5.4).

1.5.4.5 Stability

Three aliquots each of the low and high unprocessed QC samples of ALS, AML and HCZ were stable at -70 ± 5 °C for 36 days (long term stability) in human plasma, (Table 1.5.5). Also, three aliquots each of the low and high unprocessed QC samples of ALS, AML and HCZ were found to be stable over 6.0 hours in human plasma at room temperature (23-30 °C) (short term stability). After 6.0 hours the samples were processed, analyzed and compared with nominal concentrations, (Table 1.5.5). Auto-sampler stability was determined by analyzing three aliquots each of low and high QC samples of ALS, AML and HCZ that were stable for 6.0 hours after sample processing, (Table 1.5.5). Three aliquots each of low and high unprocessed quality control samples were stored at -70 ± 5 °C and subjected to three freeze and thaw cycles. After the completion of third cycle the samples were processed, analysed and results were compared with nominal values, (Table 1.5.5). Working solutions of 320 ng mL^1 of ALS and HCZ as well

as 20 ng mL^{1} and 100 ng mL^{-1} of AML and IS, respectively, were found to be stable for 6 days at 2-8 °C and at room temperature (23-30 °C) for 6 hours, (Table 1.5.6).

Table 1.5.1 Recovery results for ALS, AML and HCZ from spiked human plasma

QC sample	Concentration of drug in plasma (ng mL^{-1})			Mean Recovery %			CV			n
	ALS	AML	HCZ	ALS	AML	HCZ	ALS	AML	HCZ	
Low	6.00	0.90	15.0	88.32	86.63	83.84	2.56	4.08	2.66	5
Medium	160.00	10.00	160.0	90.36	88.32	85.37	4.50	5.28	3.02	5
High	320.00	20.00	320.0	92.85	90.05	88.62	2.02	2.74	2.30	5

CV, coefficient of variation; n, number of determinations.

Table 1.5.2 Summary for ALS, AML and HCZ calibration standards results in spiked human plasma

Conc. of drug in plasma (ng mL^{-1})			Mean conc. found (ng mL^{-1})			± S.D.			CV			Recovery %			n
ALS	AML	HCZ	ALS	AML	HCZ	ALS	AML	HCZ	ALS	AML	HCT	ALS	AML	HCT	
2.00	0.30	5.00	2.16	0.30	4.73	0.14	0.02	0.06	9.63	13.03	16.98	108.15	99.33	94.50	5
6.00	0.90	15.00	6.05	0.92	14.52	0.12	0.01	0.02	4.04	4.26	4.60	100.75	102.67	96.82	5
40.00	5.00	40.00	39.14	4.78	40.83	0.90	0.09	0.03	6.02	8.20	3.03	97.84	95.5	102.08	5
80.00	10.00	80.00	79.38	10.00	79.83	2.05	0.09	0.09	7.18	3.91	5.99	99.23	99.96	99.78	5
160.00	15.00	160.00	160.49	15.07	157.81	1.67	0.14	0.23	2.70	4.05	8.93	100.31	100.49	98.63	5
320.00	20.00	320.00	328.49	20.25	323.45	2.80	0.30	0.47	2.33	6.77	9.28	102.65	101.25	101.08	5
400.00	25.00	400.00	400.19	25.72	396.13	2.85	0.37	0.36	1.92	6.64	5.84	100.05	102.87	99.03	5

S.D., standard deviation; CV, coefficient of variation; n, number of determinations

Table 1.5.3 Characteristics and results of the proposed LC-MS/MS method for simultaneous determination of ALS, AML and HCZ in spiked human plasma

Item	**ALS**	**AML**	**HCZ**
Linearity range (ng mL^{-1})	2.0 – 400.0	0.30– 25.0	5.0 – 400.0
Regression equation (Y) [a]: Slope (b)	0.374	0.221	0.373
Intercept (a)	0.301	0.064	0.850
Regression coefficient (r^2)	0.9997	0.9989	0.9998

[a] Y=a+bC, where C is the concentration in ng/ml and Y is the peak area ratio.

Table 1.5.4 Intra-day and inter-day results of ALS, AML and HCZ in human plasma

QC sample	Conc. Of ALS (ng mL^{-1})	Intra-day assay			Inter-day assay		
		Found ± S.D.	CV	Recovery %	Found ± S.D.	CV	Recovery %
Low	6.00	6.48 ± 0.03	0.42	107.97	6.60 ± 0.19	2.83	110.01
Medium	160.00	149.52 ± 1.53	1.02	93.45	146.61 ± 6.46	4.40	91.63
High	320.00	290.52 ± 4.56	1.57	90.79	298.71 ± 7.33	2.45	93.35
	Conc. of AML (ng mL^{-1})	Intra-day assay			Inter-day assay		
		Found ± S.D.	CV	Recovery %	Found ± S.D.	CV	Recovery %
Low	0.90	0.85 ± 0.03	3.41	94.43	0.82 ± 0.02	2.49	91.18
Medium	10.00	9.24 ± 0.49	3.63	92.39	9.27 ± 0.30	2.98	92.66
High	20.00	18.03 ± 2.69	0.73	90.15	18.27 ± 0.33	1.83	91.34
	Conc. of HCZ (ng mL^{-1})	Intra-day assay			Inter-day assay		
		Found ± S.D.	CV	Recovery %	Found ± S.D.	CV	Recovery %
Low	15.00	13.61 ± 0.25	1.87	90.71	13.50 ± 0.40	2.99	89.97
Medium	160.00	148.87 ± 0.51	0.34	92.28	143.38 ± 4.60	3.21	89.01
High	320.00	283.99 ± 3.78	1.33	88.74	293.47 ± 4.44	1.51	91.71

S.D., standard deviation; CV, coefficient of variation.

Table 1.5.5 Summary of stability data of ALS in spiked human plasma

Drug	Stability term	Conc. (ng mL^{-1})	Mean conc. found (ng mL^{-1})	S.D.±	CV	Mean recovery %	n
ALS	Long term (36 days)	6.00	5.85	0.17	2.61	97.50	3
		320.00	289.27	3.95	1.36	90.40	3
	Short term (6 hours)	6.00	6.16	0.11	1.62	102.67	3
		320.00	295.22	2.83	0.96	92.26	3
	Auto-sampler (6 hours)	6.00	6.09	0.05	0.72	101.56	3
		320.00	294.76	1.93	0.65	92.11	3
	Freeze and thaw	6.00	5.67	0.31	4.60	94.50	3
		320.00	288.42	7.18	2.49	90.13	3
AML	Long term (36 days)	0.90	0.82	0.02	2.66	90.76	3
		20.00	17.98	0.72	4.00	89.88	3
	Short term (6 hours)	0.90	0.81	0.03	4.19	90.26	3
		20.00	18.09	0.28	1.54	90.44	3
	Auto-sampler (6hours)	0.90	0.81	0.02	1.95	89.92	3
		20.00	18.14	0.47	2.61	90.68	3
	Freeze and thaw	0.90	0.80	0.03	3.50	88.79	3
		20.00	17.81	0.22	1.21	89.05	3
HCZ	Long term (36 days)	15.00	13.49	0.26	1.94	89.91	3
		320.00	295.14	5.31	1.80	92.23	3
	Short term (6 hours)	15.00	13.41	0.10	0.77	89.38	3
		320.00	285.59	3.49	1.22	89.25	3
	Auto-sampler (6hours)	15.00	13.51	0.12	0.91	90.09	3
		320.00	284.88	3.51	1.23	89.03	3
	Freeze and thaw	15.00	13.15	0.29	2.22	87.67	3
		320.00	286.82	6.32	2.20	89.63	3

S.D., standard deviation; CV, coefficient of variation; n, number of determinations

Table 1.5.6 Summary of the stability data of ALS, AML, HCZ and internal standard in solution

Stability of stock solution	Conc. (ng mL^{-1})	Mean peak area at 25 ˚C after 6 hours	Mean peak area at (2-8 ˚C) after 6 days	Mean peak area of freshly prepared solution	Bias (%) at 25 ˚C after 6 hours	Bias (%) at (2-8 ˚C) after 6 days	n
ALS	320.00	241.1 x 10^4	239.9 x 10^4	242.1 x 10^4	0.40	0.89	3
AML	20.00	10.4 x 10^4	10.3 x 10^4	10.4 x 10^4	0.41	1.62	3
HCZ	320.00	10.2 x 10^4	10.0 x 10^4	10.3 x 10^4	0.81	2.18	3
IS	100.00	2.1 x 10^4	2.1 x 10^4	2.2 x 10^4	1.27	0.59	3

n, number of determinations.

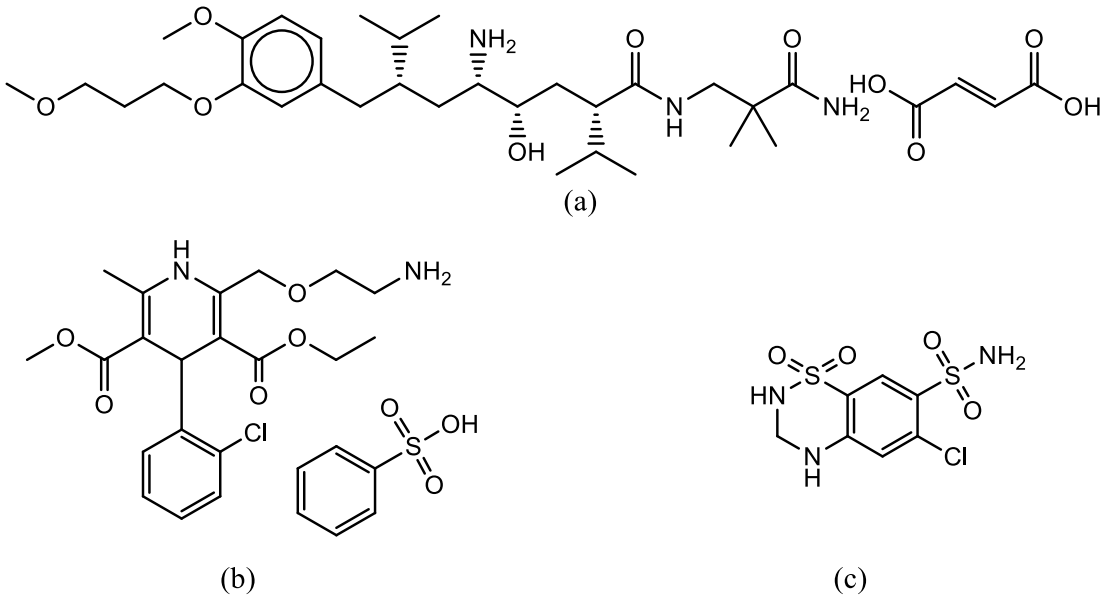

(a)

(b) (c)

Figure 1.5.1 Chemical structures of aliskiren hemifumarate (a), amlodipine besylate (b) and hydrochlorothiazide (c)

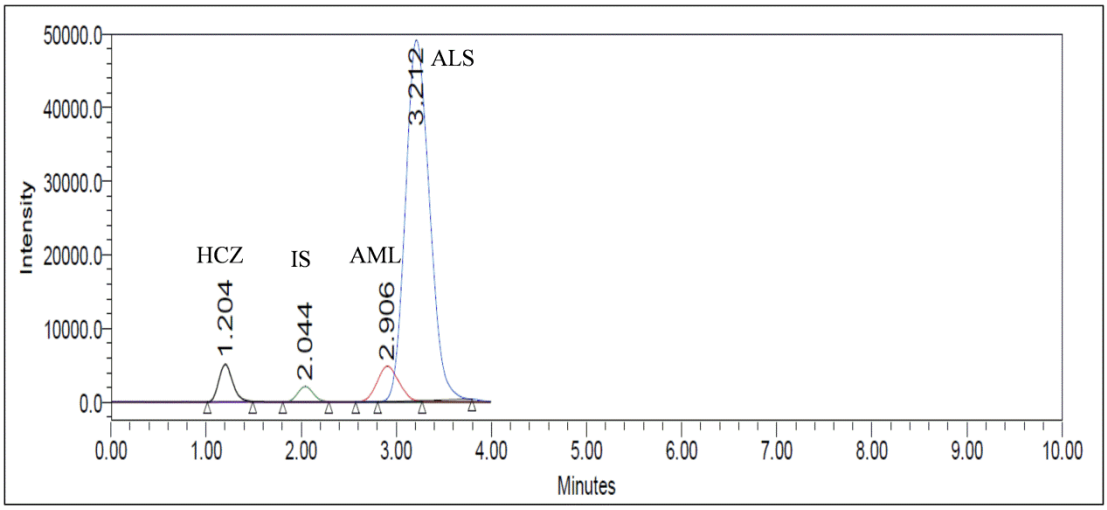

Figure 1.5.2 LC-MS/MS chromatogram of a 10 µL injection of quality control high sample showing elution of 20 ng mL^{-1} AML at 2.91 min, 160 ng mL^{-1} HCZ at 1.20 min, 160 ng mL^{-1} ALS at 3.20 min and 100 ng mL^{-1} IS at 2.04 min.

1.6 Conclusions

The study presented in section 1.2 represents the first report of a stability-indicating LC method for determination of AZL and CLT in their commercially available tablets. The proposed method has the advantages of being simple, specific, accurate and selective, so that, it was applied to the analysis of the studied drugs in their pharmaceutical dosage forms. Moreover, the suggested method permits separation of the studied drugs from their alkaline, acidic, oxidative, thermal (wet heat) or photolytic degradation products within a reasonable time. Furthermore, the proposed method was successfully applied to study the kinetics of the acidic degradation processes in the case of AZL as well as the kinetics of the alkaline degradation processes in the case of CLT, and to derive the first order degradation rate constant, half-life time ($\mathbf{t_{1/2}}$), shelf-life ($\mathbf{t_{90}}$) and the activation energy E_a of the investigated drugs.

The study presented in section 1.3 represents rapid, selective, specific and validated RP-LC method which was developed and validated for the simultaneous determination of the most important diuretics, HCZ, along with most commonly prescribed antihypertensive drugs representing different pharmacological classes, namely; ATN, VAL, MXP, ALS, AML and CND. This method is characterized by simplicity, accuracy, preciseness besides its wide range of applications, and it can be used for routine analysis and quality control of the cited drugs separately or in combinations in many dosage forms.

The proposed ion pair LC method in section 1.4 found to be reliable, simple, quick, sensitive and accurate for simultaneous determination of ALS, AML and HCZ in pharmaceutical preparation. Therefore, the proposed method can be used routinely for quality control of the cited drugs.

The proposed bio-analytical method in section 1.5 was specific, sensitive accurate and precise enough to be successfully applied to human clinical pharmacology, bioavailability, and bioequivalence studies requiring pharmacokinetic evaluation. The method employed sample preparation by liquid-liquid extraction with adequate recovery results, followed by isocratic HPLC coupled with tandem mass spectrometric detection. The LC-MS/MS method was rapid enough and capable of simultaneous estimation of ALS, AML and HCZ in human plasma with satisfactory sensitivity and precision.

References

1. Imming, P.; Sinning, C.; Meyer, A. Drugs, their targets and the nature and number of drug targets. Nat Rev Drug Discov 2006, 5 (10), 821-834.

2. The United States Pharmacopeia 30, the National Formulary 25. US Pharmacopeial Convention: Rockville, MD, 2007.

3. Moffat, A. C. Clarke's Analysis of Drugs and Poisons [Online]; The Pharmaceutical Press: London, 2006.

4. Lough, W. J.; Wainer, I. W. High Performance Liquid Chromatography Fundamental Principle and Practice. 1st ed.; Blackie academic and professional: New York,USA, 1995.

5. Hamdan, M. Pharmaceutical applications of liquid chromatography, capillary electrophoresis coupled to mass spectrometry. Process Control Qual. 1997, 10 (1-2), 113-127.

6. Lee, H. Pharmaceutical applications of liquid chromatography coupled with mass spectrometry (LC/MS). J. Liq. Chromatogr. Relat. Technol. 2005, 28 (7-8), 1161-1202.

7. Tache, F.; Udrescu, S.; Albu, F.; Micale, F.; Medvedovici, A. Greening pharmaceutical applications of liquid chromatography through using propylene carbonate-ethanol mixtures instead of acetonitrile as organic modifier in the mobile phases. J. Pharm. Biomed. Anal. 2013, 75, 230-238.

8. Locatelli, M.; Governatori, L.; Carlucci, G.; Genovese, S.; Mollica, A.; Epifano, F. Recent application of analytical methods to phase I and phase II drugs development: a review. Biomed. Chromatogr. 2012, 26 (3), 283-300.

9. Wann, M.-H. Application of LC-NMR in pharmaceutical analysis. Sep. Sci. Technol. 2005, 6 (Handbook of Pharmaceutical Analysis by HPLC), 569-579.

10. Baker, W. L.; White, W. B. Azilsartan medoxomil: a new angiotensin II receptor antagonist for treatment of hypertension. Ann. Pharmacother. 2011, 45 (Copyright (C) 2013 American Chemical Society (ACS). All Rights Reserved.), 1506-1515.

11. Kurtz, T. W.; Kajiya, T. Differential pharmacology and benefit/risk of azilsartan compared to other sartans. Vasc Health Risk Manag 2012, 8, 133-43.

12. Kusumoto, K.; Igata, H.; Ojima, M.; Tsuboi, A.; Imanishi, M.; Yamaguchi, F.; Sakamoto, H.; Kuroita, T.; Kawaguchi, N.; Nishigaki, N.; Nagaya, H. Antihypertensive, insulin-sensitising and renoprotective effects of a novel, potent and long-acting angiotensin II type 1 receptor blocker, azilsartan medoxomil, in rat and dog models. Eur J Pharmacol 2011, 669 (Copyright (C) 2013 U.S. National Library of Medicine.), 84-93.

13. Vekariya, P. P.; Joshi, H. S. Development and Validation of RP-HPLC Method for Azilsartan Medoxomil Potassium Quantitation in Human Plasma by Solid Phase Extraction Procedure. ISRN Spectroscopy 2013, 2013, 6.

14. Martindale, The Complete Drug Reference. 36th ed.; The Pharmaceutical Press: London, UK, 2009.

15. Singh, B.; Patel, D. K.; Ghosh, S. K. A reversed-phase high performance liquid chromatographic method for determination of chlorthalidone in pharmaceutical formulation. Int. J. Pharm. Pharm. Sci. 2009, 1 (Copyright (C) 2013 American Chemical Society (ACS). All Rights Reserved.), 24-29.

16. Mhaske, R. A.; Sahasrabudhe, S.; Mhaske, A. A.; Garole, D. J. RP-HPLC method for simultataneous determination of Atorvastatin calcium, Olmesartan medoxomil, Candesartan, Hydrochlorothiazide and Chlorthalidone - application to commercially available drug products. Int. J. Pharm. Sci. Res. 2012, 3 (Copyright (C) 2013 American Chemical Society (ACS). All Rights Reserved.), 793-801.

17. Woo, H.; Kim, J. W.; Han, K. M.; Lee, J. H.; Hwang, I. S.; Kim, J.; Kweon, S. J.; Cho, S.; Chae, K. R.; Han, S. Y. Simultaneous analysis of 17 diuretics in dietary supplements by HPLC and LC-MS/MS. Food Addit. Contam., Part A 2013, 30 (Copyright (C) 2013 American Chemical Society (ACS). All Rights Reserved.), 209-217.

18. Youssef, R. M.; Maher, H. M.; El-Kimary, E. I.; Hassan, E. M.; Barary, M. H. Validated stability-indicating methods for the simultaneous determination of amiloride hydrochloride, atenolol, and chlorthalidone using HPTLC and HPLC with photodiode array detector. J. AOAC Int. 2013, 96 (Copyright (C) 2013 American Chemical Society (ACS). All Rights Reserved.), 313-323.

19. Salem, H. High-performance thin-layer chromatography for the determination of certain antihypertensive mixtures. Sci. Pharm. 2004, 72 (Copyright (C) 2013 American Chemical Society (ACS). All Rights Reserved.), 157-174.

20. Ciborowski, M.; Icardo, M. C.; Mateo, J. V.; Martinez Calatayud, J. FI-chemiluminometric study of thiazides by on-line photochemical reaction. J Pharm Biomed Anal 2004, 36 (4), 693-700.

21. Parmar, K. E.; Mehta, R. S. First order derivative spectrophotometric method for simultaneous estimation of Telmisartan and Chlorthalidone in bulk and pharmaceutical dosage form. Int. Res. J. Pharm. 2013, 4 (Copyright (C) 2013 American Chemical Society (ACS). All Rights Reserved.), 224-228.

22. Lu, M.; Li, X.; Feng, Q.; Chen, G.; Zhang, L. Analysis of diuretics by capillary electrochromatography using poly(1-hexadecene-co-TMPTMA) monolithic column. Sepu 2010, 28 (Copyright (C) 2013 American Chemical Society (ACS). All Rights Reserved.), 253-259.

23. Cheng, J. W. M. Azilsartan/chlorthalidone combination therapy for blood pressure control. Integr. Blood Pressure Control 2013, 6 (Copyright (C) 2013 American Chemical Society (ACS). All Rights Reserved.), 39-48.

24. Kasimala, M. B.; Kasimala, B. B. Reverse Phase-HPLC Method Development and Validation for The Simultaneous Estimation of Azilsartan Medoxomil and Chlorthalidone in Pharmaceutical Dosage Forms Jamonline 2012, 2 (1), 117-126.

25. ICH. International conference on harmonization of technical requirements for registration of pharmaceuticals for human use. ICH Harmonised Tripartite Guideline Q1A(R2) and (Q1B), Stability Testing of New Drug Substances and Products,2003 and Stability Testing:

Photostability Testing of New Drug Substances and Products, 1996. ICH: Geneva, Switzerland.

26. ICH. ICH Harmonized Tripartite Guideline, Validation of Analytical Procedures: Text and Methodology, Q2(R1), Current Step 4 Version, Parent Guidelines on Methodology Dated November 6 1996, Incorporated in November 2005. http://www.ich.org/fileadmin/Public_Web_Site/ICH_Products/Guidelines/Quality/Q2_R1/Step4/Q2_R1__Guideline.pdf (accessed April 23, 2013).

27. SINKO, P. J. MARTIN'S PHYSICAL PHARMACY AND PHARMACEUTICAL SCIENCES: Physical Chemical and Biopharmaceutical Principles in the Pharmaceutical Sciences. 6 th ed.; Lippincott Williams & Wilkins, a Wolters Kluwer business: 530 Walnut St., Philadelphia, PA 19106, 2011.

28. Tengli, A. R.; Gurupadayya, B. M.; Soni, N. Simultaneous estimation of hydrochlorothiazide, amlodipine, and losartan in tablet dosage form by RP-HPLC. Int. J. Chem. Anal. Sci. 2013, 4 (1), 33-38.

29. El-Gindy, A.; Sallam, S.; Abdel-Salam, R. A. HPLC method for the simultaneous determination of atenolol and chlorthalidone in human breast milk. J. Sep. Sci. 2008, 31 (Copyright (C) 2013 American Chemical Society (ACS). All Rights Reserved.), 677-682.

30. Sweetman, S. Martindale: The Complete Drug Reference. The Pharmaceutical Press, London: 2007.

31. Burnier, M. Angiotensin II type 1 receptor blockers. Circulation 2001, 103 (6), 904-12.

32. Israili, Z. H. Clinical pharmacokinetics of angiotensin II (AT1) receptor blockers in hypertension. J. Hum. Hypertens. 2000, 14 Suppl 1, S73-86.

33. Belal, F. F.; Metwaly, K. M.; Amer, S. M. Development of Membrane Electrodes for the Specific Determination of Moexipril Hydrochloride in Dosage Forms and Biological Fluids. Portugaliae Electrochimica Acta 2009, 27 (4), 463-475.

34. Bonanni, L.; Dalla Vestra, M. Oral renin inhibitors in clinical practice: a perspective review. Ther. Adv. Chronic. Dis. 2012, 3 (4), 173-81.

35. Sivakumar, T.; Manavalan, R.; Muralidharan, C.; Valliappan, K. An improved HPLC method with the aid of a chemometric protocol: simultaneous analysis of amlodipine and atorvastatin in pharmaceutical formulations. J Sep Sci 2007, 30 (Copyright (C) 2013 U.S. National Library of Medicine.), 3143-53.

36. Abdollahpour, N.; Asoodeh, A.; Saberi, R.; Chamani, J. Separate and simultaneous binding effects of aspirin and amlodipine to human serum albumin based on fluorescence spectroscopic and molecular modeling characterizations: A mechanistic insight for determining usage drugs doses. J. Lumin. 2011, 131 (9), 1885-1899.

37. Johnson, J. A.; Gong, Y.; Bailey, K. R.; Cooper-DeHoff, R. M.; Chapman, A. B.; Turner, S. T.; Schwartz, G. L.; Campbell, K.; Schmidt, S.; Beitelshees, A. L.; Boerwinkle, E.; Gums, J. G. Hydrochlorothiazide and atenolol combination antihypertensive therapy: effects of drug initiation order. Clin. Pharmacol. Ther. 2009, 86 (5), 533-9.

38. White, W. B.; Stimpel, M. Long-term safety and efficacy of moexipril alone and in combination with hydrochlorothiazide in elderly patients with hypertension. J. Hum. Hypertens. 1995, 9 (11), 879-84.

39. Melian, E. B.; Jarvis, B. Candesartan cilexetil plus hydrochlorothiazide combination: a review of its use in hypertension. Drugs 2002, 62 (5), 787-816.

40. Ferdinand, K. C.; Weitzman, R.; Israel, M.; Lee, J.; Purkayastha, D.; Jaimes, E. A. Efficacy and safety of aliskiren-based dual and triple combination therapies in US minority patients with stage 2 hypertension. J. Am. Soc. Hypertens. 2011, 5 (2), 102-13.

41. Calhoun, D. A.; Lacourciere, Y.; Chiang, Y. T.; Glazer, R. D. Triple antihypertensive therapy with amlodipine, valsartan, and hydrochlorothiazide: a randomized clinical trial. Hypertens. 2009, 54 (1), 32-9.

42. Zaveri, M.; Khandhar, A. Development and validation of a RP-HPLC for the simultaneous estimation of atenolol and hydrochlorothiazide in pharmaceutical dosage forms. J. Pharm. Res. Health Care 2010, 2 (Copyright (C) 2013 American Chemical Society (ACS). All Rights Reserved.), 248-252.

43. Sa'sa, S. I.; Jalal, I. M.; Khalil, H. S. Determination of Atenolol Combinations with Hydrochlorothiazide and Chlorthalidone in Tablet Formulations by Reverse-Phase HPLC. J. Liq. Chromatogr. 1988, 11 (8), 1673-1696.

44. Havaldar, F. H.; Vairal, D. L. Simultaneous estimation of atenolol, hydrochlorothiazide, losartan, and valsartan in the pharmaceutical dosage form. Int. J. Pharm. Life Sci. 2010, 1 (Copyright (C) 2013 American Chemical Society (ACS). All Rights Reserved.), 282-289.

45. Tian, D. F.; Tian, X. L.; Tian, T.; Wang, Z. Y.; Mo, F. K. Simultaneous Determination of Valsartan and Hydrochlorothiazide in Tablets by RP-HPLC. Indian J. Pharm. Sci. 2008, 70 (3), 372-4.

46. Varghese, S. J.; Ravi, T. K. Quantitative simultaneous determination of amlodipine, valsartan, and hydrochlorothiazide in "Exforge HCT" tablets using high-performance liquid chromatography and high-performance thin-layer chromatography. J. Liq. Chromatogr. Rel. Technol. 2011, 34 (12), 981-994.

47. Şatana, E.; Altınay, Ş.; Göğer, N. G.; Özkan, S. A.; Şentürk, Z. Simultaneous determination of valsartan and hydrochlorothiazide in tablets by first-derivative ultraviolet spectrophotometry and LC. J. Pharm. Biomed. Anal. 2001, 25 (5–6), 1009-1013.

48. Shaalan, R. A.; Belal, T. S. Gradient HPLC-DAD determination of the antihypertensive mixture of amlodipine besylate, valsartan, and hydrochlorothiazide in combined pharmaceutical tablets. J. Liq. Chromatogr. Relat. Technol. 2012, 35 (Copyright (C) 2013 American Chemical Society (ACS). All Rights Reserved.), 215-230.

49. Hafez, H. M.; Abdelaziz, L. M.; Elshanawane, A. A.; Kamal, M. M. Quantitative Determination of Four Angiotensin-II-Receptor Antagonists in Presence of Hydrochlorothiazide by a Gradient Technique HPLC in their Pharmaceutical Preparations. Pharmaceut. Anal. Acta. 2012, 3, 167.

50. Hemke, A.; Bhure, M.; Anjankar, V.; Gupta, K. Validated RP-HPLC method for simultaneous determination of Amlodipine, Hydrochlorothiazide and Valsartan in

pharmaceutical formulation. Int. J. Pharm. Technol. 2013, 5 (Copyright (C) 2013 American Chemical Society (ACS). All Rights Reserved.), 5383-5392.

51. Pachauri, S.; Paliwal, S.; Srinivas, K. S.; Singh, Y.; Jain, V. Development & validation of HPLC method for analysis of some antihypertensive agents in their pharmaceutical dosage forms. J. Pharm. Sci. Res. 2010, 2 (Copyright (C) 2013 American Chemical Society (ACS). All Rights Reserved.), 459-464.

52. Anandakumar, K.; Jothieswari, D.; Subathrai, R.; Santhi, D.; Vetrichelvan, T. Validated RP-HPLC method for the simultaneous determination of amlodipine besylate, valsartan, and hydrochlorothiazide in bulk and in pharmaceutical formulation. Acta Chromatogr. 2012, 24 (1), 37-50.

53. Erturk, S.; Cetin, S. M.; Atmaca, S. Simultaneous determination of moexipril hydrochloride and hydrochlorothiazide in tablets by derivative spectrophotometric and high-performance liquid chromatographic methods. J. Pharm. Biomed. Anal. 2003, 33 (3), 505-11.

54. Raju, V. B.; Rao, A. L. Simultaneous Estimation of Moexipril and Hydrochlorthiazide in Tablet Dosage Form by RP-HPLC Method. Asian J. Chem. 2012, 24 (11), 5026.

55. Alagar Raja, M.; Ragavendra, P.; Banji, D.; Rao, K. N. V.; Chaithanya, Y.; Anusha, B.; Selvakumar, D. RP-HPLC Method for Simultaneous Estimation of Aliskiren Hemi fumarate, Hydrochlorothiazide and Amlodipine in Pharmaceutical bulk drugs and Tablet dosage form. J. Pharm. Res. 2012, 5 (8), 4580-4584.

56. Swamy, G. K.; P.Sravanthi; Surekha, M. L.; Kumar, J.; Rao, J. Validated RP-HPLC Method For The Simultaneous Determination Of Aliskiren, Hydrochlorothiazide And Amlodipine Besylate In Bulk And Pharmaceutical

Formulations. Int. J. Chem. Tech. Res. 2012, 4 (4), 1666-1673.

57. Choudhari, V. P.; Bari, N. A.; Shah, A.; Sharma, S. N.; Katariya, P. M.; Bhise, S. S. Simultaneous estimation of aliskiren and hydrochlorothiazide in pharmaceutical formulation by RP-LC-PDA. Int. J. Pharm. Sci. Rev. Res. 2012, 14 (Copyright (C) 2013 American Chemical Society (ACS). All Rights Reserved.), 10-14.

58. El-Bagary, R.; Patonay, G.; Elzahr, A.; Elkady, E.; Ebeid, W. Ion-Pair LC Method for Simultaneous Determination of Aliskiren Hemifumarate, Amlodipine Besylate and Hydrochlorothiazide in Pharmaceuticals. Chromatographia 2013, 1-8.

59. Mathrusri, A. M.; Narendra, A.; Ravi, K. K. Liquid chromatographic method for the simultaneous quantitative determination of Candesartan cilexetil and Hydrochlorthiazide in pharmaceutical dosage forms. J. Drug Delivery Ther. 2012, 2 (Copyright (C) 2013 American Chemical Society (ACS). All Rights Reserved.), 48-54.

60. Balamuralikrishna, K.; Syamasundar, B. Development and validation of high performance liquid chromatographic method for the simultaneous estimation of Candesartan cilexetil and Hydrochlorothiazide in combined tablet dosage form. Pharma Chem. 2010, 2 (Copyright (C) 2013 American Chemical Society (ACS). All Rights Reserved.), 231-237.

61. Lei, J.; Zhang, X.; Zhuo, Z.; Zhu, K.; Sun, P.; Fan, Q. HPLC-UV simultaneous determination of candesartan cilexetil and hydrochlorothiazide in compound candesartan

cilexetil tablets. Yaowu Fenxi Zazhi 2007, 27 (Copyright (C) 2013 American Chemical Society (ACS). All Rights Reserved.), 566-568.

62. Qutab, S. S.; Razzaq, S. N.; Ashfaq, M.; Shuja, Z. A.; Khan, I. U. Simple and sensitive LC-UV method for simultaneous analysis of hydrochlorothiazide and candesartan cilexetil in pharmaceutical formulations. Acta Chromatogr. 2007, 19 (Copyright (C) 2013 American Chemical Society (ACS). All Rights Reserved.), 119-129.

63. Gonzalez, O.; Iriarte, G.; Rico, E.; Ferreiros, N.; Maguregui, M. I.; Alonso, R. M.; Jimenez, R. M. LC-MS/MS method for the determination of several drugs used in combined cardiovascular therapy in human plasma. J. Chromatogr. B: Anal. Technol. Biomed. Life Sci. 2010, 878 (Copyright (C) 2013 American Chemical Society (ACS). All Rights Reserved.), 2685-2692.

64. Shah, H. J.; Kataria, N. B.; Subbaiah, G.; Patel, C. N. Simultaneous LC-MS-MS Analysis of Valsartan and Hydrochlorothiazide in Human Plasma. Chromatographia 2009, 69 (Copyright (C) 2013 American Chemical Society (ACS). All Rights Reserved.), 1055-1060.

65. Bharathi, D. V.; Hotha, K. K.; Chatki, P. K.; Satyanarayana, V.; Venkateswarlu, V. LC-MS/MS method for simultaneous estimation of candesartan and hydrochlorothiazide in human plasma and its use in clinical pharmacokinetics. Bioanal. 2012, 4 (10), 1195-204.

66. Ravisankar, P.; Devala, R. G.; Krishna, C. M.; Devadasu, C.; Srinivasa, B. P. Rapid separation of five anti-hypertensive agents - atenolol, metoprolol, hydrochlorothiazide, amlodipine and nebivolol: application to estimation of metoprolol succinate in tablet

dosage form. J. Chem. Pharm. Res. 2013, 5 (Copyright (C) 2013 American Chemical Society (ACS). All Rights Reserved.), 215-228.

67. Ahmed, M.; Jamadar, N.; Shetty, A. S. Simultaneous estimation of Atenolol and Hydrochlorothiazide in combined dosage form by UV-spectrophotometric methods. Acta Chim. Pharm. Indica 2012, 2 (Copyright (C) 2013 American Chemical Society (ACS). All Rights Reserved.), 134-142.

68. Galande, V. R.; Baheti, K. G.; Indraksha, S.; Dehghan, M. H. Estimation of Amlodipine Besylate, Valsartan and Hydrochlorothiazide in Bulk Mixture and Tablet by UV Spectrophotometry. Indian J. Pharm. Sci. 2012, 74 (1), 18-23.

69. Nikam, M. B.; Dhamane, H.; Aligave, A.; Kondawar, M. S. Simultaneous estimation of valsartan, amlodipine besylate and hydrochlorothiazide by first order derivative UV spectrophotometric method. Int. J. Pharm. Technol. 2010, 2 (Copyright (C) 2013 American Chemical Society (ACS). All Rights Reserved.), 642-650.

70. Abd, E. K. M.; El, G. A. E.; Hegazy, M.; Shokry, E. S. Novel spectrophotometric method for simultaneous determination of two binary mixtures containing hydrochlorothiazide by ratio subtraction. J. Appl. Sci. Res. 2010, 6 (Copyright (C) 2013 American Chemical Society (ACS). All Rights Reserved.), 918-926.

71. Ezzeldin, M. I.; Shokry, E.; Fouad, M. A.; Elbagary, R. I. Application of Chromatographic and Spectrophotometric Methods for The Analysis of Aliskiren and Hydrochlorothiazide Antihypertensive Combination. Int. J. Adv. Chem. 2013, 1 (2), 13-20.

72. Srivastava, B.; Bhatt, P. D.; Akhtar, J. Validated spectrophotometric method for simultaneous estimation of hydrochlorothiazide and candesartan cilexetil in tablet dosage form. J. Pharm. Res. 2011, 10 (Copyright (C) 2013 American Chemical Society (ACS). All Rights Reserved.), 106-108.

73. Erk, N. Application of first derivative UV-spectrophotometry and ratio derivative spectrophotometry for the simultaneous determination of candesartan cilexetil and hydrochlorothiazide. Pharmazie 2003, 58 (Copyright (C) 2013 American Chemical Society (ACS). All Rights Reserved.), 796-800.

74. Maguregui, M. I.; Jimenez, R. M.; Alonso, R. M. Simultaneous determination of the β-blocker atenolol and several complementary antihypertensive agents in pharmaceutical formulations and urine by capillary zone electrophoresis. J. Chromatogr. Sci. 1998, 36 (Copyright (C) 2013 American Chemical Society (ACS). All Rights Reserved.), 516-522.

75. Hillaert, S.; Van, d. B. W. Simultaneous determination of hydrochlorothiazide and several angiotensin-II-receptor antagonists by capillary electrophoresis. J. Pharm. Biomed. Anal. 2003, 31 (Copyright (C) 2013 American Chemical Society (ACS). All Rights Reserved.), 329-339.

76. Sangoi, M. S.; Wrasse-Sangoi, M.; Oliveira, P. R.; Rolim, C. M. B.; Steppe, M. Simultaneous determination of aliskiren and hydrochlorothiazide from their pharmaceutical preparations using a validated stability-indicating MEKC method. J. Sep. Sci. 2011, 34 (15), 1859-1866.

77. Bonanni, L.; Dalla Vestra, M. Oral renin inhibitors in clinical practice: a perspective review. Therapeutic advances in chronic disease 2012, 3 (4), 173-81.

78. Sarkar, A. K.; Ghosh, D.; Das, A.; Selvan, P. S.; Gowda, K. V.; Mandal, U.; Bose, A.; Agarwal, S.; Bhaumik, U.; Pal, T. K. Simultaneous determination of metoprolol succinate and amlodipine besylate in human plasma by liquid chromatography-tandem mass spectrometry method and its application in bioequivalence study. Journal of chromatography. B, Analytical technologies in the biomedical and life sciences 2008, 873 (1), 77-85.

79. Abdollahpour, N.; Asoodeh, A.; Saberi, M. R.; Chamani, J. Separate and simultaneous binding effects of aspirin and amlodipine to human serum albumin based on fluorescence spectroscopic and molecular modeling characterizations: A mechanistic insight for determining usage drugs doses. Journal of Luminescence 2011, 131 (9), 1885-1899.

80. Tengli, A. R.; Gurupadayya, B. M.; Soni, N. Simultaneous estimation of hydrochlorothiazide, amlodipine, and losartan in tablet dosage form by RP-HPLC. International Journal of Chemical and Analytical Science 2013, 4 (1), 33-38.

81. Ferdinand, K. C.; Weitzman, R.; Israel, M.; Lee, J.; Purkayastha, D.; Jaimes, E. A. Efficacy and safety of aliskiren-based dual and triple combination therapies in US minority patients with stage 2 hypertension. Journal of the American Society of Hypertension : JASH 2011, 5 (2), 102-13.

82. Wrasse-Sangoi, M.; Sangoi, M. S.; Oliveira, P. R.; Secretti, L. T.; Rolim, C. M. Determination of aliskiren in tablet dosage forms by a validated stability-indicating RP-LC method. Journal of chromatographic science 2011, 49 (2), 170-5.

83. Swamy, G. K.; Rao, J. V. L. N. S.; Kumar, J. M. R.; Kumar, U. A.; Bikshapathi, D. V. R. N.; kumar, D. V. Analytical method development and validation of aliskiren in bulk and tablet dosage form by RP-HPLC method. Journal of Pharmacy Research 2011, 4 (3), 865-867.

84. Babu, K. S.; Rao, J. V. L. N. S.; Bhargava, K. V. A simple and sensitive method for the determination of aliskiren hemifumarate using HPLC-UV detection. Rasayan Journal of Chemistry 2011, 4 (2), 285-288.

85. pachauri, S.; paliwal, S.; Kona.S.Srinivas; YogendraSingh; Jain, V. Development & validation of HPLC method for analysis of some antihypertensive agents in their pharmaceutical dosage forms. J Pharm Sci & Res 2010, Vol.2 (8), 459-464.

86. Sangoi, M. S.; Wrasse-Sangoi, M.; Oliveira, P. R.; Rolim, C. M. B.; Steppe, M. Simultaneous determination of aliskiren and hydrochlorothiazide from their pharmaceutical preparations using a validated stability-indicating MEKC method. Separation Science 2011, 34 (15), 1859–1866.

87. WS, M.; TS, L.; FD, I.; MB, C. Development and validation of an UV spectrophotometric method for the determination of aliskiren in tablets. Quim. Nova 2010, 33 (6), 1330-1334.

88. Swamy, K. G.; Kumar, J. M. R.; Sheshagirirao, J. V. L. N.; Kumar, D. V.; RatnaMani, C.; Kumar, V. N. V. E. Validated spectrophotometric determination of Aliskiren in pharmaceutical dosage form. Journal of Pharmacy Research 2011, 4 (8), 2574-2575.

89. Aydogmus, Z. Spectrofluorimetric determination of aliskiren in dosage forms and urine. J Lumin 2012, 27 (6), 489-94.

90. Aydogmus, Z.; Sari, F.; Ulu, S. T. Spectrofluorimetric determination of aliskiren in tablets and spiked human plasma through derivatization with dansyl chloride. Journal of fluorescence 2012, 22 (2), 549-56.

91. Sharma, M.; Kothari, C.; Sherikar, O.; Mehta, P. Concurrent Estimation of Amlodipine Besylate, Hydrochlorothiazide and Valsartan by RP-HPLC, HPTLC and UV-Spectrophotometry Journal of chromatographic science [Online], 2013. DOI: 10.1093/chromsci/bms200. http://www.ncbi.nlm.nih.gov/pubmed/23293040 (accessed Jan 4).

92. Patel, D. B.; Mehta, F. A.; Bhatt, K. K. Simultaneous Estimation of Amlodipine Besylate and Indapamide in a Pharmaceutical Formulation by a High Performance Liquid Chromatographic (RP-HPLC) Method. Scientia pharmaceutica 2012, 80 (3), 581-90.

93. Jain, P. S.; Patel, M. K.; Gorle, A. P.; Chaudhari, A. J.; Surana, S. J. Stability-indicating method for simultaneous estimation of olmesartan medoxomile, amlodipine besylate and hydrochlorothiazide by RP-HPLC in tablet dosage form. Journal of chromatographic science 2012, 50 (8), 680-7.

94. Fakhari, A. R.; Nojavan, S.; Haghgoo, S.; Mohammadi, A. Development of a stability-indicating CE assay for the determination of amlodipine enantiomers in commercial tablets. Electrophoresis 2008, 29 (22), 4583-92.

95. Wankhede, S. B.; Raka, K. C.; Wadkar, S. B.; Chitlange, S. S. Spectrophotometric and HPLC methods for simultaneous estimation of amlodipine besilate, losartan potassium and hydrochlorothiazide in tablets. Indian journal of pharmaceutical sciences 2010, 72 (1), 136-40.

96. Rahman, N.; Nasrul Hoda, M. Validated spectrophotometric methods for the determination of amlodipine besylate in drug formulations using 2,3-dichloro 5,6-dicyano 1,4-benzoquinone and ascorbic acid. J Pharm Biomed Anal 2003, 31 (2), 381-92.

97. Rahman, N.; Azmi, S. N. Spectrophotometric method for the determination of amlodipine besylate with ninhydrin in drug formulations. Farmaco 2001, 56 (10), 731-5.

98. Shaalan, R. A.; Belal, T. S. Simultaneous spectrofluorimetric determination of amlodipine besylate and valsartan in their combined tablets. Drug testing and analysis 2010, 2 (10), 489-93.

99. Darwish, H. W.; Backeit, A. H. Multivariate versus classical univariate calibration methods for spectrofluorimetric data: application to simultaneous determination of olmesartan medoxamil and amlodipine besylate in their combined dosage form. Journal of fluorescence 2013, 23 (1), 79-91.

100. Hertzog, D. L.; McCafferty, J. F.; Fang, X.; Tyrrell, R. J.; Reed, R. A. Development and validation of a stability-indicating HPLC method for the simultaneous determination of

losartan potassium, hydrochlorothiazide, and their degradation products. J Pharm Biomed Anal 2002, 30 (3), 747-60.

101. Sharma, R. N.; Pancholi, S. S. Simple RP-HPLC method for determination of triple drug combination of valsartan, amlodipine and hydrochlorothiazide in human plasma. Acta Pharm 2012, 62 (1), 45-58.

102. Joshi, S. J.; Karbhari, P. A.; Bhoir, S. I.; Bindu, K. S.; Das, C. RP-HPLC method for simultaneous estimation of bisoprolol fumarate and hydrochlorothiazide in tablet formulation. J Pharm Biomed Anal 2010, 52 (3), 362-71.

103. Meyyanathan, S. N.; Rajan, S.; Muralidharan, S.; Birajdar, A. S.; Suresh, B. A Validated RP-HPLC Method for Simultaneous Estimation of Nebivolol and Hydrochlorothiazide in Tablets. Indian journal of pharmaceutical sciences 2008, 70 (5), 687-9.

104. Tian, D. F.; Tian, X. L.; Tian, T.; Wang, Z. Y.; Mo, F. K. Simultaneous Determination of Valsartan and Hydrochlorothiazide in Tablets by RP-HPLC. Indian journal of pharmaceutical sciences 2008, 70 (3), 372-4.

105. Huang, T.; He, Z.; Yang, B.; Shao, L.; Zheng, X.; Duan, G. Simultaneous determination of captopril and hydrochlorothiazide in human plasma by reverse-phase HPLC from linear gradient elution. J Pharm Biomed Anal 2006, 41 (2), 644-8.

106. Bharathi, D. V.; Hotha, K. K.; Chatki, P. K.; Satyanarayana, V.; Venkateswarlu, V. LC-MS/MS method for simultaneous estimation of candesartan and hydrochlorothiazide in human plasma and its use in clinical pharmacokinetics. Bioanalysis 2012, 4 (10), 1195-204.

107. Salvadori, M. C.; Moreira, R. F.; Borges, B. C.; Andraus, M. H.; Azevedo, C. P.; Moreno, R. A.; Borges, N. C. Simultaneous determination of losartan and hydrochlorothiazide in human plasma by LC/MS/MS with electrospray ionization and its application to pharmacokinetics. Clin Exp Hypertens 2009, 31 (5), 415-27.

108. Rajasekhar, D.; Kumara, I. J.; Venkateswarlu, P. High performance liquid chromatography/negative ion electrospray tandem mass spectrometry method for the measurement of hydrochlorothiazide in human plasma: application to a comparative bioavailability study. Eur J Mass Spectrom (Chichester, Eng) 2009, 15 (6), 715-21.

109. Liu, F.; Xu, Y.; Gao, S.; Zhang, J.; Guo, Q. Determination of hydrochlorothiazide in human plasma by liquid chromatography/tandem mass spectrometry. J Pharm Biomed Anal 2007, 44 (5), 1187-91.

110. nalwade, S.; reddy, V. r.; rao, D. d.; rao, I. k. Rapid simultaneous determination of telmisartan, amlodipine besylate and hydrochlorothiazide in a combined poly pill dosage form by stability-indicating ultra performance liquid chromatography. Scientia pharmaceutica 2011, 79, 69–84.

111. El-Gindy, A.; Ashour, A.; Abdel-Fattah, L.; Shabana, M. M. Spectrophotometric and HPTLC-densitometric determination of lisinopril and hydrochlorothiazide in binary mixtures. J Pharm Biomed Anal 2001, 25 (5-6), 923-31.

112. Alagar Raja, M.; Ragavendra, P.; Banji, D.; Rao, K. N. V.; Chaithanya, Y.; Anusha, B.; Selvakumar, D. RP-HPLC Method for Simultaneous Estimation of Aliskiren Hemi

fumarate, Hydrochlorothiazide and Amlodipine in Pharmaceutical bulk drugs and Tablet dosage form. J Pharm Res 2012, 5 (8), 4580-4584.

113. Swamy, G. K.; P.Sravanthi; Surekha, M. L.; Kumar, J.; Rao, J. Validated RP-HPLC Method For The Simultaneous Determination Of Aliskiren, Hydrochlorothiazide And Amlodipine Besylate In Bulk And Pharmaceutical

Formulations. Int J ChemTech Res 2012, 4 (4), 1666-1673.

114. ICH Topic Q2B Note for Guidance on Validation of Analytical Procedures: Methodology. http://www.uam.es/personal_pas/txrf/MU5.pdf.

115. The British Pharmacopoeia 2007, The Stationery Office: London; Electronic version [Online].

116. The United States Pharmacopeal Convention. The United States Pharmacopoeia (USP 30), National Formulary (NF 25), Asian edition. Rockville, Maryland (USA) 2007, pp. 2287 and 251.

117. Bonanni, L.; Vestra, M. D. Oral renin inhibitors in clinical practice: a perspective review. Therapeutic Advances in Chronic Disease 2012, 3 (4), 173-181.

118. Sarkar, A. K.; Ghosh, D.; Das, A.; Selvan, P. S.; Gowda, K. V.; Mandal, U.; Bose, A.; Agarwal, S.; Bhaumik, U.; Pal, T. K. Simultaneous determination of metoprolol succinate and amlodipine besylate in human plasma by liquid chromatography-tandem mass spectrometry method and its application in bioequivalence study. Journal of

chromatography. B, Analytical technologies in the biomedical and life sciences 2008, 873 (1), 77-85.

119. Abdollahpoura, N.; Asoodehb, A.; Saberic, M. R.; Chamani, J. Separate and simultaneous binding effects of aspirin and amlodipine to human serum albumin based on fluorescence spectroscopic and molecular modeling characterizations: A mechanistic insight for determining usage drugs doses. Luminescence 2011, 131 (9), 1885-1899.

120. Ferdinand, K. C.; Weitzman, R.; Israel, M.; Lee, J.; Purkayastha, D.; Jaimes, E. A. Efficacy and safety of aliskiren-based dual and triple combination therapies in US minority patients with stage 2 hypertension. Journal of the American Society of Hypertension 2011, 5 (2), 102-113.

121. Wrasse-Sangoi, M.; Sangoi, M. S.; Oliveira, P. R.; Secretti, L. T.; Rolim, C. M. Determination of aliskiren in tablet dosage forms by a validated stability-indicating RP-LC method. Journal of chromatographic science 2011, 49 (2), 170-175.

122. Babu, K. S.; Rao, J. V. L. N. S.; Bhargava, K. V. A simple and sensitive method for the determination of aliskiren hemifumarate using HPLC-UV detection. Rasayan Journal of Chemistry 2011, 4 (2), 285-288.

123. Pachauria, S.; Paliwal, S.; Srinivas, K.; Singha, Y.; Jain, V. Development & validation of HPLC method for analysis of some antihypertensive agents in their pharmaceutical dosage forms. Journal of Pharmaceutical Science and Research 2010, 2 (8), 459-464.

124. Belal, F.; Walash, M.; El-Enany, N.; Zayed, S. Highly sensitive HPLC method for assay of aliskiren in human plasma through derivatization with 1-naphthyl isocyanate using UV

detection. Journal of chromatography. B, Analytical technologies in the biomedical and life sciences 2013, 933, 24-29.

125. REKULAPALLY, V. K.; RAO, V. U. Stability indicating RP-HPLC method development and validation for simultaneous of Aliskiren, amlodipine and hydrochlorothiazide in tablet dosage form. International Journal of Pharmacy and Pharmaceutical Sciences 2014, 6 (1), 724-730.

126. Belal, F.; Walash, M.; El-Enany, N.; Zayed, S. Simultaneous determination of aliskiren and hydrochlorothiazide in tablets and spiked human urine by ion-pair liquid chromatography. Pharmazie 2013, 68 (12), 933-938.

127. Sangoi, M. S.; Wrasse-Sangoi, M.; Oliveira, P. R.; Rolim, C. M. B.; Steppe, M. Simultaneous determination of aliskiren and hydrochlorothiazide from their pharmaceutical preparations using a validated stability-indicating MEKC method. Journal of Separation Science 2011, 34 (15), 1859-1866.

128. Wrasse-Sangoi, M.; Secretti, L. T.; Diefenbach, I. F.; Rolim, C. M. B.; Sangoi, M. d. S. Development and validation of an UV spectrophotometric method for the determination of aliskiren in tablets. Química Nova 2010, 33, 1330-1334.

129. Swamy, K. G.; Kumar, J. M. R.; Sheshagirirao, J. V. L. N.; Kumar, D. V.; RatnaMani, C.; Kumar, V. N. V. E. Validated spectrophotometric determination of Aliskiren in pharmaceutical dosage form. Journal of Pharmacy Research 2011, 4 (8), 2574-2575.

130. Aydogmus, Z. Spectrofluorimetric determination of aliskiren in dosage forms and urine. Luminescence 2012, 27 (6), 489-494.

131. Aydogmus, Z.; Sari, F.; Ulu, S. T. Spectrofluorimetric determination of aliskiren in tablets and spiked human plasma through derivatization with dansyl chloride. Journal of fluorescence 2012, 22 (2), 549-556.

132. Ezzeldin, M. I.; Shokry, E.; Fouad, M. A.; Elbagary, R. I. Application of Chromatographic and Spectrophotometric Methods for The Analysis of Aliskiren and Hydrochlorothiazide Antihypertensive Combination. International Journal of Advanced Chemistry 2013, 1 (2), 13-20.

133. Sharma, M.; Kothari, C.; Sherikar, O.; Mehta, P. Concurrent Estimation of Amlodipine Besylate, Hydrochlorothiazide and Valsartan by RP-HPLC, HPTLC and UV-Spectrophotometry Journal of chromatographic science [Online], 2013. DOI: 10.1093/chromsci/bms200. http://www.ncbi.nlm.nih.gov/pubmed/23293040 (accessed Jan 4).

134. Patel, D. B.; Mehta, F. A.; Bhatt, K. K. Simultaneous Estimation of Amlodipine Besylate and Indapamide in a Pharmaceutical Formulation by a High Performance Liquid Chromatographic (RP-HPLC) Method. Scientia pharmaceutica 2012, 80 (3), 581-590.

135. Jain, P. S.; Patel, M. K.; Gorle, A. P.; Chaudhari, A. J.; Surana, S. J. Stability-indicating method for simultaneous estimation of olmesartan medoxomile, amlodipine besylate and hydrochlorothiazide by RP-HPLC in tablet dosage form. Journal of Chromatographic Science 2012, 50 (8), 680-687.

136. Fakhari, A. R.; Nojavan, S.; Haghgoo, S.; Mohammadi, A. Development of a stability-indicating CE assay for the determination of amlodipine enantiomers in commercial tablets. Electrophoresis 2008, 29 (22), 4583-4592.

137. Wankhede, S. B.; Raka, K. C.; Wadkar, S. B.; Chitlange, S. S. Spectrophotometric and HPLC methods for simultaneous estimation of amlodipine besilate, losartan potassium and hydrochlorothiazide in tablets. Indian journal of pharmaceutical sciences 2010, 72 (1), 136-140.

138. Rahman, N.; Nasrul Hoda, M. Validated spectrophotometric methods for the determination of amlodipine besylate in drug formulations using 2,3-dichloro 5,6-dicyano 1,4-benzoquinone and ascorbic acid. Journal of pharmaceutical and biomedical analysis 2003, 31 (2), 381-392.

139. Rahman, N.; Azmi, S. N. Spectrophotometric method for the determination of amlodipine besylate with ninhydrin in drug formulations. Farmaco 2001, 56 (10), 731-735.

140. Shaalan, R. A.; Belal, T. S. Simultaneous spectrofluorimetric determination of amlodipine besylate and valsartan in their combined tablets. Drug testing and analysis 2010, 2 (10), 489-493.

141. Darwish, H. W.; Backeit, A. H. Multivariate versus classical univariate calibration methods for spectrofluorimetric data: application to simultaneous determination of olmesartan medoxamil and amlodipine besylate in their combined dosage form. Journal of fluorescence 2013, 23 (1), 79-91.

142. Hertzog, D. L.; McCafferty, J. F.; Fang, X.; Tyrrell, R. J.; Reed, R. A. Development and validation of a stability-indicating HPLC method for the simultaneous determination of losartan potassium, hydrochlorothiazide, and their degradation products. Journal of pharmaceutical and biomedical analysis 2002, 30 (3), 747-760.

143. Sharma, R. N.; Pancholi, S. S. Simple RP-HPLC method for determination of triple drug combination of valsartan, amlodipine and hydrochlorothiazide in human plasma. Acta Pharmaceutica 2012, 62 (1), 45-58.

144. Joshi, S. J.; Karbhari, P. A.; Bhoir, S. I.; Bindu, K. S.; Das, C. RP-HPLC method for simultaneous estimation of bisoprolol fumarate and hydrochlorothiazide in tablet formulation. Journal of pharmaceutical and biomedical analysis 2010, 52 (3), 362-371.

145. Meyyanathan, S. N.; Rajan, S.; Muralidharan, S.; Birajdar, A. S.; Suresh, B. A Validated RP-HPLC Method for Simultaneous Estimation of Nebivolol and Hydrochlorothiazide in Tablets. Indian journal of pharmaceutical sciences 2008, 70 (5), 687-689.

146. Tian, D. F.; Tian, X. L.; Tian, T.; Wang, Z. Y.; Mo, F. K. Simultaneous Determination of Valsartan and Hydrochlorothiazide in Tablets by RP-HPLC. Indian journal of pharmaceutical sciences 2008, 70 (3), 372-374.

147. Huang, T.; He, Z.; Yang, B.; Shao, L.; Zheng, X.; Duan, G. Simultaneous determination of captopril and hydrochlorothiazide in human plasma by reverse-phase HPLC from linear gradient elution. Journal of pharmaceutical and biomedical analysis 2006, 41 (2), 644-648.

148. Bharathi, D. V.; Hotha, K. K.; Chatki, P. K.; Satyanarayana, V.; Venkateswarlu, V. LC-MS/MS method for simultaneous estimation of candesartan and hydrochlorothiazide in

human plasma and its use in clinical pharmacokinetics. Bioanalysis 2012, 4 (10), 1195-1204.

149. Salvadori, M. C.; Moreira, R. F.; Borges, B. C.; Andraus, M. H.; Azevedo, C. P.; Moreno, R. A.; Borges, N. C. Simultaneous determination of losartan and hydrochlorothiazide in human plasma by LC/MS/MS with electrospray ionization and its application to pharmacokinetics. Clinical and Experimental Hypertension 2009, 31 (5), 415-427.

150. Rajasekhar, D.; Kumara, I. J.; Venkateswarlu, P. High performance liquid chromatography/negative ion electrospray tandem mass spectrometry method for the measurement of hydrochlorothiazide in human plasma: application to a comparative bioavailability study. European journal of mass spectrometry 2009, 15 (6), 715-721.

151. Liu, F.; Xu, Y.; Gao, S.; Zhang, J.; Guo, Q. Determination of hydrochlorothiazide in human plasma by liquid chromatography/tandem mass spectrometry. Journal of pharmaceutical and biomedical analysis 2007, 44 (5), 1187-1191.

152. Nalwade, S.; Ranga Reddy, V.; Durga Rao, D.; Koteswara Rao, I. Rapid simultaneous determination of telmisartan, amlodipine besylate and hydrochlorothiazide in a combined poly pill dosage form by stability-indicating ultra performance liquid chromatography. Scientia pharmaceutica 2011, 79 (1), 69-84.

153. El-Gindy, A.; Ashour, A.; Abdel-Fattah, L.; Shabana, M. M. Spectrophotometric and HPTLC-densitometric determination of lisinopril and hydrochlorothiazide in binary mixtures. Journal of pharmaceutical and biomedical analysis 2001, 25 (5-6), 923-931.

154. Alagar Raja, M.; Ragavendra, P.; Banji, D.; Rao, K. N. V.; Chaithanya, Y.; Anusha, B.; Selvakumar, D. RP-HPLC Method for Simultaneous Estimation of Aliskiren Hemi fumarate, Hydrochlorothiazide and Amlodipine in Pharmaceutical bulk drugs and Tablet dosage form. Journal of Pharmacy Research 2012, 5 (8), 4580-4584.

155. Swamy, G. K.; P.Sravanthi; Surekha, M. L.; Kumar, J.; Rao, J. Validated RP-HPLC Method For The Simultaneous Determination Of Aliskiren, Hydrochlorothiazide And Amlodipine Besylate In Bulk And Pharmaceutical Formulations. International Journal of ChemTech Research 2012, 4 (4), 1666-1673.

156. El-Bagary, R.; Patonay, G.; Elzahr, A.; Elkady, E.; Ebeid, W. Ion-Pair LC Method for Simultaneous Determination of Aliskiren Hemifumarate, Amlodipine Besylate and Hydrochlorothiazide in Pharmaceuticals. Chromatographia 2014, 77 (3-4), 257-264.

157. Salim, M. M.; Ebeid, W. M.; El-Enany, N.; Belal, F.; Walash, M.; Patonay, G. Simultaneous determination of aliskiren hemifumarate, amlodipine besylate, and hydrochlorothiazide in their triple mixture dosage form by capillary zone electrophoresis. Journal of Separation Science 2014, n/a-n/a.

158. Guidance for Industry: Bioanalytical Method Validation, U.S. Department of Health and Human Services, Food and Drug Administration Centre for Drug Evaluation and Research (CDER), Center for Veternary Medicine (CVM). 2001.

159. Sherwood, C. A.; Eastham, A.; Lee, L. W.; Risler, J.; Mirzaei, H.; Falkner, J. A.; Martin, D. B. Rapid optimization of MRM-MS instrument parameters by subtle alteration of precursor and product m/z targets. Journal of proteome research 2009, 8 (7), 3746-3751.

160. Vaidyanathan, S.; Jermany, J.; Yeh, C.; Bizot, M. N.; Camisasca, R. Aliskiren, a novel orally effective renin inhibitor, exhibits similar pharmacokinetics and pharmacodynamics in Japanese and Caucasian subjects. British journal of clinical pharmacology 2006, 62 (6), 690-8.

161. Mascoli, V.; Kuruganti, U.; Bapuji, A. T.; Wang, R.; Damle, B. Pharmacokinetics of a novel orodispersible tablet of amlodipine in healthy subjects. J. Bioequivalence Bioavailability 2013, 5 (Copyright (C) 2014 American Chemical Society (ACS). All Rights Reserved.), 76-79.

162. Patel, R. B.; Patel, U. R.; Rogge, M. C.; Shah, V. P.; Prasad, V. K.; Selen, A.; Welling, P. G. Bioavailability of hydrochlorothiazide from tablets and suspensions. J Pharm Sci 1984, 73 (3), 359-61.

2 SEPARATION AND DETERMINATION OF SELECTED PHARMACEUTICAL COMPOUNDS USING CAPILLARY ELECTROPHORESIS

2.1 Introduction

Capillary electrophoresis (CE) is a separation technique depends on different migration of solutes in an electric field. Electrophoresis is performed in narrow-bore capillaries filled with background electrolyte (BGE). Driving forces in CE are electrophoretic migration and the electro-osmotic flow (EOF) [1, 2].

Compared with other techniques, the instrumentation of CE is simple consisting of electrodes, sample introduction systems, a capillary column, a power supply, a detector, and liquid-handling systems. Detection can be achieved with on-line (UV/diode-array spectrophotometric, spectrofluorimetric or electrochemical detectors) or external detectors (mass spectrometer) [3].

There are five major modes of operation of CE: capillary zone electrophoresis (CZE, based on analytes' charge-to-size ratios) also referred to as free solution or free flow capillary electrophoresis, micellar electrokinetic chromatography (MEKC, based on chromatographic partition of analytes between micelles and the BGE), capillary isoelectric focusing (CIEF, based on analytes' isoelectric points), capillary gel electrophoresis (CGE, based on analytes' size/molecular weight ratio) and capillary isotachophoresis (CITP, based on moving boundaries) [3, 4].

Separation in CZE mode is based upon differences in charge-to-size ratios for each analyte in the sample. The larger this ratio, the higher the mobility and the faster an ion migrates in the applied electrical field [2]. The migration velocity *v* of an ion (cm/sec) in an electric field is

equal to the product of the field strength *E* and the electrophoretic mobility μ_{ep}. The electrophoretic mobility is in turn proportional to the ionic charge on the analyte and inversely proportional to frictional retarding factors. The electric field acts only on ions [4]. If two ionized species differ either in charge or in the frictional forces they experience in moving through the buffer because of the structural variations, they will migrate in a different velocity and separate from each other. Neutral species are not separated using CZE. When a high potential is applied across a capillary column containing a BGE, EOF is usually produced, in which the BGE migrates toward the cathode or the anode. EOF is caused by the electric double layer that occurs at the silica/solution interface. Above pH 3, the inside wall of a silica capillary is negatively charged due to ionization of the surface silanol groups (Si-OH). Buffer cations accumulate in an electrical double layer adjacent to the negative surface of the silica capillary. The cations in the diffuse outer layer are attracted toward the cathode dragging the bulk solvent along with them. The rate of EOF is generally higher than the electrophoretic migration nobilities of the analyzed ions [2, 4]. Figure (1) represents a simplified diagram of CZE system [5].

Capillary electrophoresis has grown from a simple to a sophisticated method because of several innovations during recent decades. This growth has expanded applications of CE to various analytes including pharmaceuticals.

A major advantage of CE is the availability of various modes, which enable the separation and analysis of different compounds ranging from inorganic species to biopolymers. It is well accepted that CZE and MEKC are still mainly employed for drug analysis. Nevertheless, various techniques have been established to improve CE selectivity, sensitivity, efficiency, applicability, or flexibility.

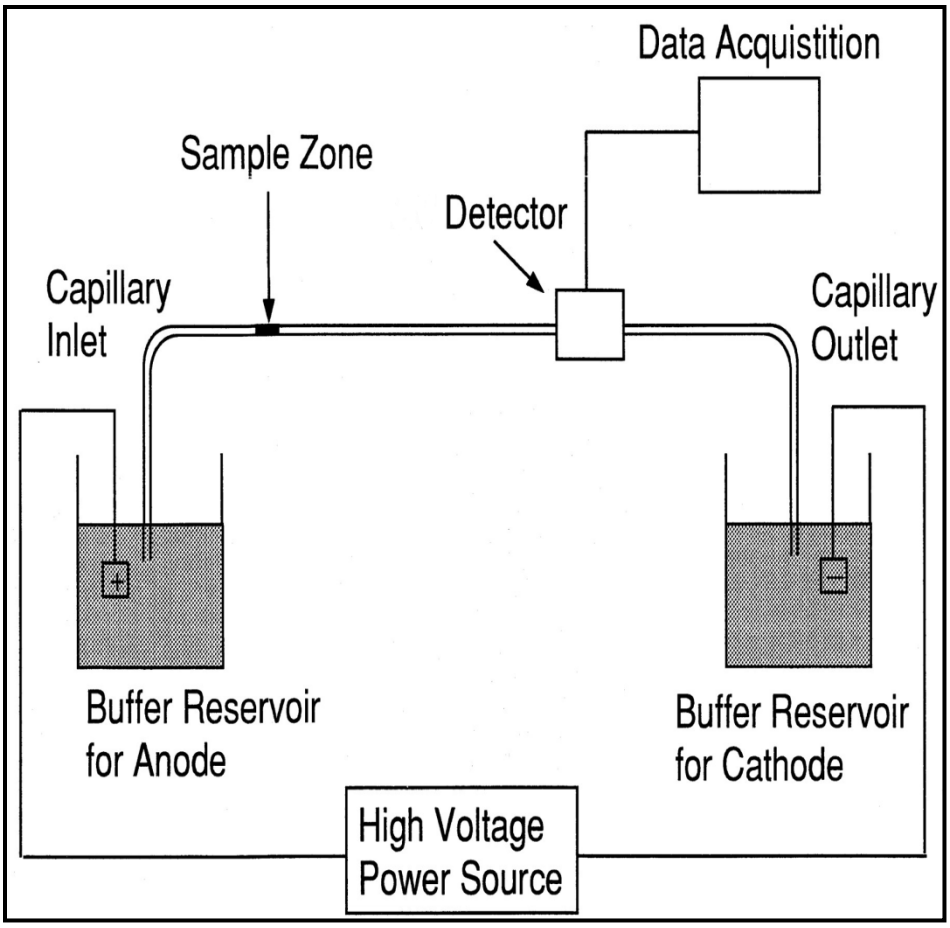

Figure 2.1.1 Simplified diagram for typical CE Instrument Configuration

Numerous applications of CE in drug analysis are reported daily and reviews on CE for drug analysis are regularly published. In 2011, Hendrickx et al. [6] surveyed the applicability of capillary electrophoresis to analyze drug impurity mixtures, formulations, biological samples, and chiral compounds. Suntornsuk [3] reviewed the recent advances of CE in pharmaceutical analysis and their applications in assay of active pharmaceutical ingredients, drug impurity testing, chiral drug separation, and determination in biological fluids between 2008 to 2009. In 2009, Gilpin and Gilpin [7] reported separation-based (including CE), and other methods for analysis of active ingredients and related drugs in bulk and formulations during 2007 - 2008.

Separation Science and Technology published a series of reviews on CE including the role of CE in drug substance and drug product development [8], the need for CE methods in pharmacopeial monographs [9], CE in impurity profiling of drugs [10], and the role of CE in biopharmaceutical development and quality control [11]. In 2007, Suntornsuk [12] surveyed recent applications of CE in pharmaceutical analysis published during 2005–2007. Altria et al. [13] reviewed use of CE for analysis of small-molecule pharmaceuticals in 2006. CE reviews on some classes of drugs have also been published, for example metal-based drugs [14], and sulfonamides [15].

2.2 Simultaneous determination of valsartan, amlodipine besylate and hydrochlorothiazide using capillary zone electrophoresis (CZE)

Pharmazie (2015) 70: 368–373

DOI 10.1691/ph.2015.4134

A capillary zone electrophoresis method was developed for simultaneous determination of valsartan (VAL), amlodipine besylate (AML) and hydrochlorothiazide (HCZ) in their combined tablets. Separation was achieved on fused silica capillary by applying a potential of 15 kV (positive polarity) and a running buffer containing 40 mM phosphate buffer at pH 7.5 with UV detection at 230 nm. The samples were injected hydrodynamically for 3 s at 0.5 psi and the temperature of the capillary cartridge was kept at 25 °C. Pyrazinoic acid was used as an internal standard. The method was validated according to ICH guidelines regarding specificity, linearity, limits of detection and quantitation, accuracy and precision. The method showed satisfactory linearity in the ranges of 10-200, 2-20 and 2-20 µg mL^{-1} with LODs of 1.82, 0.39, 0.65 µg mL^{-1} and LOQs of 5.51, 1.17, 1.96 µg mL^{-1} for VAL, AML and HCZ, respectively. The proposed method was successfully applied for the analysis of the studied drugs in their laboratory prepared mixtures and co-formulated tablets. The results were compared with reported methods and no significant difference was found statistically. The proposed method can be used for quality control of the cited medications in ordinary laboratories.

2.2.1 Introduction

Valsartan (VAL) chemically, (S)-N-valeryl-N-([2'-(1H-tetrazol-5-yl)biphenyl-4-yl]-methyl)-vali ne (Fig. 2.2.1a), is a potent, highly selective, and orally active non peptide

antagonist on AT1-receptor subtype [16]. Angiotensin receptor blockers are a major class of antihypertensive therapies due to their powerful lowering effects on blood pressure and excellent tolerability [17]. Amlodipine besylate (AML), (3-Ethyl 5-methyl (4RS)-2-[(2-aminoethoxy)methyl]-4-(2-chlorophenyl)-6-methyl-1,4-dihydropyridine-3,5-dicarboxylate benzenesulphonate) (Fig.2.2.1b) is a long acting dihydropyridine calcium channel blocker that prevents the transmembrane influx of calcium ions into vascular smooth muscles and cardiac muscles [18]. Also, it is a direct peripheral arterial vasodilator that reduces peripheral vascular resistance and hence lowers blood pressure [19]. Hydrochlorothiazide (HCZ) is an orally potent diuretic and antihypertensive agent which inhibits active chloride reabsorption and thus increases the excretion of sodium chloride and water [20]. It is chemically 6-chloro-1, 1-dichloro-3, 4, dihydro -2H-1, 2, 4-benzothiadiazine-7-sulphanomide1, 1-dioxide (Fig.2.2.1c). Triple combination therapy of VAL, AML and HCZ proved to be effective and well tolerated in treating hypertensive high-risk patients [21]. Literature survey revealed methods using HPLC [22-24], LC-MS [25-27], CE [28, 29], UV spectrophotometric [30, 31] and spectroflourimetric [32] techniques reported for estimation of VAL either alone or in combination with other agents. Methods such as HPLC [33-35], LC/MS/MS [36, 37], CE [38], UV-spectrophotometry [39-41] and spectroflourimetry [32, 42] are reported for estimation of AML either alone or in combination with other agents. Also, methods such as HPLC [43-48], LC-MS [49-51], UPLC [52] and UV- spectrophotometry [53] are reported for the estimation of HCZ alone or in combination with other anti-hypertensive agents. There are many methods reported for the simultaneous determination of the three medications in different matrices such as HPLC [44, 54, 55], and UV-spectrophotometry [56]. To the best of our knowledge, no capillary electrophoresis method was reported yet for the simultaneous determination of the studied medications either in pharmaceutical preparations or in biological fluids. CE has a lot of

proved successful applications in the field of pharmaceutical analysis such as assay of drugs, determination of impurities, chiral separation, and in the analysis of pharmaceutical excipients. The advantages of using CE for pharmaceutical analysis include its reliability and low cost of analysis, reductions in solvent consumption and disposal, and the possibility of rapid method development and feasibility of a high degree of automation. Moreover, CE allows a single set of separation conditions to be applied for a wide range of analyses, introducing efficiency savings [57, 58]. Recently, CE techniques have been applied for the simultaneous determination of co-formulated medication in their dosage forms [29, 38].

2.2.2 Investigation, results and discussion

The goal of this study was to develop and validate a reliable, accurate, inexpensive, selective and efficient method using capillary electrophoresis that could be used for routine quality control analysis of VAL, AML and HCZ simultaneously in their co-formulated tablets. VAL, AML and HCZ are co-formulated in a medicinally recommended ratio of 12.8:1.1:1. Analysis of such mixture with strong spectral overlapping is challenging. The proposed CZE method allowed the separation and simultaneous quantification of the three medications in a reasonable time less than 15 min with satisfactory accuracy and precision in their co-formulated dosage form.

Figure 2.2.2, shows a typical electropherogram for a laboratory prepared mixture of the three drugs under the described electrophoretic conditions. The migration times for VAL, AML and HCZ were 12.74, 5.21 and 6.45 min., respectively.

The proposed CZE method was applied to the simultaneous determination of VAL, AML and HCZ in laboratory prepared mixtures in the medicinally recommended ratio of 12.8:1.1:1. Furthermore, the proposed method was successfully applied for their determination in their co-

formulated tablets (Fig. 2.2.3). The results shown in (Tables 2.2.1, 2.2.2) are in good agreement with those obtained using the comparison method [55]. The comparison method was performed on RP-C18 column using a mobile phase consisting of acetonitrile: methanol: 50 mM phosphate buffer adjusted to pH 3 with orthophosphoric acid (20: 50: 30, v/v/v) at a flow rate of 1.0 mL min^{-1} in and the eluents were monitored at 239 nm. Statistical analysis of the results obtained using Student's t-test and variance ratio F-test revealed no significant difference between the performance of the methods regarding the accuracy and precision, respectively.

2.2.2.1 Optimization of the CE conditions

In CZE, the background electrolyte (BGE) type as well as its pH and its concentration are crucial for optimizing the separation of the ionizable analytes as they determine the degree of the analyte ionization, its electrophoretic mobility and the magnitude of the electroosmotic flow (EOF). As AML has pK_a value of 9.5 and HCZ has pK_a values of 8.8 and 9.9, they are positively charged at pH 7.5. On the other hand, VAL has pKa values of 3.6 and 4.7 and it is negatively charged at the same pH. Several capillaries of different length and internal diameter as well as different pHs and molarities of phosphate buffer were tested for CZE analysis and the results were evaluated taking into consideration different parameters such as migration time, resolution, peak shape, height, baseline noise and the electric current produced.

2.2.2.1.1 Effect of phosphate buffer pH

The effect of buffer pH was investigated within the range of 5.0–8.0 at a 40mM phosphate buffer concentration. Electropherograms showed in (Fig. 2.2.4) demonstrated that the four compounds needed longer time to be separated at pH lower than 6.5. Also, both resolution and migration times decreased with increasing the pH. Taking into consideration the ionization

percentage of the analytes, resolution, peak symmetry and migration time, pH 7.5 was selected as the optimum pH for separation (Fig. 2.2.4).

2.2.2.1.2 Effect of phosphate buffer concentration

Buffer concentration has also a significant effect on the separation performance through its influence on the EOF and the current produced in the capillary. The effect of phosphate running buffer concentrations was examined by varying the concentration from 5 to 50 mM with the increase in phosphate buffer concentration, both resolution and migration times increased. A 40mM concentration of phosphate buffer was chosen in order to achieve reliable electrolyte background for analysis while maintaining reasonable run time, good resolution and acceptable current (≈ 78μA), (Fig. 2.2.5).

2.2.2.1.3 Effect of applied voltage

The applied voltage effect was investigated under the optimized conditions selected above from 5 to 20 kV. As expected, increasing the applied voltage increases the EOF, leading to shorter separation time and higher efficiencies. However, lowering the applied voltage than 15 kV decreases the EOF so the separation time will be high and increasing the applied voltage exhibits higher currents and produces Joule's heating. To limit this heating inside the capillary, the maximum applied voltage was chosen from an Ohm's plot (current versus voltage) and it was found to be 15 kV (current (≈ 78μA)).

2.2.2.1.4 Effect of injection time

Injection time affects the peak width and peak height. Sample solutions were hydrodynamically injected at 0.5 psi while the injection time was varied from 1.0 to 4.0 s. After 3.0 s, the peak widths of VAL, HCZ and IS were increased and the peak shapes were deformed, so 3.0 s was selected as the optimum injection time, (Fig. 2.2.6).

2.2.2.1.5 Selection of the internal standard (IS)

The use of IS is recommended to compensate for injection errors, minor fluctuations effect of the migration time and improve the quantitative analysis. Then pyrazinoic acid was chosen as it possesses pK_a value 2.9 [59] and its molecular weight is less than VAL so it will be negatively charged under the optimized condition and as expected it eluted after VAL.

2.2.2.1.6 Selection of the detection wavelength

In order to optimize sensitivity and detection limit of the method, a multiwavelength detection system (190 – 300 nm) was used in the CE system. For simultaneous determination of VAL, AML and HCZ, reasonable detection sensitivities were obtained at 230 nm (bandwidth 20 nm), (Fig. 2.2.7, Table 2.2.3).

2.2.2.2 Validation of the method

Validation of the proposed CZE method was performed with respect to stability, linearity, range, specificity, limit of detection (LOD), limit of quantitation (LOQ), accuracy and precision according to the ICH Guidelines [http://www.fda.gov/downloads/Regulator%20yInformation/Guidances/UCM128049.pdf].

2.2.2.2.1 Linearity

A linear relationship was established by plotting the peak area ratio (the studied drug peak area/IS peak area) against the corresponding drug concentration in the range of 10–200, 2-20 and 2-20 µg mL^{-1} for VAL, AML and HCZ, respectively. Statistical analysis of the data gave high value for the correlation coefficient (r) of the regression equation, small values of the standard deviation of residuals ($S_{y/x}$), of intercept (S_a), and of slope (S_b), and small value of the percentage relative standard deviation, (Table 2.2.4). These data proved the linearity of the calibration graphs.

2.2.2.2.2 Limit of quantitation (LOQ) and limit of detection (LOD)

LOQ and LOD were calculated according to ICH Q2 (R1) recommendations. Results are given in (Table 2.2.4).

2.2.2.2.3 Accuracy and precision

To prove the accuracy of the proposed method, the recovery percentage results of the assay of VAL, AML and HCZ were compared with those of the reference methods [60, 61]. Statistical analysis of the results using Student's t-test and variance ratio F-test revealed no significant difference between the performance of the two methods regarding accuracy and precision, (Supplementary materials Table 2.2.5). The reference methods depend on the analysis of VAL, AML and HCZ using HPLC. Repeatability (intra-day) and intermediate precision (inter-day) were assessed using three concentrations and three replicates of each concentration. The relative standard deviations were found to be very small indicating reasonable repeatability and intermediate precision of the proposed method, (Table 2.2.1).

2.2.2.2.4 Stability

Stability of the standard solutions of VAL, AML and HCZ, stored at 2 ˚C, were evaluated at various time points over 3 months. The concentrations of freshly prepared solutions and those aged for 2 months were calculated by the method developed and the difference between them was found to be less than 0.3 %. These solutions can therefore be used during this interval of time without the results being affected.

2.2.2.2.5 Specificity

The specificity of the method was investigated by observing any interference encountered from common tablet excipients and it was confirmed that the signals measured was caused only by the analytes. Each film-coated tablet of Exforge HCT® contains the following

inactive ingredients: colloidal silicon dioxide, crospovidone, hypromellose, iron oxide red, iron oxide yellow, iron oxide black, magnesium stearate, microcrystalline cellulose, polyethylene glycol, povidone, talc, and titanium dioxide. It was found that the excipients did not interfere with the results of the proposed method. As shown in (Fig. 2.2.3) the tablets electropherogram did not show any additional peaks when compared to VAL, AML and HCZ laboratory prepared mixture electropherogram which confirm the specificity of the method.

2.2.3 Experimental

2.2.3.1 Instruments

The assay was developed and validated using a Beckman P/ACE 5510 system (Fullerton, CA, U.S.A) equipped with an autosampler, a photodiode array (PDA) detector, a temperature controlling system(4 - 40 ^{o}C) and power supply able to deliver up to 30 kV. Beckman P/ACE^{TM} station software (version 1.2) was used for the instrument control, data acquisition and analysis. Electrophoretic analyses were performed in a fused silica capillary (Polymicro Technologies, Phoenix, AZ, U.S.A) of 57.0-cm-long (50.0-cm effective length) and 75.6 µm i.d. in normal mode, applying a voltage of 15 kV. The wavelength for analysis was 230 nm, hydrodynamic injection of samples for 3 s under a pressure of 0.5 psi and the temperature of the capillary cartridge was 25 ^{o}C.

The BGE was filtered using 0.2 µm Anatop 25 Whatman inorganic membrane filter (Maidstone, England) and degassed using Branson Ultrasonic 5510 degasser (Danbury, CT, U.S.A). A Sym**pH**only (SB20) pH-meter (Thermo Orion Beverly, MA, U.S.A) was used for pH measurements. Deionized water was prepared using a Barnstead NANO pure DIamond Analytical (USA) ultrapure water system.

2.2.3.2 Materials and reagents

All the chemicals used were of Analytical Reagent grade, and the solvents were of HPLC grade. Pharmaceutical grade valsartan USP was supplied Zydus, batch Number: VSK1MK A02B (certified to contain 99.40%). Amlodipine besylate (certified to contain 99.75%) was kindly supplied by Global Nabi Co., (Giza -Egypt). Hydrochlorothiazide (certified to contain 99.93%) was supplied by AstraZeneca - Cairo, - Egypt (Under license of AstraZeneca, Sweden). Methanol and Pyrazinoic acid (certified to contain 99%) were obtained from (Sigma-Aldrich, MO, U.S.A). Exforge HCT® 160/10/12.5 mg tablets each labeled to contain 160 mg Valsartan, 13.9 mg amlodipine besylate and 12.5 mg hydrochlorothiazide were purchased from commercial sources in the local market. Sodium hydroxide, sodium dihydrogen phosphate (J.T. Baker,NJ, U.S.A) and Orthophosphoric acid 85% (Fisher Scientific, NJ, U.S.A)) and methanol (Sigma-Aldrich, MO, U.S.A) were used.

2.2.3.3 Standard and working solutions

2.2.3.3.1 Standard solutions

Stock solutions 2000 µg mL^{-1} of VAL and 1000 µg mL^{-1} of AML, HCZ and IS were prepared in a solvent composed of methanol and water (10: 90, v/v), 10% methanol. Working solutions were prepared by further dilution of AML and HCZ stock solutions with 10% methanol to give a final concentration of 200 µg mL^{-1}.

2.2.3.3.2 Background running electrolyte (BGE)

The optimized BGE solution consisted of 40 mM sodium dihydrogen phosphate buffer adjusted to pH 7.5 with 1M NaOH and filtered through a 0.2 µm membrane filter.

2.2.3.4 Electrophoretic procedure

Before the first use, the capillary was conditioned by flushing with 1M NaOH for 90 min, then with water for 30 min and BGE for 30 min at 0.5 psi pressure. At the beginning of each working day, the capillary was rinsed with 0.1M NaOH for 10 min, water for 5 min and then with BGE for 5 min at 20 psi pressure. Before each injection, the capillary was preconditioned with 0.1M NaOH (5 min), water (5 min) and BGE (5 min) at 20 psi pressure to maintain proper reproducibility of run-to-run injections. Injection was carried out under hydrodynamic pressure at 0.5 psi for 3 s. A diode-array UV detector was set at 230 nm with a bandwidth of 20 nm. The capillary temperature was kept constant at 25 ˚C and a voltage of 15 kV was applied.

2.2.3.5 Procedures

2.2.3.5.1 Construction of the calibration graphs

Accurate aliquots of VAL stock solution as well as AML and HCZ working solutions were transferred into a series of 4-mL vials so that the final concentrations were in the range of 10-200 µg mL^{-1} for VAL, 2-20 µg mL^{-1} for AML and 2-20 µg mL^{-1} for HCZ. A constant 100µL IS stock solution was added and the volume was diluted to 4 mL with 10% methanol. The peak area ratio (peak area of the studied drug/ peak area of IS) was plotted versus the final concentration of each drug in µg mL^{-1} to get the calibration graphs. Alternatively, the corresponding regression equations were derived.

2.2.3.5.2 Analysis of VAL/AML/HCZ laboratory prepared mixture

Accurate aliquots of VAL stock solution as well as AML and HCZ working solutions keeping the pharmaceutical ratio of 12.8:1.1:1 were transferred into a series of 4-mL vials, diluted with 10% methanol after addition of 100µL IS and mixed well. The above procedure

described under "section 2.5.1" was then applied. The percentage recoveries were calculated using the corresponding regression equations.

2.2.3.5.3 Analysis of the studied drugs in their co-formulated tablets

Ten tablets of Exforge HCT® 160-10-12.5 were weighed and then crushed to a fine powder. An accurately weighed amount of the finely powdered tablets, equivalent to 50.00 mg VAL, 4.30 mg AML and 3.91 mg HCZ, was transferred to 25 mL volumetric flask. Twenty milliliters of methanol were added and the solution was sonicated for 30 min. The solution was completed to volume with the same solvent and then filtered through Whatman filter paper and filtered again using 0.2 µm Whatman inorganic membrane filter. For analysis, different aliquots from the prepared sample solution, spiked with 100 µL IS stock solution, were diluted to 4 mL using 10% methanol. The above procedure described under "section 2.5.1" was then applied. The percentage recoveries were calculated by referring to the corresponding regression equations.

Table 2.2.1 Accuracy and precision data for the determination of VAL, AML and HCZ by the proposed CZE method

Concentration of VAL ($\mu g\ mL^{-1}$)	Intra-day assay Recovery % ± S.D [a]	Inter-day assay Recovery % ± S.D [a]	Comparison method Recovery %
32.00	101.42 ± 1.40	100.90 ± 0.57	98.04
96.00	99.44 ± 0.32	100.26 ± 1.16	100.64
128.00	99.38 ± 1.35	99.71 ± 1.60	98.66
Mean ± S.D.	100.08 ± 1.16	100.29 ± 0.60	99.11 ± 1.36
Student *t* test	0.94 (2.78)	1.38 (2.78)	
F	1.37 (19.00)	5.21 (19.00)	
Concentration of AML ($\mu g\ mL^{-1}$)	Intra-day assay Recovery % ± S.D [a]	Inter-day assay Recovery % ± S.D [a]	Comparison method Recovery %
2.75	101.60 ± 1.71	99.63 ± 2.96	102.20
8.25	99.56 ± 2.05	99.56 ± 2.48	99.70
13.75	101.52 ± 0.59	100.54 ± 1.49	100.09
Mean ± S.D.	100.89 ± 1.16	99.91 ± 0.55	100.66 ± 1.35
Student *t* test	0.23 (2.78)	0.89 (2.78)	
F	1.37 (19.00)	6.10 (19.00)	
Concentration of HCZ ($\mu g\ mL^{-1}$)	Intra-day assay Recovery % ± S.D [a]	Inter-day assay Recovery % ± S.D [a]	Comparison method Recovery %
2.50	100.31 ± 0.88	98.84 ± 1.35	100.28
7.50	100.84 ± 0.59	99.96 ± 0.78	99.77
12.50	99.65 ± 0.89	100.94 ± 1.16	100.07
Mean ± S.D.	100.27 ± 0.60	99.91 ± 1.05	100.04 ± 0.26
Student *t* test	0.60 (2.78)	0.20 (2.78)	
F	5.26 (19.00)	16.33 (19.00)	

[a] Mean and standard deviation of three determinations

Table 2.2.2 Assay results for the determination of the studied drugs in Exforge HCT® 160/10/12.5 mg tablets

Compound	Proposed method			Comparison method
	Amount taken ($\mu g\ mL^{-1}$)	Amount found ($\mu g\ mL^{-1}$)	Recovery %	Recovery %
VAL	32.00	32.26	100.80	99.41
	64.00	64.97	101.52	99.28
	96.00	97.42	101.48	101.58
	128.00	127.64	99.72	99.32
	160.00	163.18	101.99	99.32
Mean ± S.D.			101.10 ± 0.88	99.78 ± 1.01
Student *t* test			2.21 (2.31)	
F			1.30 (6.39)	
AML	2.75	2.82	102.59	97.93
	5.50	5.58	101.55	99.95
	8.25	8.35	101.21	101.78
	11.00	11.03	100.30	99.97
	13.75	13.96	101.52	99.45
Mean ± S.D.			101.43 ± 0.82	99.82 ± 1.38
Student *t* test			2.26 (2.31)	
F			2.82 (6.39)	
HCZ	2.50	2.57	102.96	97.20
	5.00	5.07	101.37	99.52
	7.50	7.63	101.72	102.67
	10.00	10.06	100.57	100.34
	12.50	12.84	102.71	99.00
Mean ± S.D.			101.87 ± 0.98	99.75 ± 2.00
Student *t* test			2.13 (2.31)	
F			4.15 (6.39)	

Each result is the average of three separate determinations.

The values between parentheses are the tabulated t and F values at $P = 0.05$.

Table 2.2.3 Effect of detection wavelength on VAL, AML, HCZ and IS: (16 μg mL^{-1} of AML, 16 μg mL^{-1} of HCZ, 160 μg mL^{-1} of VAL and 100 μg mL^{-1} of IS)

Wavelength (nm)	Peak Area				Peak Area Ratio to IS		
	AML	HCZ	VAL	IS	AML	HCZ	VAL
203	66265	146077	1841391	365774	0.181	0.399	5.034
210	52578	109062	1825075	363935	0.144	0.300	5.015
220	32218	134227	1489437	258277	0.125	0.520	5.767
230	27050	148232	1048758	124057	0.218	1.195	8.454
240	27816	82551	769974	65863	0.422	1.253	11.691
250	25836	26766	621544	76513	0.388	0.350	8.123
260	17552	35390	562031	170272	0.103	0.208	3.301

Table 2.2.4 Performance data for the determination of the studied drugs by the proposed CZE method

Parameter	VAL	AML	HCZ
Linearity range (µg mL^{-1})	10-200	2-20	2-20
Intercept (*a*)	-0.0837	-0.0047	0.0154
Slope (*b*)	0.0637	0.0123	0.0453
Correlation coefficient (*r*)	0.9999	0.9998	0.9995
S.D. of residuals ($S_{y/x}$)	0.052	0.002	0.0114
S.D. of intercept (S_a)	0.035	0.001	0.0089
S.D. of slope (S_b)	0.0004	0.0001	0.0007
% RSD	3.362	3.357	3.164
% Error	1.368	1.380	1.304
LOD (µg mL^{-1})	1.819	0.385	0.647
LOQ (µg mL^{-1})	5.513	1.166	1.960

Table 2.2.5 Assay results for the determination of the studied drugs in pure form by the CZE and reference methods

Compound	Proposed method			Reference method
	Amount taken ($\mu g\ mL^{-1}$)	Amount found ($\mu g\ mL^{-1}$)	Recovery %	Recovery %
VAL	32.00	31.942	99.82	99.78
	64.00	64.124	100.19	100.47
	96.00	95.129	99.09	99.98
	128.00	128.190	100.15	99.68
	160.00	158.834	99.27	100.16
Mean ± S.D.			99.70± 0.50	100.01± 0.32
Student *t* test			1.17 (2.31)	
F			2.56 (6.39)	
AML	2.75	2.740	99.63	100.07
	5.50	5.585	101.55	97.69
	8.25	8.309	100.71	102.13
	11.00	11.033	100.30	100.11
	13.75	13.902	101.11	99.52
Mean ± S.D.			100.66± 0.74	99.90± 1.59
Student *t* test			0.97 (2.31)	
F			4.61 (6.39)	
HCZ	2.50	2.552	102.08	99.48
	5.00	4.936	98.72	102.02
	7.50	7.519	100.25	101.44
	10.00	9.815	98.15	100.99
	12.50	12.442	99.53	99.25
Mean ± S.D.			99.74± 1.53	100.64± 1.22
Student *t* test			1.02 (2.31)	
F			1.57 (6.39)	

Each result is the average of three separate determinations.
The values between parentheses are the tabulated t and F values at $P = 0.05$.

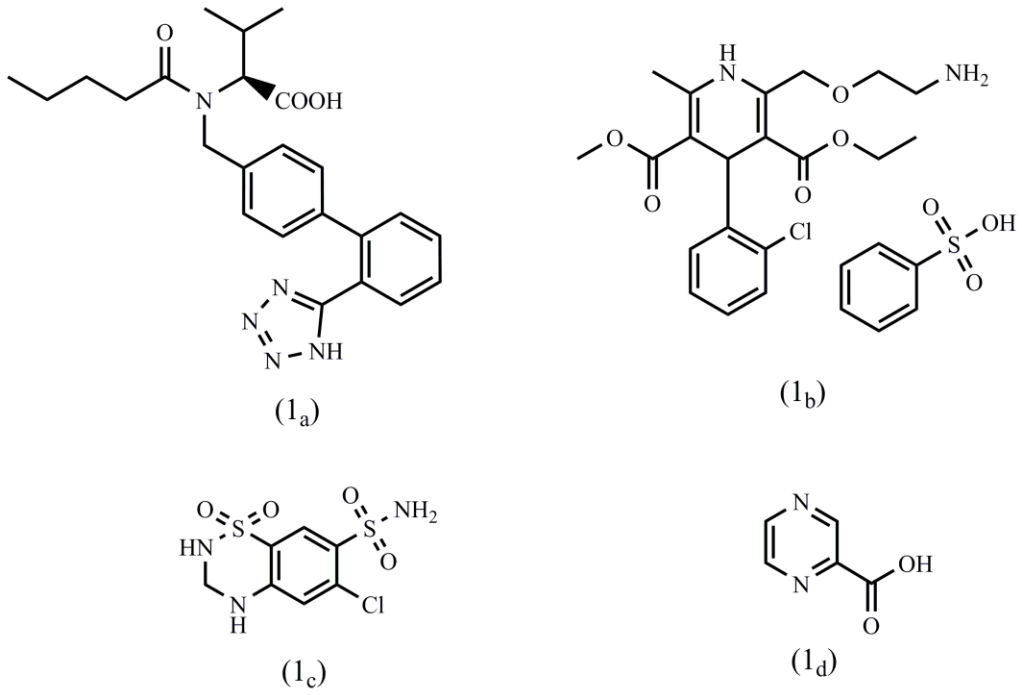

Figure 2.2.1 The structural formulae for the studied drugs; (a) valsartan (VAL), (b) amlodipine besylate (AML), (c) hydrochlorothiazide (HCZ) and (d) Pyrazinoic acid (IS)

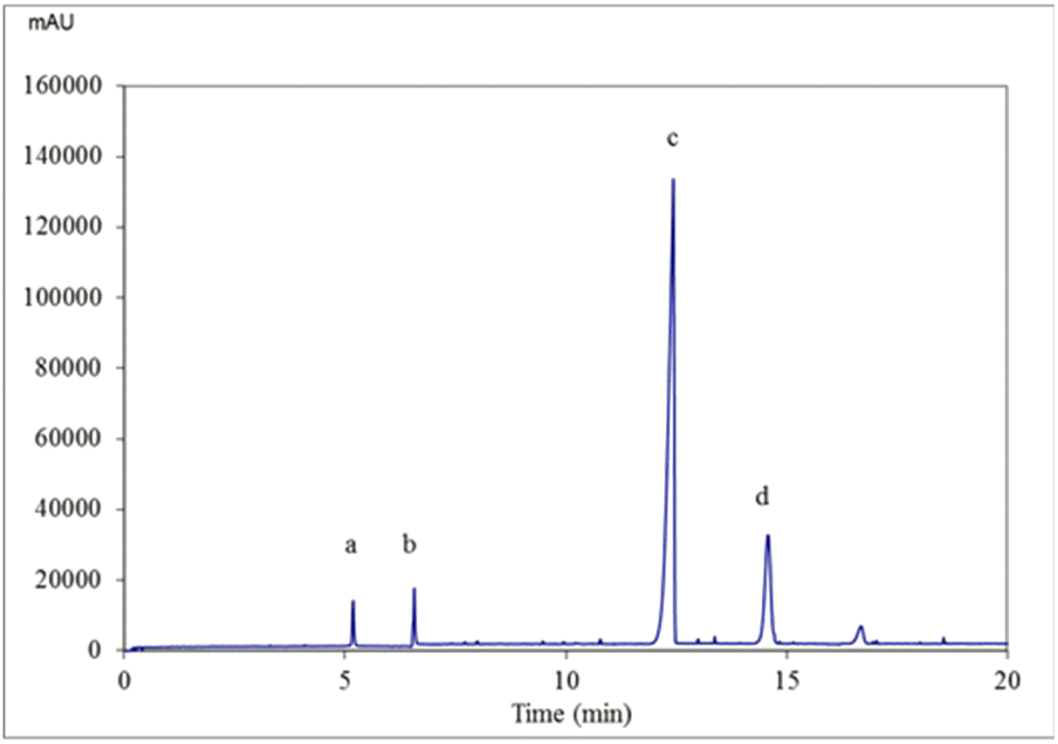

Figure 2.2.2 Typical electropherogram for a laboratory prepared mixture; (a) 11 µg mL^{-1} AML, (b) 10 µg mL^{-1} HCZ, (c) 128 µg mL^{-1} VAL and (d) 100 µg mL^{-1} IS under the described electrophoretic conditions

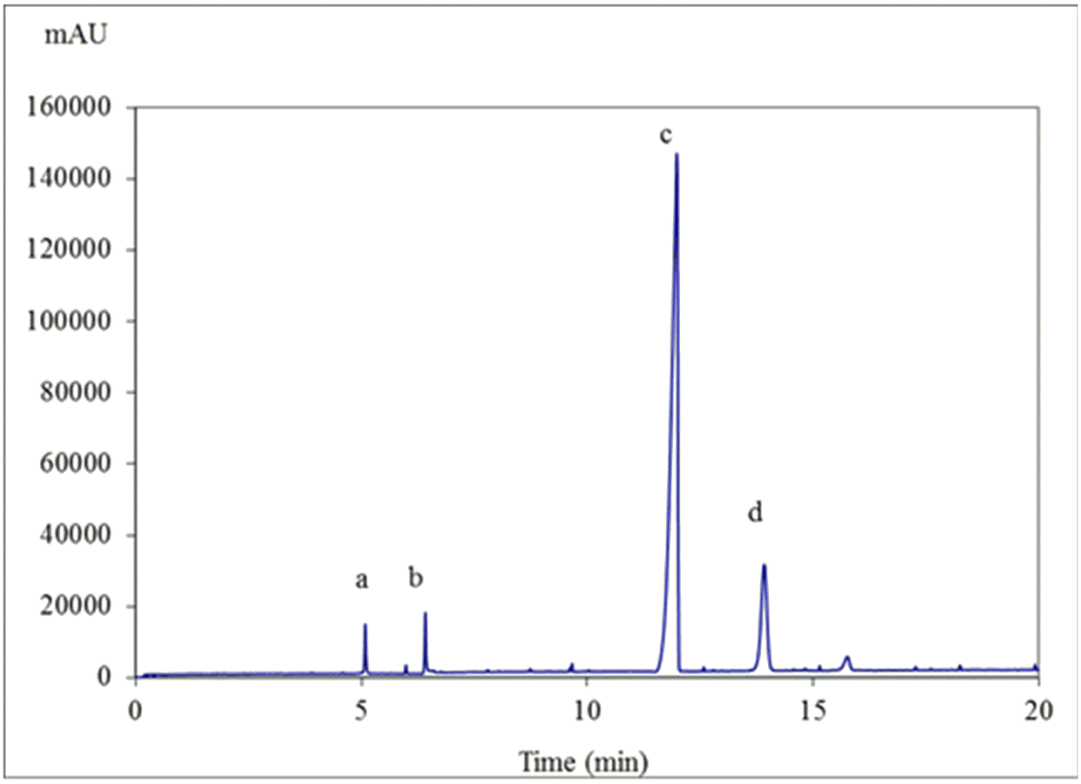

Figure 2.2.3 Application of the proposed method for the simultaneous determination of VAL, AML and HCZ in their co-formulated tablets; (a) 11 µg mL^{-1} AML, (b) 10 µg mL^{-1} HCZ, (c) 128 µg mL^{-1} VAL and (d) 100 µg mL^{-1} IS under the described electrophoretic conditions

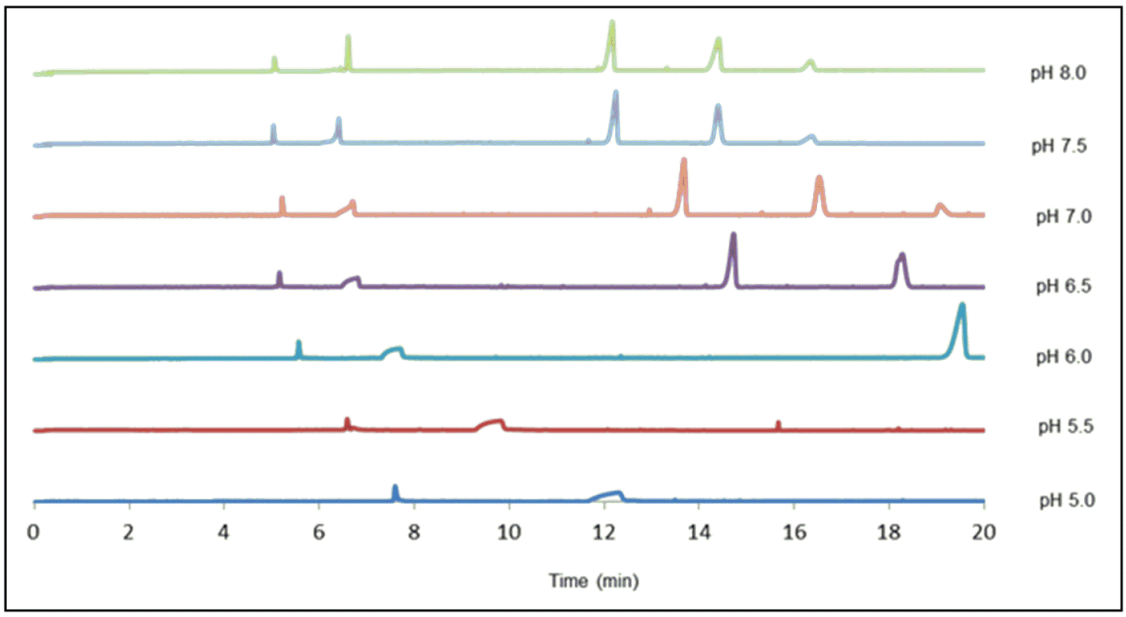

Figure 2.2.4 Effect of phosphate buffer pH; operating conditions: 40mM phosphate buffer, injection (3 s), 15 kV, 25 ◦C, 210 nm (bandwidth 20 nm). (12 μg mL^{-1} AML, 30 μg mL^{-1} HCZ, 192 μg mL^{-1} VAL and 100 μg mL^{-1} IS)

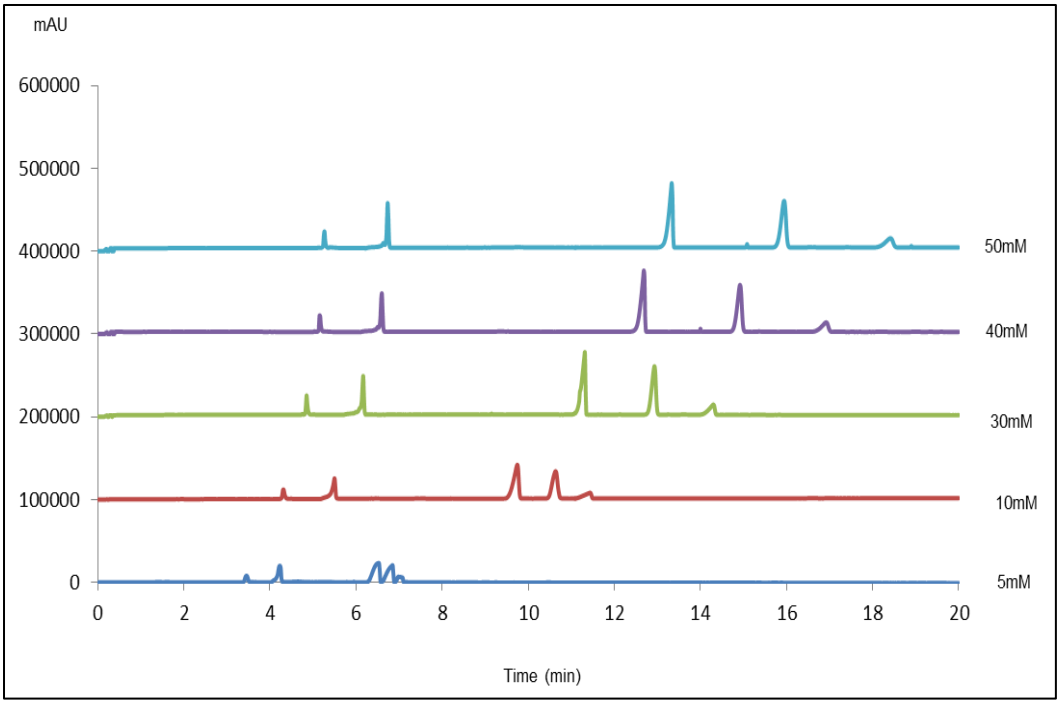

Figure 2.2.5 Effect of phosphate buffer concentration.

Operating conditions: pH 7.5 phosphate buffer, injection (3 s), 15 kV, 25 ◦C, 210 nm (bandwidth 20 nm). (12 μg mL^{-1} AML, 30 μg mL^{-1} HCZ, 192 μg mL^{-1} VAL and 100 μg mL^{-1} IS)

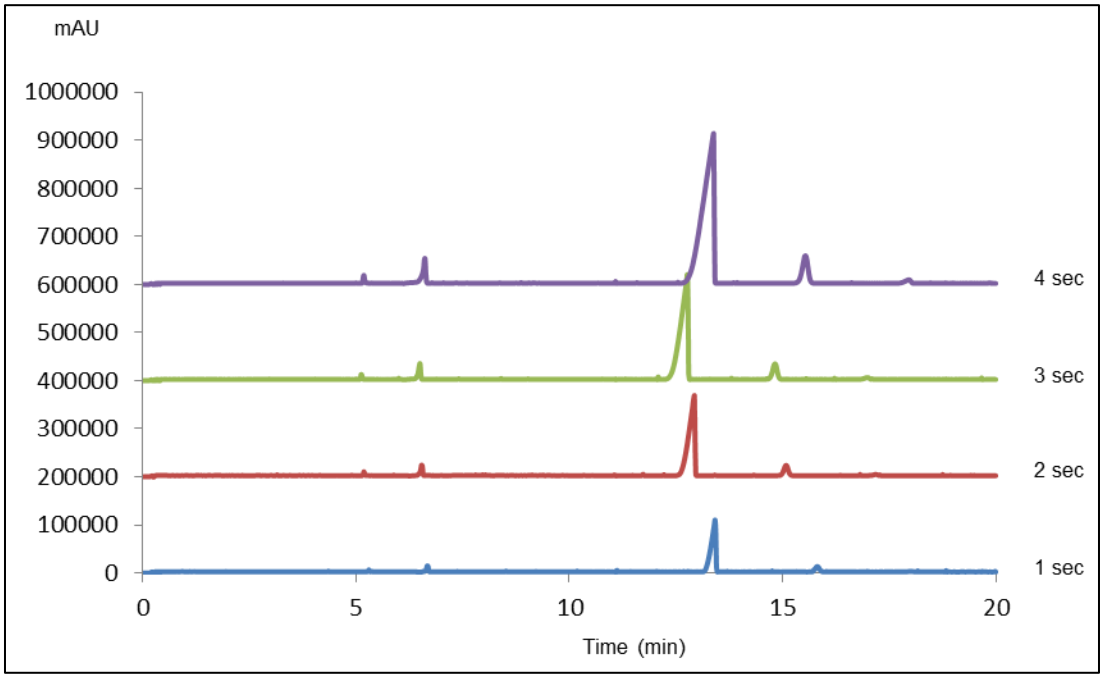

Figure 2.2.6 Effect of injection time.

Operating conditions: pH 7.5 phosphate buffer, injection (3 s), 15 kV, 25 ◦C, 210 nm (bandwidth 20 nm). (12 μg mL^{-1} AML, 30 μg mL^{-1} HCZ, 192 μg mL^{-1} VAL and 100 μg mL^{-1} IS)

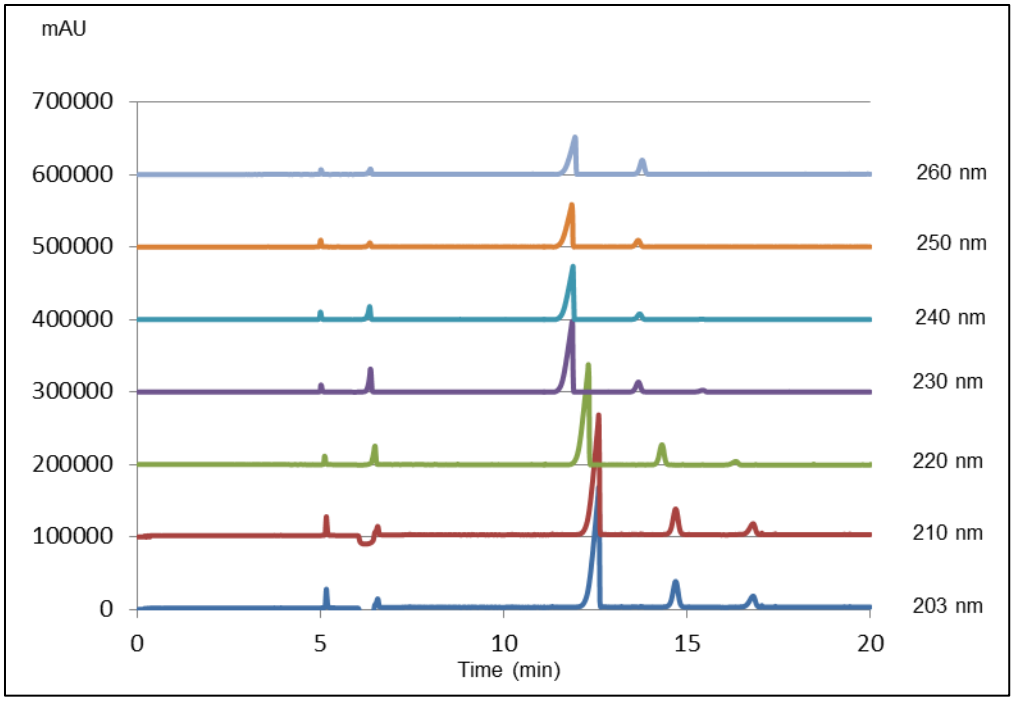

Figure 2.2.7 Selection of the detection wavelength.

Operating conditions: 40mM phosphate buffer, pH 7.5, injection (3 s), 15 kV, 25 ◦C. (16 μg mL^{-1} AML, 16 μg mL^{-1} HCZ, 160 μg mL^{-1} VAL and 100 μg mL^{-1} IS)

2.3 Simultaneous determination of aliskiren hemifumarate, amlodipine besylate, and hydrochlorothiazide in their triple mixture dosage form by capillary zone electrophoresis

Journal of Separation Science (2014) 37(9-10):1206-1213

DOI 10.1002/jssc.201301140

A novel, specific, reliable and accurate capillary zone electrophoresis (CZE) method was developed and validated for the simultaneous determination of aliskiren hemifumarate (ALS), amlodipine besylate (AML) and hydrochlorothiazide (HCZ) in their triple mixture dosage form AMTURNIDE®. Separation was carried out in fused silica capillary (57.0 cm total length and 50.0 cm effective length, 75.6 µm i.d.) by applying a potential of 17 KV (positive polarity) and a running buffer consisting of 40 mM phosphate buffer at pH 6.0 with UV detection at 245 nm. The samples were injected hydrodynamically for 2 s at 0.5 psi and the temperature of the capillary cartridge was kept at 25 °C. Meoxipril (MXP) was used as internal standard (IS). The method was suitably validated with respect to specificity, linearity, limit of detection and quantitation, accuracy, precision, and robustness. The method showed good linearity in the ranges of 1-10, 2.5-25 and 30-300 µg/mL with limits of detection of 0.11, 0.33 and 5.83 µg/mL and limits of quantification of 0.33, 1.01 and 17.65µg/mL for AML, HCZ and ALS, respectively. The proposed method was successfully applied for the analysis of the studied drugs in their laboratory prepared mixtures and co-formulated tablets without any interfering peaks. The estimated amounts of AML, HCZ and ALS were almost identical with the certified values, and their percentage relative standard deviation values (%R.S.D.) were found to be ≤ 1.80% (n = 3).

The results were compared to reference methods and no significant difference was found statistically.

2.3.1. Introduction

Aliskiren hemifumarate (ALS), (2(S), 4(S), 5(S), 7(S)-N- (2-carbamoyl- 2- methylpropyl) -5-amino-4-hydroxy2,7diisopropyl-8-[4-methoxy-3-(3-methoxypropoxy) phenyl] octanamide hemifumarate) (Fig 2.3.1a) is the first direct renin inhibitor (DRI) suitable for oral administration [62]. ALS reduces baseline systolic and diastolic blood pressure (BP) by directly inhibiting the catalytic activity of renin system at its rate-limiting step [62]. Therefore, ALS is used as a new effective treatment for hypertension alone and extra antihypertensive activity can be achieved when it is used in combination therapy [63]. Amlodipine besylate (AML), 2-[(2-Aminoethoxy)methyl]-4-(2–chlorophenyl)-1,4–dihydro–6–methyl–3,5–pyridinedicarboxylic acid 3–ethyl 5–methyl ester [64] (Fig 2.3.1b) is an oral dihydropyridine calcium channel blocker, which acts only on the L-type channel to produce its pharmacological effect [65]. Like most of the second generation dihydropyridine derivatives, AML has greater selectivity for the vascular smooth muscle than myocardial tissue and therefore their main effect is vasodilatation [66]. AML is used alone or in combination with other medicines for the treatment of chronic stable angina and in the management of mild-to-moderate essential hypertension [65]. Hydrochlorothiazide (HCZ), 6-chloro-1, 1-dichloro-3, 4, dihydro -2H-1, 2, 4-benzoliadiazine-7-sulphanomide1, 1-dioxide [64] (Fig 2.3.1c) is a potent oral thiazide diuretic and antihypertensive agent. HCZ affects the renal tubular mechanisms of electrolytes reabsorption, directly increasing excretion of sodium salt and chloride in approximately equivalent amount [67]. The ALS/AML/HCZ triple combination therapy in patients with moderate to severe hypertension was well tolerated and provided clinically significant BP reductions and effective BP control [68].

Literature survey revealed several reported methods for the determination of ALS in pharmaceutical preparation or biological fluids alone or in combination with other anti-hypertensive agents. These methods include HPLC [69-73], CE [74], UV-spectrophotometry [75, 76] and spectroflourimetry [77, 78]. Several methods have also been reported for the estimation of AML alone or in combination with other anti-hypertensive agents such as HPLC [79-81], LC-MS [82], CE [83], UV-spectrophotometric[41, 84, 85] and spectroflourimetric [86, 87]. For HCZ determination alone or in combination with other anti-hypertensive agents, several methods like HPLC [88-93], LC-MS [94-97], UPLC [98] and UV- spectrophotometric [99] have been described.

Regarding ALS, AML and HCZ simultaneous analysis, only two RP-HPLC methods [100, 101] have been reported for the simultaneous determination of the triple mixture either in pure form or in their co-formulated dosage form. Rao et al [100] described a RP-HPLC method for determination of the drugs in their dosage form using C18 column and a complex mobile phase consisting of acetonitrile: methanol: 50mM phosphate buffer(pH 3) in the ratio of 20:50:30% v/v. Moreover, the linearity range of ALS practically will not allow proper simultaneous determination of the three drugs in their co-formulated tablets. However, Selvakumar et al [101] reported a RP-HPLC method using 20 mM potassium dihydrogen phosphate buffer (pH 6.5): methanol: acetonitrile (55:10:35 v/v) as mobile phase for determination of the triple mixture in pure form only. The samples were separated with poor sensitivity on C8 column within a long run time of 16 min.

To the best of our knowledge, no CZE method has been yet described for the simultaneous determination of ALS, AML and HCZ in their triple co-formulated dosage form.

The use of capillary electrophoresis (CE) methods for pharmaceutical analysis has become increasingly popular in recent years. The wide range of pharmaceutical applications for

which its use has proved successful, include assay of drugs, determination of drug-related impurities, physicochemical measurements of drug molecules, chiral separation, and the analysis of vitamins and pharmaceutical excipients. The advantages of using CE for pharmaceutical analysis include its speed and low cost of analysis, reductions in solvent consumption and disposal, and the possibility of rapid method development. CE also offers the possibility that a single set of separation conditions can be applied for a wide range of analyses, giving efficiency savings [6, 102]. Recently, CE techniques have been applied to the simultaneous determination of co-formulated drugs in dosage form [3, 103].

The goal of this study is to develop and validate a reliable, accurate, inexpensive, selective and sensitive method using capillary electrophoresis that could be applied to the routine quality control analysis of ALS, AML and HCZ simultaneously in bulk drug samples and in combined dosage formulation. The studied drugs; ALS, AML and HCZ, are co-formulated in a medicinally recommended ratio of 23.9:1.0:1.8, respectively. Analysis of such mixture with strong spectral overlapping is challenging. The proposed CZE method allowed the separation and quantitation of the three drugs with satisfied accuracy and precision. The developed CZE method has the advantages of being more simple, sensitive, accurate and faster for quality control and routine analysis of ALS, HCZ and AML triple mixture in comparison with the reported methods [100, 101]. Moreover, this method consumes no organic solvent so it can be considered a green method.

2.3.2. Experimental

2.3.2.1. Instruments

The assay was developed and validated using a Beckman P/ACE 5510 system (Fullerton, CA, U.S.A) equipped with an autosampler, a photodiode array (PDA) detector, a temperature

controlling system (4 ºC - 40 ºC) and power supply able to deliver up to 30 KV. Beckman P/ACE^{TM} station software (version 1.2) was used for the instrument control, data acquisition and analysis. Electrophoretic analyses were performed in a fused silica capillary (Polymicro Technologies, Phoenix, AZ, U.S.A) of 57.0-cm-long (50.0-cm effective length) and 75.6 µm i.d. in normal mode, applying a voltage of 17 KV. The wavelength for analysis was 245 nm, hydrodynamic injection of samples for 2 s under a pressure of 0.5 psi and the temperature of the capillary cartridge was kept at 25 ºC. The background running buffer (BRB) was filtered using 0.2 µm Anatop 25 Whatman inorganic membrane filter (Maidstone, England) and degassed using Branson Ultrasonic 5510 degasser (Danbury, CT, U.S.A). A Sym**pH**only (SB20) pH-meter (Thermo Orion Beverly, MA, U.S.A) was used for pH measurements. Deionized water was prepared using a Barnstead NANO pure DIamond Analytical (USA) ultrapure water system.

2.3.2.2. Materials and reagents

All the chemicals used were of Analytical Reagent grade, and the solvents were of HPLC grade. Aliskiren hemifumarate (certified to contain 99.51%) was supplied by Novartis Pharmaceuticals Corporation East, New Jersey, USA. Amlodipine besylate (certified to contain 99.75%) was kindly supplied by Global Nabi Co., Giza, Egypt. Hydrochlorotiazide (certified to contain 99.93%) was supplied by AstraZeneca - Cairo, Egypt. Moexipril hydrochloride was purchased from Sigma-Aldrich (Saint Louis, MO, USA) with labeled purity > 98%. Amturnide® 300-10-25 mg tablets; batch # NDC 0078-0614-15 (Novartis Pharmaceuticals Corporation East, New Jersey, USA 07936) were purchased from commercial sources in the USA market. Each labeled to contain 331.5 mg aliskiren hemifumarate (equivalent to 300 mg aliskiren as a free base), 13.87 mg amlodipine besylate (equivalent to 10 mg amlodipine as a free base) and 25 mg hydrochlorothiazide, sodium hydroxide, acetic acid and sodium dihydrogen phosphate (J.T.

Baker,NJ, U.S.A), orthophosphoric acid 85%, sodium acetate and boric acid (Fisher Scientific, NJ, U.S.A), acetonitrile, methanol and ethanol (Sigma-Aldrich, MO, U.S.A) were used.

2.3.2.3. Standard and sample solutions

2.3.2.3.1. Standard solutions

Stock solutions 1.0 mg/mL of AML, HCZ, MXP and 4.0 mg/mL of ALS were prepared by dissolving 25 mg of AML, HCZ, MXP and 100 mg of ALS separately in 25 mL of solvent composed of methanol and water (10:90 v/v). Working solutions were prepared by further dilution of the stock solutions with the same solvent to give a final desired concentration. The solutions were stable for one week when kept in the refrigerator at 2 ^{o}C.

2.3.2.3.2. Background electrolyte (BGE)

Optimized BGE solution was 40 mM sodium dihydrogen phosphate buffer adjusted to pH 6 with 1 M NaOH [104] and filtered through a 0.2 µm membrane filter.

2.3.2.4. Electrophoretic procedure

Before the first use, the capillary was conditioned by flushing with 1.0 M NaOH for 60 min, then with water for 30 min and BGE for 30 min at 0.5 psi pressure. At the beginning of each working day, the capillary was rinsed with 0.1 M NaOH for 10 min, water for 5 min and then with BGE for 5 min at 20 psi pressure. Before each injection, the capillary was preconditioned with 0.1 M NaOH (5 min), water (5 min) and BGE (5 min) at 20 psi pressure to maintain proper repeatability of run-to-run injections. Injection was carried out under hydrodynamic pressure at 0.5 psi for 2 s. PDA detector was set at 245 nm with a bandwidth of 20 nm. The capillary temperature was kept constant at 25 ˚C and a voltage of 17 kV was applied (positive polarity).

2.3.2.5. Procedures

2.3.2.5.1. Construction of calibration graphs

Aliquots of the suitable drug stock or working standard solutions were transferred into a series of 4-mL vials so that the final concentrations were in the range of 1-10 µg/mL for AML, 2.5-25 µg/mL for HCZ and 30-300 µg/mL for ALS. A constant 100 µL MXP stock solution was added (final concentration of 25 µg/mL) and the volumes were diluted to 4 mL with a solvent composed of methanol and water (10:90 v/v). The peak area ratio (peak area of the studied drug/ peak area of MXP) was plotted versus the final concentration of each drug in µg/mL to get the calibration graph. Alternatively, the corresponding regression equations were derived.

2.3.2.5.2. Analysis of the cited drugs separately

Aliquots of ALS, AML and HCZ standard solutions covering the working concentration ranges were transferred into a series of 4-mL vials, diluted with a solvent composed of methanol and water (10:90 v/v) after addition of 100 µL MXP and mixed well. The above procedure described under "Construction of calibration graphs" was then applied. The percentages found were calculated by referring to the calibration graphs, or using the corresponding regression equations.

2.3.2.5.3. Analysis of ALS/AML/HCZ laboratory prepared mixtures

Aliquots of ALS, AML and HCZ standard solutions keeping the pharmaceutical ratio of 23.9:1.0: 1.8 m/m/m were transferred into a series of 4-mL vials, diluted with a solvent composed of methanol and water (10:90 v/v) after addition of 100 µL MXP and mixed well. The above procedure described under "Construction of calibration graphs" was then applied. The percentages found were calculated by referring to the calibration graphs, or using the

corresponding regression equations.

2.3.2.5.4. Analysis of the studied drugs in Amturnide® co-formulated tablets

Ten tablets were weighed and finely pulverized after decoating by careful rubbing with a clean tissue wetted with methanol. An accurately weighed amount of the fine powder (0.2748 gm) equivalent to 4.000 mg ALS, 0.167 mg AML and 0.301 mg HCZ was transferred to 10-mL volumetric flask and 6 mL of a solvent composed of methanol and water (10:90 v/v) was added. The flask was sonicated for 30 min and vortex mixing for 15 min by Fisher vortex (Fisher Scientific), and then diluted to the mark with the same solvent. The solution was filtered through Whatmann filter paper and then filtered again using 0.2 µm Whatmann inorganic membrane filter. For analysis, appropriate aliquots from the prepared sample solution, spiked with 100 µL MXP stock solution, was diluted to 4 mL using the same solvent. The above procedure described under "Construction of calibration graphs" was then applied. The percentages found were calculated by referring to the calibration graphs, or using the corresponding regression equations. All solutions were filtered through a 0.2 µm membrane filter and degassed for 5 min before injection to the CE system.

2.3.3. Results and discussion

The proposed method offered the separation and quantification of the studied drugs in their co-formulated tablets in a single run (less than 7 min) with good resolution. Figure 2.3.2 shows a typical electropherogram for a synthetic mixture of the studied drugs under the described electrophoretic conditions. The retention times for AML, ALS, HCZ and MXP were 4.2, 4.4, 5.4 and 6.8 min., respectively. A large peak width of HCZ and MXP compared to AML and ALS was observed. The contributors to the peak width may be analyte wall interactions (wall adsorption) and/or electromigration dispersion [105-107]. The proposed method offers good

sensitivity as about 0.11 µg/mL of AML, 0.33 of HCZ and 5.83 µg/mL of ALS could be detected.

2.3.3.1. Optimization of CE conditions

In CZE, the buffer type, pH and concentration is the key strategy for optimizing the separation of ionizable analytes as it determines the degree of the analyte ionization, its electrophoretic mobility and the magnitude of EOF. Several running buffers such as phosphate, acetate and borate at different pHs and molarities were tested for CZE analysis and the best results were obtained in phosphate buffer taking into consideration different parameters (migration time, resolution, peak shape, height, baseline noise and the electric current produced).

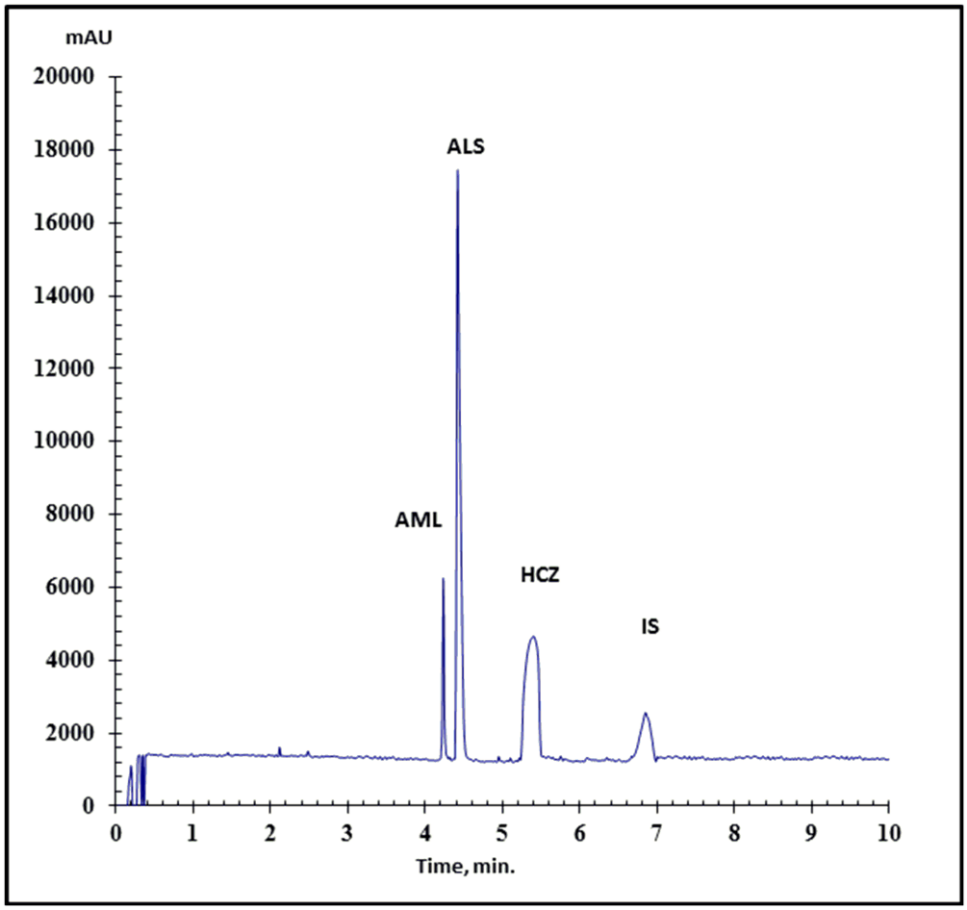

Figure 2.3.1 Typical electropherogram of synthetic mixture of 8 µg/mL of AML (4.2 min), 240 µg/mL ALS (4.4 min), 20 µg/mL HCZ (5.4 min) and 25 µg/mL MXP (6.8 min).

Operating conditions: 40 mM phosphate buffer (pH 6), injection (2 s at 0.5 psi), 17 kV, 25 ˚C, 245 nm (bandwidth 20 nm)

2.3.3.1.1. Effect of phosphate buffer pH

The effect of the buffer pH was investigated within the range of 5.0–7.0 at a 40 mM phosphate buffer concentration. The results demonstrated that the studied compounds were easily separated in this pH range and both resolution and migration times decreased with increasing pH. At pH less than 5, the separation of the sample matrix will take long time. At pH more than 7 overlapping of ALS peak with AML peak was noticed. pH 6.0 was selected as optimum pH as it gave a good compromise regarding resolution, peak symmetry and migration time (Fig. 2.3.3). As ALS has pK_a value of 9.49 [108], AML has pK_a value of 8.6 [109] and HCZ has pK_a values 7.0 and 9.09 [110, 111], ALS and AML are positively charged at pH 6.0 and can be analyzed and separated from the unionized HCZ by CZE. In fact, at this pH value HCZ neither underwent protonation nor deprotonation and as such remained a neutral compound thus migrated with the EOF.

2.3.3.1.2. Effect of phosphate buffer concentration

Buffer concentration has also a significant effect on the separation performance through its influence on the EOF and the current produced in the capillary. The effect of phosphate concentration of running buffer was examined by varying the concentration from 10 to 50 mM. As shown in Figure 2.3.4, with an increasing in phosphate concentration, both resolution and migration times increased. A 40 mM concentration of phosphate buffer was chosen in order to reduce the analysis time while maintaining good resolution (≈ 2.9, 8.8, 3.4, respectively) and acceptable current (≈ 41μA).

2.3.3.1.3. Effect of organic modifiers

The addition of organic modifiers to the running buffer was considered because they affect several parameters such as viscosity, dielectric constant and Zeta potential. In order to investigate the effect of organic modifiers, methanol, ethanol and acetonitrile were added at

various concentrations (5, 10 and 15% v/v) to the running background electrolyte of 40 mM phosphate buffer pH 6.0. No appreciable improvements were observed, but migration times increased significantly with the addition of organic modifiers. Therefore, no organic modifiers were incorporated in the proposed analysis method (Fig. 2.3.5).

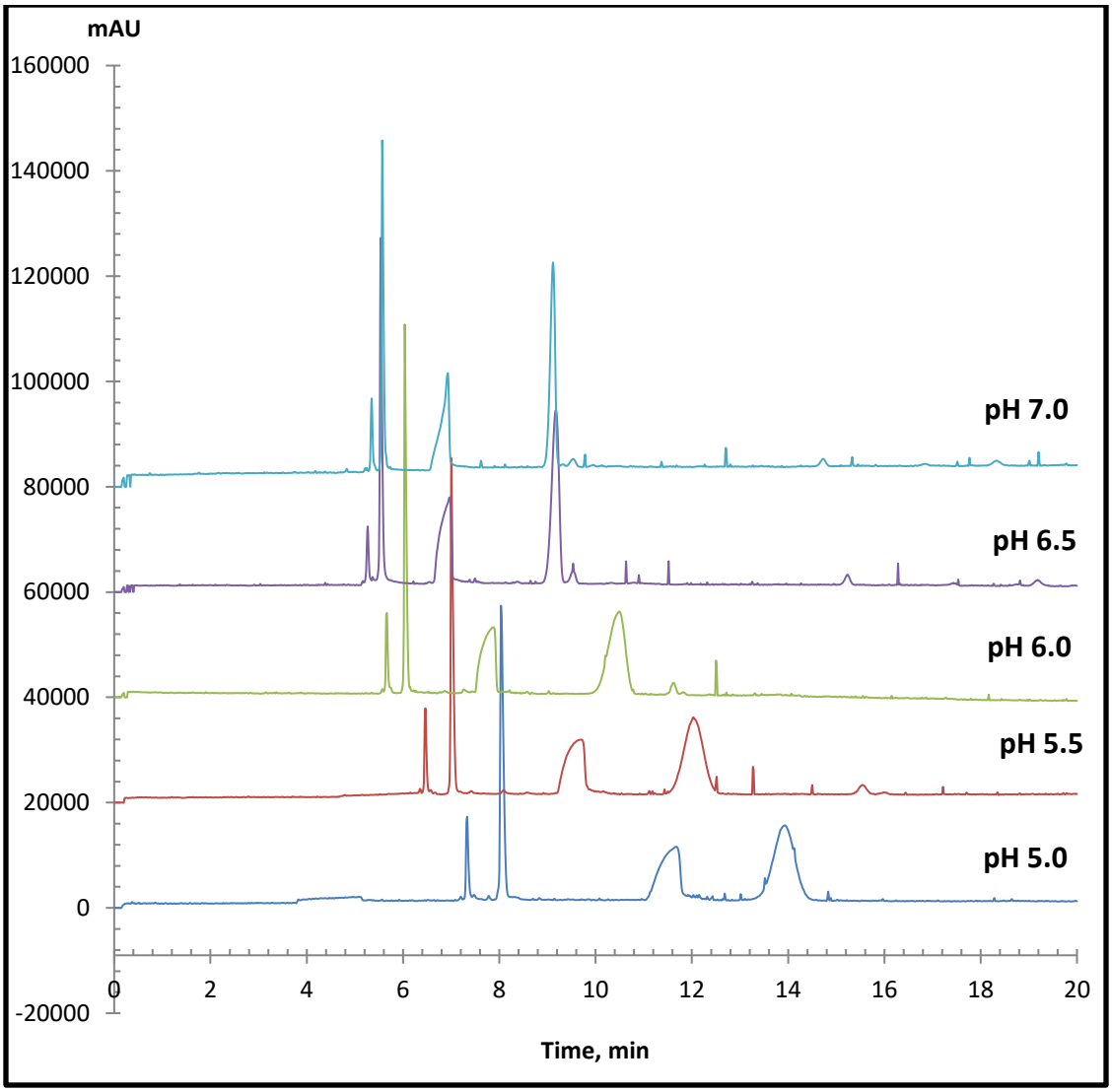

Figure 2.3.2 Effect of phosphate buffer pH on separation of the studied drugs. Operating conditions: 40 mM phosphate buffer, injection (2 s, 0.5 psi), 17 kV, 25 ˚C, 245 nm (bandwidth 20 nm). Peak names and drugs conc.: are as given in Figure 2.3.1.

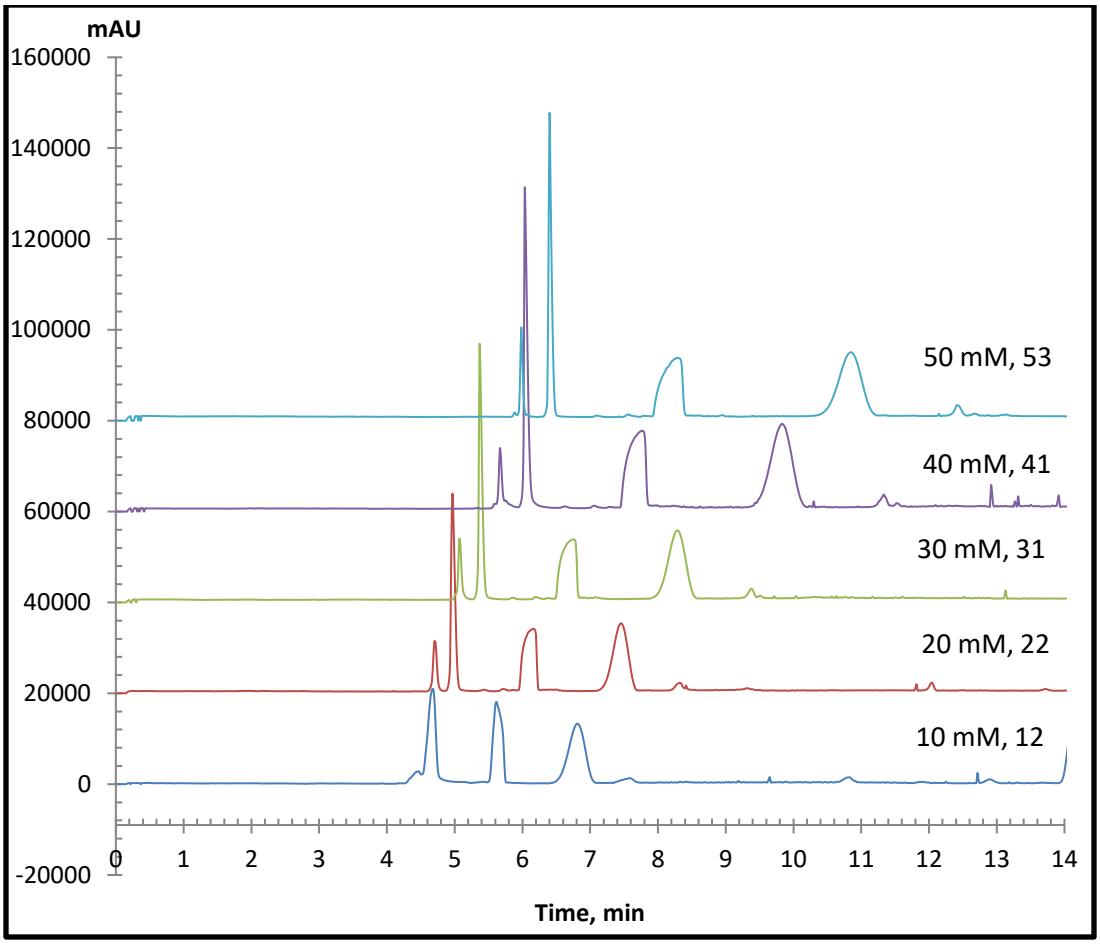

Figure 2.3.3 Effect of phosphate buffer conc. on separation of the studied drugs. Operating conditions: phosphate buffer (pH 6), injection (2 s, 0.5 psi), 17 kV, 25 ◦C, 245 nm (bandwidth 20 nm). Peak names and drugs conc.: are as given in figure 2 and the produced current (µA) is written.

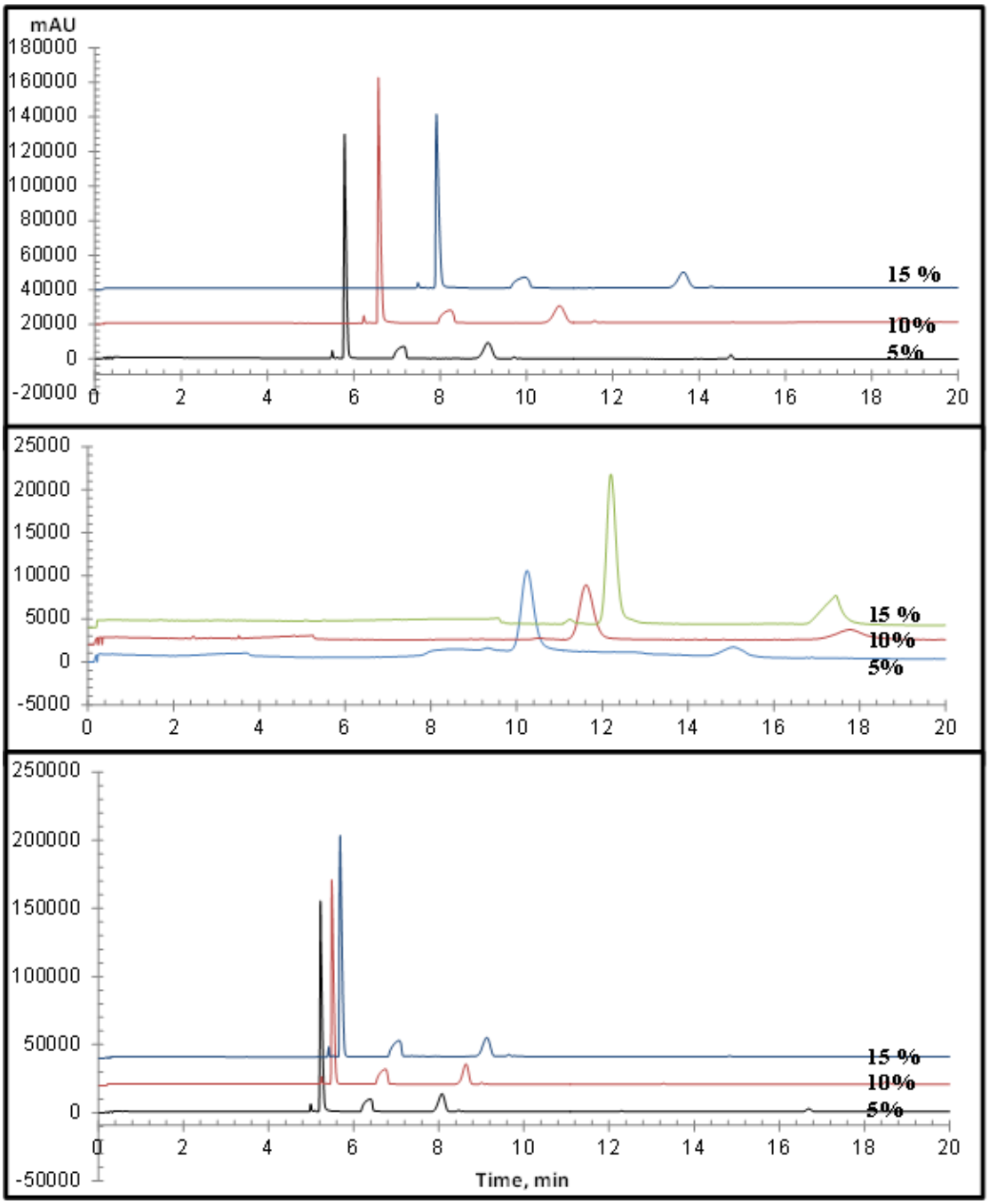

Figure 2.3.4 Effect of organic modifiers on separation of the studied drugs (A) methanol, (B) ethanol, and (C) acetonitrile.

Operating conditions: 40 mM phosphate buffer (pH 6), injection (2 s, 0.5 psi), 17 kV, 25 ˚C, 245 nm (bandwidth 20 nm). Peak names and drugs conc.: are as given in figure 2.3.2.

2.3.3.1.4. Effect of applied voltage

The applied voltage effect was investigated under the optimized conditions selected above from 5 to 20 kV. As expected, increasing the applied voltage increases the EOF, leading to shorter analysis time and higher efficiencies as shown in Figure 2.3.6. However, lowering the applied voltage to less than 10 kV decreases the EOF so the time for separation was more than 20 min and increasing applied voltage to more than 20 kV exhibited higher currents and produced Joule's heating. To limit this heating inside the capillary, the maximum applied voltage was chosen from an Ohm's plot (current vs voltage). The selected voltage was 17 kV (current (≈ 41 µA).

2.3.3.1.5. Effect of injection time

Injection time affects the peak width and peak height. Sample solutions were hydrodynamically injected at 0.5 psi while the injection time was varied from 1.0 to 5.0 s. After 3.0 s, the peak widths of the studied compounds were increased and the peak shapes were deformed, so 2.0 s was selected as the optimum injection time (Fig. 2.3.7).

2.3.3.1.6. Effect of capillary cartridge temperature

Controlling the temperature of the capillary cartridge is important in capillary electrophoresis. The viscosity of the running buffer is dependent on capillary temperature, so changes in temperature cause changes in EOF, electrophoretic mobilities and injection volume. The influence of the temperature on analysis was investigated at 20, 25 and 30 ˚C. As shown in Figure 2.3.8, the selected temperature was 25 ˚C because it provided the best resolution and the generated current was not more than 42 µA.

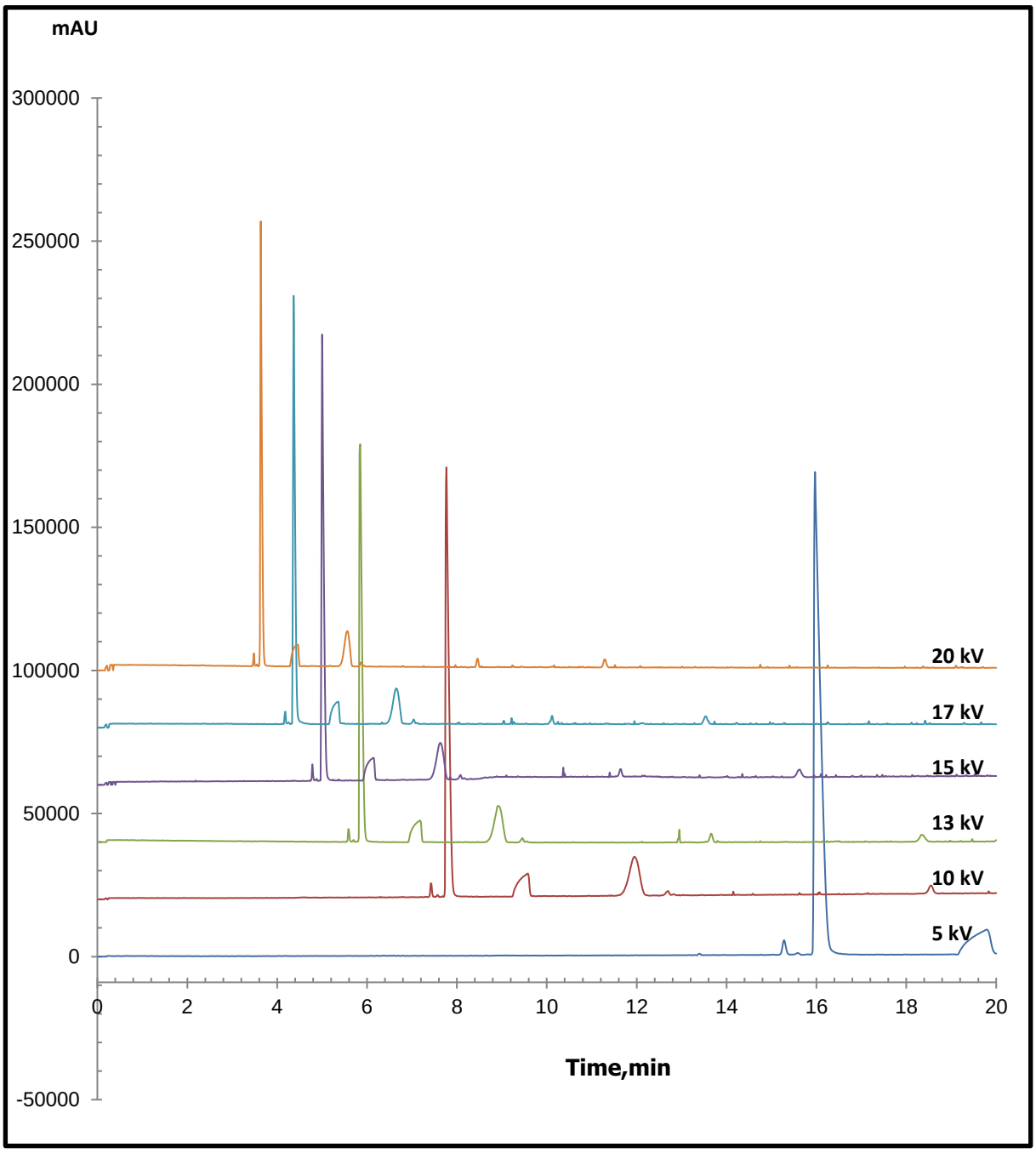

Figure 2.3.5 Effect of applied voltage (kV) on separation of the studied drugs.

Operating conditions: 40 mM phosphate buffer (pH 6), injection (2 s, 0.5 psi), 25 ˚C, 245 nm (bandwidth 20 nm). Peak names and drugs conc.: are as given in figure 2.3.2.

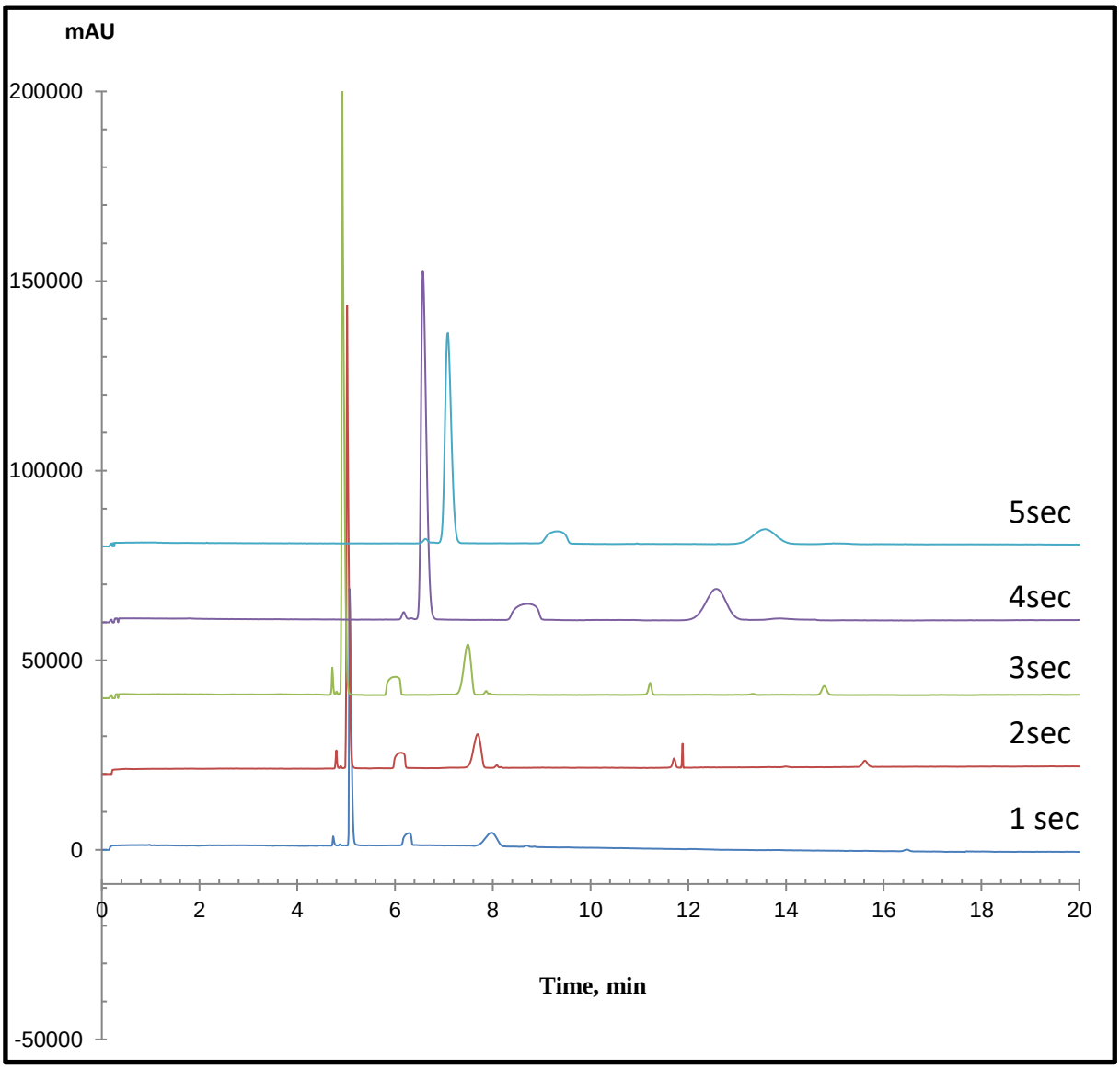

Figure 2.3.6 Effect of injection time (sec.) on separation of the studied drugs.

Operating conditions: 40 mM phosphate buffer (pH 6), 17 kV, 25 ˚C, 0.5 psi, 245 nm (bandwidth 20 nm). Peak names and drugs conc.: are as given in figure 2.32.

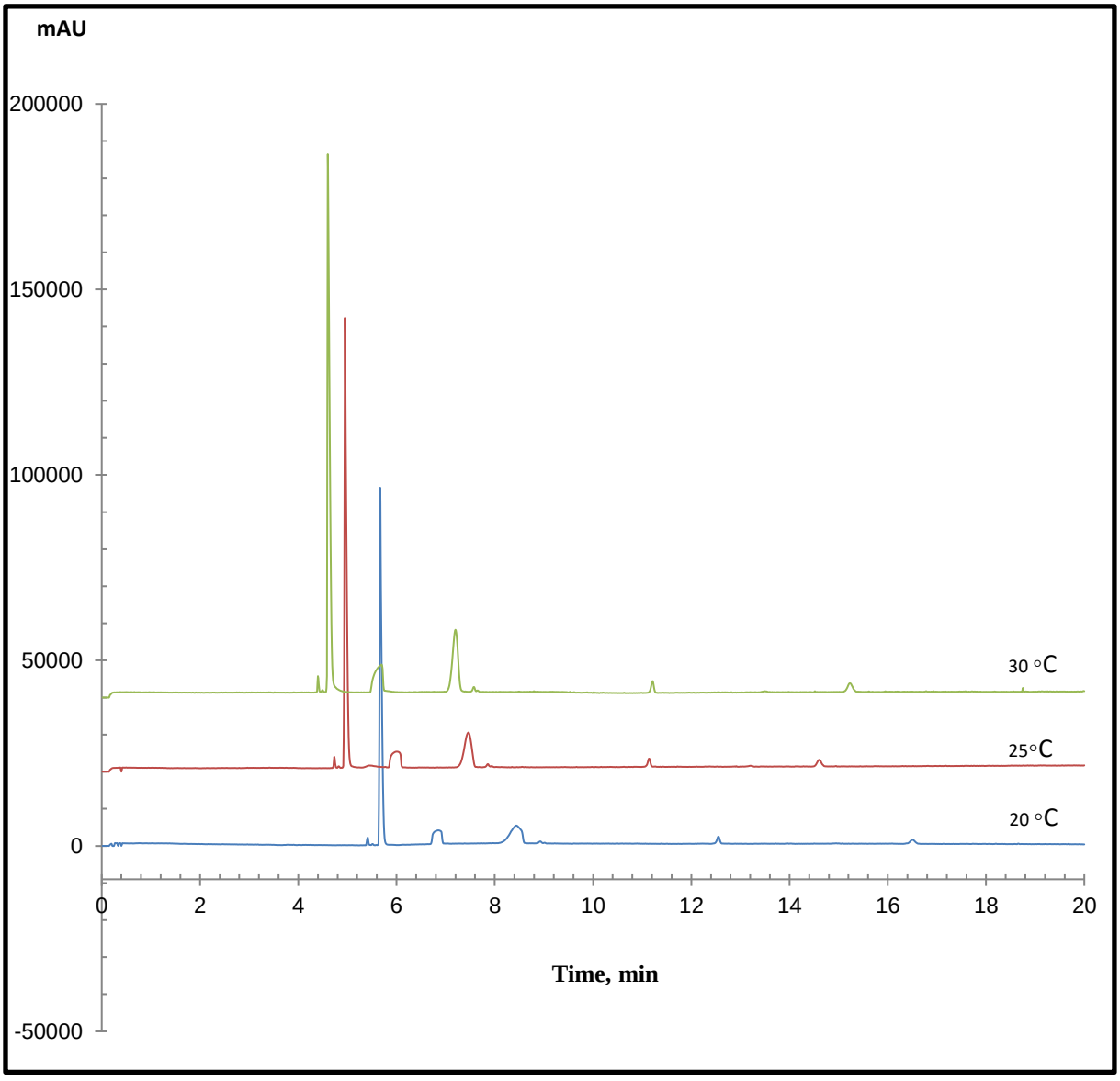

Figure 2.3.7 Effect of capillary cartridge temperature (˚C) on separation of the studied drugs. Operating conditions: 40 mM phosphate buffer (pH 6), 17 kV, 2 sec, 0.5 psi, 245 nm (bandwidth 20 nm). Peak names and drugs conc.: are as given in figure 2.3.2.

2.3.3.1.7. Selection of internal standard (IS)

The use of IS is recommended to compensate for injection errors, minor fluctuations effect of the migration time and improve the quantitative analysis. Then MXP was chosen as it possesses pk_a value of 5.4 [112] and its molar mass is high (535.03 g/mol) so it will be negatively charged under the optimized condition and as expected it eluted after HCZ [11].

2.3.3.1.8. Selection of the detection wavelength

In order to optimize sensitivity and detection limit of the method, a multi wavelength detection system (190–300 nm) was used in the CE system. For the simultaneous determination of the triple mixture, the maximum detection sensitivities were obtained at 245 nm (bandwidth 20 nm). Figure 2.3.9 shows the effect of detection wavelength on the proposed CZE method. Optimum electrophoretic conditions for the CZE determination of the studied drugs are summarized in Table 2.3.1. At 5.4 minutes on the electropherogram (Fig. 2.3.2), this distinct wide CE peak corresponds to the migration time of HCZ (neutral analyte at pH 6.0) which also corresponds to the EOF. The electroosmotic mobility (μ_{eof}), apparent mobility (μ_a) and effective mobility (μ_e) was calculated and the data were abridged in Table 2.3.2. The subsequent apparent mobility (μ_{ap}) of HCZ is determined to be 5.2×10^{-4} cm^2/Vs (the electroosmotic mobility (μ_{eof})) and its effective mobility (μ_e) is equal to zero as it is neutral compound under the optimized conditions. On the other hand, AML retained overall positive charge under the operating conditions and thus is first to be eluted in the CZE process (the small positive ion migrated the fastest). ALS also retained overall positive charge and migrate with different mobility rate than AML according to charge-to-size ratio. MXP (IS) at pH 6.0 becomes negatively charged and migrated eventually towards the cathode due to the higher force of EOF. Negatively charged species exhibit higher migration time and consequently negative effective mobilities.

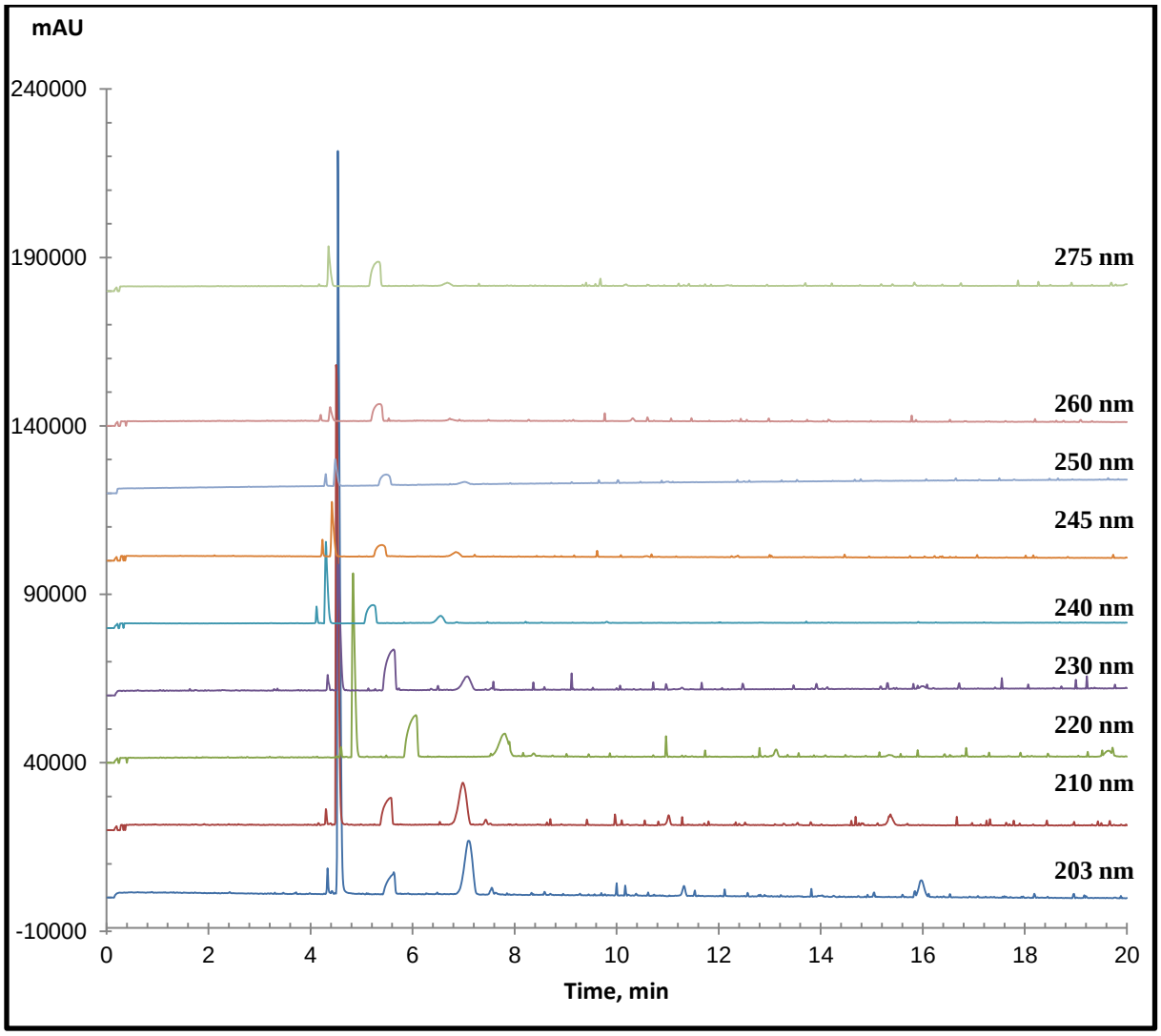

Figure 2.3.8 Selection of the detection wavelength.

Operating conditions: Operating conditions: 40mM phosphate buffer (pH 6), injection (2 s, 0.5 psi), 17 kV, 25 ˚C. Peak names and drugs conc.: are as given in figure 2.3.2.

Table 2.3.1 Typical electrophoretic conditions for the CZE determination of the studied drugs

Capillary	Fused silica capillary (57.0 cm total length and 50.0 cm effective length, 75.6 µm id)
BGE	40 mM phosphate buffer at pH 6.0
Applied Voltage	Normal (positive) polarity, + 17 kV
Detector	DAD at 245 nm
Bandwidth	20 nm
Sample Injection	Hydrodynamic injection for 2 s under a pressure of 0.5 psi
capillary Cartridge Temperature	25 ^{o}C
Sample Solvent	Methanol and water (10:90 v/v).

Table 2.3.2 Mobilities and migration times of the studied compounds using CZE

Analyte	Average Migration time (s)	Electroosmotic mobility (μ_{eof}) ($\times 10^{-4}$ cm^2/ Vs)	Apparent mobility (μ_a) ($\times 10^{-4}$ m^2/Vs)	Effective mobility (μ_e) ($\times 10^{-4}$ cm^2/ Vs)
EOF	**324**	**5.2**		
AML	252		6.7	1.5
ALS	264		6.4	1.2
HCZ	324		5.2	0
MXP	408		4.1	-1.1

2.3.3.2. Validation

Validation of the proposed CZE method was performed with respect to linearity and range, specificity, limit of detection, limit of quantitation, accuracy, precision and robustness according to the ICH Guidelines [113]

2.3.3.2.1. Linearity and Range

A linear relationship was established by plotting the peak area ratio (the studied drug peak area / IS peak area) against the drug concentration in µg/mL as shown in Figures 2.3.10-2.3.12. The concentration ranges were found to be linear in the range of 1-10 µg/mL, 2.5-25 µg/mL and 30-300 µg/mL for AML, HCZ and ALS, respectively. Linear regression analysis of the data gave the following equations:

P = 0.0110 C - 0.0009	(r=0.9999)	for AML
P = 0.0203 C + 0.1298	(r=0.9999)	for HCZ
P = 0.0122 C + 0.0846	(r=0.9998)	for ALS

Where: P is the peak area, C is the concentration of the drug in µg/mL and r is the correlation coefficient.

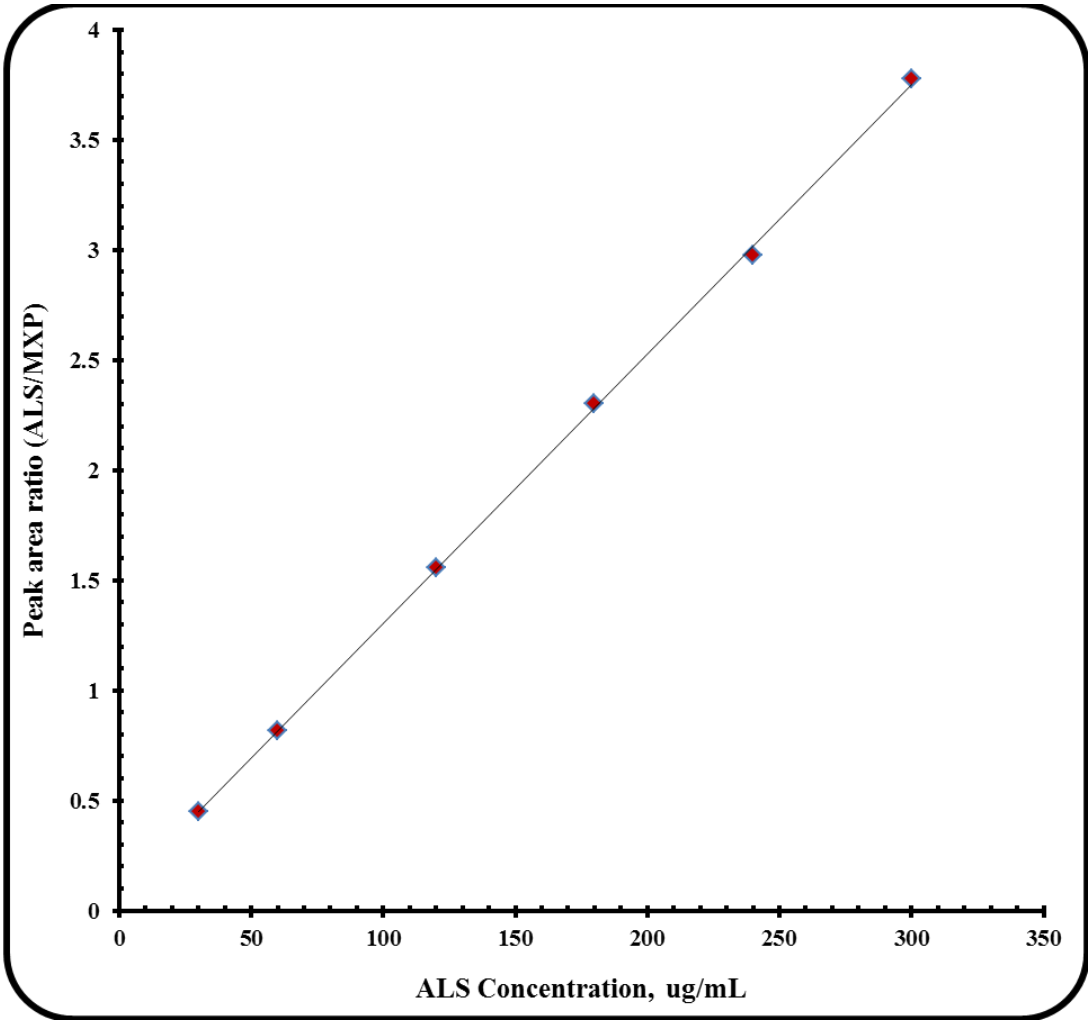

Figure 2.3.9 Calibration curve for the CZE determination of ALS

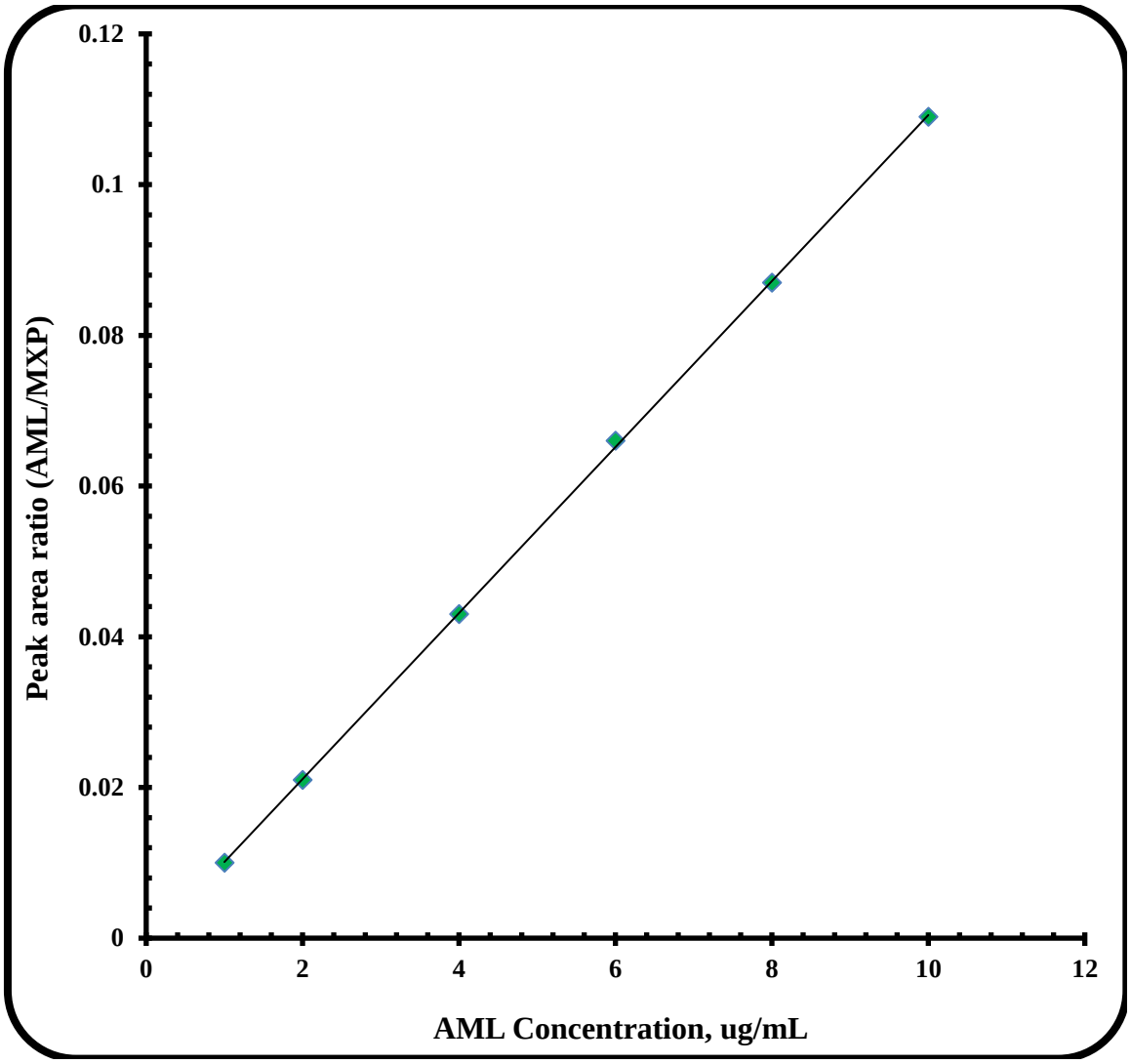

Figure 2.3.10 Calibration curve for the CZE determination of AML.

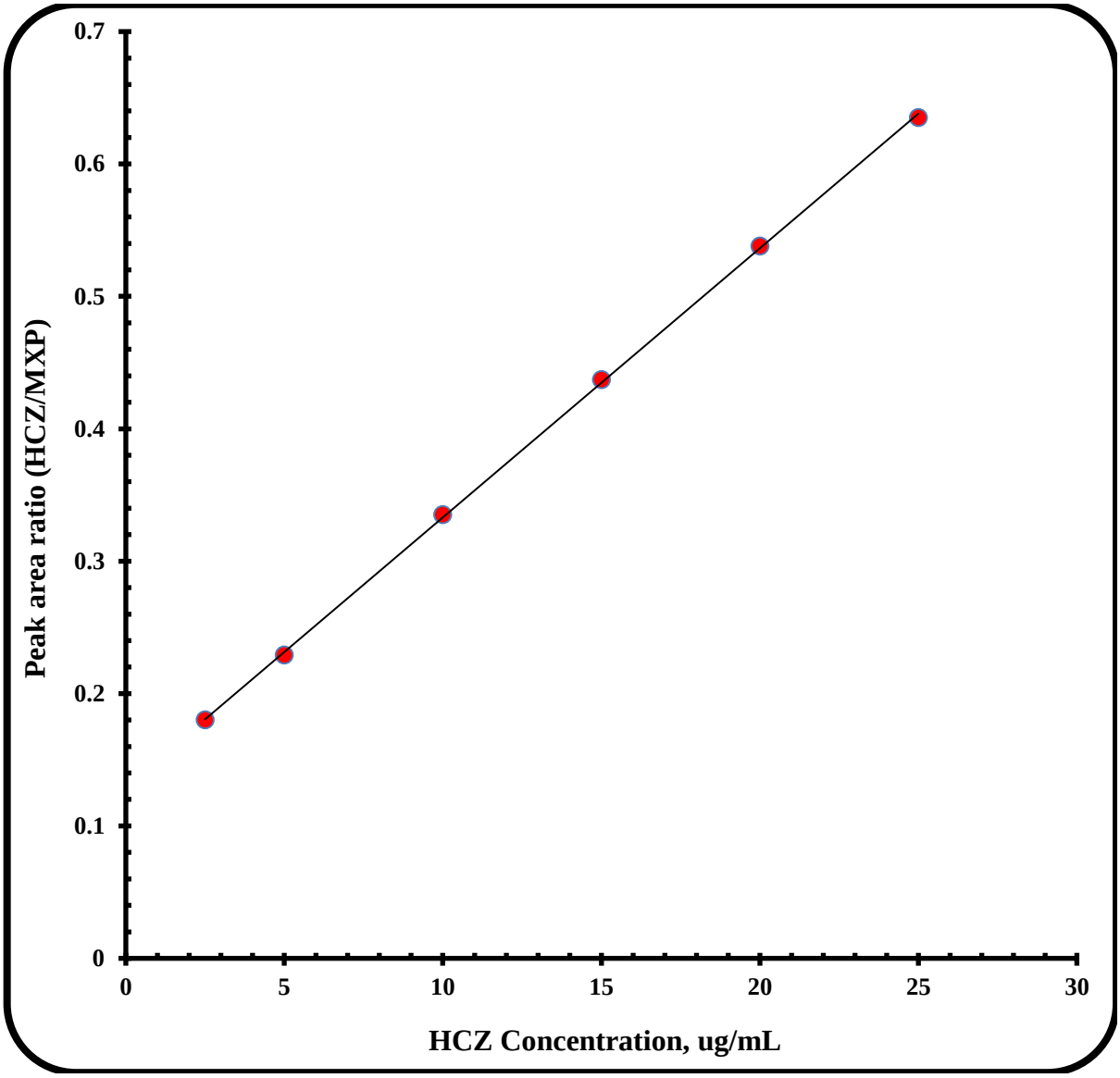

Figure 2.3.11 Calibration curve for the CZE determination of HCZ.

The statistical analysis of the data [114] gave high values of the correlation coefficient (r) of the regression equations, small values of the standard deviation of residuals ($S_{y/x}$), of intercept (S_a), and of slope (S_b), and small values of the percentage relative standard deviation and the percentage relative error (Table 2.3.3). These data proved the linearity of the calibration graphs and indicated the high accuracy and precision of the proposed method.

2.3.3.2.2. Limit of Detection (LOD) and Limit of Quantitation (LOQ)

LOQ and LOD were calculated according to ICH Q2R1 recommendations using the following equations [113]:

$$LOQ = 10\ S_a/b \text{ and } LOD = 3.3\ S_a/b$$

Where S_a = standard deviation of the intercept and b = slope of the calibration curve.

The limit of quantitation (LOQ) was determined by establishing the lowest concentration that can be measured and below which the calibration graph is nonlinear. The limit of detection (LOD) [115] [115] [115] [238] [225] was determined by establishing the minimum level at which the analyte can be reliably detected. LOQ values were found to be 0.33, 1.01 and 17.65 µg/mL while, LOD values were found to be 0.11, 0.33 and 5.83 µg/mL for AML, HCZ and ALS, respectively. The results are shown in Table 2.3.3.

Table 2.3.3 Performance data for the determination of the studied drugs by the proposed CZE method

Parameter	AML	HCZ	ALS
Linearity and range (µg/mL)	1-10	2.5-25	30-300
Intercept (a)	-0.0009	0.1298	0.0846
Slope (b)	0.0110	0.0203	0.0122
Correlation coefficient (r)	0.9999	0.9999	0.9998
S.D. of residuals ($S_{y/x}$)	0.0005	0.0026	0.0277
S.D. of intercept (S_a)	0.0004	0.0021	0.0215
S.D. of slope (S_b)	0.0001	0.0002	0.0001
Percentage relative standard deviation, % RSD	0.79	0.67	0.80
Limit of detection, LOD (µg/mL)	0.11	0.33	5.83
Limit of quantitation, LOQ (µg/mL)	0.33	1.01	17.65

2.3.3.2.3. Accuracy

To prove the accuracy of the proposed method, the results of the assay of ALS, AML and HCZ, both in pure form and in pharmaceutical preparations were compared with those of the comparison method [116]. Statistical analysis [114] of the results using Student's t-test and variance ratio F-test revealed no significant difference between the performance of the two methods regarding the accuracy (Tables 2.3.4 - 2.3.6). The comparison method [116] depends on the analysis of ALS, AML and HCZ triple mixture by ion-pair LC using C18 column, acetonitrile: 25 mM octane sulphonic acid sodium salt monohydrate (60: 40 v/v) as the mobile phase and UV detection at 232 nm.

2.3.3.2.4. Precision

2.3.3.2.4.1. Repeatability

Intra-day precision (repeatability) was performed through replicate analysis of three concentrations of the studied drugs in pure forms on three successive times (Table 2.3.7).

Table 2.3.4 Assay results for the determination of the studied drugs in pure forms by the CZE and comparison methods

Compound	Proposed method			Comparison method (HPLC) [116]
	Amount taken (μg/mL)	Amount found (μg/mL)	% Found	% Found
AML	1.00	0.990	99.00	100.7
	2.00	1.990	99.55	99.78
	4.00	3.990	99.78	99.34
	6.00	6.080	101.4	100.4
	8.00	7.990	99.89	
	10.0	9.990	99.91	
Mean ± S.D.			99.92± 0.79	100.1± 0.60
t			0.28 (2.31)	
F			1.73 (9.01)	
HCZ	2.50	2.490	99.68	100.0
	5.00	4.950	99.00	99.22
	10.0	10.10	100.7	101.1
	15.0	15.10	100.6	99.57
	20.0	20.10	100.4	
	25.0	24.90	99.64	
Mean ± S.D.			100.0± 0.67	99.98± 0.82
t			0.04(2.31)	
F			1.50 (5.41)	
ALS	30.0	30.00	100.1	101.2
	60.0	60.20	100.3	99.14
	120	120.5	100.5	99.66
	180	181.8	101.1	100.5
	240	237.1	98.79	
	300	302.7	100.9	
Mean ± S.D.			100.3± 0.81	100.1± 0.91
t			0.26(2.31)	
F			1.27 (5.41)	

N.B. Each result is the average of three separate determinations.

The values between parentheses are the tabulated t and F values at P = 0.05 [114].

Table 2.3.5 Assay results for the determination of the studied drugs in their laboratory prepared mixture and comparison methods

Ratio	Compound	Proposed method			Comparison method [116]
		Amount taken (μg/mL)	Amount found (μg/mL)	% Found	% Found
AML: HCZ: ALS 1.0 : 1.8: 23.9 m/m/m	**AML**	3.14	3.150	100.29	100.52
		7.50	7.500	99.97	99.35
		10.0	10.01	100.06	100.24
	Mean ± S.D.			100.11± 0.17	100.04± 0.61
	% RSD			0.17	
	t			0.22 (2.36)	
	F			1.68 (19.29)	
	HCZ	5.65	5.610	99.26	99.18
		13.5	13.71	101.58	100.84
		18.0	18.05	100.27	99.71
	Mean ± S.D.			100.37± 1.17	99.91± 0.85
	% RSD			1.16	
	t			0.18(2.36)	
	F			1.62 (5.79)	
	ALS	75.0	73.94	98.59	98.63
		179	177.9	99.27	101.05
		239	238.0	99.61	99.82
	Mean ± S.D.			99.16± 0.52	99.83± 2.21
	% RSD			0.52	
	t			0.65(2.36)	
	F			2.27 (5.79)	

N.B. Each result is the average of three separate determinations.

The values between parentheses are the tabulated t and F values at P = 0.05 [114].

Table 2.3.6 Assay results for the determination of the studied drugs in their co-formulated tablets and comparison methods.

Dosage Form	Compound	Proposed method			Comparison method (HPLC)[116]
		Amount taken (μg/mL)	Amount found (μg/mL)	% Found[a]	% Found[a]
AMTURNIDE® 300-10-25 mg tablets[b]	**AML**	3.14	3.180	101.2	98.88
		7.50	7.500	99.98	100.86
		10.0	10.10	101.1	99.85
	Mean ± S.D.			100.75± 0.67	99.86± 0.99
	% RSD			0.67	
	t			0.09 (2.36)	
	F			1.56 (5.79)	
	HCZ	5.65	5.720	101.3	99.82
		13.5	13.60	100. 9	100.2
		18.0	17.70	98.4	99.97
	Mean ± S.D.			100.2± 1.59	99.98± 0.17
	% RSD			1.58	
	t			0.05(2.36)	
	F			15.29 (19.29)	
	ALS	75.0	75.10	100.1	99.28
		179	182.0	101.8	101.6
		239	242.0	101.2	99.32
	Mean ± S.D.			101.1± 0.85	100.1± 1.32
	% RSD			0.84	
	t			0.29(2.36)	
	F			2.68 (5.79)	

[a] Each result is the average of three separate determinations.

[b] Labeled to contain 331.5 mg aliskiren hemifumarate (equivalent to 300 mg aliskiren as a free base), 13.87 mg amlodipine besylate (equivalent to 10 mg amlodipine as a free base) and 25 mg

hydrochlorothiazide; manufactured by Novartis Pharmaceuticals Corporation East, NJ, USA; batch # NDC 0078-0614-15. Nominal contents of AML = 10.07 mg as free base, of HCZ = 25.05 mg as free base and of ALS = 303.30 mg as free base per tablet.The values between parentheses are the tabulated t and F values at P = 0.05 [114].

2.3.3.2.4.2. Intermediate Precision

Inter-day precision (Intermediate precision) was assessed using three concentrations of the studied drugs in pure forms and three replicates of each concentration on three successive days. The results are summarized in Table 2.3.7. The relative standard deviations and percentage relative errors were found to be very small indicating excellent repeatability and intermediate precision of the proposed method.

2.3.3.2.5. Robustness

The robustness of the proposed method was evaluated by the constancy of the peak area ratio with the deliberated changes in the experimental parameters; these parameters include (phosphate buffer pH 6.0 ± 0.2, Phosphate buffer concentration 40 ± 5 mM, applied voltage 17 ± 2 kV and capillary cartridge temperature 25 ± 2 ◦C). Analyses were carried out in triplicate and only one parameter was changed in the experiments at a time. These changes didn’t greatly affect the peak area ratio and migration times of the studied drugs (Table 2.3.8).

Table 2.3.7 Precision data for the determination the studied drugs by the proposed CZE method

	Parameters	**AML** concentration (μg/mL)			**HCZ** concentration (μg/mL)			**ALS** concentration (μg/mL)		
		3.14	**7.50**	**10.00**	**5.65**	**13.50**	**18.00**	**75.00**	**179.25**	**239.00**
Intra-day	Amount found[a] (μg/mL)	3.17	7.41	9.96	5.72	13.51	17.87	75.02	178.68	239.60
		3.11	7.57	10.21	5.65	13.63	17.97	75.72	179.36	242.08
		3.16	7.63	10.14	5.62	13.72	17.67	74.92	180.95	243.71
	($\bar{x}$)	100.18	100.47	101.03	100.26	100.90	99.10	100.29	100.23	101.17
	±S.D.	1.05	1.50	1.29	0.87	0.79	0.85	0.59	0.65	0.87
	%RSD	1.05	1.49	1.28	0.87	0.78	0.86	0.58	0.65	0.86
Inter-day	Amount found[a] (μg/mL)	3.21	7.42	10.09	5.66	13.85	18.12	75.97	181.56	239.60
		3.11	7.49	9.81	5.74	13.65	18.25	76.56	180.49	244.64
		3.18	7.68	9.97	5.62	13.63	17.98	75.22	177.58	243.73
	($\bar{x}$)	100.83	100.40	99.57	100.43	101.54	100.64	101.22	100.35	101.53
	±S.D.	1.48	1.80	1.41	1.14	0.88	0.76	0.89	1.15	1.13
	%RSD	1.47	1.80	1.41	1.13	0.87	0.75	0.88	1.14	1.11

[a] Each result is the average of three separate determinations

Table 2.3.8 Robustness data for the determination the studied drugs by the proposed CZE method

Parameters		Migration times (min.)			Peak area ratios		
		AML	**ALS**	**HCZ**	**AML**	**ALS**	**HCZ**
Optimized condition		**4.20**	**4.40**	**5.40**	**0.066**	**2.976**	**0.538**
Buffer pH	**5.82**	4.33	4.51	5.59	0.065	2.961	0.534
	6.21	4.05	4.25	5.15	0.067	2.979	0.538
Buffer concocent-ration (mM)	**35**	4.10	4.25	5.20	0.064	2.969	0.537
	45	4.25	4.80	5.55	0.069	2.994	0.528
Applied voltage (kV)	**15**	4.76	4.98	6.13	0.076	2.606	0.524
	20	3.46	3.62	4.43	0.076	2.645	0.561
Capillary temp. (ºC)	**23**	4.40	4.65	5.83	0.068	2.805	0.537
	27	4.08	4.25	4.95	0.066	2.928	0.585

N.B. Each result is the average of three separate determinations.

2.3.3.2.6. Specificity

The specificity of the method was investigated by observing any interference encountered from common tablet excipients and it was confirmed that the signals measured was caused only by the analytes. Each film-coated tablet of Amturnide® contains the following inactive ingredients: colloidal silicon dioxide, crospovidone, hypromellose, iron oxide red, iron oxide yellow, iron oxide black, magnesium stearate, microcrystalline cellulose, polyethylene glycol, povidone, talc, and titanium dioxide. It was found that these compounds did not interfere with the results of the proposed method. As shown in Figures 2.3.13, 2.3.14 the tablets did not show any additional peak when compared to the synthetic mixture electropherogram which confirm the specificity of the method (Table 2.3.6).

2.3.3.3. Analysis of AML, HCZ and ALS in laboratory prepared mixtures and co-formulated tablets

The proposed CZE method was applied to the simultaneous determination of **AML**, **HCZ** and **ALS** in laboratory prepared mixtures in the medicinally recommended ratio of 1.0: 1.8: 23.9 m/m/m, respectively (Fig. 2.3.13). Furthermore, the proposed method was successfully applied to their determination in co-formulated tablets (Fig. 2.3.14). The average percent found of different concentrations were based on the average of three replicate determinations. The results shown in Tables 2.3.5,2.3.6 are in good agreement with those obtained using a comparison method [116]. Statistical analysis of the results obtained using Student's t-test and variance ratio F-test [114] revealed no significant difference between the performance of the two methods regarding the accuracy and precision, respectively.

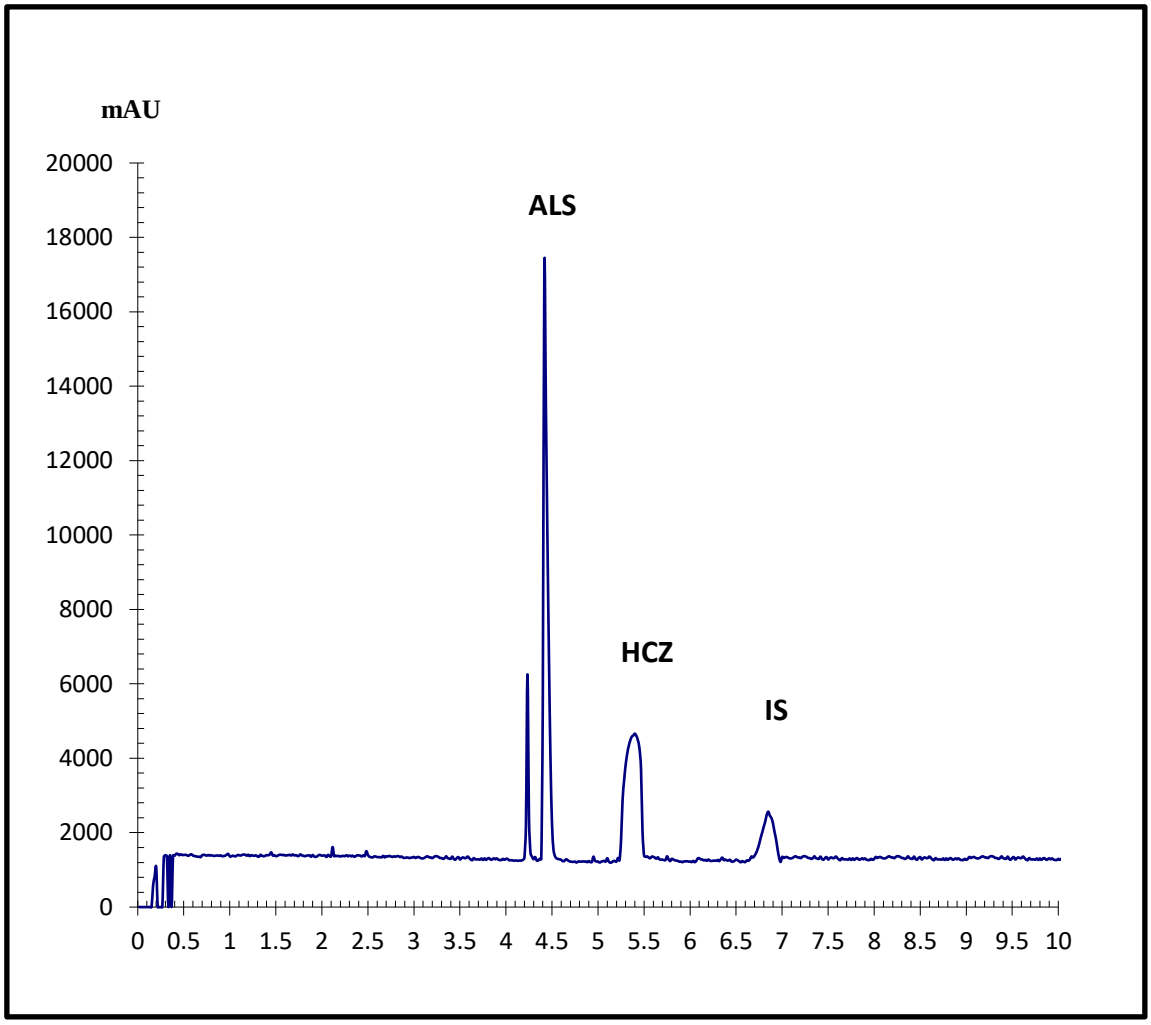

Figure 2.3.12 Application of the proposed method for the simultaneous determination of a laboratory prepared mixture of 8 μg/mL of AML, 240 μg/mL ALS, 20 μg/mL HCZ and 25 μg/mL MXP (IS).

Operating conditions: 40mM phosphate buffer (pH 6), injection (2 s, 0.5 psi), 17 kV, 25 ˚C and DAD at 245 nm (bandwidth 20)

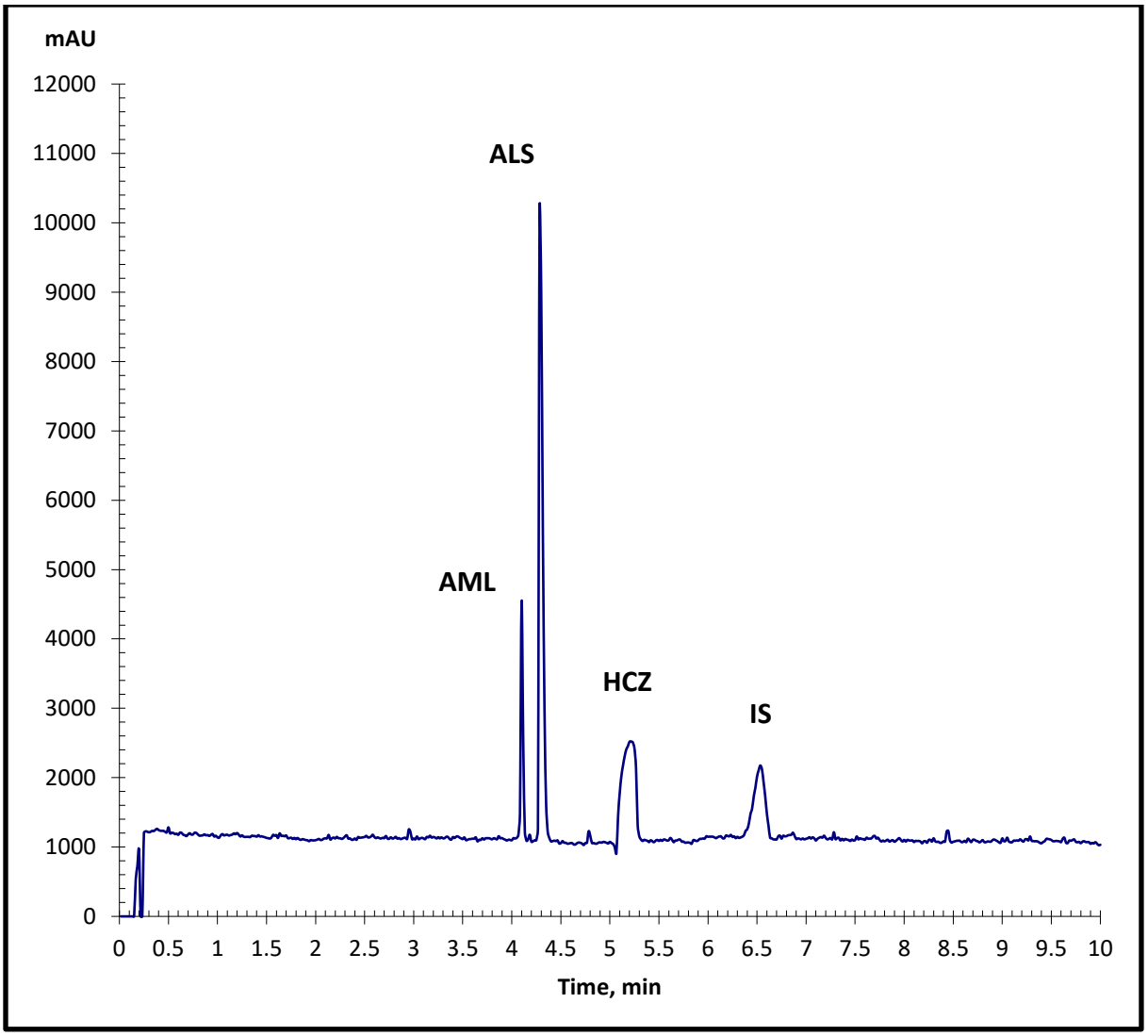

Figure 2.3.13 Application of the proposed method for the simultaneous determination of the studied drugs in Amturnide® tablets (7.5 µg/mL of AML, 179.25 µg/mL ALS, 13.5 µg/mL HCZ and 25 µg/mL MXP; IS).

Operating conditions: 40 mM phosphate buffer (pH 6), injection (2 s, 0.5 psi), 17 kV, 25 ˚C and DAD at 245 nm (bandwidth 20)

2.4 Conclusions

In section 2.2, a new, simple, accurate, selective and validated CZE method was developed for the simultaneous determination of VAL, AML and HCZ in ternary mixture. The proposed method has distinct advantages regarding reliability, selectivity and operation cost. LOD of 1.82, 0.39, 0.65 μg mL^{-1} and LOQ of 5.51, 1.17, 1.96 μg mL^{-1} for VAL, AML and HCZ, respectively were obtained. Moreover, this method was successfully applied for the analysis of the three medications in their laboratory prepared mixtures and co-formulated tablets.

In section 2.3, a novel, simple, accurate and precise CZE method was explored for the simultaneous determination of AML, HCZ and ALS in triple mixture. The developed method has distinct advantages regarding analysis time, sensitivity and cost compared with those of the previously reported methods. Limits of detection of 0.11, 0.33 and 5.83 μg/mL and limits of quantitation of 0.33, 1.01 and 17.65 μg/mL for AML, HCZ and ALS, respectively were obtained. The good validation criteria of the proposed method allow its utilization for quality control laboratories. In addition, it is a good analytical tool for the simultaneous analysis of the studied drugs in their co-formulated tablets. Moreover, the analysis of the same therapeutic class drugs in a single run has the advantage of a unique sample extraction procedure and a shorter analytical run, thus reducing the overall turnaround time. In addition, this method consumes no organic solvents and thus it can be classified as green chemistry.

Finally, the proposed methods can be used for the quality control of the cited drugs in ordinary laboratories.

References

1. Craxì, A.; Pawlotsky, J. M.; Wedemeyer, H.; Bjoro, K.; Flisiak, R.; Forns, X.; Mondelli, M.; Peck-Radosavljevic, M.; Rosenberg, W.; Sarrazin, C.; Jacobson, I.; Dusheiko, G. European Association for the Study of the Liver (EASL): Clinical Practice Guidelines: management of hepatitis C virus infection. Journal of hepatology 2011, 55 (2), 245-64.
2. Skoog, D. A.; West, D. M.; Holler, F. J.; Crouch, S. R. Fundamentals of Analytical Chemistry. 8th ed.; Saunders College Publishing: Philadelphia, 2004.
3. Suntornsuk, L. Recent advances of capillary electrophoresis in pharmaceutical analysis. Analytical and bioanalytical chemistry 2010, 398 (1), 29-52.
4. The United States Pharmacopoeia 30, the National Formulary 25 [Online]; US Pharmacopeial Convention: Rockville, MD, 2007.
5. Vetuschi, C.; Ragno, G. Fourth UV derivative spectrophotometry for the simultaneous assay of atenolol and chlorthalidone in pharmaceuticals. Int. J. Pharm. 1990, 65 (Copyright (C) 2013 American Chemical Society (ACS). All Rights Reserved.), 177-81.
6. Hendrickx, A.; Mangelings, D.; Heyden, Y. V. Capillary methods for drug analysis. Journal of AOAC International 2011, 94 (3), 667-702.
7. Gilpin, R. K.; Gilpin, C. S. Pharmaceuticals and related drugs. Analytical chemistry 2009, 81 (12), 4679-94.
8. Grosche, O.; Zeitz, M. 5 Role of CE in drug substance and drug product development. In Separation Science and Technology, Satinder, A.; Jimidar, M. I., Eds. Academic Press: New York, 2008; Vol. Volume 9, pp 95-121.

9. Holzgrabe, U. 11 The need for CE methods in pharmacopoeial monographs. In Separation Science and Technology, Satinder, A.; Jimidar, M. I., Eds. Academic Press: New York, 2008; Vol. Volume 9, pp 245-258.
10. Mallampati, S.; Pauwels, J.; Hoogmartens, J.; Van Schepdael, A. 12 CE in impurity profiling of drugs. In Separation Science and Technology, Satinder, A.; Jimidar, M. I., Eds. Academic Press: New York, 2008; Vol. Volume 9, pp 259-315.
11. Guo, A.; Camblin, G.; Han, M.; Meert, C.; Park, S. 14 Role of CE in biopharmaceutical development and quality control. In Separation Science and Technology, Satinder, A.; Jimidar, M. I., Eds. Academic Press: New York, 2008; Vol. Volume 9, pp 357-532.
12. Suntornsuk, L. Capillary electrophoresis in pharmaceutical analysis: a survey on recent applications. Journal of chromatographic science 2007, 45 (9), 559-77.
13. Altria, K.; Marsh, A.; Sanger-van de Griend, C. Capillary electrophoresis for the analysis of small-molecule pharmaceuticals. Electrophoresis 2006, 27 (12), 2263-82.
14. Timerbaev, A. R.; Keppler, B. K. Capillary electrophoresis of metal-based drugs. Analytical biochemistry 2007, 369 (1), 1-7.
15. Hoff, R.; Kist, T. B. Analysis of sulfonamides by capillary electrophoresis. Journal of separation science 2009, 32 (5-6), 854-66.
16. Criscione, L.; Gasparo, M. D.; Buhlmayer, P.; Whitebread, S.; Ramjoue, H. P.; Wood, J. Pharmacological profile of valsartan: a potent, orally active, nonpeptide antagonist of the angiotensin II AT1-receptor subtype. Br J. Pharmacol. 1993, 110 (2), 761-71.
17. Asmar, R. Targeting effective blood pressure control with angiotensin receptor blockers. Int. J. Clin. Pract. 2006, 60 (3), 315-20.

18. El-Gindy, A.; Sallam, S.; Abdel-Salam, R. A. HPLC method for the simultaneous determination of atenolol and chlorthalidone in human breast milk. J. Sep. Sci. 2008, 31 (4), 677-82.

19. Abdollahpour, N.; Asoodeh, A.; Saberi, M. R.; Chamani, J. Separate and simultaneous binding effects of aspirin and amlodipine to human serum albumin based on fluorescence spectroscopic and molecular modeling characterizations: A mechanistic insight for determining usage drugs doses. J. Luminesc. 2011, 131 (9), 1885-1899.

20. Tengli, A. R.; Gurupadayya, B. M.; Soni, N. Simultaneous estimation of hydrochlorothiazide, amlodipine, and losartan in tablet dosage form by RP-HPLC. Int. J. Chem. Anal. Sci. 2013, 4 (1), 33-38.

21. Calhoun, D. A.; Lacourciere, Y.; Chiang, Y. T.; Glazer, R. D. Triple antihypertensive therapy with amlodipine, valsartan, and hydrochlorothiazide: a randomized clinical trial. Hypertens. 2009, 54 (1), 32-9.

22. Kocyigit, K. B.; Unsalan, S.; Rollas, S. Determination and validation of Ketoprofen, Pantoprazole and Valsartan together in human plasma by high performance liquid chromatography. Pharmazie 2006, 61, 586-589.

23. Daneshtalab, N.; Lewanczuk, R. Z.; F, J. High performance liquid chromatographic analysis of angiotensin II receptor antagonist Valsartan using a liquid extraction method. J. Chromatogr. B Analyt. Technol. Biomed. Life Sci. 2002, 766, 345-359.

24. Gonzalez, L.; Lopez, J. A.; Alonso, R. M.; Jimenez, R. M. Fast screening method for the determination of angiotensin II receptor antagonists in human plasma by high performance liquid chromatography with fluorimetric detection. J. Chromatogr. A 2002, 949, 49-60.

25. Koseki, N.; Kawashita, H.; Hara, H.; Niina, M.; Tanaka, M.; Kawai, R.; Nagae, Y.; Masuda, N. Development and validation of a method for quantitative determination of Valsartan in human plasma by liquid chromatography-tandem mass spectrometry. J. Pharm. Biomed. Anal. 2007, 43, 1769-1774.

26. Li, H.; Wang, Y.; Jiang, Y.; Tang, Y.; Wang, J.; Zhao, L.; Gu, J. A liquid chromatography tandem mass spectrometry method for the simultaneous quantification of Valsartan and Hydrochlorothiazide in human plasma J. Chromatogr. B Analyt. Technol. Biomed. Life Sci. 2007, 852, 436-442.

27. Senthamil, S. P.; Gowda, V. K.; Mandal, U.; Solomon, W. D.; Pal, T. K. Simultaneous determination of fixed dose combination of Nebivolol and Valsartan in human plasma by liquid chromatographic-tandem mass spectrometry and its application to pharmacokinetic study. J. Chromatogr. B Analyt. Technol. Biomed. Life Sci. 2007, 858, 143-150.

28. Hillaert, S.; Bossche, V. W. Simultaneous determination of Hydrochlorothiazide and several angiotensin II receptor antagonists by capillary electrophoresis. J. Pharm. Biomed. Anal. 2003, 31, 329-339.

29. Alnajjar, A. O. Validation of a capillary electrophoresis method for the simultaneous determination of amlodipine besylate and valsartan in pharmaceuticals and human plasma. J. AOAC Int. 2011, 94 (2), 498-502.

30. Satana, E.; Altinay, S.; Goger, N. G.; Ozkan, S. J.; Senturk, Z. J. Simultaneous determination of Valsartan and Hydrochlorothiazide in tablets by first derivative ultraviolet spectrophotometry and LC J. Pharm. Biomed. Anal. 2001, 25, 1009-1013.

31. Tatar, S.; Saglik, S. Comparison of UV - and second derivative spectrophotometric and LC methods for the determination of Valsartan in pharmaceutical formulation. J. Pharm. Biomed. Anal. 2002, 30, 371-375.

32. Shaalan, R. A.; Belal, T. S. Simultaneous spectrofluorimetric determination of amlodipine besylate and valsartan in their combined tablets. Drug Test. Anal. 2010, 2 (10), 489-93.

33. Sharma, M.; Kothari, C.; Sherikar, O.; Mehta, P. Concurrent Estimation of Amlodipine Besylate, Hydrochlorothiazide and Valsartan by RP-HPLC, HPTLC and UV-Spectrophotometry. J. Chromatogr. Sci. 2014, 52 (1), 27-35.

34. Patel, D. P.; Mehta, F. A.; Bhatt, K. K. Simultaneous Estimation of Amlodipine Besylate and Indapamide in a Pharmaceutical Formulation by a High Performance Liquid Chromatographic (RP-HPLC) Method. Sci. Pharm. 2012, 80 (3), 581-90.

35. Jain, P. S.; Patel, M. K.; Gorle, A. P.; Chaudhari, A. J.; Surana, S. J. Stability-indicating method for simultaneous estimation of olmesartan medoxomile, amlodipine besylate and hydrochlorothiazide by RP-HPLC in tablet dosage form. J. Chromatogr. Sci. 2012, 50 (8), 680-7.

36. Pilli, N. R.; Inamadugu, J. K.; Mullangi, R.; Karra, V. K.; Vaidya, J. R.; Rao, J. V. Simultaneous determination of atorvastatin, amlodipine, ramipril and benazepril in human plasma by LC-MS/MS and its application to a human pharmacokinetic study. Biomed. Chromatogr. 2011, 25 (4), 439-49.

37. Yacoub, M.; Awwad, A. A.; Alawi, M.; Arafat, T. Simultaneous determination of amlodipine and atorvastatin with its metabolites; ortho and para hydroxy atorvastatin; in human plasma by LC-MS/MS. J. Chromatogr. B Analyt. Technol. Biomed. Life Sci. 2013, 917-918, 36-47.

38. Fakhari, A. R.; Nojavan, S.; Haghgoo, S.; Mohammadi, A. Development of a stability-indicating CE assay for the determination of amlodipine enantiomers in commercial tablets. Electrophoresis 2008, 29 (22), 4583-4592.

39. Wankhede, S. B.; Raka, K. C.; Wadkar, S. B.; Chitlange, S. S. Spectrophotometric and HPLC methods for simultaneous estimation of amlodipine besilate, losartan potassium and hydrochlorothiazide in tablets. Indian J. Pharm. Sci. 2010, 72 (1), 136-40.

40. Rahman, N.; Hoda, M. N. Validated spectrophotometric methods for the determination of amlodipine besylate in drug formulations using 2,3-dichloro 5,6-dicyano 1,4-benzoquinone and ascorbic acid. J. Pharm. Biomed. Anal. 2003, 31 (2), 381-92.

41. Rahman, N.; Azmi, S. N. Spectrophotometric method for the determination of amlodipine besylate with ninhydrin in drug formulations. Farmaco 2001, 56 (10), 731-5.

42. Darwish, H. W.; Backeit, A. H. Multivariate versus classical univariate calibration methods for spectrofluorimetric data: application to simultaneous determination of olmesartan medoxamil and amlodipine besylate in their combined dosage form. J. Fluoresc. 2013, 23 (1), 79-91.

43. Hertzog, D. L.; McCafferty, J. F.; Fang, X.; Tyrrell, R. J.; Reed, R. A. Development and validation of a stability-indicating HPLC method for the simultaneous determination of losartan potassium, hydrochlorothiazide, and their degradation products. J. Pharm. Biomed. Anal. 2002, 30 (3), 747-60.

44. Sharma, R. N.; Pancholi, S. S. Simple RP-HPLC method for determination of triple drug combination of valsartan, amlodipine and hydrochlorothiazide in human plasma. Acta Pharmaceutica 2012, 62 (1), 45-58.

45. Joshi, S. J.; Karbhari, P. A.; Bhoir, S. I.; Bindu, K. S.; Das, C. RP-HPLC method for simultaneous estimation of bisoprolol fumarate and hydrochlorothiazide in tablet formulation. J. Pharm. Biomed. Anal. 2010, 52 (3), 362-71.

46. Meyyanathan, S. N.; Rajan, S.; Muralidharan, S.; Birajdar, A. S.; Suresh, B. A Validated RP-HPLC Method for Simultaneous Estimation of Nebivolol and Hydrochlorothiazide in Tablets. Indian J. Pharm. Sci. 2008, 70 (5), 687-9.

47. Tian, D. F.; Tian, X. L.; Tian, T.; Wang, Z. Y.; Mo, F. K. Simultaneous Determination of Valsartan and Hydrochlorothiazide in Tablets by RP-HPLC. Indian J. Pharm. Sci. 2008, 70 (3), 372-4.

48. Huang, T.; He, Z.; Yang, B.; Shao, L.; Zheng, X.; Duan, G. Simultaneous determination of captopril and hydrochlorothiazide in human plasma by reverse-phase HPLC from linear gradient elution. J. Pharm. Biomed. Anal. 2006, 41 (2), 644-8.

49. Bharathi, D. V.; Hotha, K. K.; Chatki, P. K.; Satyanarayana, V.; Venkateswarlu, V. LC-MS/MS method for simultaneous estimation of candesartan and hydrochlorothiazide in human plasma and its use in clinical pharmacokinetics. Bioanal. 2012, 4 (10), 1195-204.

50. Salvadori, M. C.; Moreira, R. F.; Borges, B. C.; Andraus, M. H.; Azevedo, C. P.; Moreno, R. A.; Borges, N. C. Simultaneous determination of losartan and hydrochlorothiazide in human plasma by LC/MS/MS with electrospray ionization and its application to pharmacokinetics. Clin. Exp. Hypertens. 2009, 31 (5), 415-27.

51. Rajasekhar, D.; Kumara, I. J.; Venkateswarlu, P. High performance liquid chromatography/negative ion electrospray tandem mass spectrometry method for the measurement of hydrochlorothiazide in human plasma: application to a comparative bioavailability study. Eur. J. Mass Spectrom. 2009, 15 (6), 715-21.

52. Nalwade, S.; Ranga Reddy, V.; Durga Rao, D.; Koteswara Rao, I. Rapid simultaneous determination of telmisartan, amlodipine besylate and hydrochlorothiazide in a combined poly pill dosage form by stability-indicating ultra performance liquid chromatography. Sci. Pharm. 2011, 79 (1), 69-84.

53. El-Gindy, A.; Ashour, A.; Abdel-Fattah, L.; Shabana, M. M. Spectrophotometric and HPTLC-densitometric determination of lisinopril and hydrochlorothiazide in binary mixtures. J. Pharm. Biomed. Anal. 2001, 25 (5-6), 923-31.

54. Varghese, S. J.; Ravi, T. K. Quantitative Simultaneous Determination of Amlodipine, Valsartan and hydrochlorothiazide in "Exforge HCT" Tablets Using High-Performance Liquid Chromatography and High-Performance Thin-Layer Chromatography. J. Liq. Chromatogr. Rel. Tech. 2011, 34 (12), 981-994.

55. Anandakumar, K.; Jothieswari, D.; Subathrai, R.; Santhi, D.; Vetrichelvan, T. Validated RP-HPLC method for the simultaneous determination of amlodipine besylate, valsartan, and hydrochlorothiazide in bulk and in pharmaceutical formulation. Acta Chromatogr. 2012, 24 (1), 37-50.

56. Galande, V. R.; Baheti, K. G.; Indraksha, S.; Dehghan, M. H. Estimation of Amlodipine Besylate, Valsartan and Hydrochlorothiazide in Bulk Mixture and Tablet by UV Spectrophotometry. Indian J. Pharm. Sci. 2012, 74 (1), 18-23.

57. Hendrickx, A.; Mangelings, D.; Heyden, Y. V. Capillary methods for drug analysis. J. AOAC Int. 2011, 94 (3), 667-702.

58. Altria, K. D.; Filbey, S. D. Quantitative Pharmaceutical analysis by Capillary Electrophoresis. J Liq. Chromatogr. 1993, 16 (11), 2281-2292.

59. Billes, F. Ionization equilibrium constants of pyrazine derivatives and ion conformations. Kémiai közlemények 1980, 54 (2-3), 359.

60. BP. The British Pharmacopoeia, The Stationery Office, London, U.K. 2009.

61. USP. The United States Pharmacopeal Convention, The United States Pharmacopoeia (USP 30), National Formulary (NF 25), Asian edition Maryland, U.S.A., 2007; Vol. 32, p 2287, 3445.

62. Riccioni, G.; Vitulano, N.; D'Orazio, N.; Bellocci, F. Aliskiren, the first approved renin inhibitor: Clinical application and safety in the treatment of hypertension. Advances in therapy 2009, 26 (7), 700-10.

63. Bonanni, L.; Dalla Vestra, M. Oral renin inhibitors in clinical practice: a perspective review. Ther Adv Chronic Dis 2012, 3 (4), 173-81.

64. Clarke's Analysis of Drugs and Poisons [Online]; 3rd ed; The Pharmaceutical Press: London ; Electronic version, 2006.

65. John M. Beale, J.; Block, J. H. Organic Medicinal and Pharmaceutical Chemistry. 12th ed.; Lippincott Williams&Wilkins,a Wolters Kluwer business Philadelphia, 2011.

66. Abdollahpour, N.; Asoodeh, A.; Saberi, M. R.; Chamani, J. Separate and simultaneous binding effects of aspirin and amlodipine to human serum albumin based on fluorescence spectroscopic and molecular modeling characterizations: A mechanistic insight for determining usage drugs doses. Journal of Luminescence 2011, 131 (9), 1885-1899.

67. Tengli, A. R.; Gurupadayya, B. M.; Soni, N. Simultaneous estimation of hydrochlorothiazide, amlodipine, and losartan in tablet dosage form by RP-HPLC. International Journal of Chemical and Analytical Science 2013, (0), 1-6.

68. Murray, A. V.; Koenig, W.; Garcia-Puig, J.; Patel, S.; Uddin, A.; Zhang, J. Safety and efficacy of aliskiren/amlodipine/hydrochlorothiazide triple combination in patients with moderate to severe hypertension: a 54-week, open-label study. Journal of clinical hypertension 2012, 14 (12), 821-7.

69. Wrasse-Sangoi, M.; Sangoi, M. S.; Oliveira, P. R.; Secretti, L. T.; Rolim, C. M. Determination of aliskiren in tablet dosage forms by a validated stability-indicating RP-LC method. Journal of chromatographic science 2011, 49 (2), 170-5.

70. Swamy, G. K.; Rao, J. V. L. N. S.; Kumar, J. M. R.; Kumar, U. A.; Bikshapathi, D. V. R. N.; Kumar, D. V. Analytical method development and validation of aliskiren in bulk and tablet dosage form by RP-HPLC method. Journal of Pharmacy Research 2011, 4 (3), 865-867.

71. Babu, K. S.; Rao, J. V. L. N. S.; Bhargava, K. V. A simple and sensitive method for the determination of aliskiren hemifumarate using HPLC-UV detection. Rasayan Journal of Chemistry 2011, 4 (2), 285-288.

72. pachauri, S.; paliwal, S.; Kona.S.Srinivas; YogendraSingh; Jain, V. Development & validation of HPLC method for analysis of some antihypertensive agents in their pharmaceutical dosage forms. J Pharm Sci & Res 2010, Vol.2 (8), 459-464.

73. Belal, F.; Walash, M.; El-Enany, N.; Zayed, S. Highly sensitive HPLC method for assay of aliskiren in human plasma through derivatization with 1-naphthyl isocyanate using UV detection. Journal of chromatography. B, Analytical technologies in the biomedical and life sciences 2013, 933, 24-9.

74. Sangoi, M. S.; Wrasse-Sangoi, M.; Oliveira, P. R.; Rolim, C. M.; Steppe, M. Simultaneous determination of aliskiren and hydrochlorothiazide from their pharmaceutical preparations using a validated stability-indicating MEKC method. J Sep Sci 2011.

75. WS, M.; TS, L.; FD, I.; MB, C. Development and validation of an UV spectrophotometric method for the determination of aliskiren in tablets. Quim. Nova 2010, 33 (6), 1330-1334.

76. Swamy, K. G.; Kumar, J. M. R.; Sheshagirirao, J. V. L. N.; Kumar, D. V.; RatnaMani, C.; Kumar, V. N. V. E. Validated spectrophotometric determination of Aliskiren in pharmaceutical dosage form. Journal of Pharmacy Research 2011, 4 (8), 2574-2575.

77. Aydogmus, Z. Spectrofluorimetric determination of aliskiren in dosage forms and urine. Luminescence : the journal of biological and chemical luminescence 2012, 27 (6), 489-94.

78. Aydogmus, Z.; Sari, F.; Ulu, S. T. Spectrofluorimetric determination of aliskiren in tablets and spiked human plasma through derivatization with dansyl chloride. Journal of fluorescence 2012, 22 (2), 549-56.

79. Sharma, M.; Kothari, C.; Sherikar, O.; Mehta, P. Concurrent Estimation of Amlodipine Besylate, Hydrochlorothiazide and Valsartan by RP-HPLC, HPTLC and UV-Spectrophotometry. Journal of chromatographic science 2013.

80. Patel, D. B.; Mehta, F. A.; Bhatt, K. K. Simultaneous Estimation of Amlodipine Besylate and Indapamide in a Pharmaceutical Formulation by a High Performance Liquid Chromatographic (RP-HPLC) Method. Scientia pharmaceutica 2012, 80 (3), 581-90.

81. Jain, P. S.; Patel, M. K.; Gorle, A. P.; Chaudhari, A. J.; Surana, S. J. Stability-indicating method for simultaneous estimation of olmesartan medoxomile, amlodipine besylate and hydrochlorothiazide by RP-HPLC in tablet dosage form. Journal of chromatographic science 2012, 50 (8), 680-7.

82. Sarkar, A. K.; Ghosh, D.; Das, A.; Selvan, P. S.; Gowda, K. V.; Mandal, U.; Bose, A.; Agarwal, S.; Bhaumik, U.; Pal, T. K. Simultaneous determination of metoprolol succinate and amlodipine besylate in human plasma by liquid chromatography-tandem mass spectrometry method and its application in bioequivalence study. Journal of chromatography. B, Analytical technologies in the biomedical and life sciences 2008, 873 (1), 77-85.

83. Fakhari, A. R.; Nojavan, S.; Haghgoo, S.; Mohammadi, A. Development of a stability-indicating CE assay for the determination of amlodipine enantiomers in commercial tablets. Electrophoresis 2008, 29 (22), 4583-92.

84. Wankhede, S. B.; Raka, K. C.; Wadkar, S. B.; Chitlange, S. S. Spectrophotometric and HPLC methods for simultaneous estimation of amlodipine besilate, losartan potassium and hydrochlorothiazide in tablets. Indian journal of pharmaceutical sciences 2010, 72 (1), 136-40.

85. Rahman, N.; Nasrul Hoda, M. Validated spectrophotometric methods for the determination of amlodipine besylate in drug formulations using 2,3-dichloro 5,6-dicyano 1,4-benzoquinone and ascorbic acid. J Pharm Biomed Anal 2003, 31 (2), 381-92.

86. Shaalan, R. A.; Belal, T. S. Simultaneous spectrofluorimetric determination of amlodipine besylate and valsartan in their combined tablets. Drug testing and analysis 2010, 2 (10), 489-93.

87. Darwish, H. W.; Backeit, A. H. Multivariate versus classical univariate calibration methods for spectrofluorimetric data: application to simultaneous determination of olmesartan medoxamil and amlodipine besylate in their combined dosage form. Journal of fluorescence 2013, 23 (1), 79-91.

88. Hertzog, D. L.; McCafferty, J. F.; Fang, X.; Tyrrell, R. J.; Reed, R. A. Development and validation of a stability-indicating HPLC method for the simultaneous determination of losartan potassium, hydrochlorothiazide, and their degradation products. J Pharm Biomed Anal 2002, 30 (3), 747-60.

89. Sharma, R. N.; Pancholi, S. S. Simple RP-HPLC method for determination of triple drug combination of valsartan, amlodipine and hydrochlorothiazide in human plasma. Acta Pharm 2012, 62 (1), 45-58.

90. Joshi, S. J.; Karbhari, P. A.; Bhoir, S. I.; Bindu, K. S.; Das, C. RP-HPLC method for simultaneous estimation of bisoprolol fumarate and hydrochlorothiazide in tablet formulation. J Pharm Biomed Anal 2010, 52 (3), 362-71.

91. Meyyanathan, S. N.; Rajan, S.; Muralidharan, S.; Birajdar, A. S.; Suresh, B. A Validated RP-HPLC Method for Simultaneous Estimation of Nebivolol and Hydrochlorothiazide in Tablets. Indian journal of pharmaceutical sciences 2008, 70 (5), 687-9.

92. Tian, D. F.; Tian, X. L.; Tian, T.; Wang, Z. Y.; Mo, F. K. Simultaneous Determination of Valsartan and Hydrochlorothiazide in Tablets by RP-HPLC. Indian journal of pharmaceutical sciences 2008, 70 (3), 372-4.

93. Huang, T.; He, Z.; Yang, B.; Shao, L.; Zheng, X.; Duan, G. Simultaneous determination of captopril and hydrochlorothiazide in human plasma by reverse-phase HPLC from linear gradient elution. J Pharm Biomed Anal 2006, 41 (2), 644-8.

94. Bharathi, D. V.; Hotha, K. K.; Chatki, P. K.; Satyanarayana, V.; Venkateswarlu, V. LC-MS/MS method for simultaneous estimation of candesartan and hydrochlorothiazide in human plasma and its use in clinical pharmacokinetics. Bioanalysis 2012, 4 (10), 1195-204.

95. Salvadori, M. C.; Moreira, R. F.; Borges, B. C.; Andraus, M. H.; Azevedo, C. P.; Moreno, R. A.; Borges, N. C. Simultaneous determination of losartan and hydrochlorothiazide in human plasma by LC/MS/MS with electrospray ionization and its application to pharmacokinetics. Clin Exp Hypertens 2009, 31 (5), 415-27.

96. Rajasekhar, D.; Kumara, I. J.; Venkateswarlu, P. High performance liquid chromatography/negative ion electrospray tandem mass spectrometry method for the measurement of hydrochlorothiazide in human plasma: application to a comparative bioavailability study. Eur J Mass Spectrom (Chichester, Eng) 2009, 15 (6), 715-21.

97. Liu, F.; Xu, Y.; Gao, S.; Zhang, J.; Guo, Q. Determination of hydrochlorothiazide in human plasma by liquid chromatography/tandem mass spectrometry. J Pharm Biomed Anal 2007, 44 (5), 1187-91.

98. nalwade, S.; reddy, V. r.; rao, D. d.; rao, I. k. Rapid simultaneous determination of telmisartan, amlodipine besylate and hydrochlorothiazide in a combined poly pill dosage form by stability-indicating ultra performance liquid chromatography. Scientia pharmaceutica 2011, 79, 69–84.

99. El-Gindy, A.; Ashour, A.; Abdel-Fattah, L.; Shabana, M. M. Spectrophotometric and HPTLC-densitometric determination of lisinopril and hydrochlorothiazide in binary mixtures. J Pharm Biomed Anal 2001, 25 (5-6), 923-31.

100. Swamy, K. G.; P.Sravanthi; Surekha, M. L.; Kumar, J.; Rao, J. Validated RP-HPLC Method For The Simultaneous Determination Of Aliskiren, Hydrochlorothiazide And Amlodipine Besylate In Bulk And Pharmaceutical Formulations. International Journal of ChemTech Research 2012, 4 (4), 1666-1673.

101. Alagar Raja, M.; Ragavendra, P.; Banji, D.; Rao, K. N. V.; Chaithanya, Y.; Anusha, B.; Selvakumar, D. RP-HPLC Method for Simultaneous Estimation of Aliskiren Hemi fumarate, Hydrochlorothiazide and Amlodipine in Pharmaceutical bulk drugs and Tablet dosage form. Journal of Pharmacy Research 2012, 5 (8), 4580-4584.
102. Nishi, H. Capillary electrophoresis of drugs: current status in the analysis of pharmaceuticals. Electrophoresis 1999, 20 (15-16), 3237-58.
103. Ha, P. T.; Hoogmartens, J.; Van Schepdael, A. Recent advances in pharmaceutical applications of chiral capillary electrophoresis. J Pharm Biomed Anal 2006, 41 (1), 1-11.
104. The British Pharmacopoeia [Online]; The Stationery Office: London, 2009.
105. Xuan, X.; Li, D. Joule heating effects on peak broadening in capillary zone electrophoresis. J. Micromech. Microeng. 2004, 14 (8), 1171-1180.
106. Gas, B.; Stedry, M.; Kenndler, E. Peak broadening in capillary zone electrophoresis. Electrophoresis 1997, 18 (12-13), 2123-2133.
107. Huang, X.; Coleman, W. F.; Zare, R. N. Analysis of factors causing peak broadening in capillary zone electrophoresis. J. Chromatogr. 1989, 480, 95-110.
108. Wood, J. M.; Maibaum, J.; Rahuel, J.; Grutter, M. G.; Cohen, N. C.; Rasetti, V.; Ruger, H.; Goschke, R.; Stutz, S.; Fuhrer, W.; Schilling, W.; Rigollier, P.; Yamaguchi, Y.; Cumin, F.; Baum, H. P.; Schnell, C. R.; Herold, P.; Mah, R.; Jensen, C.; O'Brien, E.; Stanton, A.; Bedigian, M. P. Structure-based design of aliskiren, a novel orally effective renin inhibitor. Biochemical and biophysical research communications 2003, 308 (4), 698-705.
109. van Zwieten, P. A. Amlodipine: an overview of its pharmacodynamic and pharmacokinetic properties. Clinical cardiology 1994, 17 (9 Suppl 3), III3-6.

110. Vujic, Z.; Mulavdic, N.; Smajic, M.; Brboric, J.; Stankovic, P. Simultaneous analysis of irbesartan and hydrochlorothiazide: an improved HPLC method with the aid of a chemometric protocol. Molecules 2012, 17 (3), 3461-74.

111. Moffat, A. C. Clarke's Analysis of Drugs and Poisons [Online]; The Pharmaceutical Press: London, 2006.

112. Liederer, B. Case Study: Moexipril Hydrochloride: A Prodrug of Moexiprilat. In Prodrugs, Stella, V.; Borchardt, R.; Hageman, M.; Oliyai, R.; Maag, H.; Tilley, J., Eds. Springer New York: 2007; Vol. V, pp 1289-1297.

113. ICH Harmonized Tripartite Guideline, Validation of Analytical Procedures: Text and Methodology, Q2(R1), Current Step 4 Version, Parent Guidelines on Methodology Dated November 6 1996, Incorporated in November 2005. http://www.ich.org/products/guidelines/quality/article/quality-guidelines.html. ICH Harmonized Tripartite Guideline, Validation of Analytical Procedures: Text and Methodology, Q2(R1), Current Step 4 Version, Parent Guidelines on Methodology Dated November 6 1996, Incorporated in November 2005. http://www.ich.org/products/guidelines/quality/article/quality-guidelines.html (accessed April 10th, 2013).

114. Miller, J. N.; Miller, J. C. Statistics and Chemometrics for Analytical Chemistry. 5th ed.; Pearson Education Limited: Harlow, England, 2005.

115. Burugula, L.; Mullangi, R.; Pilli, N. R.; Makula, A.; Lodagala, D. S.; Kandhagatla, R. Simultaneous determination of sitagliptin and simvastatin in human plasma by LC-MS/MS and its application to a human pharmacokinetic study. Biomed. Chromatogr. 2013, 27 (1), 80-87.

116. El-Bagary, R.; Patonay, G.; Elzahr, A.; Elkady, E.; Ebeid, W. Ion-Pair LC Method for Simultaneous Determination of Aliskiren Hemifumarate, Amlodipine Besylate and Hydrochlorothiazide in Pharmaceuticals. Chromatographia 2013, 1-8.

3 SPECTROMETRIC DETERMINATION OF SOME SELECTED PHARMACEUTICAL COMPOUNDS

3.1 Introduction

Fluorescence spectrometry, by virtue of its great inherent sensitivity, finds wide applications in quantitative studies of rates of degradation, metabolism and excretion of drugs where other analytical techniques are not sufficiently sensitive [1]. The two main advantages of fluorimetric analysis are that, it is capable of measuring much lower concentrations than spectrophotometric analysis, and that it is potentially more selective because both the excitation and emission wavelengths can be varied and because not every compound fluoresce. Moreover, measuring the synchronous fluorescence spectra of analytes with overlapping emission spectra can help also to increase the selectivity of the spectrfluorimetric technique [2]. Fluorimetric analysis is typically sensitive down to 10^{-8} to 10^{-9} M concentration, depending on the intensity of the excitation source, the quantum efficiency and molar absorptivity of the analyte [3].

Different compounds can be assayed fluorimetrically by procedures utilizing, either their inherent fluorescence or the fluorescence of suitable derivatives of them. The most important application of fluorimetry is in the analysis of pharmaceuticals, clinical samples, food products, and natural products. The sensitivity and selectivity of the method make it a particularly valuable tool in these fields. Moreover, several inorganic species can be determined fluorometrically based on either direct formation of fluorescent chelates or the measurement of the decrease in fluorescence intensity due to the quenching action of the substance being determined [4].

Fluorescence techniques are based on the measurement of emitted photons of an excited analyte. Fluorescence can be enhanced by increasing the radiative rate of a molecule. In particular, shielding the fluorescent molecule from quenching impurities and/or solvent

molecules can be used to achieve this enhancement. Surfactant organized assemblies such as micelles, reversed micelles, and microemulsions have been used extensively to enhance the fluorescence. It is well known that the addition of a surfactant at a concentration above its critical micellar concentration to a given fluorophore solution increases the molar absorptivity and/or the fluorescence quantum yield of the fluorophore [5, 6].

The enhanced fluorescence in micellar media may be attributed to stabilization and/or protection of the excited singlet state, which hinders decay by quenching, and other non-radiative deactivation processes. The radiative relaxation process of the analyte is modified when it is solubilized in the micellar system because the micelle not only protects the analyte from quenching molecules but also modifies the physical properties of the environment around it, i.e., viscosity, polarity, etc. The enhancement was found to be dependent on the structure of the surfactant and the analyte [7, 8].

This enhancement facilitates the use of this technique as a complementary means for the detection and identification of fluorescent compounds. This general observation has been used to improve the performance of spectrofluorimetric methods of various analytes and active drugs [9-20].

3.2 Steady-state and synchronous spectrofluorimetric methods for simultaneous determination of aliskiren hemifumarate and amlodipine besylate in dosage forms

Luminescence (2014) 29(7): 878-83

DOI 10.1002/bio.2636

Aliskiren hemifumarate (ALS) and amlodipine besylate (AML) were simultaneously determined by two different spectrofluorimetric techniques. The first technique depends on direct measuring of the steady state fluorescence intensities of ALS and AML at 313 nm and 452 nm upon excitation at 290 and 375 nm, respectively, in a solvent composed of methanol and water (10:90 *v/v*). The second technique utilizes synchronous fluorimetric quantitative screening of the emission spectra of ALS and AML at 272 and 366 nm, respectively using $\Delta\lambda$ of 97 nm. Effects of different solvents and surfactants on relative fluorescence intensity were studied. The method was validated according to ICH guidelines. Linearity, accuracy and precision were found to be satisfactory in both techniques over the concentration ranges of 1 – 15 and 0.4 – 4 μg ml^{-1} for ALS and AML, respectively. In the first technique, LOD and LOQ were estimated and found to be 0.256 and 0.776 μg ml^{-1} for ALS as well as 0.067 and 0.204 μg ml^{-1} for AML, respectively. Also, LOD and LOQ were calculated in the synchronous method and found to be 0.293 and 0.887 μg ml^{-1} for ALS as well as 0.034 and 0.103 μg ml^{-1} for AML, respectively. The methods were successfully applied for the determination of the two drugs in their co-formulated tablets. The results were compared statistically with reference methods and no significant difference was found. The developed methods are rapid, sensitive, cheap and accurate for the quality control and

routine analysis of the cited drugs in bulk and in pharmaceutical preparations without pre-separation.

3.2.1. Introduction

Aliskiren hemifumarate, (2(S), 4(S), 5(S), 7(S)-N- (2-carbamoyl- 2- methylpropyl) -5-amino-4-hydroxy2,7 diisopropyl-8-[4-methoxy-3-(3-methoxypropoxy)phenyl] octanamide hemifumarate) (Fig. 1.3.1f), is the first orally active direct renin inhibitor. It may provide higher protection from hypertension [21]. Also, its efficacy to decrease systolic and diastolic blood pressure could be compared to other first-line antihypertensive agents. Additional advantages can be achieved when it is used in combination with other antihypertensive drugs [21]. Amlodipine besylate (AML), (3-Ethyl 5-methyl (4RS)-2-[(2-aminoethoxy) methyl]-4-(2-chlorophenyl)-6-methyl-1,4-dihydropyridine-3,5-dicarboxylate benzenesulphonate) (Fig. 1.3.1g), is a long-acting dihydropyridine calcium channel blocker that inhibits the influx of calcium ions into vascular and cardiac muscles [22]. Amlodipine acts directly on vascular smooth and reduces peripheral vascular resistance and blood pressure [23]. Combination therapy of ALS and AML proved to be effective and well tolerated in treating hypertensive patients [24].

Literature survey revealed LC [25-28], CE [29], UV-spectrophotometric [30, 31] and spectrofluorimetric [32, 33] methods reported for the estimation of aliskiren hemifumarate alone or in combination with other anti-hypertensive agents. Also, LC [34-36], LC/MS/MS [22], CE [37], UV-spectrophotometric [38-40] and spectrofluorimetric [41, 42] methods are reported for estimation of amlodipine alone or in combination with other agents. To the best of our knowledge, there are no reported direct or synchronous spectrofluorimetric methods for determination of ALS either alone or in combination with AML without the need for derivatization methodologies. Thus, the

aim of the present study was to develop validated, sensitive, simple, rapid, cheap and precise spectrofluorimetric procedures for analysis of ALS and AML in bulk drug samples and in their combined dosage formulations. The developed methods are suitable for quality control and routine analysis of ALS in its commercial dosage forms either alone or co-formulated with AML.

3.2.2. Experimental

3.2.2.1. Materials and Reagents

All the chemicals used in the present studies were of analytical reagent grade and the solvents were of HPLC grade.

Working standard of ALS (certified to contain 99.51%) was kindly supplied by Novartis Pharmaceuticals Corporation (East, New Jersey- USA 07936). AML (certified to contain 99.75%) was kindly supplied by Global Nabi Co., (Giza- Egypt). Hydrochlorothiazide (HCZ) (certified to contain 99.93%) was supplied by AstraZeneca (Cairo- Egypt) (Under license of AstraZeneca, Sweden). Tekamlo® 150/10 mg tablets labeled to contain 165.8 mg ALS and 13.9 mg AML per each tablet were purchased from commercial sources in the local market. Methanol, Sodium dodecyl sulphate (SDS), cetyl trimethyl ammonium bromide (CTAB), hydroxymethyl cellulose (HMC) and Triton® X-100 were obtained from Sigma-Aldrich, MO, USA. β-Cyclodextrin (β-CD) (TCI, Tokyo Kasei, Japan). Orthophosphoric acid 85% and hydrochloric acid (Fisher Scientific, NJ, USA) were used. Sodium hydroxide and sodium dihydrogen phosphate were purchased from J.T. Barker, NJ, USA. Phosphate buffer (0.2 M, pH 4) solution was freshly prepared. SDS, CTAB, β-CD, HMC and Triton® X-100 were prepared as 1% w/v aqueous solutions. Also, 0.1N NaOH and 0.1N HCl were prepared.

3.2.2.2. Instruments

A LS 55 Fluorescence Spectrometer, 120 V (PerkinElmer, Waltham, MA, USA), equipped with a high energy pulsed xenon source for excitation, variable slit and holographic gratings was used. Fluorescence spectra and measurements were recorded using PekinElmer FL WinLab™ software. A 1 cm quartz cell was used. A VWR SympHoly (SB20) pH meter (Thermo Orion, Beverly, MA, USA) was used for pH measurements. Deionized water was prepared using a Barnstead NANO pure Dlamond Analytical ultrapure water system (Thermo Fischer Scientific, Waltham, MA, USA).

3.2.2.3. Standard solutions

Ten mg of ALS, AML and HCZ were accurately weighed and transferred separately into 10 mL volumetric flasks. Then, they were dissolved and made up to volume with methanol to give concentrations of 1000 μg mL^{-1} for each. Further dilutions were made separately using the same solvent to prepare 100 μg mL^{-1} of AML and HCZ.

3.2.2.4. Procedures

3.2.2.4.1. Linearity and construction of calibration graphs

Aliquots of ALS and AML standard stock solutions were separately transferred into two series of 10 ml Fisherbrand disposable tubes to give final concentrations of 1–15 and 0.4–4 μg mL^{-1} for ALS and AML, respectively, then completed to 500 μL with methanol. Finally, 4.5 mL deionized water were added to each tube to reach final volume of 5 mL, the contents were mixed well. Relative fluorescence intensity (RFI) was measured in two ways. In the first technique, it was measured directly against a solvent blank at 313 and 452 nm upon excitation at 290 and 375 nm for ALS and AML, respectively. Excitation and emission slit width of 4.5 were used in the

case of ALS as well as 8 in the case of AML, (Fig. 3.2.1). In the second technique, RFI of the synchronous spectrofluorimetric spectra were measured against a solvent blank using Δλ of 97 at 272 and 366 nm for ALS and AML, respectively, (Fig. 3.2.2). The excitation and emission slit width were 8. RFI was plotted versus the corresponding final drug concentration of ALS and AML (µg mL^{-1}) to obtain the calibration graphs and regression equations. Figures (3.2.3 – 3.2.6) show linear relationships which were established by plotting the RFI against ALS and AML concentrations in µg mL^{-1}. Linear regression analysis of the data gave the following equations:

RFI_{ALS} = 063.679C + 7.138 (r=0.9999); (Conventional method) eq. (1)

RFI_{AML}= 241.398C + 0.417 (r=0.9998); (Conventional method) eq. (2)

RFI_{ALS} = 060.459C + 28.911 (r=0.9999); (Synchronous method) eq. (3)

RFI_{AML}= 233.118C – 0.214 (r=0.9999); (Synchronous method) eq. (4)

Where: RFI is the relative fluorescence intensity, C is the concentration of ALS or AML in µg mL^{-1} and r is the correlation coefficient.

3.2.2.4.2. Analysis of ALS and AML laboratory prepared mixtures

Aliquots of ALS and AML standard stock solutions were accurately transferred into a series of 10 mL Fisherbrand disposable tubes to give final concentrations of 4.8 – 14.4 and 0.4 – 1.2 µg mL^{-1} for ALS and AML, respectively. The procedure described under "Linearity and construction of calibration graphs" was then applied. The recovery percentage was calculated using the corresponding regression equation. Tables 3.2.1 and 3.2.2 show the mean percentage recoveries ± S.D. of ALS and AML using the proposed methods.

3.2.2.4.3. Sample preparation and application to Dosage Form

Twenty tablets of Tekamlo® were weighed and finely powdered. A portion of the powder equivalent to ALS (50 mg) and AML (4.192 mg) was introduced into a 50 mL volumetric and

sonicated with 30 mL methanol for 15 minutes, and then diluted to the mark with methanol. The solution was filtered through Whatman filter paper. The procedure described under "Linearity and construction of calibration graphs" was then applied. The recovery percentage was calculated using the corresponding regression equations. Standard addition technique was applied and the concentrations of the examined drugs were calculated using the corresponding regression equation. Tables (3.2.3 – 3.2.6) show the mean percentage recoveries ± S.D. of ALS and AML using the proposed methods.

3.2.2.5. Validation

The suggested analytical method was validated according to ICH guidelines with respect to certain parameters such as linearity, LOD and LOQ, accuracy, precision, specificity and stability.

3.2.2.5.1. Linearity

The linearity of the method was established by spiking a series of standard mixtures in the range 1–15 and 0.4–4 µg mL^{-1} of ALS and AML, respectively. The procedure described under "Linearity and construction of calibration graphs" was applied. Linear regression was applied and standard deviation of slope (Sb), standard deviation of intercept (Sa), correlation coefficient (r) and standard error (Es) were determined.

3.2.2.5.2. Limit of detection & Limit of quantification

Detection and quantification limits were determined through dilution method using S/N approach. LOD was considered as the minimum concentration with a signal to noise ratio of at

least three (S/N˜3), while LOQ was taken as a minimum concentration with a signal to noise ratio of at least ten (S/N˜10).

3.2.2.5.3. Accuracy

Accuracy was determined in terms of percent recovery. A set of standard mixtures at six different concentration levels 4.8, 7.2, 9.6, 12, 13.2, 14.4 µg mL^{-1} of ALS and 0.4, 0.6, 0.8, 1, 1.1, 1.2 µg mL^{-1} of AML were prepared. The procedure described under "Linearity and construction of calibration graphs" was then applied. The percentage recoveries of ALS and AML were calculated.

3.2.2.5.4. Precision

Method precision was determined both in terms of repeatability (intra-day reproducibility) and intermediate precision (inter-day reproducibility) using three different concentration levels 2, 6, 12 µg mL^{-1} of ALS and 0.6, 1.8, 3.4 µg mL^{-1} of AML.

3.2.2.5.5. Specificity

Specificity was examined by analyzing ALS and AML in their laboratory prepared mixtures and pharmaceutical dosage forms to detect any interference caused by the combined drugs present in dosage formulations or the co-formulated excipients. Also, specificity was checked by analyzing 12 µg mL^{-1} ALS and 0.5 µg mL^{-1} AML in their triple mixture with 0.5, 1 and 2 µg mL^{-1} of HCZ. The percentage recovery and standard deviation were calculated.

3.2.2.5.6. Stability

The stability studies of ALS and AML samples were carried out over a period of 72h at 2–80 °C (refrigerator) and standard stock solutions for one month at 2–80 °C.

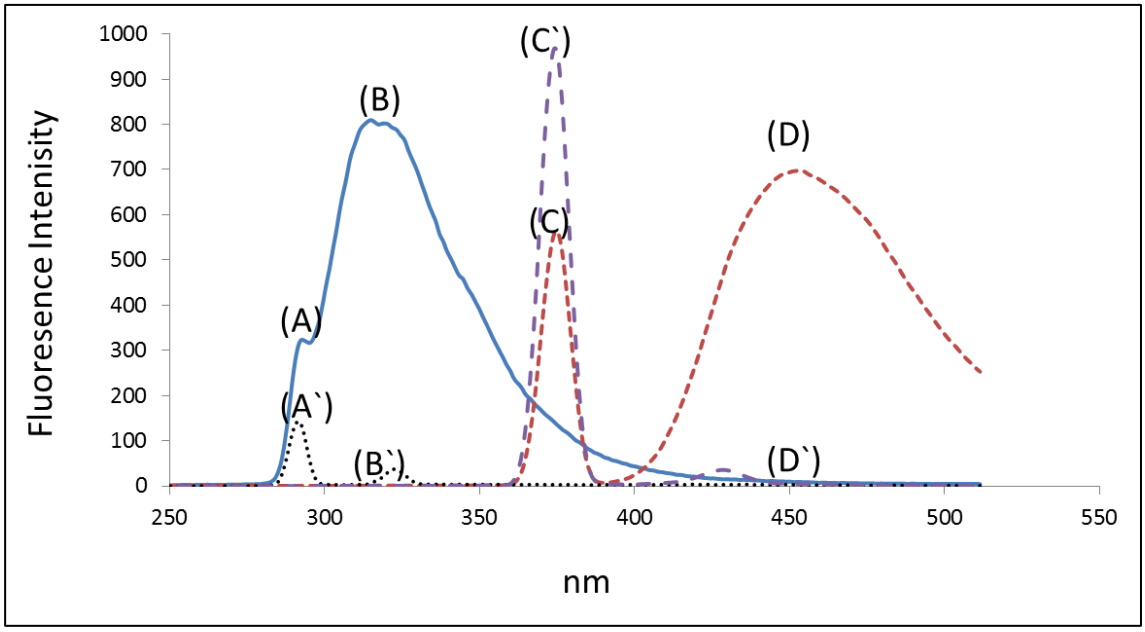

Figure 3.2.1 Excitation (A, C) and direct fluorescence spectra of (B, D) of ALS and AML respectively (ALS: 12 µg mL^{-1} and AML: 3 µg mL^{-1}) in a solvent composed of methanol and water (10:90, v/v) and (A`, B`, C`, D`) for blank solvent composed of methanol and water (10:90, v/v). Where (A, C, A`, C`) are the excitation spectra and (B, D, B`, D`) are the emission spectra

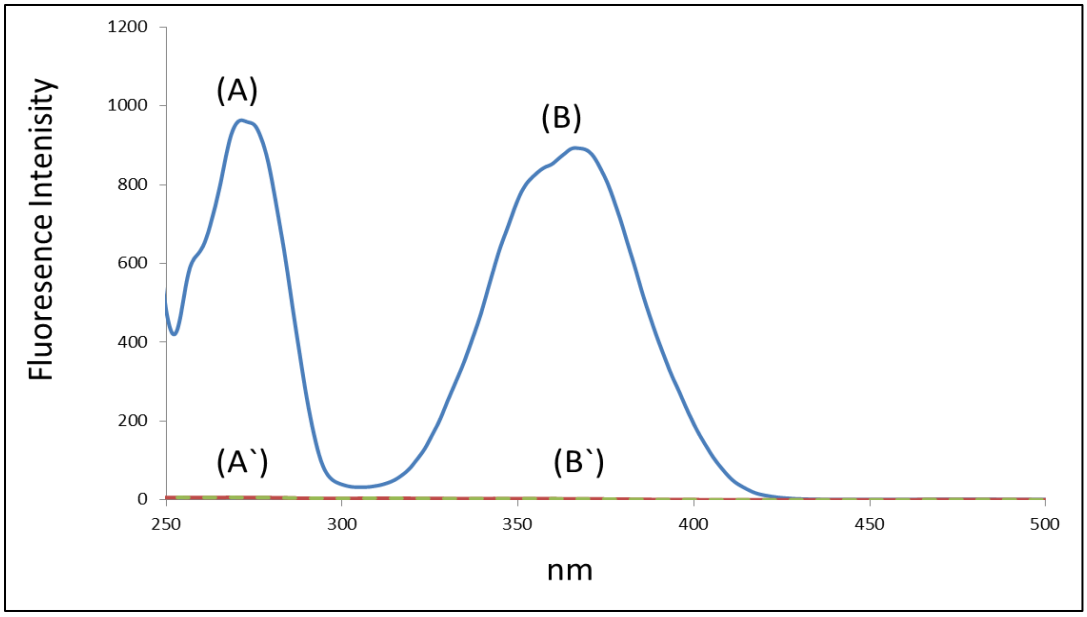

Figure 3.2.2 Synchronous fluorescence spectra of (A) ALS (12 µg mL^{-1}), (B) AML (3 µg mL^{-1}) in a solvent composed of methanol and water (10:90, v/v) and (A, B`) solvent composed of methanol and water (10:90, v/v)

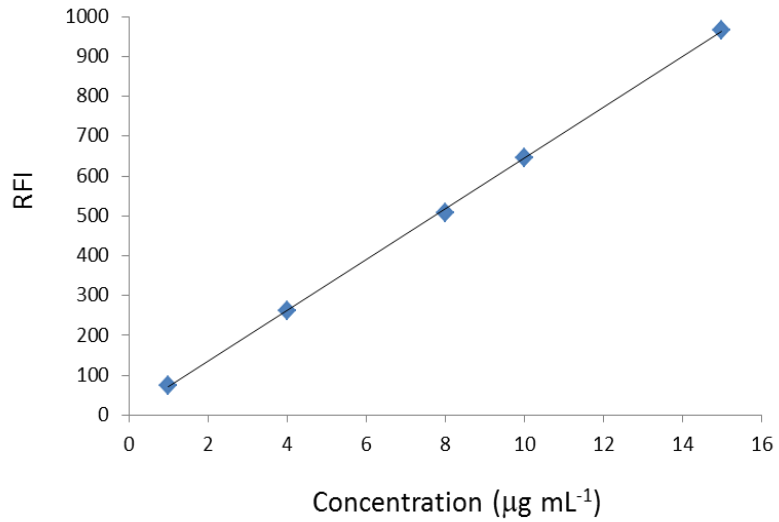

Figure 3.2.3 Standard calibration curve for determination of ALS by the proposed conventional spectrofluorimetric method

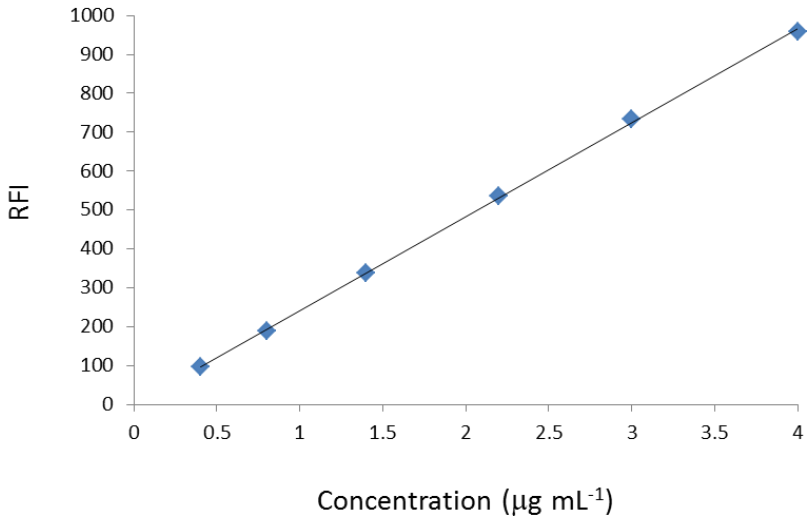

Figure 3.2.4 Standard calibration curve for determination of AML by the proposed conventional spectrofluorimetric method

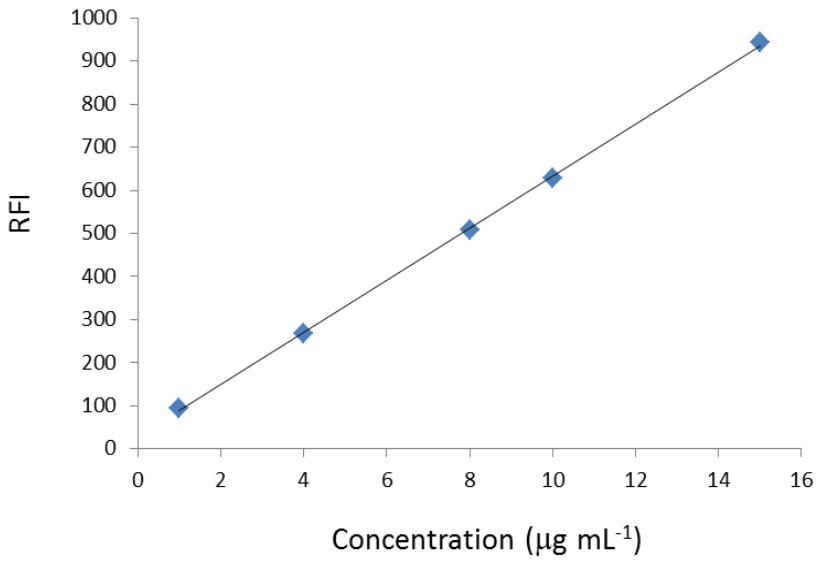

Figure 3.2.5 Standard calibration curve for determination of ALS by the proposed synchronous spectrofluorimetric method

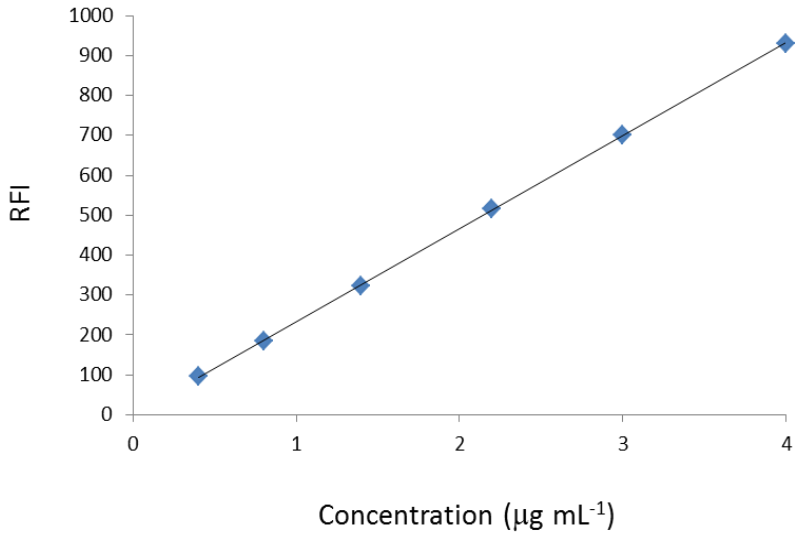

Figure 3.2.6 Standard calibration curve for determination of AML by the proposed synchronous spectrofluorimetric method

Table 3.2.1 Determination of ALS and AML using the conventional spectrofluorimetric method

$RFI_{ALS} = 063.679C + 7.138$
$RFI_{AML} = 241.398C + 0.417$

Mixture No	Amount taken [µg/ml]		ALS			AML		
	ALS	**AML**	RFI of **ALS**	Found [µg/ml]	Recovery %	RFI of **AML**	Found [µg/ml]	Recovery %
1	4.8	0.4	303	96	4.870	0.396	101.47	98.99
2	7.2	0.6	456	148	7.273	0.611	101.01	101.89
3	9.6	0.8	593	196	9.424	0.810	98.17	101.28
4	12.0	1.0	747	241	11.843	0.997	98.69	99.66
5	13.2	1.1	822	264	13.021	1.092	98.64	99.26
6	14.4	1.2	936	295	14.811	1.220	102.85	101.69
Mean					**100.14**			**100.46**
± S.D.					**1.90**			**1.30**
± S.E.					**0.78**			**0.53**

Table 3.2.2 Determination of ALS and AML using the synchronous spectrofluorimetric method

$RFI_{ALS} = 060.459C + 28.911$
$RFI_{AML} = 233.118C - 0.214$

Mixture No	Amount taken [µg/ml]		ALS			AML		
	ALS	**AML**	RFI of **ALS**	Found [µg/ml]	Recovery %	RFI of **AML**	Found [µg/ml]	Recovery %
1	4.8	0.4	317	92	4.765	0.396	99.27	98.89
2	7.2	0.6	459	139	7.114	0.597	98.80	99.53
3	9.6	0.8	599	187	9.429	0.803	98.22	100.39
4	12.0	1.0	757	231	12.043	0.992	100.36	99.18
5	13.2	1.1	832	254	13.283	1.090	100.63	99.14
6	14.4	1.2	906	279	14.507	1.198	100.74	99.81
Mean					**99.67**			**99.49**
± S.D.					**1.05**			**0.54**
± S.E.					**0.43**			**0.22**

Table 3.2.3 Determination of ALS using the conventional spectrofluorimetric method

RFI_{ALS} = 063.679C + 7.138

Mixture No	Amount of ***ALS*** (µg/ml)		RFI of ***ALS***		Amount of ***ALS*** found (µg/ml)			Recovery %	
	Tablet	Added	Tablet	Tablet & added	Tablet	Tablet & added	Added	Tablet	Added
1	6	4	363	616	5.813	9.786	3.973	96.88	99.33
2	6	6	363	748	5.813	11.859	6.046	96.88	100.77
3	6	9	363	939	5.813	14.858	9.045	96.88	100.50
4	9	4	551	806	8.767	12.769	4.002	97.41	100.06
5	9	5	551	876	8.767	13.869	5.102	97.41	102.03
6	9	6	551	940	8.767	14.874	6.107	97.41	101.78
Mean								**97.14**	**100.74**
± S.D.								**0.29**	**1.03**
± S.E.								**0.12**	**0.42**

Table 3.2.4 Determination of AML using the conventional spectrofluorimetric method

RFI_{AML} = 241.398C + 0.417

Mixture No	Amount of ***AML*** (µg/ml)		RFI of ***AML***		Amount of ***AML*** found (µg/ml)			Recovery %	
	Tablet	Added	Tablet	Tablet & added	Tablet	Tablet & added	Added	Tablet	Added
1	0.503	0.4	115	213	0.475	0.881	0.406	94.38	101.49
2	0.503	1.0	115	355	0.475	1.469	0.994	94.38	99.42
3	0.503	2.0	115	602	0.475	2.492	2.017	94.38	100.87
4	0.754	0.6	179	323	0.740	1.336	0.597	98.06	99.42
5	0.754	1.0	179	422	0.740	1.746	1.007	98.06	100.66
6	0.754	2.0	179	671	0.740	2.778	2.038	98.06	101.91
Mean								**96.22**	**100.63**
± S.D.								**2.02**	**1.03**
± S.E.								**0.82**	**0.42**

Table 3.2.5 Determination of ALS using the synchronous spectrofluorimetric method.

RFI_{ALS} = 060.459C + 28.911

Mixture No	Amount of ***ALS*** (µg/ml)		RFI of ***ALS***		Amount of ***ALS*** found (µg/ml)			Recovery %	
	Tablet	Added	Tablet	Tablet & added	Tablet	Tablet & added	Added	Tablet	Added
1	6	4	376	621	5.749	9.793	4.045	95.81	101.11
2	6	6	376	738	5.749	11.728	5.980	95.81	99.66
3	6	9	376	925	5.749	14.821	9.073	95.81	100.81
4	9	4	563	801	8.834	12.770	3.937	98.15	98.41
5	9	5	563	869	8.834	13.895	5.061	98.15	101.23
6	9	6	563	928	8.834	14.871	6.037	98.15	100.62
Mean								**96.98**	**100.31**
± S.D.								**1.28**	**1.08**
± S.E.								**0.52**	**0.44**

Table 3.2.6 Determination of AML using the synchronous spectrofluorimetric method

RFI_{AML}= 233.118C – 0.214

Mixture No	Amount of ***AML*** (µg/ml)		RFI of ***AML***		Amount of ***AML*** found (µg/ml)			Recovery %	
	Tablet	Added	Tablet	Tablet & added	Tablet	Tablet & added	Added	Tablet	Added
1	0.503	0.4	113	205	0.486	0.880	0.395	96.56	98.66
2	0.503	1.0	113	351	0.486	1.507	1.021	96.56	102.09
3	0.503	2.0	113	588	0.486	2.523	2.038	96.56	101.88
4	0.754	0.6	174	313	0.747	1.344	0.596	99.06	99.38
5	0.754	1.0	174	409	0.747	1.755	1.008	99.06	100.81
6	0.754	2.0	174	649	0.747	2.785	2.038	99.06	101.88
Mean								**97.81**	**100.78**
± S.D.								**1.37**	**1.46**
± S.E.								**0.56**	**0.59**

3.2.3. Results and Discussion:

The goal of the present investigation was to develop validated, sensitive, simple and rapid specrofluorimetric analytical methods for simultaneous determination and quantification of **ALS** and **AML** in pharmaceutical preparations. Also, many trials were attempted to enhance the intensity of the emission bands and increase molar absorptivity and quantum yield through selection of proper solvent and addition of surfactants at concentrations above their critical micellar concentration in order to perform micelles or reversed micelles able to stabilize the exited singlet states and delay the decay process. The fluorescence performance of **ALS** was studied in various solvents and micellar media and a solvent composed of methanol and water (10:90 v/v) was chosen as no one of the studied media caused significant enhancement in RFI of ALS (Fig. 3.2.1 and 3.2.2).

3.2.3.1. Optimization of the experimental conditions

3.2.3.1.1. Effect of different organized media

The fluorescence properties of ALS in various micellar media were studied using anionic surfactant (SDS), cationic surfactant (CTAB) and non-ionic surfactant (Triton® X-100) and different macromolecules, like β-Cyclodextrin (β-CD) and hydroxyl methyl cellulose (HMC). ALS has pKa above 9 so it will be positively charged under acidic conditions obtained by adding phosphate buffer (pH 4). No one of the examined surfactants showed significant enhancement in RFI of ALS, (Fig. 3.2.7).

3.2.3.1.2. Effect of the diluting solvent

For the steady state spectrofluorimetric procedure, the influence of different diluting solvents on RFI of ALS was investigated using water, methanol, phosphate buffer solution at pH

4, 0.1N HCl and 0.1N NaOH to give final solutions containing 10% v/v methanol for each. Water was chosen as diluting solvent as it showed a good RFI compared with methanol but it is friendlier to the environment and with much less blank readings, (Fig. 3.2.8).

3.2.3.1.3. Selection of Δλ in the synchronous spectrofluorimetric method

To separate entirely synchronous fluorescence peaks of ALS and AML, the synchronous fluorescence spectra of the mixtures were recorded using different Δλ. It was found that Δλ of 97 nm is suitable for simultaneous determination of ALS and AML in their medicinally recommended ratio of (12: 1), respectively. The result was showed in (Fig. 3.2.2), where the maximum synchronous fluorescence peaks of ALS and AML were at 272 and 366 nm, respectively. Obviously, no significant interference would occur in their combined formulation`s ratio.

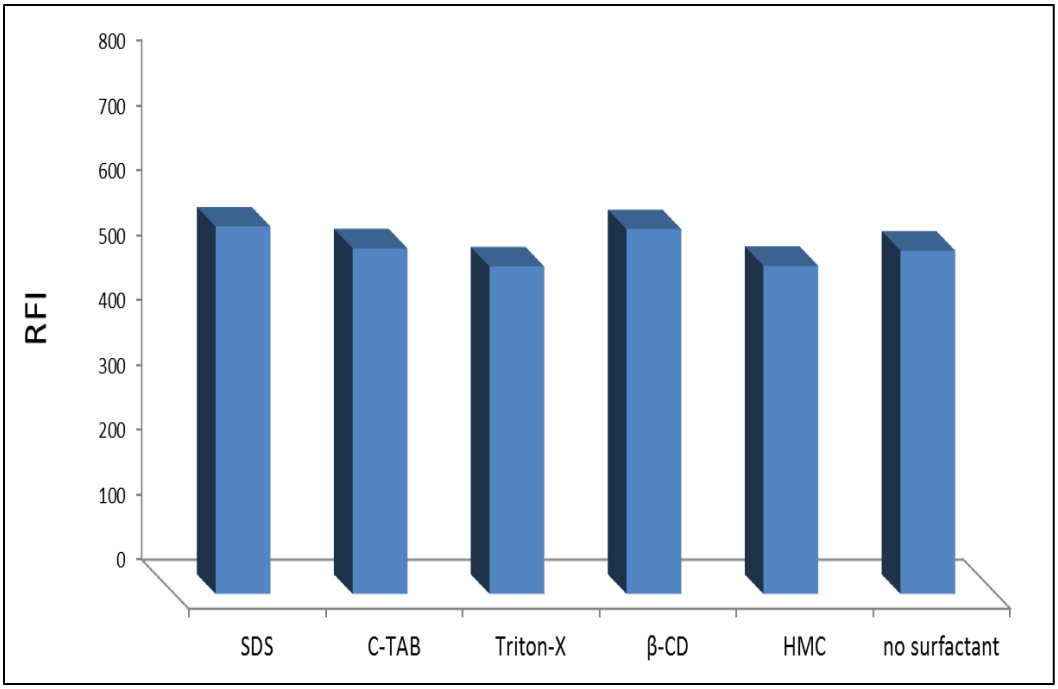

Figure 3.2.7 Effect of type of surfactant (1mL of 1% solution for each) on the RFI of ALS (8 µg mL^{-1})

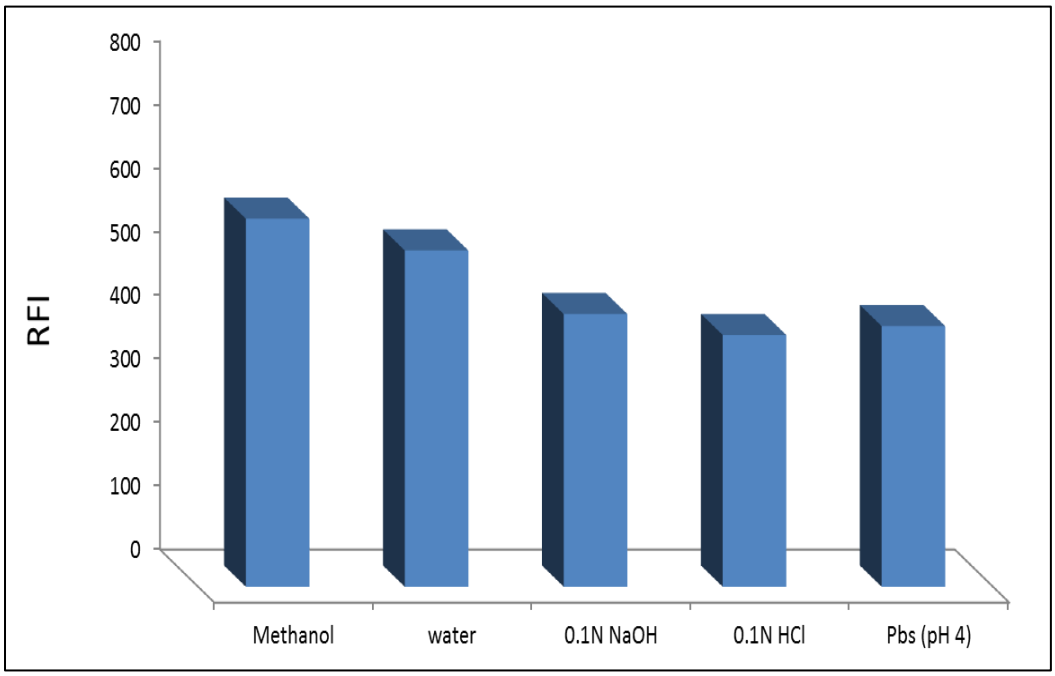

Figure 3.2.8 Effect of different diluting solvents on the RFI of ALS (8 µg mL^{-1})

3.2.3.2. Validation

3.2.3.2.1. Linearity and Range

The linearity of the calibration curves was validated by the high value of correlation coefficients (r) of the regression equation, small values of the standard deviation of residuals (Sy/x) and small value of the percentage relative error (Table 3.2.7). The analytical data of the calibration curves including standard deviations for the slope and intercept (Sb, Sa) are summarized in (Table 3.2.7). These data proved the linearity of the calibration graphs.

3.2.3.2.2. Limit of Detection (LOD) and Limit of Quantitation (LOQ)

LOQ and LOD were calculated according to ICH Q2R1 recommendations using the following equations:

$$LOQ = 10\ S_a/b \text{ and } LOD = 3.3\ S_a/b$$

Where: S_a = standard deviation of the intercept and b = slope of the calibration curve.

LOQ was determined by establishing the lowest concentration that can be measured and below which the calibration graph is nonlinear. LOD was determined by establishing the minimum level at which the analyte can be reliably detected. LOD and LOQ were estimated and found to be 0.256 and 0.776 μg mL^{-1} for ALS as well as 0.067 and 0.204 μg mL^{-1} for AML, respectively. Also, LOD and LOQ were calculated in the synchronous method and found to be 0.293 and 0.887 μg mL^{-1} for ALS as well as 0.034 and 0.103 μg mL^{-1} for AML, respectively. The results are shown in Table 3.2.7.

3.2.3.2.3. Accuracy

Accuracy of the results was calculated by % recovery of 6 different concentrations of the two drugs analyzed by the proposed spectrofluorimetric methods. The results obtained including

the mean of the recovery and standard deviations are displayed in (Table 3.2.7). To prove the accuracy and utility of the proposed method, the results of the assay of ALS and AML with the proposed spectrofluorimetric methods were compared with those of the reference methods [26, 43]. Statistical analysis of the results using Student's t-test and variance ratio F-test revealed no significant difference between the performance of the developed methods and reference methods regarding the accuracy and precision, respectively (Table 3.2.8). The reference method [26] and pharmacopeal method [43] depend on the analysis of ALS and AML, respectively, using RP-HPLC.

3.2.3.2.4. Precision

Repeatability (intra-day, n=3) and intermediate precision (inter-day, n=3) were checked using three different concentrations at low, medium and high level of the standard curve. Relative standard deviations were calculated to check the precision of the method, (Table 3.2.9). The relative standard deviations and percentage relative errors were found to be very small indicating reasonable repeatability and intermediate precision of the proposed method.

3.2.3.2.5. Specificity

The specificity of the methods was investigated by observing any interference encountered from the excipients of the tablets. It was shown that these compounds do not interfere with the proposed method (Table 3.2.7). It was also found that ALS and AML do not interfere with each other either in their laboratory prepared mixtures or in their co-formulated tablets (Table 3.2.7). Moreover, the steady state method showed better results and higher tolerance in presence of 1 µg mL^{-1} HCZ for the determination of ALS and AML than the synchronous method (Table 3.2.7). So, the steady state method is more reliable to be used for simultaneous determination of ALS and AML in presence of HCZ specifically in the medicinally

recommended ratio of (12:0.5:1), respectively, in their co-formulated tablets, Amturnide® (Table 3.2.7).

3.2.3.2.6. Stability

Results from the stability studies of standard stock solutions indicated that they were stable for one month at 2–8 °C with satisfactory recovery percentage of about 98%. These solutions can therefore be used during this interval of time without the results being affected.

Table 3.2.7 Performance data and results of the proposed spectrofluorimetric methods for the simultaneous determination of ALS and AML

Item	**Conventional fluorescence**		**Synchronous fluorescence**	
	ALS	AML	ALS	AML
Linearity range (μg mL^{-1})	1 – 15	0.4 – 4	1 – 15	0.4 – 4
LOD (μg mL^{-1})	0.256	0.067	0.293	0.034
LOQ (μg mL^{-1})	0.776	0.204	0.887	0.103
Regression equation (Y) [a]: Slope (b)	63.679	241.398	60.459	233.118
Standard deviation of slope (S_b)	0.548	2.114	0.595	1.031
Intercept (a)	7.1382	0.4170	28.9113	- 0.2143
Standard deviation of intercept (S_a)	4.942	4.928	5.362	2.403
Regression coefficient (r)	0.9999	0.9998	0.9999	0.9999
Standard deviation of residuals ($S_{y/x}$)	5.937	6.480	6.442	3.159
%Error	1.292	0.448	1.378	0.467
Results	(Recovery ± S.D.)			
Drug in bulk	101.33 ± 0.91	99.81 ± 0.84	100.74 ± 0.88	100.68 ± 0.72
Drugs in lab. mixture	100.14 ± 1.90	100.46 ± 1.30	99.67 ± 1.05	99.49 ± 0.54
Drugs in lab. Mixture with HCZ	100.72 ± 1.58	100.02 ± 0.35	95.68 ± 1.39	99.86 ± 0.77
Tekamlo® 150/10 mg tablets	97.14 ± 0.29	96.22 ± 2.02	96.98 ± 1.28	97.81 ± 1.37
Drug spiked to dosage form	100.74 ± 1.03	100.63 ± 1.03	100.31 ± 1.08	100.78 ± 1.46

[a] Y=a+bC, where C is the concentration in μg mL^{-1} and Y is the peak area.
[b] 95% confidence limit.

Table 3.2.8 Statistical comparison between analysis results of pure samples of the studied drugs using spectrofluorimetric methods and those of the reference methods

Statistical Term	ALS			AML		
	Reported method [6]	Conventional fluorescence	Synchronous fluorescence	Reported method [24]	Conventional fluorescence	Synchronous fluorescence
Mean	101.10	101.33	100.74	99.90	99.81	100.68
±S.D.	1.64	0.91	0.88	1.59	0.84	0.72
±S.E.	0.73	0.37	0.36	0.71	0.34	0.29
%RSD	1.62	0.90	0.87	1.59	0.84	0.72
n	5	6	6	5	6	6
V	2.69	0.83	0.77	2.53	0.71	0.52
Student`s t test		0.783 (1.833*)	1.003 (1.833*)		0.180 (1.833*)	1.312 (1.833*)
F-test		3.241 (6.260*)	3.494 (6.260*)		3.563 (6.260*)	4.865 (6.260*)

* Figures in parentheses are the theoretical t and F values at (p= 0.05) and n is the number of experiments.

Table 3.2.9 Intra-and inter-day validation for the spectrofluorimetric determination of ALS and AML

Concentration of ALS (μg mL^{-1})	**Intra-day assay**		**Inter-day assay**	
	Direct fluorescence	Synchronous fluoresence	Direct fluorescence	Synchronous fluoresence
	Found ± RSD[a]	Found ± RSD[a]	Found ± RSD[a]	Found ± RSD[a]
2	1.997 ± 0.79	1.959 ± 2.97	2.004 ± 1.18	1.967 ± 1.90
6	5.975 ± 1.35	6.006 ± 1.26	5.996 ± 1.32	5.942 ± 1.74
12	12.021 ± 0.72	12.092 ± 1.54	11.955 ± 1.13	12.056 ± 1.20
Concentration of AML (μg mL^{-1})	**Intra-day assay**		**Inter-day assay**	
	Direct fluorescence	Synchronous fluoresence	Direct fluorescence	Synchronous fluoresence
	Found ± RSD[a]	Found ± RSD[a]	Found ± RSD[a]	Found ± RSD[a]
0.6	0.609 ± 1.42	0.591 ± 1.51	0.604 ± 1.55	0.601 ± 2.09
1.8	1.797 ± 0.96	1.813 ± 0.90	1.814 ± 1.13	1.835 ± 1.26
3.4	3.397 ± 0.46	3.394 ± 0.58	3.419 ± 0.97	3.396 ± 0.41

[a] Mean and standard deviation of three determinations

3.3 Spectrophotometric and Spectrofluorimetric Studies on Azilsartan Medoxomil and Chlorthalidone to be Utilized in their Determination in Pharmaceuticals

Analytical Chemistry Insights (2014) 7; 9:33-40

DOI: 10.4137/ACI.S13768

The angiotensin II receptor blocker, Azilsartan medoxomil (AZL) was determined spectrophotometrically and spectrfluorimetrically in its combination with chlorthalidone (CLT). The UV-spectrophotometric technique depends on simultaneous measurement of the first derivative spectra for AZL and CLT at 286 nm and 257 nm, respectively, in methanol. The spectrofluorimetric technique depends on measurement of the fourth derivative of the synchronous spectra intensities of AZL in presence of CLT at 298 nm in methanol. Effects of different solvents on spectrophotometric and spectrfluorimetric responses were studied. For, the spectrofluorimetric study, the effect of pH and micelle assisted fluorescence enhancement were also studied. The method was validated according to ICH guidelines. Linearity, accuracy and precision were found to be satisfactory over the concentration ranges of 8 – 50 and 2 – 20 µg mL^{-1} for AZL and CLT, respectively, in the spectrophotometric method as well as 0.01 - 0.08 µg mL^{-1} for AZL in the spectrofluorimetric method. The methods were successfully applied for the determination of the studied drugs in their co-formulated tablets. The developed methods are inexpensive and simple for the quality control and routine analysis of the cited drugs in bulk and in pharmaceuticals.

3.3.1 Introduction

Azilsartan medoxomil (AZL), (5-Methyl-2-oxo-1,3-dioxol-4yl) methyl 2-ethoxy-1-{[2`-(5-oxo-4,5-dihydro-1,2,4-oxadiazol-3-yl)biphenyl-4-yl]methyl}-1H-benzimidazole-7-carboxylate, (Fig. 1.2.1a). AZL is practically insoluble in water, freely soluble in methanol, dimethylsulfoxide, soluble in acetic acid, slightly soluble in acetone, and acetonitrile and sparingly soluble in tetrahydrofuran and 1-octanol [44]. Azilsartan, the active metabolite of AZL, is a novel non-peptide angiotensin II type 1 (AT_1) receptor blocker (ARB), was recently approved for treatment of hypertension [45]. It has a superior ability to control systolic blood pressure (BP) relative to other widely used ARBs. Greater antihypertensive effects of AZL might be due in part to its unusually potent and persistent ability to inhibit binding of angiotensin II to AT_1 receptors [46]. Preclinical studies have indicated that AZL may also beneficially affect cellular mechanisms of cardio-metabolic disease and insulin sensitizing activity [47]. There is only one reported method [44] for determination of AZL alone and it was applied to analysis in plasma. Chlorthalidone (CLT), (2-chloro-5- (1-hydroxy-3-oxoiso-indolin-1-yl) benzenesulfonamide), (Fig. 1.2.1b), is an orally taken thiazide-like diuretic for controlling hypertension and edema, including that associated with heart failure [48]. CLT has been determined in different matrices either alone or in combination with other medications using LC [49, 50], LC/MS/MS [51], HPTLC [52, 53], chemiluminometry [54], spectrophotometry [55] and CE [56] techniques. Binary combination therapies of AZL and CLT proved to induce significant reductions in systolic and diastolic BP in patients with mild to severe hypertension [57]. Accordingly, it is desirable to develop validated simple analytical methods for assay of AZL in its combination with CLT either in their synthetic mixtures or in their combined pharmaceutical preparations. Regarding simultaneous determination of CLT and AZL, there is only one LC reported method [58], done on a symmetry

C18 column with a mobile phase consisting of methanol: Water: Acetonitrile : 0.1% Ortho phosphoric acid (30:35:15:5, v/v/v/v) at λ of 251 nm. To the best of our knowledge there is no spectrophotometric or spectrofluorimetric methods developed for determination of AZL either alone or in its combination with CLT. Hence, the aim of these studies was to develop and validate simple, rapid and inexpensive analytical methods using spectrophotometric and spectrofluorimetric techniques for determination of AZL in its combination with CLT to be applied to their determination in pharmaceuticals. These newly developed and validated methods can be used for routine analysis and quality control of the cited medications either separately or in combinations without pre-separation.

3.3.2 Experimental

3.2.2.1 Materials and reagents

All the chemicals used in the present studies were of analytical reagent grade and the solvents were of HPLC grade.

CLT (certified to contain 98%) was supplied by Ark Pharm. Inc., IL 60048 USA. AZL (certified to contain 98%) was supplied by D-L Chiral Chemicals, LLC., NJ 08540 USA. Edarbcyclor® 40-25 mg tablets; batch # NDC 64764-0994-30 (Takeda Pharmaceutical Company Limited, Tokyo, Japan) each labeled to contain 42.68 mg of azilsartan kamedoxomil (equivalent to 40 mg AZL) and 25 mg CLT were purchased from commercial sources in local market. Methanol, Sodium dodecyl sulphate (SDS), cetyl trimethyl ammonium bromide (CTAB), and hydroxymethyl cellulose (HMC) were obtained from Sigma-Aldrich, MO, USA. β-Cyclodextrin (β-CD) (TCI, Tokyo Kasei, Japan). O-phosphoric acid 85% and hydrochloric acid (Fisher Scientific, NJ, USA) were used. Sodium hydroxide and sodium dihydrogen phosphate were purchased from J.T. Baker,

NJ, USA. Phosphate buffer solutions (PBS) (0.02 M) were freshly prepared. SDS, CTAB, β-CD and HMC were prepared as 1% w/v aqueous solutions. Also, 0.1N NaOH and 0.1N HCl were prepared.

3.3.2.2 Instruments

A Lambda 20 UV/VIS spectrometer (Perkin Elmer, Massachusetts, USA) was used for the spectrophotometric measurements whereas a LS 55 Fluorescence spectrometer, 120V (Perkin Elmer, Massachusetts, USA) was used for the spectrofluorimetric measurements. Spectrophotometric measurements and data handling were performed using UV WinLab 1.22 software whereas fluorescence spectra measurements and data handling were performed using FL WinLab™ software. Quartz cells (1 cm) were used. A VRW SympHoly (SB20) pH-meter (Thermo Orion. Beverly, MA, USA) was used for pH measurements. Deionized water was prepared using a Barnstead NANO pure Dlamond Analytical ultrapure water system (Thermo Fischer Scientific, Waltham, MA, USA).

3.3.2.3 Standard solutions

10 mg of AZL and CLT were accurately weighed and transferred separately into 10 mL volumetric flasks. Then, they were dissolved and made up to volume with methanol to give concentrations of 1000 μg mL-1 for each. Further dilutions were made separately using the same solvent to prepare 1 μg mL^{-1} solutions for each.

3.3.2.4 Procedures

3.3.2.4.1 Linearity and construction of calibration graphs for the spectrophotometric technique

Aliquots of AZL and CLT standard stock solutions (1000 μg mL^{-1}) were separately transferred into two series of 10 mL Fisherbrand disposable tubes to give final concentrations of 8–50 and 2–20 μg mL^{-1} for AZL and CLT, respectively, then completed to 5 mL with methanol

and the contents were mixed well. The absorbance spectra were recorded against a methanol blank and then the first derivative spectra were obtained (number of points = 18), (Fig. 3.3.1). The amplitudes at 286 nm and 257 nm for AZL and CLT, respectively, were measured then plotted versus the corresponding final drug concentration of AZL and CLT (µg mL^{-1}) to obtain the calibration graphs and the regression equations. Figures (3.3.2 & 3.3.3) show linear relationships which were established by plotting first derivative of the spectra for AZL or CLT at 286 nm and 257 nm against AZL and CLT concentrations in µg mL^{-1}. Linear regression analysis of the data gave the following equations:

$$1D_{AZL} = 0.0075C + 0.0064 \quad (r=0.9998); \qquad \text{eq. (1)}$$

$$1D_{CLT} = 0.0224C - 0.0154 \quad (r=0.9999); \qquad \text{eq. (2)}$$

Where: 1D is the first derivative of the spectra for AZL or CLT at 286 nm and 257 nm, respectively. C is the concentration of AZL or CLT in µg mL^{-1} and r is the correlation coefficient.

3.3.2.4.2 Linearity and construction of calibration graphs for the spectrofluorimetric technique

Aliquots of AZL standard stock solution (1 µg mL^{-1}) were transferred into a series of 10 ml Fisherbrand disposable tubes to give final concentrations in the range of 0.01-0.08 µg mL^{-1}. Then, completed to 5 mL with methanol and the contents were mixed well. Relative fluorescence intensity (RFI) of the synchronous spectrofluorimetric spectra were recorded against a solvent blank using ($\Delta\lambda$= 110 nm, slit width for excitation and emission= 10 nm) and then the fourth derivatives were obtained (number of points = 90), (Fig. 3.3.4). The amplitudes of the fourth derivative of the synchronous spectra at 298 nm were measured and plotted versus the corresponding final drug concentration of AZL (µg mL^{-1}) to obtain the calibration graphs and regression equations. Figures (3.3.5 – 3.3.7) show linear relationships which were established by

plotting the RFI of AZL or CLT against their concentrations in μg mL^{-1}. Linear regression analysis of the data gave the following equations:

$4D_{AZL} = 789.1C + 0.7876$ (r=0.9998); (Synchronous method) eq. (3)

$RFI_{AZL} = 6289.8C + 41.996$ (r=0.9991); (Conventional method) eq. (4)

$RFI_{AML} = 3922.4C + 3.534$ (r=0.9996); (Conventional method) eq. (5)

Where: 4D is the fourth derivative of the synchronous fluorescence for AZL, RFI is the relative fluorescence intensity, C is the concentration of AZL or CLT in μg mL^{-1} and r is the correlation coefficient.

3.3.2.4.3 Preparation of AZL and CLT laboratory prepared mixtures

For the spectrophotometric method, aliquots of AZL and CLT standard stock solutions (1000 μg mL^{-1}) were accurately transferred into a series of 10 ml Fisherbrand disposable tubes to give final concentrations of 9.6, 16.0, 24.0 μg mL^{-1} for AZL and 6.0, 10.0, 15.0 μg mL^{-1} for CLT. The procedure described under "section 2.2.4.2" was then applied. For the spectrofluorimetric method, aliquots of AZL and CLT standard stock solutions (1 μg mL^{-1}) were accurately transferred into a series of 10 ml Fisherbrand disposable tubes to give final concentrations of 0.0384, 0.0576, 0.0768 μg mL^{-1} for AZL and 0.0240, 0.0360, 0.0480 μg mL^{-1} for CLT. The procedure described under "section 2.2.4.3" was then applied. For both methods, the percentage recoveries were calculated using the corresponding regression equation. Table (3.3.1) shows the mean percentage recoveries ± S.D. of AZL and CLT using the proposed methods.

3.3.2.4.4 Sample preparation and application to dosage form

Ten tablets of Edarbcyclor® were weighed and finely powdered after removal of the coat

using a tissue moistened with methanol. A portion of the powder equivalent to AZL (40 mg) and CLT (25 mg) was introduced into a 25 mL volumetric flask and completed to volume with methanol. The solutions were sonicated for 30 min then filtered through a Whatman filter paper and then filtered again using 0.2 µm a Whatman inorganic membrane filter. For spectrophotometric analyses, different aliquots from the prepared sample solutions were scanned and manipulated using the same procedure described under section "2.2.4.2". For the spectrofluorimetric analyses, further dilutions were prepared and different aliquots from the prepared sample solutions were scanned and manipulated using the same procedure described under section "2.2.4.3". The percentage recoveries were calculated by referring to the corresponding regression equations. Table (3.3.1) shows that the mean percentage recoveries ± S.D. of ALS and AML using the proposed methods.

3.3.2.5 Validation

The suggested analytical methods were validated according to ICH guidelines with respect to certain parameters such as linearity, LOD and LOQ, accuracy, precision, specificity and stability.

3.3.3 Results and discussion

The goal of the present investigations was to perform spectrophotometric and spectrophotometric studies on AZL and CLT in order to develop validated, rapid, sensitive, simple, inexpensive and selective spectrophotometric and specrofluorimetric methods for quantification of AZL in its combination with CLT. These studies focused on factors that enhance the absorbance or the intensities of the emission bands of each analyte separately and in their combination.

3.3.3.1 Optimization of experimental conditions for the spectrophotometric technique

For the spectrophotometric technique, the effect of different diluting solvents such as methanol, 0.1N HCl and 0.1N NaOH on absorbance was studied. 0.1N NaOH showed a slightly higher response for both drugs, (Fig. 3.3.8). This solvent can be used for ordinary UV measurements of AZL or CLT separately at 260 nm and 232 nm, respectively. Methanol was used as a convenient diluting solvent with satisfactory linearities in the range 8-50 and 2-20 µg mL^{-1} for AZL and CLT at 242 nm and 266 nm, respectively, (Fig. 3.3.1). The spectra of AZL and CLT in all the studied solvents showed severe overlap, (Fig. 3.3.1). Obtaining the first derivative for the absorbance spectra of the analyzed drugs was able to resolve such overlapping between AZL and CLT, only in methanol, to be utilized for their simultaneous quantitative determination at 286 nm and 257 nm, respectively, (Fig.3.3.9).

3.3.3.2 Optimization of experimental conditions for the spectrofluorimetric technique

3.3.3.2.1. Effect of diluting solvent

AZL is freely soluble in methanol so it was added to the solvent media in at least 10% of the final volume then either methanol, 0.1N HCl, 0.1N NaOH or PBS was added to complete the volume. The influence of these different diluting solvents on the relative fluorescence intensity (RFI) of AZL and CLT was studied and methanol was chosen as it showed the highest RFI, (Fig. 3.3.10).

3.3.3.2.2 Effect of pH

The effect of pH on RFI of AZL and CLT was investigated and pH 7.5 was found to give slightly higher RFI for AZL as its pKa values is 6.1 and it will have higher ionization percentage

at that pH, (Fig. 3.3.11). For CLT (pKa = 9.4), it is highly ionized at all the studied pHs so the effect of the studied pH values was not significant, (Fig. 3.3.11).

3.3.3.2.3 Effect of different organized media

The fluorescence properties of AZL and CLT in various micellar media were studied using anionic surfactant (SDS), cationic surfactant (CTAB) and different macromolecules; (β-CD) and (HMC). Micelles or reversed micelles are able to stabilize the exited singlet state and delay the decay process and thus may enhance the intensity of the emission bands [59]. PBS of pH 7.5 was used in this study to allow proper ionization of both analytes. None of the examined surfactants showed significant enhancement in RFI of AZL and CLT, (Fig. 3.3.12).

3.3.3.2.4 Techniques and parameters settings

Satisfactory linearities were obtained for AZL and CLT in methanol at 381 nm and 330 nm, upon excitation at 260 nm, respectively, at slit width of excitation and emission of 10 nm, (Fig. 3.3.13), (Table 3.3.1). However, the spectra of AZL and CLT in all of the studied solvents showed severe overlap so they cannot be used for their simultaneous determination, (Fig. 3.3.13). Also, synchronous fluorescence was not able to resolve such overlap at (λ= 10 – 300 nm, slit width for excitation and emission= 5 - 10 nm), (Fig. 3.3.4). Obtaining the fourth derivative for the synchronous fluorescence spectra (λ=110 nm, slit width for excitation and emission= 10 nm) of the analyzed drugs was able to resolve such overlap between AZL and CLT, only in methanol, to be utilized for quantitative determination of AZL in presence of CLT at 298 nm in their medicinally recommended ratio of (1.6: 1), respectively, (Fig. 3.3.14).

3.3.3.3 Validation of the proposed methods

3.3.3.3.1 Linearity and range

Linear relationships between the responses of AZL or CLT and their corresponding concentrations were obtained. The regression equation y = bC ± a for each drug was also computed. In these studies, five concentrations for AZL or CLT were used. The linearity of the calibration curves was validated by the high value of correlation coefficients (r) of the regression equation, small values of the standard deviation of residuals (Sy/x) and small value of the percentage relative error (Table 3.3.1). The analytical data of the calibration curves including standard deviations for the slope and intercept (Sb, Sa) are summarized in (Table 3.3.1). These data indicate the linearity of the calibration graphs.

3.3.3.3.2 Limit of detection and limit of quantification

LOQ and LOD were calculated according to ICH recommendations [51]. LOD was considered as the minimum concentration with a signal to noise ratio of at least three (S/N˜3), while LOQ was taken as a minimum concentration with a signal to noise ratio of at least ten (S/N˜10). Results are given in (Table 3.3.1).

3.3.3.3.3 Accuracy and precision

The satisfactory recovery results for the assay of AZL and/with CLT in their synthetic mixtures indicate the accuracy of the method, (Table, 3.3.2). Repeatability (intra-day) and intermediate precision (inter-day) were assessed using three concentrations and three replicates of each concentration. The relative standard deviations were found to be very small indicating reasonable repeatability and intermediate precision of the proposed method (Table 3.3.3).

3.3.3.3.4 Specificity

The specificity of the method was investigated by observing any interference encountered from common tablet excipients and it was confirmed that the signals measured was caused only by the analytes. The inactive ingredients in Edarbcylor® are: mannitol, microcrystalline cellulose, fumaric acid, sodium hydroxide, hydroxypropyl cellulose, crospovidone, magnesium stearate, hypromellose 2910, talc, titanium dioxide, ferric oxide red, polyethylene glycol 8000, and printing ink gray F1. It was found that the excipients did not interfere with the results, (Table 3.3.2). For the spectrophotometric method, it was found that AZL and CLT can be determined simultaneously either in their laboratory prepared mixtures or in their co-formulated tablets, (Table 3.3.2). On the other hand, the spectrofluorimetric method was only able to determine AZL in presence of CLT in methanol, (Table 3.3.2).

3.3.3.3.5 Stability

Stabilities of the standard stock solutions of AZL and CLT, stored at 2 – 8 °C, were evaluated at various time points over 1 month. The concentrations of freshly prepared solutions and those aged for 1 month were calculated by the methods developed and the difference between them was found to be less than 2%. Also, the prepared solutions for analysis were found to be stable for at least 3 days at 2 – 8 °C and for a day at room temperature. These solutions can therefore be used during this interval of time without the results being affected.

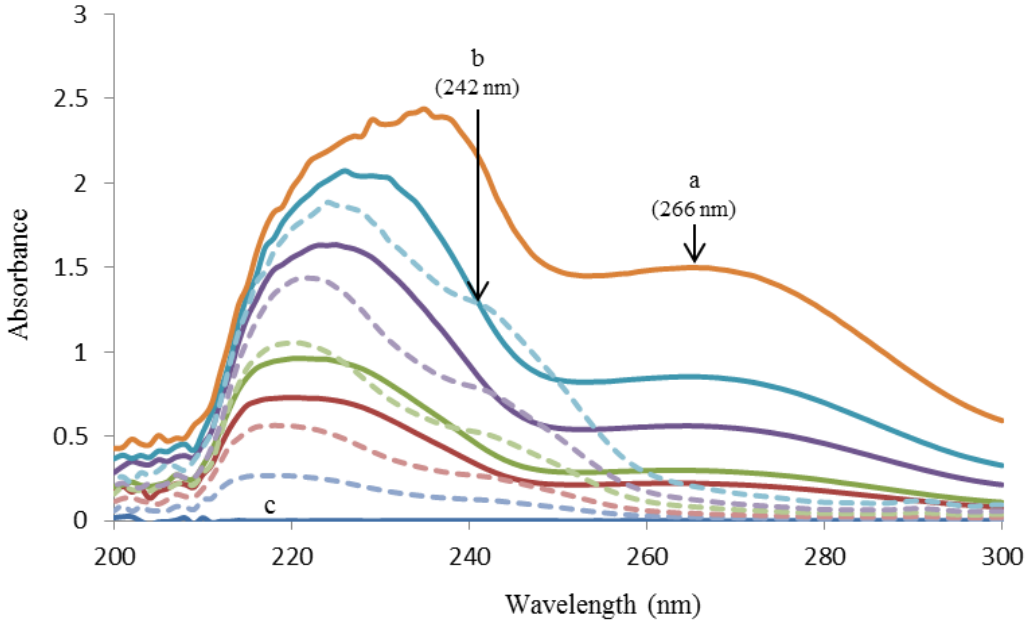

Figure 3.3.1 Zero order UV-absorbance spectra of (a) 8, 12, 20, 30, 50 µg mL^{-1} AZL and (b) 2, 4, 8, 12, 20 µg mL^{-1} CLT against (c) methanol blank

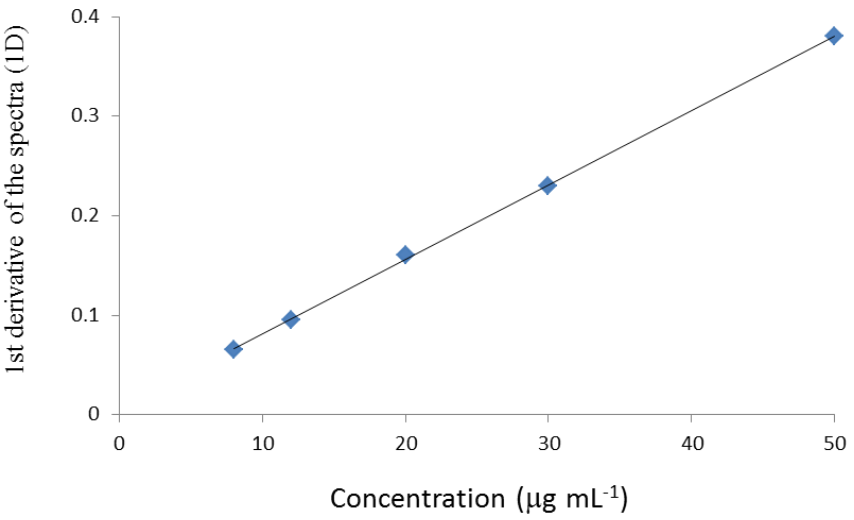

Figure 3.3.2 Standard calibration curve for determination of AZL by the proposed spectrophotometric method

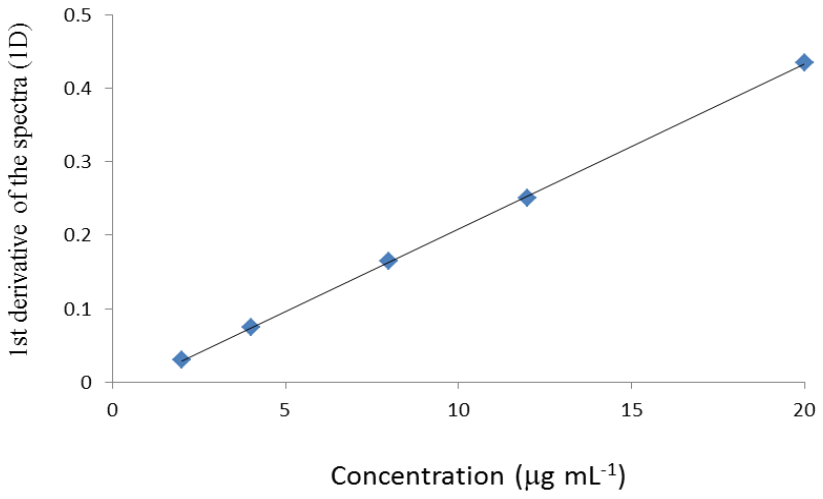

Figure 3.3.3 Standard calibration curve for determination of CLT by the proposed spectrophotometric method

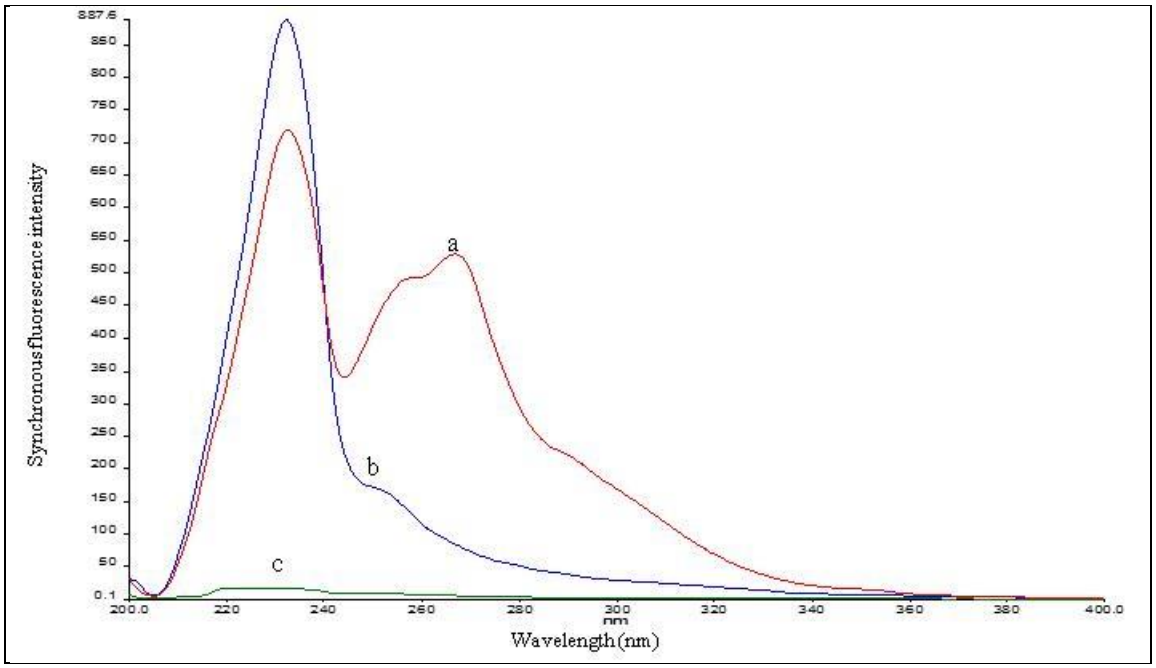

Figure 3.3.4 Synchronous fluorescence spectra for 0.06 µg mL^{-1} of (a) AZL and (b) CLT upon excitation at 260 nm against (c) methanol blank using the described parameters

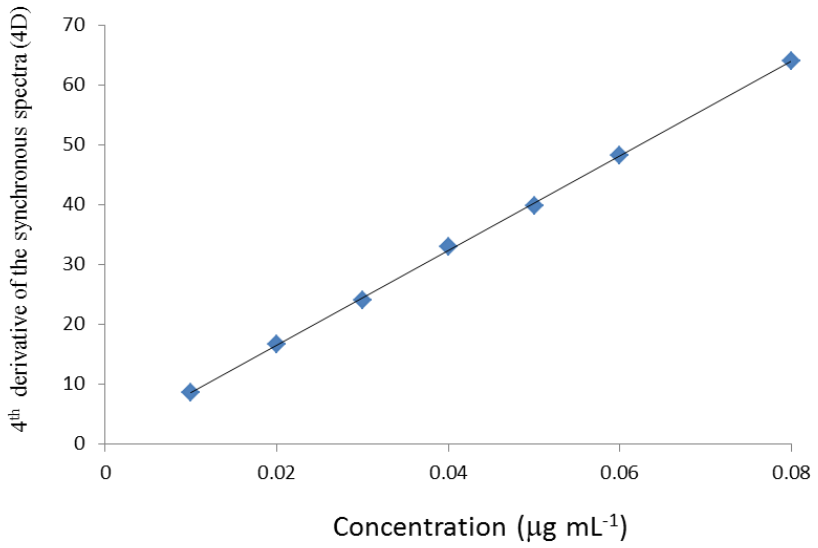

Figure 3.3.5 Standard calibration curve for determination of AZL by the proposed synchronous spectrofluorimetric method

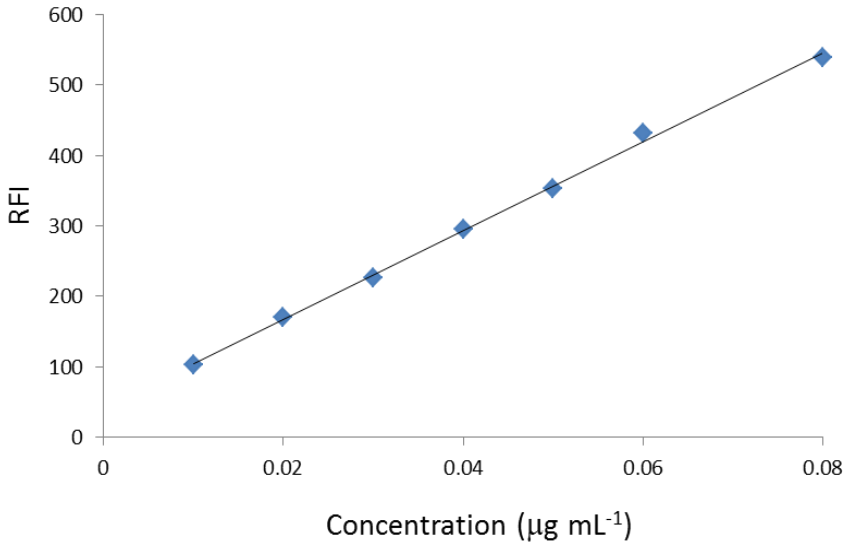

Figure 3.3.6 Standard calibration curve for determination of AZL by the proposed Conventional spectrofluorimetric method

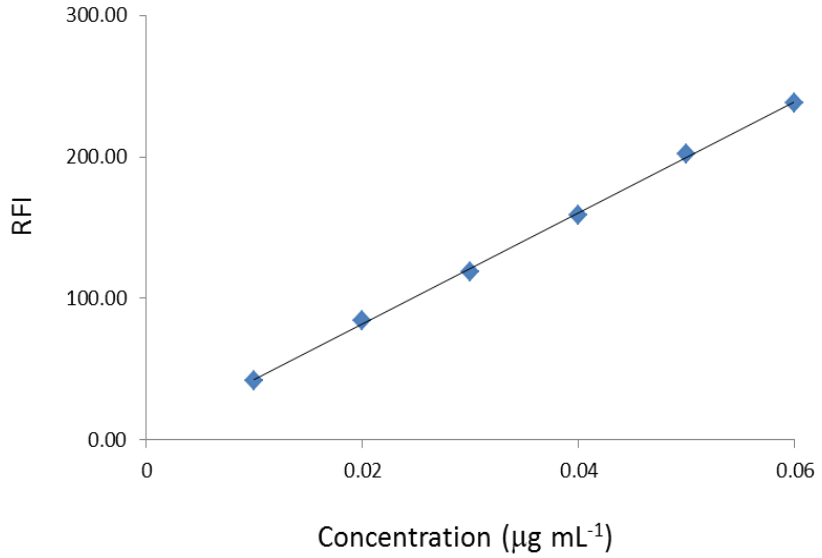

Figure 3.3.7 Standard calibration curve for determination of CLT by the proposed Conventional spectrofluorimetric method

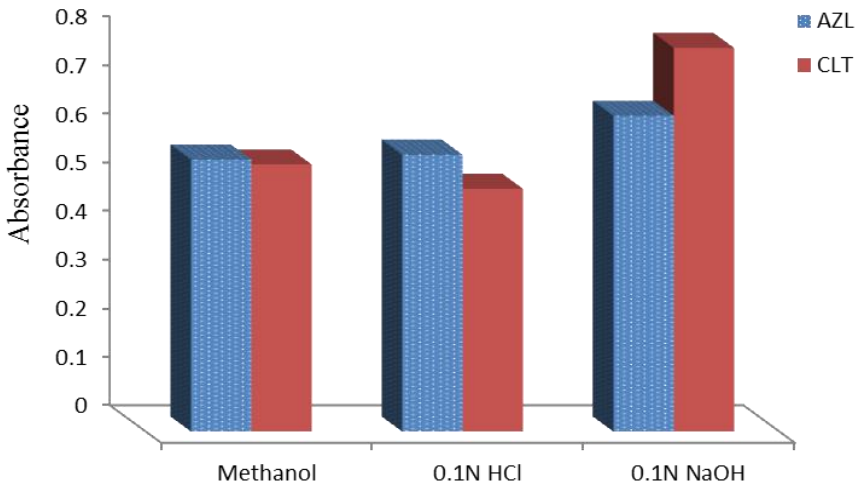

Figure 3.3.8 Effect of different diluting solvents on the Zero order UV-absorbance spectra of (a) 20 µg mL^{-1} of AZL at 260 nm and (b) 8 µg mL^{-1} of CLT at 232 nm

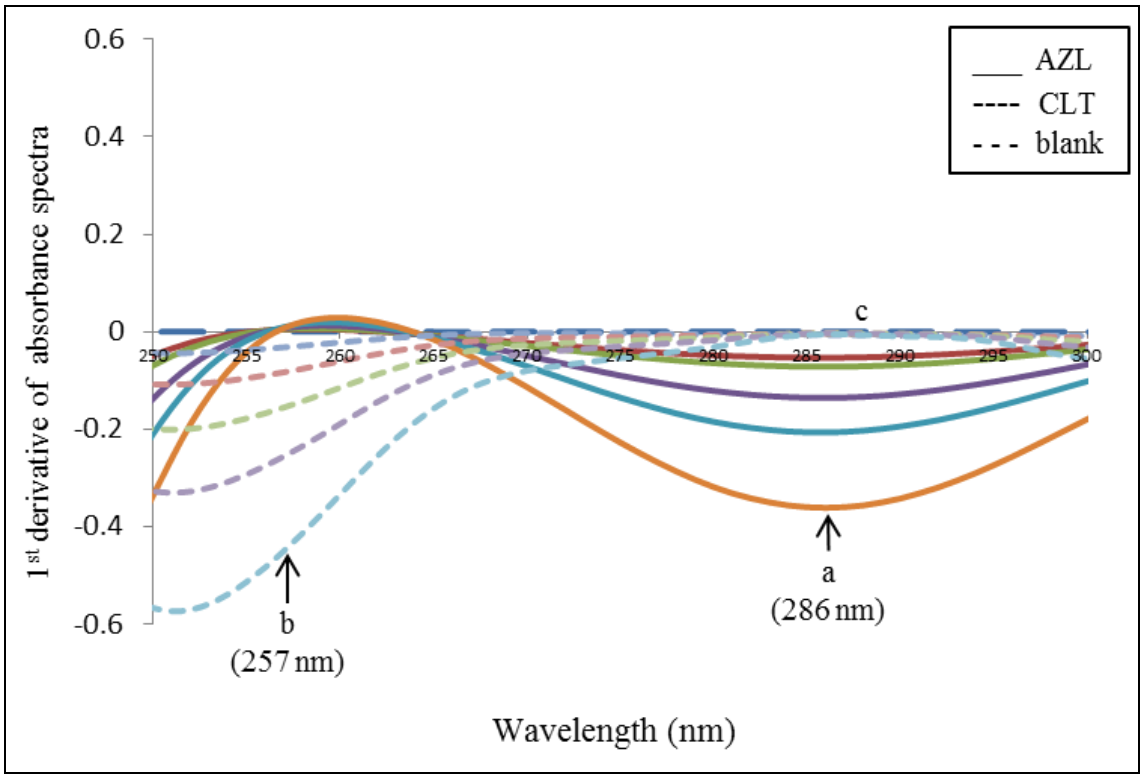

Figure 3.3.9 First derivative for the spectra of (a) 8, 12, 20, 30, 50 µg mL^{-1} of AZL and (b) 2, 4, 8, 12, 20 µg mL^{-1} CLT against (c) methanol blank

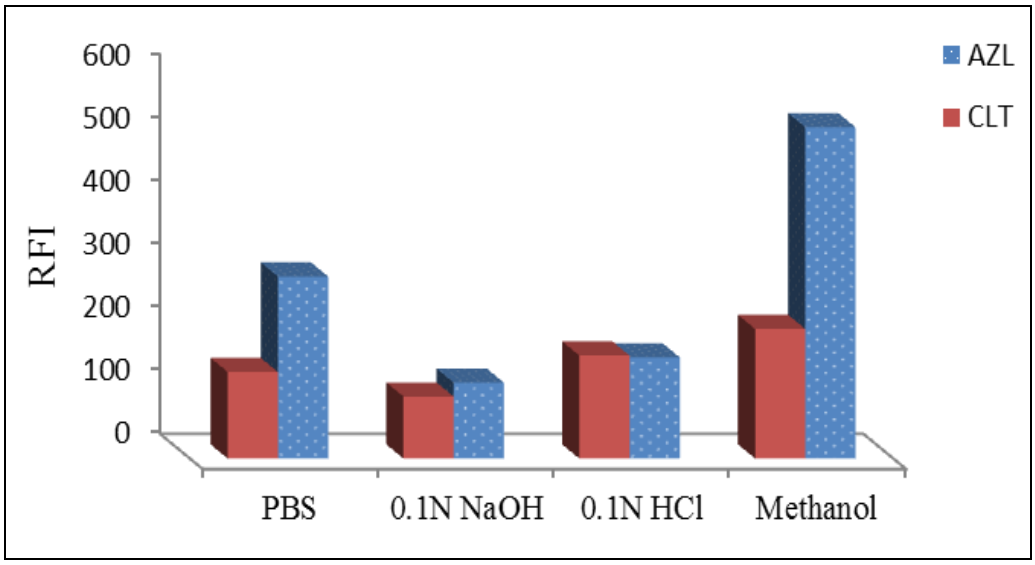

Figure 3.3.10 Effect of different diluting solvents on the relative conventional fluorescence intensities for 0.02 µg mL^{-1} of AZL and CLT at 381 nm upon excitation at 260 nm using the described parameters

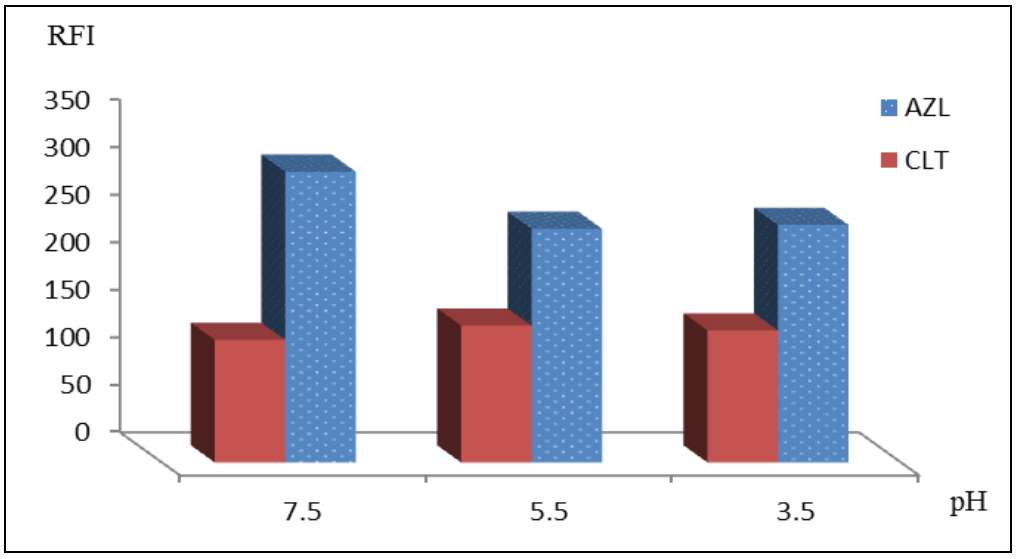

Figure 3.3.11 Effect of pH of PBS on the relative conventional fluorescence intensities for 0.02 µg mL^{-1} of AZL and CLT at 381 nm upon excitation at 260 nm using the described parameters

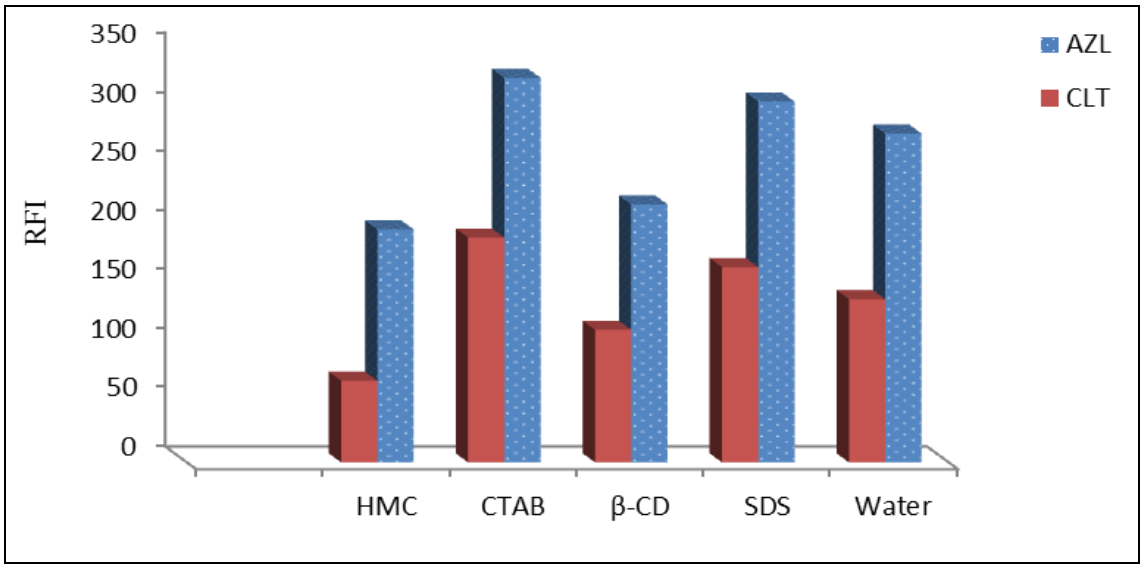

Figure 3.3.12 Effect of different surfactants (1 mL of 1% solution for each) on the relative conventional fluorescence intensities for 0.02 µg mL^{-1} of AZL and CLT at 381 nm upon excitation at 260 nm using the described parameters

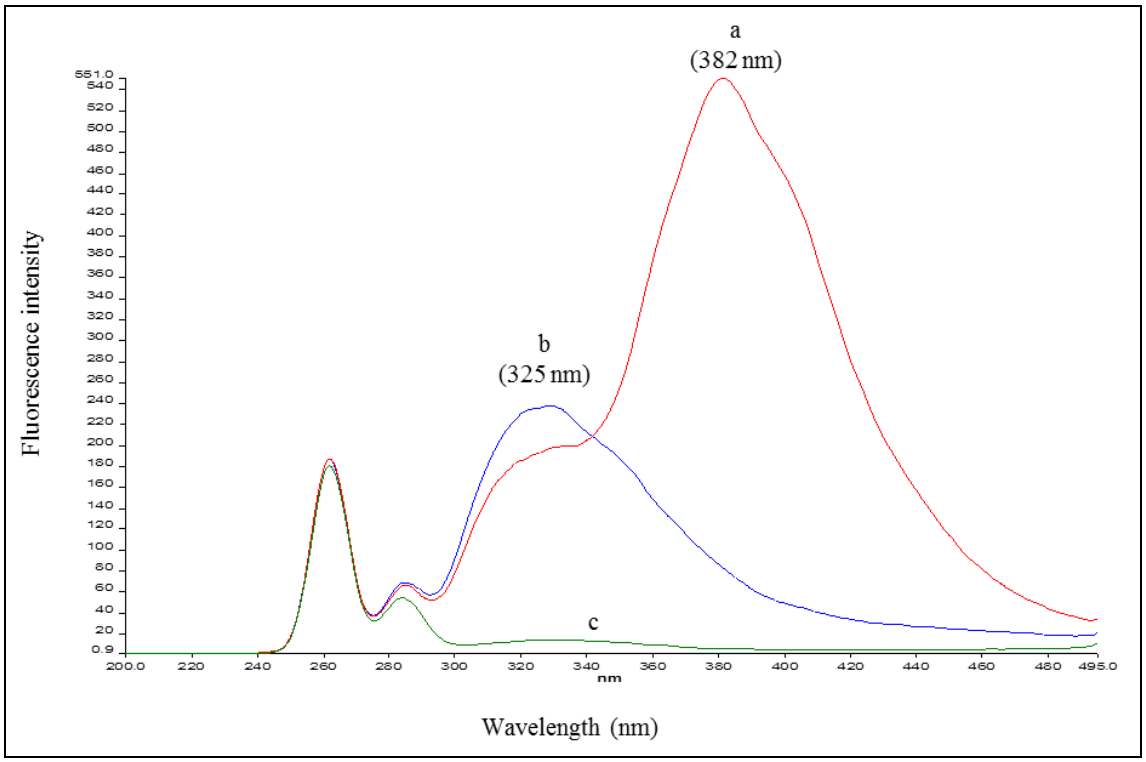

Figure 3.3.13 Conventional emission spectra for 0.06 µg mL^{-1} of (a) AZL and (b) CLT upon excitation at 260 nm against (c) methanol blank using the described parameters

Table 3.3.1 Performance data and results of the proposed spectroscopic methods

Item	Spectrophotometric technique		Spectrofluorimetric technique		
	AZL (1D)	CLT (1D)	AZL (4D)	AZL (381 nm)	CLT (330 nm)
Limit of detection, LOD ($\mu g\ mL^{-1}$)	0.977	0.296	0.001	0.001	0.002
Limit of quantitation, LOQ ($\mu g\ mL^{-1}$)	2.960	0.897	0.003	0.004	0.005
Intercept (a)	0.0064	-0.0154	0.7876	41.996	3.5339
Slope (b)	0.0075	0.0224	789.1	6289.8	3922.4
Correlation coefficient (r)	0.9998	0.9999	0.9998	0.9991	0.9996
S.D. of residuals (Sy/x)	0.003	0.003	0.478	4.396	2.576
S.D. of intercept (Sa)	0.002	0.002	0.267	2.469	2.043
S.D. of slope (Sb)	0.001	0.001	8.048	74.453	61.598
Percentage relative error, % Error	0.75	0.55	0.76	0.94	1.23
Linearity range ($\mu g\ mL^{-1}$)	8.00-50.00	2.00-20.00	0.01-0.08	0.01-0.08	0.01-0.06
Mean recovery ± %R.S.D.	99.55± 1.69	100.62± 1.24	99.94± 0.80	99.54± 2.09	100.61± 2.75

Table 3.3.2 Intra-and inter-day validation for the spectroscopic methods

	Medication	Concentration (µg mL^{-1})	Intra-day assay Found ± %R.S.D [a]	Inter-day assay Found ± %R.S.D [a]
Spectrophotometric Technique	AZL	12.000	12.619 ± 0.63	12.124 ± 1.68
		20.000	20.124 ± 2.02	20.258 ± 1.01
		30.000	29.813 ± 1.23	29.457 ± 1.19
	CLT	4.000	4.028 ± 0.32	4.051 ± 0.64
		8.000	7.905 ± 1.63	8.054 ± 1.66
		12.000	11.923 ± 1.08	11.789 ± 1.58
Spectrofluorimetric Technique	AZL	0.015	0.015 ± 2.09	0.015 ± 2.92
		0.030	0.030 ± 2.22	0.030 ± 2.77
		0.050	0.050 ± 1.36	0.050 ± 2.88

[a] Mean and standard deviation of three determinations

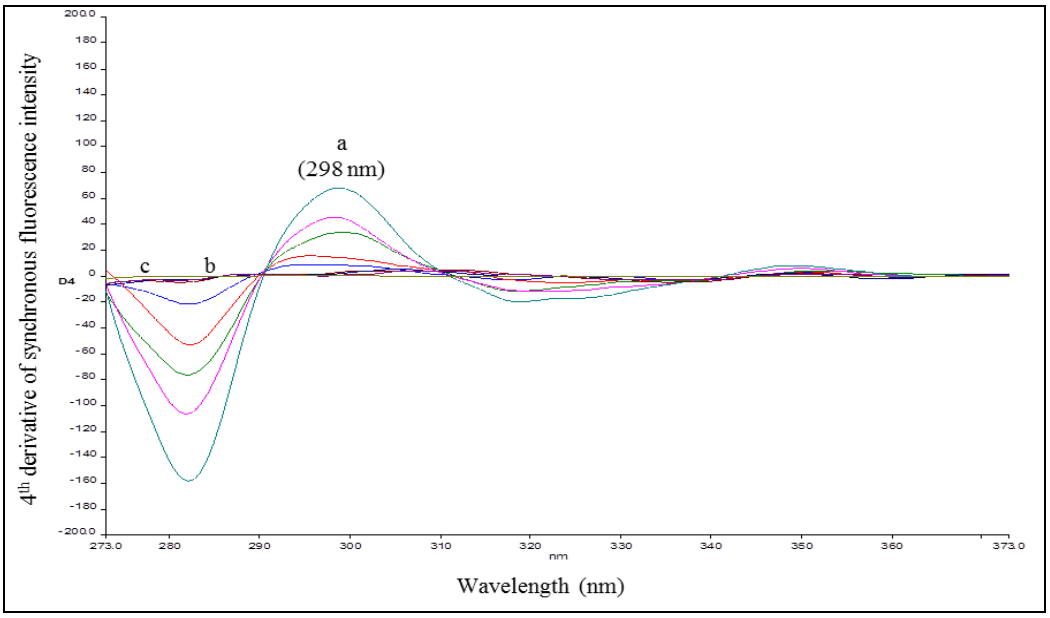

Figure 3.3.14 Fourth derivative of the synchronous fluorescence spectra for (a) 0.01, 0.02, 0.04, 0.06, 0.08 µg mL^{-1} of AZL and (b) 0.01, 0.02, 0.03 0.04, 0.06 µg mL^{-1} of CLT against (c) methanol blank using the described parameters

Table 3.3.3 Assay results for the determination of the studied drugs in their laboratory prepared mixtures and dosage form

	Compound	Synthetic mixtures (CLT: AZL) (1.0: 1.6)			Dosage form (Edarbcyclor® tablets)		
		Amount taken ($\mu g\ mL^{-1}$)	Amount found ($\mu g\ mL^{-1}$)	% Found	Amount taken ($\mu g\ mL^{-1}$)	Amount found ($\mu g\ mL^{-1}$)	% Found
Spectrophotometric technique	**CLT**	6.000	6.045	100.74	6.000	6.045	97.95
		10.000	9.839	98.39	10.000	10.286	99.10
		18.000	17.875	99.31	18.000	17.875	101.71
	Mean recovery%			**99.48**			**99.59**
	± %R.S.D.			**1.19**			**1.93**
	AZL	9.600	9.813	102.22	9.600	9.813	100.45
		16.000	15.813	98.83	16.000	16.480	101.17
		28.800	28.480	98.89	28.800	28.480	100.48
	Mean recovery%			**99.98**			**100.70**
	± %R.S.D.			**1.94**			**0.40**
Spectrofluorimetric technique	**AZL**	0.0384	0.039	101.26	0.0384	0.037	97.40
		0.0576	0.058	100.12	0.0576	0.057	99.30
		0.0768	0.077	100.47	0.0768	0.076	98.80
	Mean recovery%			**100.62**			**98.50**
	± %R.S.D.			**0.58**			**1.00**

Each result is the average of three separate determinations.

3.4 Conclusions

In section 3.2, rapid, sensitive, and simple spectrofluorimetric methods were developed and validated for simultaneous determination of ALS and AML in bulk and in dosage forms. The proposed methods have many advantages regarding analysis time, sensitivity and cost compared with those of the previously reported methods. Also, the proposed methods are less pollutant to far extent as no harmful reagents are used. Moreover, lower values for LOD and LOQ could be obtained easily by controlling the slit width of excitation and emission which could allow determination of these drugs separately in plasma using the steady state spectrofluorimetric method. Moreover, the direct steady state method showed good tolerance and could be applied for the determination of ALS and AML in their co-formulated tablets with HCZ.

In section 3.3, rapid, sensitive, inexpensive and simple spectrophotometric and spectrofluorimetric methods were developed and validated for determination of AZL in its combination with CLT either in their laboratory prepared mixtures or in their combined pharmaceutical formulation. The proposed methods have many advantages regarding analysis time, sensitivity and cost.

Finally, the proposed methods can be used for the quality control of the cited drugs in ordinary laboratories.

References

1. Munson, J. W. Pharmaceutical Analysis, Part A. Marcel Dekker: NY, USA, 1981.
2. Xiao, Y.; Wang, H. Y.; Han, J. Simultaneous determination of carvedilol and ampicillin sodium by synchronous fluorimetry. Spectrochimica acta. Part A, Molecular and biomolecular spectroscopy 2005, 61 (4), 567-73.
3. Bauer, H. H.; Christian, G. D.; O' Reilly, J. E. Instrumental Analysis. Allyn and Bacon: London, 1978.
4. Skoog, D. A.; Holler, F. J.; Crouch, S. R. Principles of Instrumental Analysis. 6th ed.; Thamson Brooks/Cole: Canda, 2007.
5. McLntire, G. L.; Dorsey, J. G. Micelles in Analytical Chemistry. Critical Reviews in Analytical Chemistry 1990, 21 (4), 257-278.
6. Hinze, W. L.; Singh, H. N.; Baba, Y.; Harvey, N. G. Micellar enhanced analytical fluorimetry. TrAC Trends in Analytical Chemistry 1984, 3 (8), 193-199.
7. Tran, C. D.; Van Fleet, T. A. Micellar induced simultaneous enhancement of fluorescence and thermal lensing. Analytical Chemistry 1988, 60 (22), 2478-2482.
8. Singh, H.; Hinze, W. L. Micellar Enhanced Spectrofluorimetric Methods: Application to the Determination of Pyrene. Analytical Letters 1982, 15 (3), 221-243.
9. Jalali, F.; Afshoon, A.; Shamsipur, M. Micellar-enhanced spectrofluorimetric determination of ketoconazole in cetyltrimethylammonium bromide medium. Chem. Anal. (Warsaw, Pol.) 2007, 52 (1), 115-123.
10. Sabry, S. M. Determination of flufenamic and mefenamic acids in pharmaceutical preparations using organized media. Anal. Chim. Acta 1998, 367 (1-3), 41-53.

11. Shah, J.; Jan, M. R.; Khan, M. N.; Inayatullah. Development and validation of micellar-enhanced spectrofluorimetric method for determination of sulpiride in pharmaceutical formulations and biological samples. Tenside, Surfactants, Deterg. 2012, 49 (6), 451-457.
12. Wang, C. C.; Masi, A. N.; Fernandez, L. On-line micellar-enhanced spectrofluorimetric determination of rhodamine dye in cosmetics. Talanta 2008, 75 (1), 135-40.
13. Yang, G.-J.; Liu, P.; Qu, X.-L.; Ming, S.; Wang, C.-Y.; Qu, Q.-S.; Hu, X.-Y.; Leng, Z.-Z. Micellar-enhanced spectrofluorimetric determination of trazodone hydrochloride in human urine and serum. Anal. Lett. 2007, 40 (1), 151-162.
14. Alarfaj, N. A.; Aly, F. A. Micelle-Enhanced Spectrofluorimetric Method for Determination of Cholesterol-Reducing Drug Ezetimibe in Dosage Forms. J. Fluoresc. 2012, 22 (1), 9-15.
15. Alarfaj, N. A.; El-Tohamy, M. F. Determination of the anti-viral drug Ribavirin in dosage forms via micelle-enhanced spectrofluorimetric method. Luminescence 2013, 28 (2), 190-194.
16. Salama, N. N. A.; Salem, M. Y.; Abd El Halim, L. M.; Abdel Fattah, L. E. Spectrofluorimetric and spectrophotometric stability-indicating methods for the analysis of veralipride in presence of its degradants and in spiked human plasma. Chin. J. Chem. 2012, 30 (1), 183-189.
17. Kaur, K.; Singh, B.; Malik, A. K. Micelle enhanced spectrofluorimetric method for the determination of ofloxacin and lomefloxacin in human urine and serum. Thai J. Pharm. Sci. 2010, 34 (2), 58-66.
18. Manzoori, J. L.; Amjadi, M. Spectrofluorimetric and micelle-enhanced spectrofluorimetric methods for the determination of gemfibrozil in pharmaceutical preparations. J. Pharm. Biomed. Anal. 2003, 31 (3), 507-513.

19. Ocana, J. A.; Barragan, F. J.; Callejon, M. Spectrofluorimetric and micelle-enhanced spectrofluorimetric determination of gatifloxacin in human urine and serum. J. Pharm. Biomed. Anal. 2005, 37 (2), 327-332.
20. Walash, M. I.; Belal, F.; El-Enany, N.; Eid, M.; El-Shaheny, R. N. Stability-indicating micelle-enhanced spectrofluorimetric method for determination of loratadine and desloratadine in dosage forms. Luminescence 2011, 26 (6), 670-679.
21. Bonanni, L.; Dalla Vestra, M. Oral renin inhibitors in clinical practice: a perspective review. Ther Adv Chronic Dis 2012, 3 (4), 173-81.
22. Sarkar, A. K.; Ghosh, D.; Das, A.; Selvan, P. S.; Gowda, K. V.; Mandal, U.; Bose, A.; Agarwal, S.; Bhaumik, U.; Pal, T. K. Simultaneous determination of metoprolol succinate and amlodipine besylate in human plasma by liquid chromatography-tandem mass spectrometry method and its application in bioequivalence study. J Chromatogr B Analyt Technol Biomed Life Sci 2008, 873 (1), 77-85.
23. Abdollahpour, N.; Asoodeh, A.; Saberi, M. R.; Chamani, J. Separate and simultaneous binding effects of aspirin and amlodipine to human serum albumin based on fluorescence spectroscopic and molecular modeling characterizations: A mechanistic insight for determining usage drugs doses. Journal of Luminescence 2011, 131 (9), 1885-1899.
24. Littlejohn, T. W., 3rd; Trenkwalder, P.; Hollanders, G.; Zhao, Y.; Liao, W. Long-term safety, tolerability and efficacy of combination therapy with aliskiren and amlodipine in patients with hypertension. Curr Med Res Opin 2009, 25 (4), 951-9.
25. Wrasse-Sangoi, M.; Sangoi, M. S.; Oliveira, P. R.; Secretti, L. T.; Rolim, C. M. Determination of aliskiren in tablet dosage forms by a validated stability-indicating RP-LC method. J Chromatogr Sci 2011, 49 (2), 170-5.

26. Swamy, G. K.; Rao, J. V. L. N. S.; Kumar, J. M. R.; Kumar, U. A.; Bikshapathi, D. V. R. N.; kumar, D. V. Analytical method development and validation of aliskiren in bulk and tablet dosage form by RP-HPLC method. Journal of Pharmacy Research 2011, 4 (3), 865-867.

27. Babu, K. S.; Rao, J. V. L. N. S.; Bhargava, K. V. A simple and sensitive method for the determination of aliskiren hemifumarate using HPLC-UV detection. Rasayan Journal of Chemistry 2011, 4 (2), 285-288.

28. pachauri, S.; paliwal, S.; Kona.S.Srinivas; YogendraSingh; Jain, V. Development & validation of HPLC method for analysis of some antihypertensive agents in their pharmaceutical dosage forms. J Pharm Sci & Res 2010, Vol.2 (8), 459-464.

29. Sangoi, M. S.; Wrasse-Sangoi, M.; Oliveira, P. R.; Rolim, C. M. B.; Steppe, M. Simultaneous determination of aliskiren and hydrochlorothiazide from their pharmaceutical preparations using a validated stability-indicating MEKC method. Separation Science 2011, 34 (15), 1859–1866.

30. WS, M.; TS, L.; FD, I.; MB, C. Development and validation of an UV spectrophotometric method for the determination of aliskiren in tablets. Quim. Nova 2010, 33 (6), 1330-1334.

31. Swamy, K. G.; Kumar, J. M. R.; Sheshagirirao, J. V. L. N.; Kumar, D. V.; RatnaMani, C.; Kumar, V. N. V. E. Validated spectrophotometric determination of Aliskiren in pharmaceutical dosage form. Journal of Pharmacy Research 2011, 4 (8), 2574-2575.

32. Aydogmus, Z. Spectrofluorimetric determination of aliskiren in dosage forms and urine. Luminescence : the journal of biological and chemical luminescence 2012, 27 (6), 489-94.

33. Aydogmus, Z.; Sari, F.; Ulu, S. T. Spectrofluorimetric determination of aliskiren in tablets and spiked human plasma through derivatization with dansyl chloride. J Fluoresc 2012, 22 (2), 549-56.

34. Sharma, M.; Kothari, C.; Sherikar, O.; Mehta, P. Concurrent Estimation of Amlodipine Besylate, Hydrochlorothiazide and Valsartan by RP-HPLC, HPTLC and UV-Spectrophotometry. J Chromatogr Sci 2013.

35. Patel, D. B.; Mehta, F. A.; Bhatt, K. K. Simultaneous Estimation of Amlodipine Besylate and Indapamide in a Pharmaceutical Formulation by a High Performance Liquid Chromatographic (RP-HPLC) Method. Sci Pharm 2012, 80 (3), 581-90.

36. Jain, P. S.; Patel, M. K.; Gorle, A. P.; Chaudhari, A. J.; Surana, S. J. Stability-indicating method for simultaneous estimation of olmesartan medoxomile, amlodipine besylate and hydrochlorothiazide by RP-HPLC in tablet dosage form. J Chromatogr Sci 2012, 50 (8), 680-7.

37. Fakhari, A. R.; Nojavan, S.; Haghgoo, S.; Mohammadi, A. Development of a stability-indicating CE assay for the determination of amlodipine enantiomers in commercial tablets. Electrophoresis 2008, 29 (22), 4583-92.

38. Wankhede, S. B.; Raka, K. C.; Wadkar, S. B.; Chitlange, S. S. Spectrophotometric and HPLC methods for simultaneous estimation of amlodipine besilate, losartan potassium and hydrochlorothiazide in tablets. Indian J Pharm Sci 2010, 72 (1), 136-40.

39. Rahman, N.; Nasrul Hoda, M. Validated spectrophotometric methods for the determination of amlodipine besylate in drug formulations using 2,3-dichloro 5,6-dicyano 1,4-benzoquinone and ascorbic acid. J Pharm Biomed Anal 2003, 31 (2), 381-92.

40. Rahman, N.; Azmi, S. N. Spectrophotometric method for the determination of amlodipine besylate with ninhydrin in drug formulations. Farmaco 2001, 56 (10), 731-5.

41. Shaalan, R. A.; Belal, T. S. Simultaneous spectrofluorimetric determination of amlodipine besylate and valsartan in their combined tablets. Drug testing and analysis 2010, 2 (10), 489-93.

42. Darwish, H. W.; Backeit, A. H. Multivariate versus classical univariate calibration methods for spectrofluorimetric data: application to simultaneous determination of olmesartan medoxamil and amlodipine besylate in their combined dosage form. J Fluoresc 2013, 23 (1), 79-91.

43. Tambe, V.; Vichare, V.; Kandekar, U. Spectrophotometric simultaneous determination of Atenolol and Hydrochlorothiazide in combined dosage form by simultaneous equation, absorption ratio and first order derivative spectroscopy methods. Int. J. Pharm. Sci. Rev. Res. 2010, 5 (Copyright (C) 2013 American Chemical Society (ACS). All Rights Reserved.), 151-155.

44. Vekariya, P. P.; Joshi, H. S. Development and Validation of RP-HPLC Method for Azilsartan Medoxomil Potassium Quantitation in Human Plasma by Solid Phase Extraction Procedure. ISRN Spectroscopy 2013, 2013, 6.

45. Baker, W. L.; White, W. B. Azilsartan medoxomil: a new angiotensin II receptor antagonist for treatment of hypertension. Ann. Pharmacother. 2011, 45 (Copyright (C) 2013 American Chemical Society (ACS). All Rights Reserved.), 1506-1515.

46. Kurtz, T. W.; Kajiya, T. Differential pharmacology and benefit/risk of azilsartan compared to other sartans. Vasc Health Risk Manag 2012, 8, 133-43.

47. Kusumoto, K.; Igata, H.; Ojima, M.; Tsuboi, A.; Imanishi, M.; Yamaguchi, F.; Sakamoto, H.; Kuroita, T.; Kawaguchi, N.; Nishigaki, N.; Nagaya, H. Antihypertensive, insulin-sensitising and renoprotective effects of a novel, potent and long-acting angiotensin II type 1 receptor blocker, azilsartan medoxomil, in rat and dog models. Eur J Pharmacol 2011, 669 (Copyright (C) 2013 U.S. National Library of Medicine.), 84-93.

48. Martindale, The Complete Drug Reference [Online]; 36th Ed ed; The Pharmaceutical Press: London, UK, 2009.

49. Singh, B.; Patel, D. K.; Ghosh, S. K. A reversed-phase high performance liquid chromatographic method for determination of chlorthalidone in pharmaceutical formulation. Int. J. Pharm. Pharm. Sci. 2009, 1 (Copyright (C) 2013 American Chemical Society (ACS). All Rights Reserved.), 24-29.

50. Mhaske, R. A.; Sahasrabudhe, S.; Mhaske, A. A.; Garole, D. J. RP-HPLC method for simultataneous determination of Atorvastatin calcium, Olmesartan medoxomil, Candesartan, Hydrochlorothiazide and Chlorthalidone - application to commercially available drug products. Int. J. Pharm. Sci. Res. 2012, 3 (Copyright (C) 2013 American Chemical Society (ACS). All Rights Reserved.), 793-801.

51. Woo, H.; Kim, J. W.; Han, K. M.; Lee, J. H.; Hwang, I. S.; Kim, J.; Kweon, S. J.; Cho, S.; Chae, K. R.; Han, S. Y. Simultaneous analysis of 17 diuretics in dietary supplements by HPLC and LC-MS/MS. Food Addit. Contam., Part A 2013, 30 (Copyright (C) 2013 American Chemical Society (ACS). All Rights Reserved.), 209-217.

52. Youssef, R. M.; Maher, H. M.; El-Kimary, E. I.; Hassan, E. M.; Barary, M. H. Validated stability-indicating methods for the simultaneous determination of amiloride hydrochloride, atenolol, and chlorthalidone using HPTLC and HPLC with photodiode array detector. J.

AOAC Int. 2013, 96 (Copyright (C) 2013 American Chemical Society (ACS). All Rights Reserved.), 313-323.

53. Salem, H. High-performance thin-layer chromatography for the determination of certain antihypertensive mixtures. Sci. Pharm. 2004, 72 (Copyright (C) 2013 American Chemical Society (ACS). All Rights Reserved.), 157-174.

54. Ciborowski, M.; Icardo, M. C.; Mateo, J. V.; Martinez Calatayud, J. FI-chemiluminometric study of thiazides by on-line photochemical reaction. J Pharm Biomed Anal 2004, 36 (4), 693-700.

55. Parmar, K. E.; Mehta, R. S. First order derivative spectrophotometric method for simultaneous estimation of Telmisartan and Chlorthalidone in bulk and pharmaceutical dosage form. Int. Res. J. Pharm. 2013, 4 (Copyright (C) 2013 American Chemical Society (ACS). All Rights Reserved.), 224-228.

56. Lu, M.; Li, X.; Feng, Q.; Chen, G.; Zhang, L. Analysis of diuretics by capillary electrochromatography using poly(1-hexadecene-co-TMPTMA) monolithic column. Sepu 2010, 28 (Copyright (C) 2013 American Chemical Society (ACS). All Rights Reserved.), 253-259.

57. Cheng, J. W. M. Azilsartan/chlorthalidone combination therapy for blood pressure control. Integr. Blood Pressure Control 2013, 6 (Copyright (C) 2013 American Chemical Society (ACS). All Rights Reserved.), 39-48.

58. Kasimala, M. B.; Kasimala, B. B. REVERSE PHASE-HPLC METHOD DEVELOPMENT AND VALIDATION FOR THESIMULTANEOUS ESTIMATION OF AZILSARTAN MEDOXOMIL ANDCHLORTALIDONE IN PHARMACEUTICAL DOSAGE FORMS Reverse Phase-HPLC Method Development and Validation for the Simultaneous

Estimation of Azilsartan medoxomil and Chlorthalidone in Pharmaceutical Dosage Forms. Jamonline 2012, 2 (1), 117-126.

59. Salim, M.; El-Enany, N.; Belal, F.; Walash, M.; Patonay, G. Micelle-enhanced spectrofluorimetric method for determination of sitagliptin and identification of potential alkaline degradation products using LC-MS. Luminescence 2013, 5 (10).

4 FUNCTIONALIZED SILICA NANOPARTICLES FOR ENHANCED ELECTROPHORETIC SEPARARTION OF SOME ACIDIC AND BASIC DRUGS

This chapter provides a systematic comparison of five functionalized silica nanoparticles (SNPs) that can be used as pseudo-stationary phases (PSPs) in capillary electrochromatography. Monoamine-modified SNPs (MA-SNPs), L-lysine-modified SNPs (L-SNPs), and linear poly L-lysine (LPL-SNPs) were prepared using the proper organosilane coupling agents to render a positive charge on the surface of the SNPs, whereas, cysteine-modified SNPs (CYS-SNPs) and Glutamic acid-modified SNPs (GLU-SNPs) were prepared using amino acids-based organosilane conjugate moieties to render a zwitter ionic nature and a negative charge on the surface of the SNPs at the proper pH, respectively. The SNPs were prepared using the reverse microemulsion approach with mean diameters in the range of 53.4 ± 5.9 nm to 82.7 ± 4.7 nm as shown by the TEM measurements. The differences in the electrophoretic behavior, and the ability to separate mixtures of acidic and basic drugs using these PSPs were evaluated by analyzing a mixture of ibuprofen, ketoprofen, and valsartan as well as a mixture of atenolol and propranolol as examples of acidic and basic compounds, respectively. An enhanced separation of the acidic or basic drug mixtures was achieved using LPL-SNPs. Also, MA-SNPs resulted in fast and enhanced separation of the acidic drugs mixture using the reversed polarity mode. Both CYS-SNPs and GLU-SNPs did not show any significant change in the electroosmotic flow with non-negligible improvement in the separation of the acidic drugs mixture at pH 4 using the reversed polarity mode. These amino acids or peptides-modified SNPs can significantly help in achieving fast and efficient separation of challenging mixtures of compounds of different charges.

4.1 Introduction

The use of silica nanoparticles (SNPs) with surface modifications in different applications is a topic of growing interest. Nanochemistry has been widely used in recent years in various fields, including chemistry, physics, biology, material science, etc., because of their advantageous features [1]. The interest in nanoparticles (NPs) comes from their unique mechanical, magnetic, catalytic, electronic, optical, and biological characteristics. Size of NPs can range from 1 to 1,000 nm and can consist of biodegradable polymers, metals, inorganic, or lipid constituents [2]. The applications of NPs include catalysis, electronics, biosensors, medicines, cosmetics, imaging, bioanalysis and bio-related applications [3]. For instance, NP-based drug delivery systems have been utilized to improve human health by illuminating tumors, brain, and other cellular functions while using medical imaging [4].

Breakthroughs in the synthesis of SNPs are beneficial when designing and developing nanosized probes. SNPs can be modified with various organic groups and conjugated to molecules, which include monoclonal antibodies, DNA, or other moieties [5].

The SNPs usually consist of a polymeric structure consisting of siloxan (-Si-O-Si-O-) and high concentrations of silanol (Si-OH) groups on the outer surface and are a type of colloidal metal oxide, which can be easily modified. There are two major classes of SNPs: solid SNPs (SSNPs) and mesoporous SNPs (MSNPs). The MSNPs have many pores with a silica matrix, and SSNPs have no pores. The MSNPs, with its empty pores and channels, can be filled with various amounts of biomolecules and drugs as well as filling the gaps of molecules [6]. Controlled release of drugs from MSNPs pores is an excellent feature and can also prolong drug efficiency [6].

Functionalized SNPs also have some useful applications in the field of separation of organic molecules either by using liquid chromatography or capillary electrophoresis (CE) as they can be used as pseudostationary phases (PSP) or as additives to the mobile phase to enhance the separation performance and get better resolutions [7].

NP capillary electrophoresis is the combination of NPs and CE technology in which NPs are used as stationary or PSP to alter the electroosmotic flow (EOF), increase column capacity, and improve separation selectivity and column efficiency. The technique combines the high efficiency of CE with the high selectivity of HPLC that can be used for the separation of different types of analytes. The use of NPs-based PSPs in capillary electrochromatography (CEC) [8] has attracted the interest of many researchers because of its several merits, such as no packing or frits, fast regeneration of the column, and the absence of stationary phase carry-over effects. When NPs are used as PSPs, they are suspended in the background electrolyte and are continuously pumped through the capillary. Compared with other CEC types, NPs are much smaller than the particles used in packed columns, and improved separation efficiency is expected due to their high surface-to-volume ratio [9]. And compared with traditional micelles, NPs have higher stability and larger surface area, which make them powerful buffer additives for achieving more efficient separations [7].

NPs used in CEC usually include polymer nanoparticles, gold nanoparticles, molecularly imprinted polymer NPs, dendrimers, and SNPs. Nilsson [7] and Palmer [4] reviewed the research in the field of NPs in detail, including SNPs as well. SNPs own many advantages over other types of NPs, such as good biocompatibility, no swelling in aqueous and organic solvents, and easy post-modifications with different functional groups, etc. [10]

In the past decade, functionalized SNPs have received considerable attention and had been successfully used as PSPs for the enhanced separation of organic acids and bases, drugs and proteins [11]. SNPs used in CEC, contain hydroxyl functional groups with different binding sites on the surface. In many cases, the SNPs have to be surface coated or are derived using specific functional groups to provide additional interaction sites [12]. Achieving controlled localization of two or more different molecular functionalities on the surface of NPs would offer several profound advantages. For example, Bachmann and Gottlicher covalently modified commercially available SNPs with a combination of reversed-phase groups and negatively charged groups [13]. Also, Neiman et al. prepared one neutrally charged and two positively charged modified silica solutions for the CEC separation of aromatic acids and their structural isomers [14]. Accordingly, the development of synthetically tailored SNPs is of great significance in separation science.

EOF is a very important factor in CEC separation because analytes move through the capillary by EOF drive, as well as self-electrophoretic mobility if they are charged [15]. Knowing the direction and magnitude of the EOF will be helpful to understand the separation behavior.

Since the structures of amino acids can be easily modified, amino acids and their derivatives would be candidates to act as precursors for modifying the surface of SNPs. Also, due to their weak UV absorption and low cost, it is meaningful to use native amino acids - functionalized SNPs as additives for enhanced electrophoretic separation of chiral and achiral drugs [16]. Therefore, the design and synthesis of amino acid-functionalized SNPs could prove useful for separation and determination of pharmaceutical compounds especially for enantiomeric drugs and metabolites either alone or in combination with other chiral selectors such as cyclodextrins, antibiotics or carbohydrates.

Synthesis of SNPs is usually carried out through two sol–gel methods: the Stöber method

[17] and the water in oil reverse microemulsion (WORM) method [18]. The particles prepared by Stöber methods usually are not uniform. To overcome these shortcomings, WORM method is preferred as it results in SNPs with better monodispersity. However, a high amount of surfactants is needed in the synthesis process which necessitates extensive subsequent cleaning steps [19]. This article provides a systematic comparison of five functionalized SNPs using the WORM method; Monoamine-modified SNPs (MA-SNPs), L-lysine-modified SNPs (L-SNPs), and linear poly L-lysine (LPL-SNPs) were prepared using the proper organosilane coupling agents to render a positive charge on the surface of the SNPs, whereas, cysteine-modified SNPs (CYS-SNPs) and Glutamic acid-modified SNPs (GLU-SNPs) were prepared using amino acids-based organosilane conjugate moieties to render a zwitterionic nature and a negative charge on the surface of the SNPs at the proper pH, respectively, Fig. 4.1.

The separation of acidic compounds in unmodified capillaries is often unsatisfactory and requires higher pH buffer solutions (~neutral or alkaline) in order to produce higher cathodic EOF to surpass the anodic electrophoretic mobility of analytes. The poor separation of the acidic analytes in bare capillary can be caused by the migration of the acidic compounds in reverse direction with the EOF. Hence, the five proposed modified SNPs were explored as background electrolyte additive to investigate their effect on the EOF, and hence on the separation of two separate mixtures of acidic and basic drugs. The mixture of acidic drugs consisted of ibuprofen (IBU), Ketoprofen (KET), and Valsartan (VAL) whereas the mixture of basic drugs consisted of propranolol (PRP) and atenolol (ATN), Fig. 4.2.

These amino acids or peptides-modified SNPs can significantly help in achieving fast and efficient separation of challenging mixtures of achiral and chiral compounds of different charges.

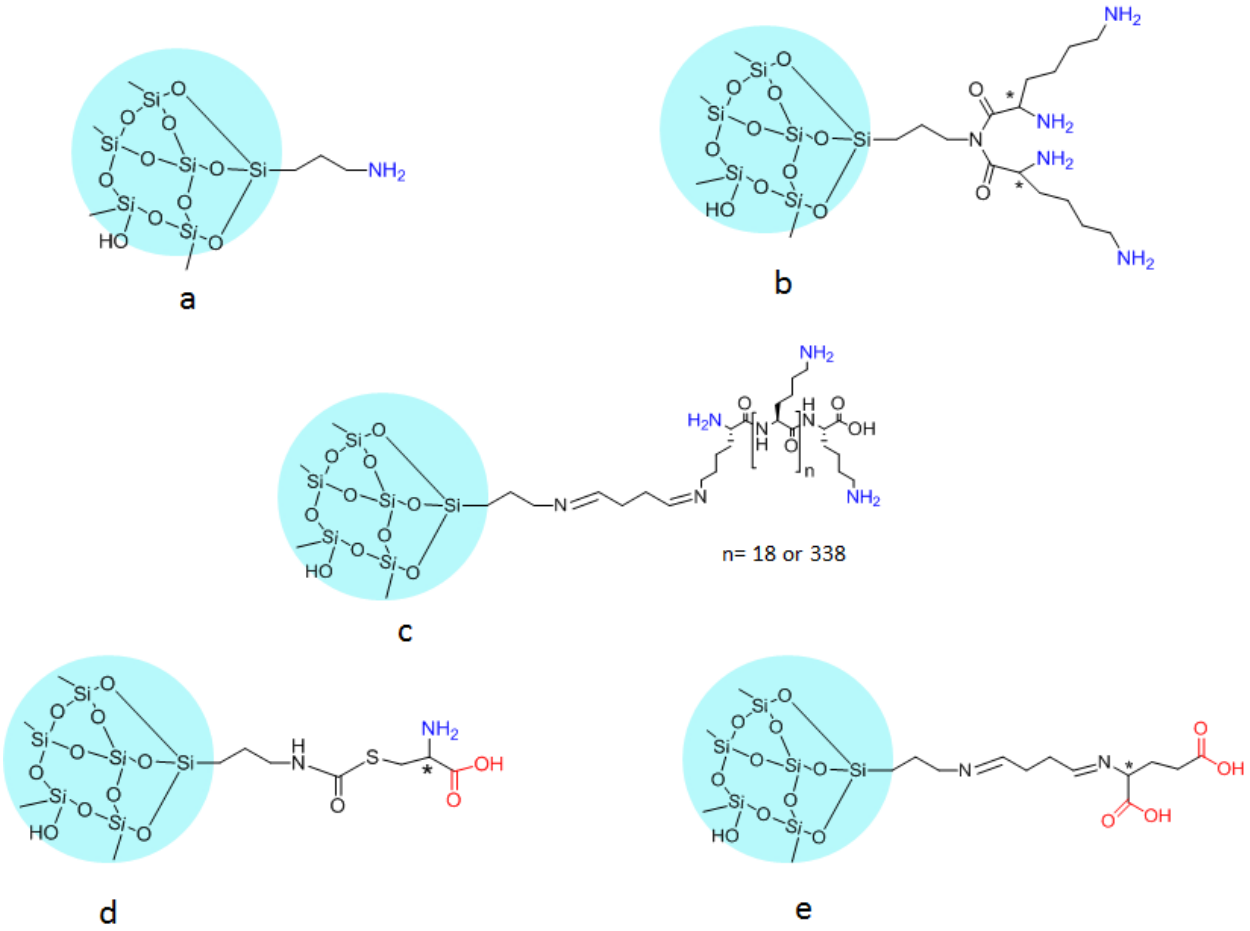

Figure 4.1 The structural formulae of the proposed amino acid-based functionalized SNPs; (a) MA-SNPs, (b) L-SNPs, (c) LPL-SNPs, (d) CYS-SNPs, and (c) GLU-SNPs

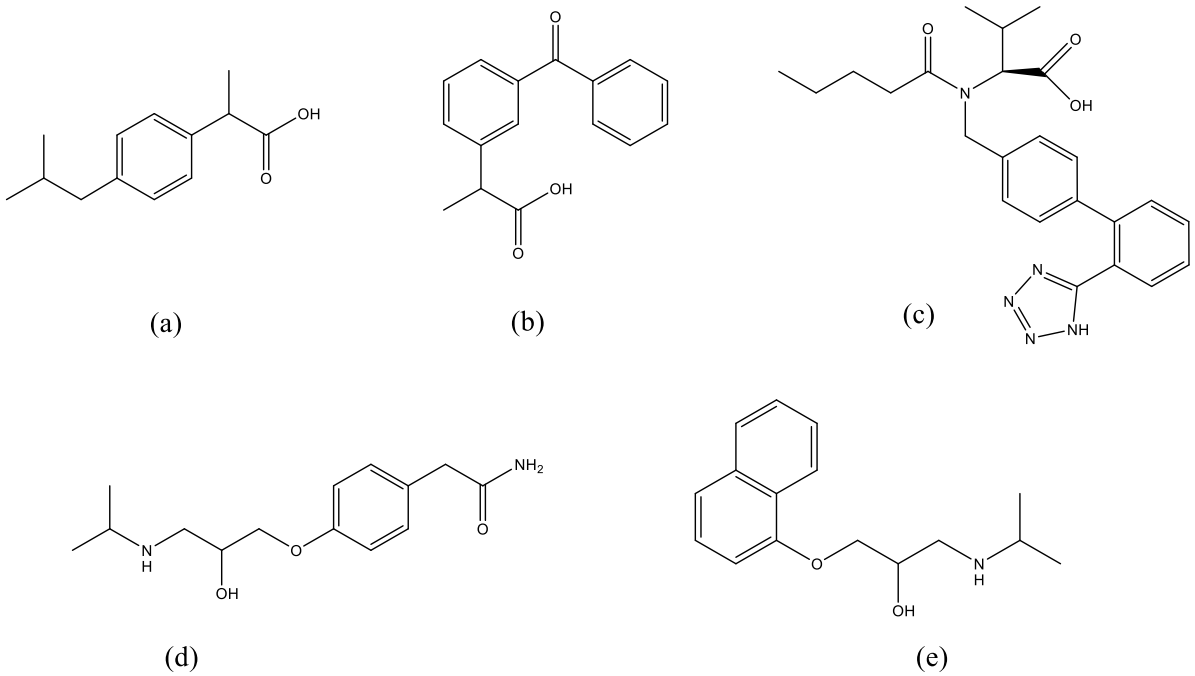

Figure 4.2 The structure formulae for (a) ibuprofen, (b) ketoprofen, (c) valsartan, (d) atenolol, and (e) propranolol

4.2 Experimental

4.2.1 Reagents and materials

All chemicals were analytical-grade unless noted otherwise. All the following chemicals were produced by Sigma-Aldrich, MO, USA: 1-heptanol (anhydrous, ≥99%), 3-aminopropyl triethoxysilane (APTES) (≥98%), tetraethyl orthosilicate (TEOS) (99.99% trace metal basis), 3-(Triethoxysilyl)propyl isocyanate (95%), Ethyl acetate, anhydrous (99.8%), tert-butyl alcohol (99.5%), (±)-propranolol hydrochloride (99%), (±)-atenolol (98%), (±)-ketoprofen (98%), sodium hydroxide (pellets, 97+%, A.C.S. reagent), cyclohexane (anhydrous, 99.5%), di-tert-butyl dicarbonate (98%), L-cysteine (97%), poly-L-lysine hydrobromide (P2636), ethanol (99.7%), dichloromethane, sodium phosphate, dibasic (98+%), potassium phosphate monobasic

(>95%), TRIS-HCl buffer, magnesium sulfate anhydrous (99.5%), potassium hydrogen sulfate (99%), sodium bicarbonate, trifluoroacetic acid (TFA), hydrochloric acid (37%), and Triton™ X-100 (laboratory grade). Fisher Scientific, Fair Lawn, NJ, produced ammonium hydroxide solution (28%). Alfa Aesar, Ward Hill, MA, produced L-glutamic acid, 99+%. Aldrich Pharmaceutical Company Inc., Milwaukee, WI, USA produced DMAP (4-Dimethylaminopyridine) (99%), 1,3-dicyclohexyl-carbodiimide (DCC) (99%), sodium hydrogen carbonate (99%), and glutaric dialdehyde (50 wt.%) solution in water. AK Scientific, Inc., Union City, CA, USA produced ±ibuprofen (98%), and L(+)-glutamic acid (99%). Pharmaceutical grade VAL USP was supplied by Zydus, batch No.: VSK1MK A02B (certified to contain 99.4%).

4.2.2 Instrumentation

Regarding instrumentation, separations were performed using a Beckman Coulter P/ACE MDQ (144001) Capillary Electrophoresis System (Fullerton, CA, USA) equipped with an autosampler and a UV detector for the CE technique. Beckman Coulter's 32 Karat™ Software 3.0 was used for the instrument control, data acquisition, and analysis. Electrophoretic analyses were performed in a fused silica capillary (Polymicro Technologies, Phoenix, AZ, USA) of 53.2 cm long (42.5 cm effective length) and 50 μm id. Prior to the first use, the capillary was successively rinsed with methanol, DI water, 1 M NaOH, DI water, 1 M NaOH, DI water, 0.1 M HCl, DI water, and 25 mM phosphate buffer (pH 5) for 20 min each. Afterwards, the capillaries were flushed with a 5 mg/mL SNPs suspension for 5 min and left to stand for 10 min, and this step was repeated three times. Nano pure water was prepared using a Barnstead NANO pure DIamond Analytical ultrapure water system (Fischer Scientific, NJ, USA). A SympHonly (SB20) pH-meter (Thermo Orion, MA, USA) was used for pH adjustment. Transmission

electron microscopy micrographs were conducted by the Zeiss LEO 912AB (Zeiss, Thornwood, NY). Scanning electron microscopy micrographs were conducted by the Tescan Vega3 LMU scanning electron microscope (TESCAN, Kohoutovice, Czech Republic) and Denton Desk II sputter coated with a gold target (Denton Vacuum, NJ, USA). 0.2 mg/mL SNPs suspensions dispersed in ethanol or water were subjected to particle size determination analysis using a Malvern Mastersizer (Malvern Instruments Ltd., Malvern, UK. The polydispersity index (PDI), and standard deviation were obtained from three independent measurements of the dispersions of SNPs. The zeta potential of particles dispersions in water was measured. NPs separation required an Allegra 64R Centrifuge (Beckman Coulter Inc., Brea, CA).

4.2.3 Synthesis of the amino acid-based conjugate moieties (ACM)

The reaction progress was monitored using silica gel 60 F254 thin layer chromatography plates (Merck EMD Millipore, Darmstadt, Germany). Open column chromatography was utilized for the purification of all final compounds using 60−200 μm, 60A classic column silica gel (Dynamic Adsorbents, Norcross, GA). The nuclear magnetic resonance spectra were obtained using high quality Kontes NMR tubes (Kimble Chase, Vineland, NJ) rated to 500 MHz and were recorded on a Bruker Avance 400 MHz spectrometer interfaced to a PC using Topspin 3.1. High-resolution accurate mass spectra were obtained at the Georgia State University Mass Spectrometry Facility using a Waters Q-TOF micro (ESI-Q-TOF) mass spectrometer.

4.2.3.1 Synthesis of L-ACM

The synthesis included three steps, (Scheme 4.1). In the first step, a 50 mL flask was charged with a solution of NaOH (0.454 g, 0.011 moles) in water (12.5 mL). Then, L-lysine (1.503 g, 0.010 moles) was added followed by tert-butyl alcohol (10 mL). The solution was cooled in an ice bath, and subsequently, di-tert-butyl dicarbonate (5.462 g, 0.025 moles) was

added in three portions over a one hour period. After the addition was completed, the reaction mixture was stirred for another hour. Then, the ice bath was removed and the reaction mixture was stirred overnight at room temperature. After that, the reaction mixture was diluted with an equal volume of ethyl acetate and acidified by the addition of a solution of $KHSO_4$ (2.3 g, 0.017 mole) in water (15 mL). The ethyl acetate layer was separated, and the aqueous phase was extracted once more with ethyl acetate. The combined ethyl acetate fractions were washed with water, separated, dried over MgSO4, filtered, and evaporated under reduced pressure. Upon drying under vacuum, the resulting yellow oil turned into yellowish white foam (di-BOC-lysine). Yield was 2.88 g (81%). In the second step, 4 0.533 g (488 μL, 1.54 mmoles) of di-BOC-lysine free acid, 167 μl (0.77 mmoles) of APTES, 36.6 mg (0.324 mmoles) of DMAP (4-Dimethylaminopyridine), and 0.32 g (1.53 mmoles) of DCC were dissolved in 15 mL of methylene chloride and stirred for 20 h at room temperature. The reaction mixture was filtered to remove N,N'-dicyclohexyl urea (DCU), washed four times with 15 mL 0.5 M sodium bicarbonate, 15 mL 0.2 N HCl, and 15 mL saturated NaCl solution, and dried over MgSO4. The solution was then concentrated under reduced pressure to obtain di-BOC-L-ACM. In the third step, the precipitate then obtained (0.5 g) was collected and was subjected for further reaction preceded by its deprotection with 1:1 trifluoroacetic acid (TFA): dichloromethane (DCM) (2 mL) and stirred for 8 hours at room temperature. The solution was then concentrated overnight under reduced pressure. Materials were recrystallized in a 3:1 acetone/methanol mixture and dried to obtain yellowish white crystals of L-ACM. Yield was 0.122 g (34% yield). MS (ESI): 478 (M+).

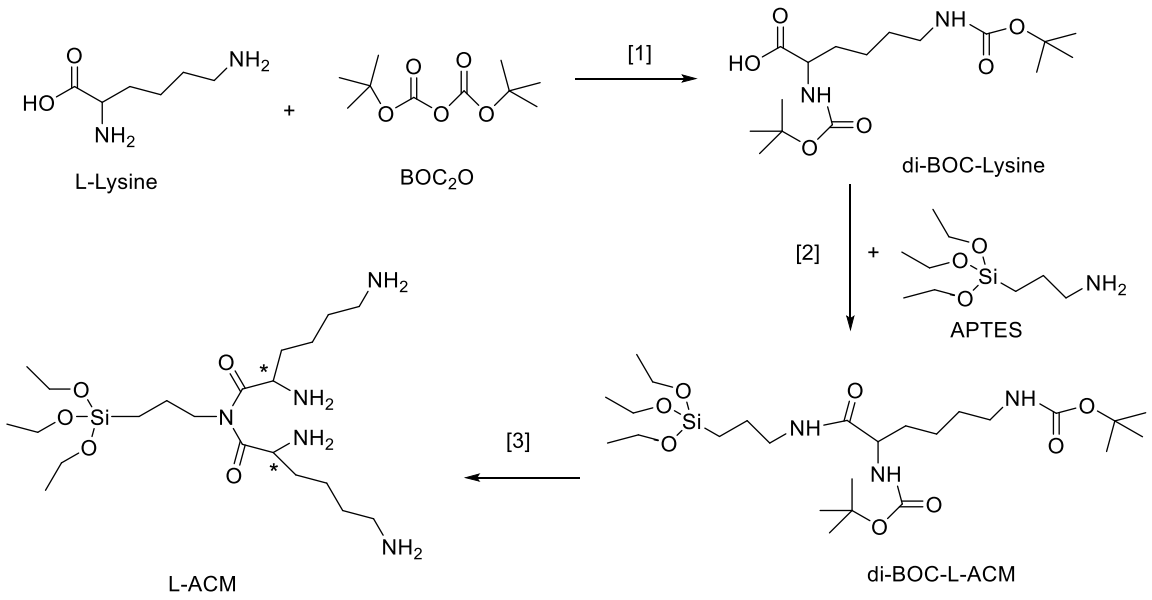

Scheme 4.1 Synthesis of L-ACM

4.2.3.2 Synthesis of the zwitter ionic L-cysteine-based conjugate moieties (CYS-ACM)

A 50-mL flask was charged with L-Cysteine (0.315 g, 2.0 mmole) in DMF (4.0 mL). Then, 3-(Triethoxysilyl)propyl isocyanate (0.519 mL, 2.10 mmole) was added. After the addition was completed, the reaction mixture was stirred for three days at room temperature. The product was filtered and washed several times with DMF. The solid was dried under reduced pressure to obtain CYS-ACM. Yield was 0.681 g (92% yield), Scheme 4.2.

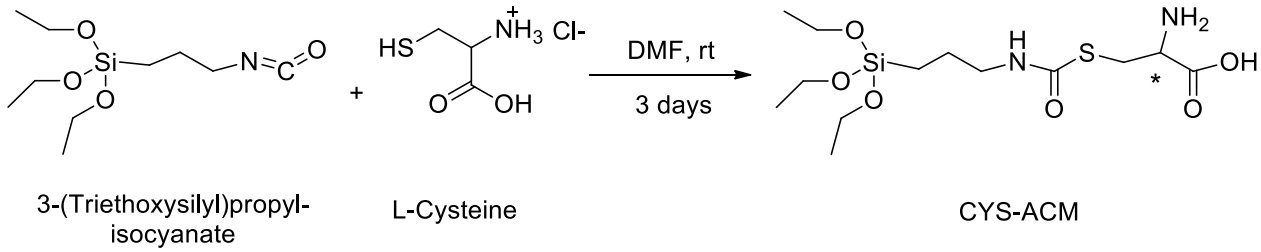

Scheme 4.2 Synthesis of CYS-ACM

4.2.4 Preparation of the functionalized SNPs

To obtain spherical SNPs with small size and narrow size distribution patterns, modified Stöber methods were used in the beginning for the synthesis of bare SNPs, MA-SNPs, L-SNPs, and CYS-SNPs then a WORM method was used for the preparation of bare SNPs, MA-SNPs, L-SNPs, LPL-SNPs, CYS-SNPs, and GLU-SNPs, (Fig. 4.3). The amounts of all reagents for each preparation method were adjusted carefully.

4.2.4.1 Preparation of bare SNPs and MA-SNPs by a modified Stöber method

MA-SNPs were prepared by modifying the Stöber method, Fig. 4.3. The first solution was a mixture of 0.930 mL TEOS and 7.50 mL ethanol, and the second solution was a mixture of 0.230 mL 28% (w/w) ammonia, 2.30 mL DI water, and 5.870 mL ethanol. With stirring, the first solution was added to the second solution. After reaction for 24 h at room temperature, APTES acting as surface functionality was added with TEOS, with the volume ratio of APTES to TEOS equals 1:1 for particle co-condensation. The total amount of functionalized trialkoxysilane reagents added corresponds to 5% of the initial amount of TEOS. The mixture was further reacted for 24 h, and the particles thus formed were centrifuged and washed with ethanol and DI water for several times, then vacuum-dried at 80 °C for 6 h. If no functionalization was intended, the reaction mixture of TEOS, ethanol, and ammonia was stirred overnight at room temperature in a similar way, and the bare SNPs thus formed were centrifuged and washed with ethanol and DI water for several times and then vacuum-dried at 80 °C for 6 h.

4.2.4.2 Synthesis of L-SNPs by a modified Stöber method

L-SNPs were prepared by modifying the Stöber method [20], Fig. 4.3. A total amount of 1 mL of TEOS (~4.5 mmol) was added to a conical flask in the presence of 12.5 mL of ethanol and 1 mL DI water. The solution was sonicated for 10 minutes, and then 0.4 mL of ammonia was

added gradually. After 24 h of reaction under stirring at room temperature (200 rpm), 0.23 mmoles (107 mg) of L-ACM was dissolved in 0.5 mL ethanol and added with extra TEOS (0.23 mmoles, 50 μL) gradually. The reaction of the obtained mixture continued for another 24 h (120 rpm), and the particles thus formed were centrifuged and washed with ethanol and DI water repeatedly, then the residue was left to dry completely at 80 °C.

4.2.4.3 Synthesis of CYS-SNPs by a modified Stöber method

CYS-SNPs were prepared by modifying the Stöber method [20], Fig. 4.3. A total amount of 0.625 mL of TEOS (~2.8 mmol) was added to a conical flask in the presence of 1 mL of methanol, 0.36 mL DI water, and 0.08 mL NH_4OH. The solution was stirred at room temperature for 24 h, and then 0.09 mmol CYS-ACM were added, and stirred for another 24 h at room temperature, and the particles thus formed were centrifuged and washed with methanol and DI water repeatedly, then the residue was left to dry completely at 80 °C.

4.2.4.4 Synthesis of bare SNPs and MA-SNPs by WORM method

Bare SNPs were prepared by modifying the WORM method. The micelles were prepared using 15.0 mL cyclohexane, 2.60 mL 1-heptanol, 3.55 mL Triton™ X-100, and 1.13 mL DI H_2O which were stirred for 10 min to generate the microemulsion. After time elapsed, 3.0 mL TEOS, and 0.12 mL ammonium hydroxide were added and the solution was stirred at low speed for 24 h. In order to modify the surface of the SNPs to prepare MA-SNPs, 0.075 mL from each of TEOS and APTES were added gradually to the reaction mixture and stirred at low speed for another 24 h at room temperature. Afterward, 5.0 mL acetone were added, and the NPs were collected by centrifugation and washed 5 times with absolute ethanol and two times with water to remove any unreacted chemicals, Fig. 4.3, then the residue was left to dry completely at 80 °C.

4.2.4.5 Synthesis of L-SNPs, and CYS-SNPs by WORM method

75.0 mg bare SNPs prepared as described in the previous section were added to a conical flask, and suspended in 7.5 mL 50 mM TRIS-HCl buffer (pH 8.0) with stirring at low speed. Afterwards, 7.5 mg L-ACM in the case of L-SNPs or 7.5 mg CYS-ACM in the case of CYS-SNPs were dissolved in 2.0 mL 90% ethanol, and added dropwise to the reaction mixture. Then, 15.0 µL TEOS and 40.0 µL ammonium hydroxide were added, and the reaction mixture was stirred for 18 h at room temperature. The NPs were collected by centrifugation and washed 3 times with each of 50 mM TRIS-HCl buffer (pH 8.0), ethanol and water to remove any unreacted chemicals, Fig. 4.3, then the residue was left to dry completely at 80 °C.

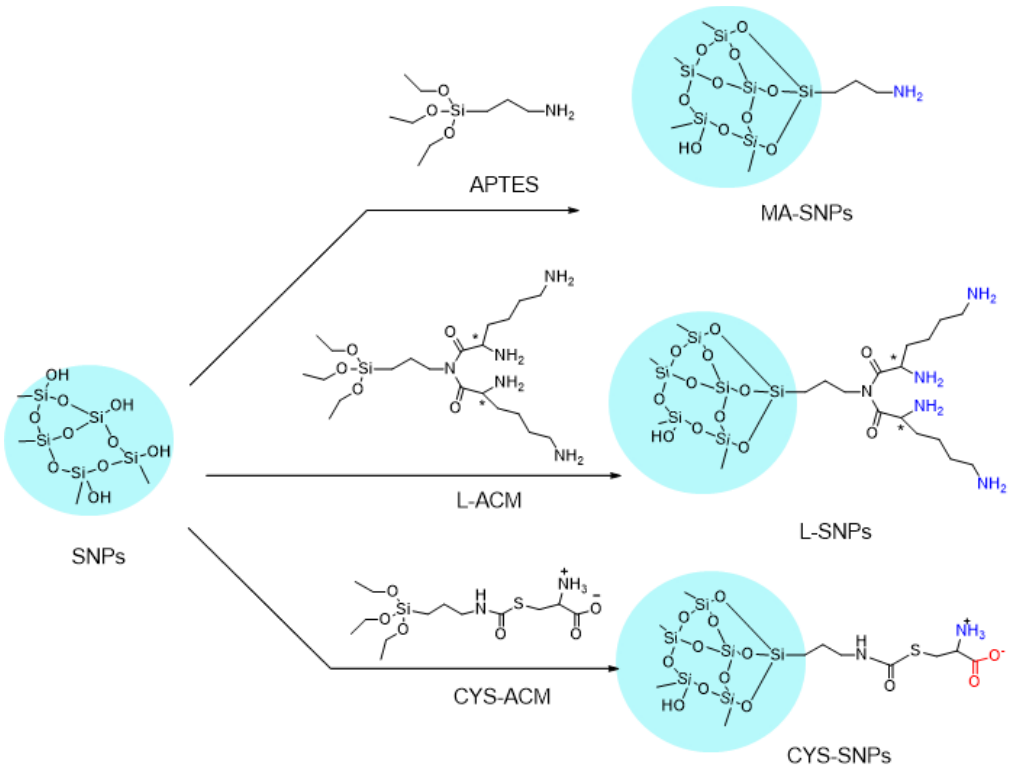

Figure 4.3 Modifying the surface of bare SNPs to prepare MA-SNPs, L-SNPs, and CYS-SNPs

4.2.4.6 Immobilization of linear poly-L-lysine or glutamic acid on the surface of MA-SNPs

The primary amino groups on the MA-SNPs carrier were modified with glutaric acid dialdehyde molecules to effectively combine with the linear poly-L-lysine (LPL) or L-glutamic acid (GLU), Fig. 4.4. In detail, 60 mg of MA-SNPs prepared by WORM method were dispersed in 5.0 mL 50 mM ammonium acetate buffer solution of pH 7.0, and then 1 mL of 50 (Wt.%) glutaric acid dialdehyde solution in water was then added to the dispersion solution, which was stirred overnight at room temperature. Samples were then centrifuged and washed with DI water four times to remove the excess reagent. Finally, the solid was dried at 60 °C in a vacuum drying oven. For the immobilizing procedure, 50 mg of carrier (Glut-MA-SNPs) were added into 2 mL of 10.0 mg/mL LPL or 7.5 mg/mL L-glutamic acid solutions prepared in 50 mM ammonium acetate buffer, pH 5. Afterwards, the mixtures were stirred gently for 12 h in an ice bath, followed by centrifugation. The collected NPs were rinsed alternately three times with the same buffer and DI water, then the residue was left to dry completely at 60 °C.

4.2.5 Characterization of the functionalized SNPs

The developed functionalized SNPs were characterized in detail by one or more of the following techniques: TEM, SEM, dynamic light scattering (DLS), zeta potential measurements, and FT-IR.

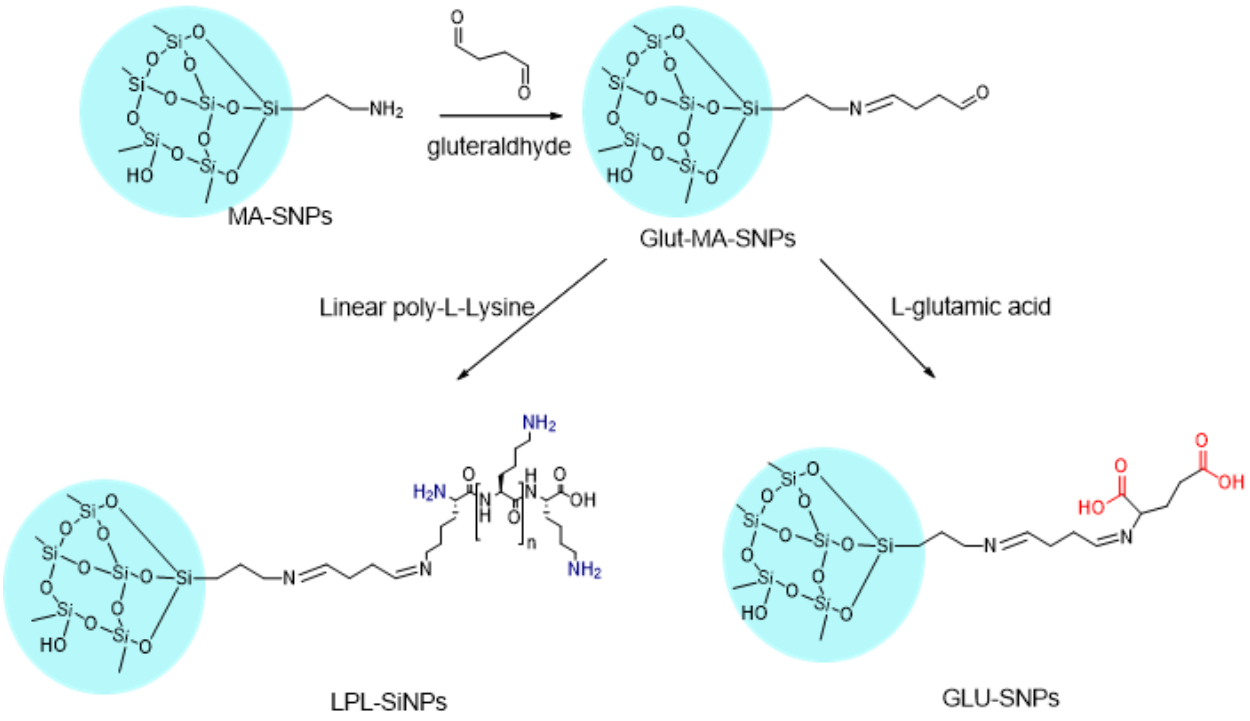

Figure 4.4 Immobilization of linear poly-L-lysine or L-glutamic acid on the surface of MA-SNPs

4.2.6 Standard and working solutions

72 mM of IBU, KET, 48 mM of ATN, PRP and 24 mM of VAL stock solutions were prepared separately in methanol. The mixture of the acidic drugs consisted of 3.6 mM IBU, 3.6 mM KET, and 1.2 mM VAL whereas the mixture of the basic drugs consisted of 2.4 mM PRP and 3.6 mM ATN which were prepared by transferring the proper aliquots from the corresponding stock solutions, and completing the volume with methanol and water to reach a final ratio of 25% methanol in DI water. The solutions were stable for one month when kept in the refrigerator at 2 oC.

4.3 Results and discussion

4.3.1 Characterization of the functionalized SNPs

The physical nature and dimensions of the particles were derived from the SEM, TEM, and DLS scans. Two sol-gel methods were used in preparing the functionalized SNPs. The NP diameter obtained from TEM images, the mean hydrodynamic particle sizes by DLS, PDI, and zeta potential values are summarized in Table 4.1 and 4.2. The NPs prepared by Stöber method had relatively larger diameters with a poor control on the monodispersity of the size and shape as shown in Fig. 4.5 and Table 4.1. SEM and TEM micrographs showed that the SNPs prepared by WORM method had a spherical shape and a narrow size distribution as can be seen in Fig.4.6 and Table 4.2. Although having different surface functional groups, the five functionalized SNPs had nearly the same shape and size morphology. The five materials were sphere-like and uniform in shape, with an average size of approximately 79 nm.

As shown in Table 4.2, the zeta potential of both the bare SNPs [21] and GLU-SNPs colloidal SNPs showed a highly negative charge of about -44 mV whereas CYS-SNPs and L-SNPs showed a relatively lower negative charge of about -37 and -35 mM, respectively. MA-SNPs showed a positive charge of +14.7 ± 4.37 mV while LPL-SNPs showed a wide range of charge deviation between -48.0 to + 60.0 mV which can be attributed to the ionization nature of the poly L-lysine protein at the neutral pH of the used dispersant.

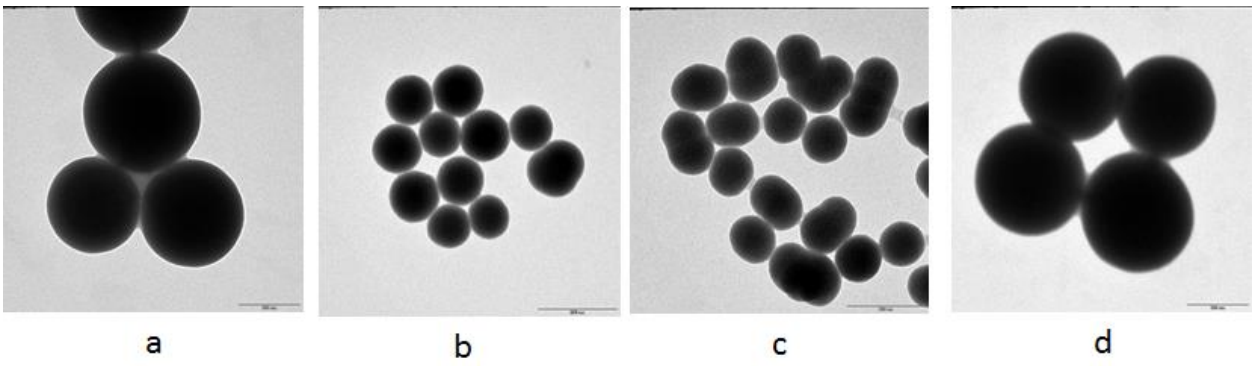

Figure 4.5 TEM photographs for SNPs prepared by Stöber method for (a) bare SNPs, (b) MA-SNPs, (c) L-SNPs, and (d) CYS-SNPs

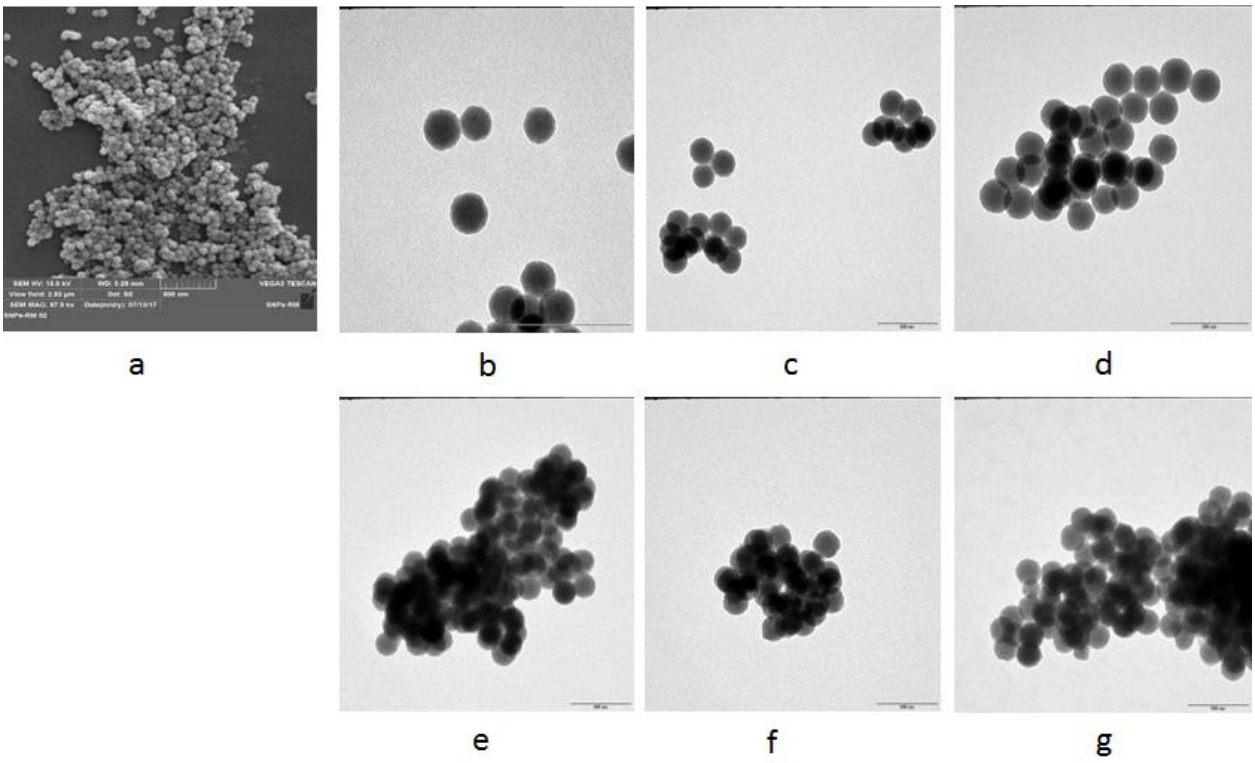

Figure 4.6 SEM and TEM photographs for SNPs prepared by WORM method. (a) SEM photographs of bare SNPs, TEM photographs for: (b) bare SNPs, (c) LPL-SNPs, (d) MA-SNPs, (e) L-SNPs, (f) CYS-SNPs, and (g) GLU-SNPs

Table 4.1 Diameter determined by TEM and DLS, polydispersity index (PDI), zeta potential of 0.1 mg/ml SNPs in ethanol (prepared by Stöber method)

SNPs	Diameter (TEM) (nm)	Diameter (DLS) (nm)	PDI	Zeta potential (mV)
Bare SNPs	343.2 ± 40.4	145.3 ± 36.45	0.402	-25.0 ± 14.9
MA-SNPs	119.8 ± 9.9	299.6 ± 119.3	0.217	+6.7 ± 5.2
L-SNPs	123.3 ± 6.3	275.4 ± 105.8	0.190	-12.3 ± 9.1
CYS-SNPs	347.7 ± 38.3	387.5 ± 41.2	0.285	-32.0 ± 5.6

Table 4.2 Diameter determined by TEM and DLS, polydispersity index (PDI), zeta potential of 0.1 mg/ml SNPs in DI water (prepared by WORM method).

SNPs	Diameter (TEM) (nm)	Diameter (DLS) (nm)	PDI	Zeta potential (mV)
Bare SNPs	58.8 ± 6.6	189.8 ± 81.7	0.242	-44.1.0 ± 11.3
MA-SNPs	77.1 ± 4.6	384.2 ± 126.6	0.254	+14.7 ± 4.37
LPL-SNPs	79.9 ± 6.3	164.2 ± 0.01	0.974	-0.36 ± 31.5
L-SNPs	77.9 ± 4.9	342.4 ± 78.1	0.656	-35.7 ± 6.31
CYS-SNPs	82.7 ± 4.7	328.3 ± 180.8	0.531	-37.2 ± 3.78
GLU-SNPs	78.1 ± 5.0	439.3 ± 51.9	0.542	-44.3 ± 3.46

FT-IR spectra of bare SNPs and amine-modified SNPs (Fig. 4.7) showed the presence of organic groups. In comparison with pure SNPs, several new absorption bands appeared in the spectrum of MA-SNPs. The peak between 3,300 and 3,500 cm^{-1} are assigned to the stretching vibration of the amino group (m-NH2), and the peaks at 1,650 and 624 cm^{-1} are the bending vibrations of the amino group (d-NH2 and s-NH2). These results confirmed the presence of functional groups on the surface of SNPs.

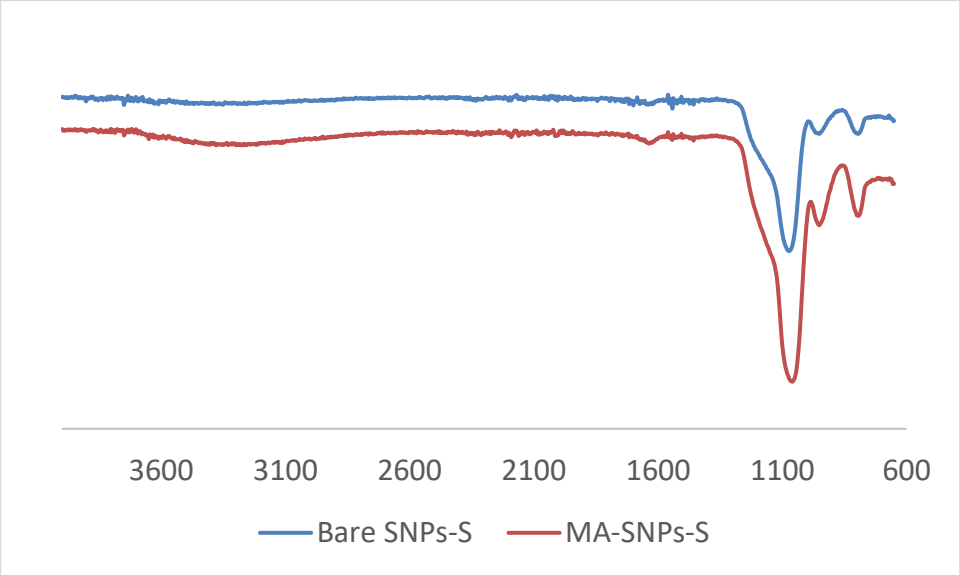

Figure 4.7 The IR spectra of bare SNPs (a), and MA-SNPs (b)

4.3.2 EOF Characteristics

EOF is a very important factor in CE separation because analytes are driven through the capillary both by the EOF and as a result of self-electrophoretic mobility if they are charged. When the amine-functionalized NPs such as MA-SNPs, L-SNPs, and LPL-SNPs are suspended in the acidic background electrolyte, they are positively charged, because of the amino groups on their surface. Thus they were adsorbed on the inner wall of the negatively charged capillary to

form a dynamic coating under acidic buffer solutions. As a result, reversed anodic EOF was obtained. Fig. 4.8 depicts the dependence of the EOF mobility of the used SNPs-based PSPs on buffer solution pH. Considering that the silica-based materials tend to dissolve in strongly alkaline solutions, the pH range of 3–8 was selected for this investigation.

From Fig. 4.8 it can be observed that only cathodic EOF can be detected by varying the pH of the running electrolyte because no suitable functional groups exist on the surface of the bare SNPs and GLU-SNPs to reverse the EOF. Moreover, bare SNPs, CYS-SNPs, L-SNPs, and GLU-SNPs did not show in significant difference in EOF from the unmodified capillary columns. With MA-SNPs and LPL-SNPs the anodic EOF velocity decreased when the buffer pH increased from 3 to 5 whereas the cathodic EOF velocity increased when the buffer pH increased from 6.5 to 8. At pH 3, the amine groups of the functionalized SNPs were protonated strongly and residual silanol groups on the capillary were partly suppressed. With increasing pH, the anodic EOF velocity decreased as the ionization of the amine groups became weaker. At pH 6.0, no EOF was observed because the net charge between the positively charged functionalized SNPs and the negatively charged capillary wall was nearly zero. Moreover, from this plot, it can be observed that an increased reversed anodic EOF can be obtained from LPL-SNPs compared with MA-SNPs at very low pH values. The amine-modified SNPs that can generate a reversed EOF should have a positive effect on the separation of charged analytes especially the acidic compounds.

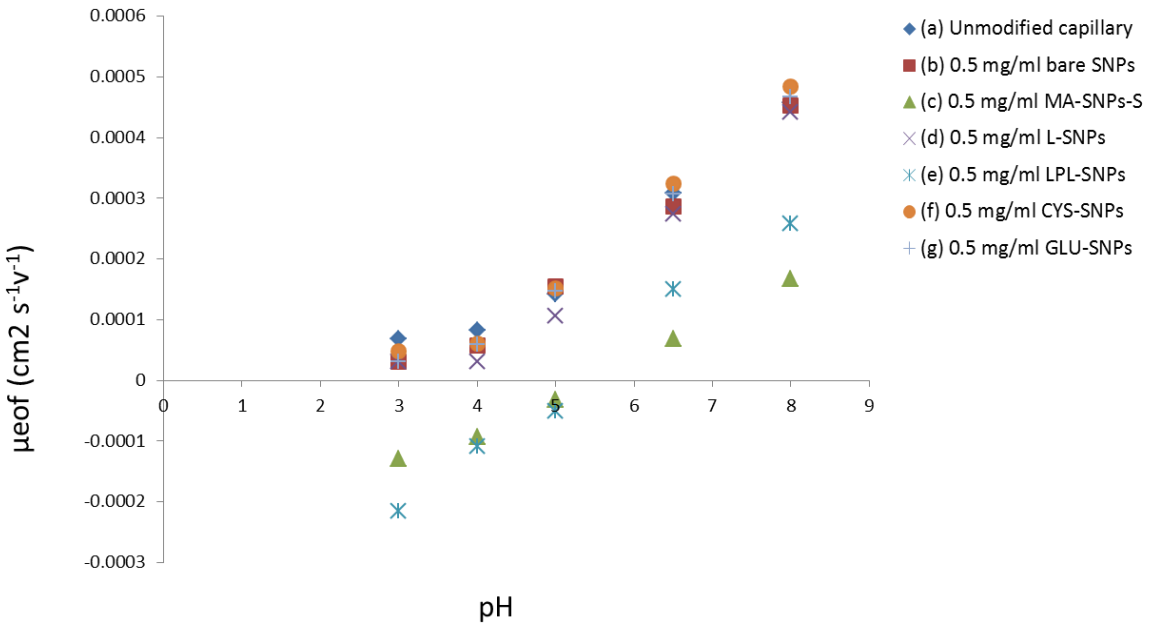

Figure 4.8 Effect of buffer pH on EOF. Experimental conditions: capillary, total length 53.2 cm, effective length 42.5 cm; buffer, 25 mmol/L KH2PO4 buffer without additives (a), with 0.5 mg/mL bare SNPs (b), with 0.5 mg/mL functionalized SNPs (c-g); detection wavelength, 214 nm; separation voltage, 20 kV or – 20 kV; hydrodynamic injection for 6 s

4.3.3 Electrophoretic Separation

4.3.3.1 Effect of modified SNPs

The separation of acidic compounds in unmodified capillary columns is often unsatisfactory because acidic compounds migrate in the reverse direction to the EOF, resulting in longer separation time [22]. For fast and efficient separation of acidic compounds, it is preferred that the analytes migrate in the same direction as the EOF (co-EOF). Because the direction of the EOF is from cathode to anode under low pH conditions in the case of MA-SNPs and LPL-SNPs (Fig. 4.8), it is expected that fast separation can be obtained for acidic compounds. Taking into

account all those aspects, three acidic drugs IBU, KET, and VAL and two basic drugs PRP and ATN were chosen as target analytes to evaluate the performance of five functionalized SNPs as buffer additives in CE. First, no NPs were added to the running buffer. However, it was difficult to observe resolved peaks of the three acidic drugs or the two basic drugs using normal polarity mode over the pH range 3.0 to 8.0 as can be seen in Fig. 4.9 and 4.10, respectively. Hence, the organically functionalized SNPs were evaluated as buffer additives to improve the separation where five different functionalized SNPs were separately added to the running buffer as PSP in the concentration of 0.5 mg/mL. A background electrolyte of pH 4 and negative polarity were used in the case of analyzing the acidic drugs, Fig. 4.11, whereas pH 3 and positive polarity were used in the case of analyzing the basic drugs, Fig. 4.12. As it can be observed in Fig. 4.11 and Table 4.3, only MA-SNPs and LPL- SNPs additives were able to resolve the three acidic analytes in less than 15 min with acceptable peak shapes. Also, only LPL-SNPs were able to resolve the two analyzed basic drugs but with a prolonged run time and poor peak shapes, Fig. 4.12, Table 4.3.

The fast and successful separation of the acidic analytes is based on the fact that the direction of EOF is from cathode to anode under lower pH conditions in the tested separation system, that is, to say that the analytes migrate in the same direction with the EOF (co-EOF).

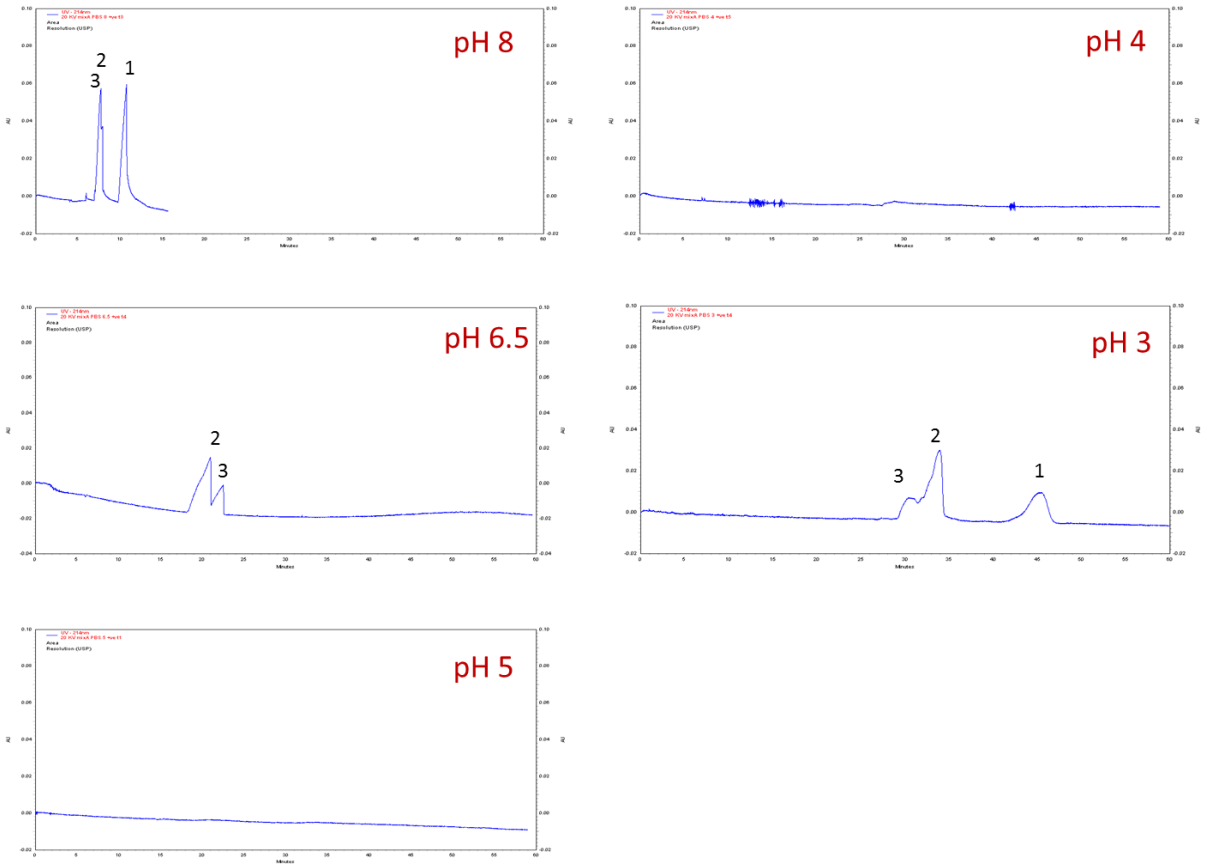

Figure 4.9 The effect of pH on the separation of the three acidic drugs without SNPs. Experimental conditions: Applied voltage 20 kV at pH 3, 4, 5, 6.5 or 8. The other conditions are the same as given in Fig. 4.8. Peak identities: 1 VAL; 2 KET; 3 IBU.

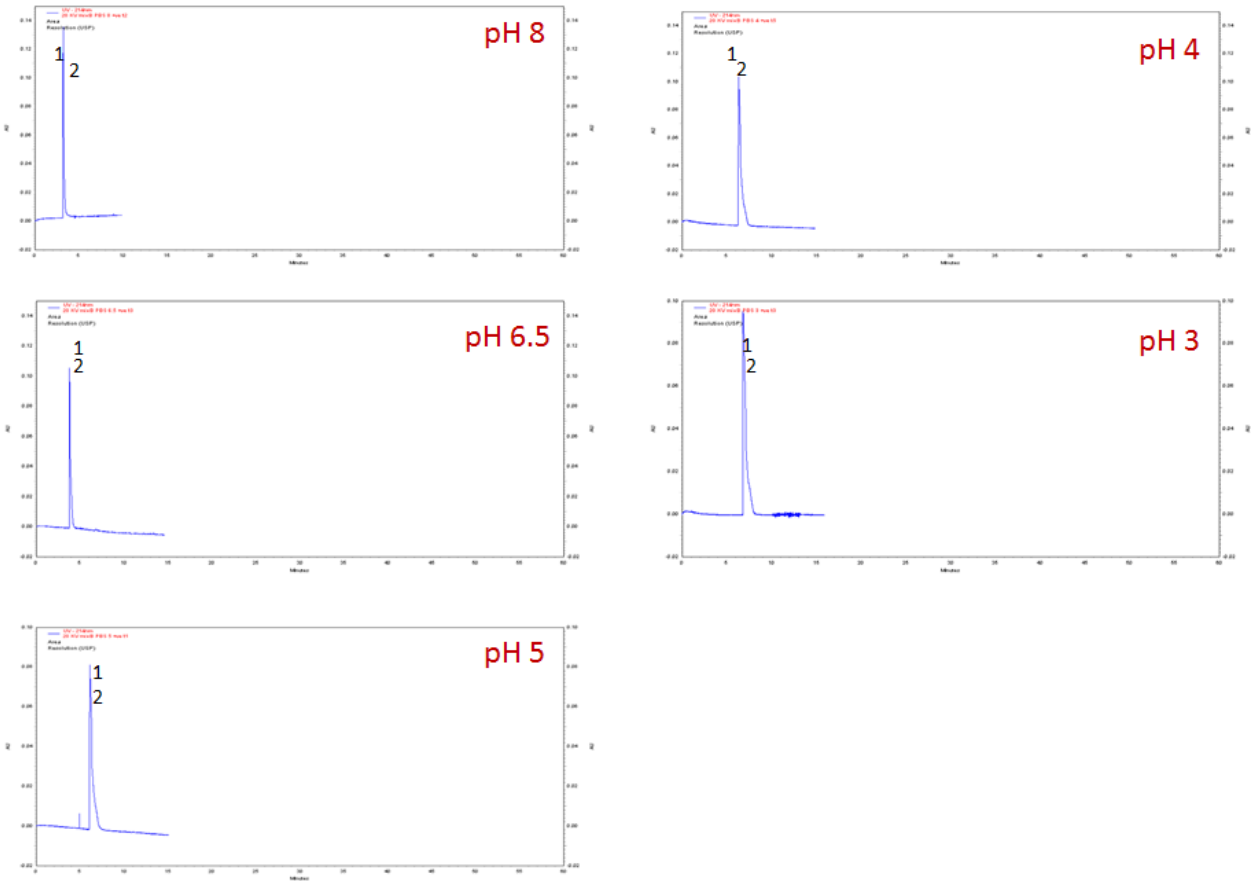

Figure 4.10 The effect of pH on the separation of the two basic drugs without SNPs. Experimental conditions: Applied voltage 20 kV at pH 3, 4, 5, 6.5 or 8. The other conditions are the same as given in Fig. 4.8. Peak identities: 1 PRP; 2 ATN

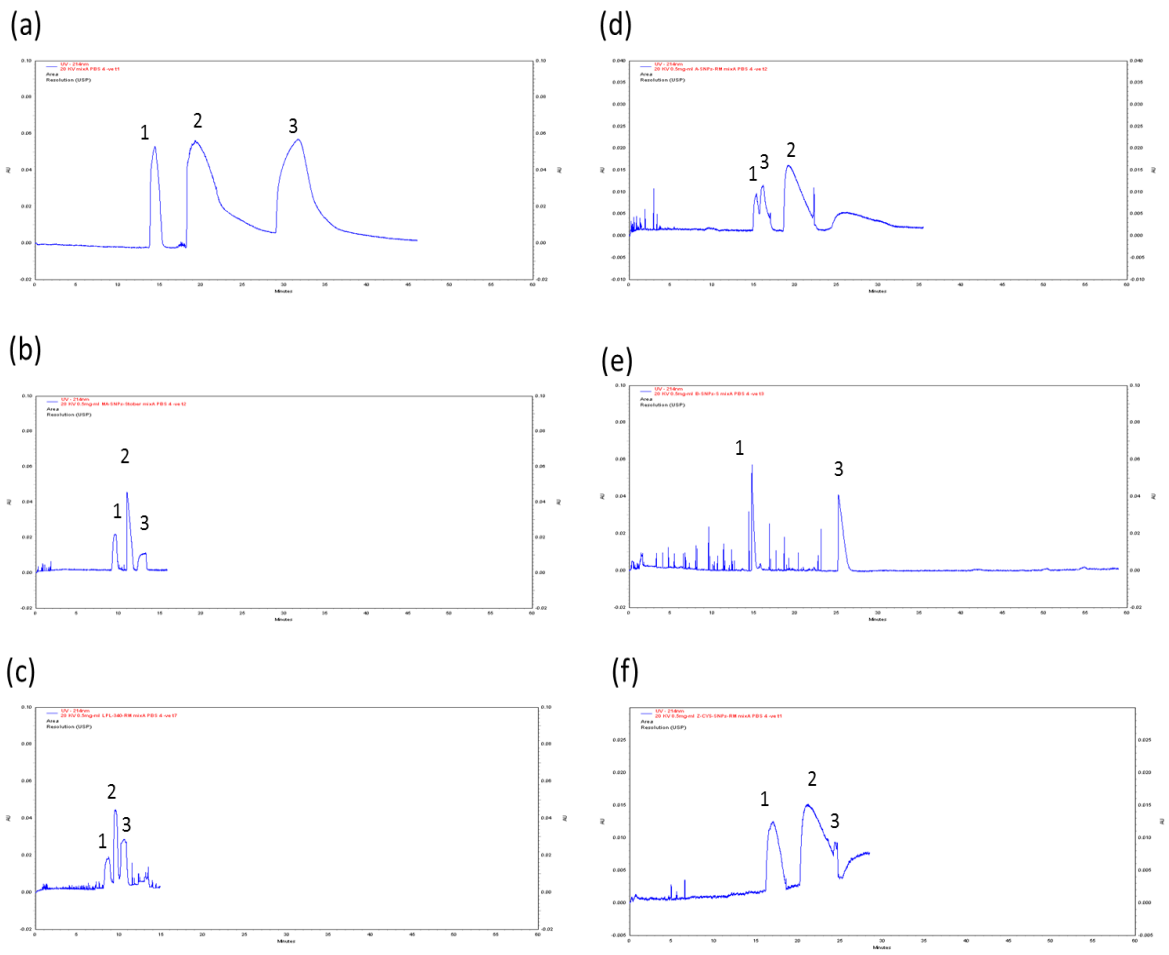

Figure 4.11 Electropherograms obtained from the three acidic drugs in the absence of SNPs (a), in the presence of MA-SNPs (b), LPL-SNPs (c), L-SNPs (d), GLU-SNPs (e), and CYS-SNPs (f). Experimental conditions: buffer, 25 mM phosphate buffer (pH 4) with (or without) 0.5 mg/mL SNPs added; applied voltage -20 kV; injection, 1psi for 6 s. The other conditions are the same as for Fig. 4.8.

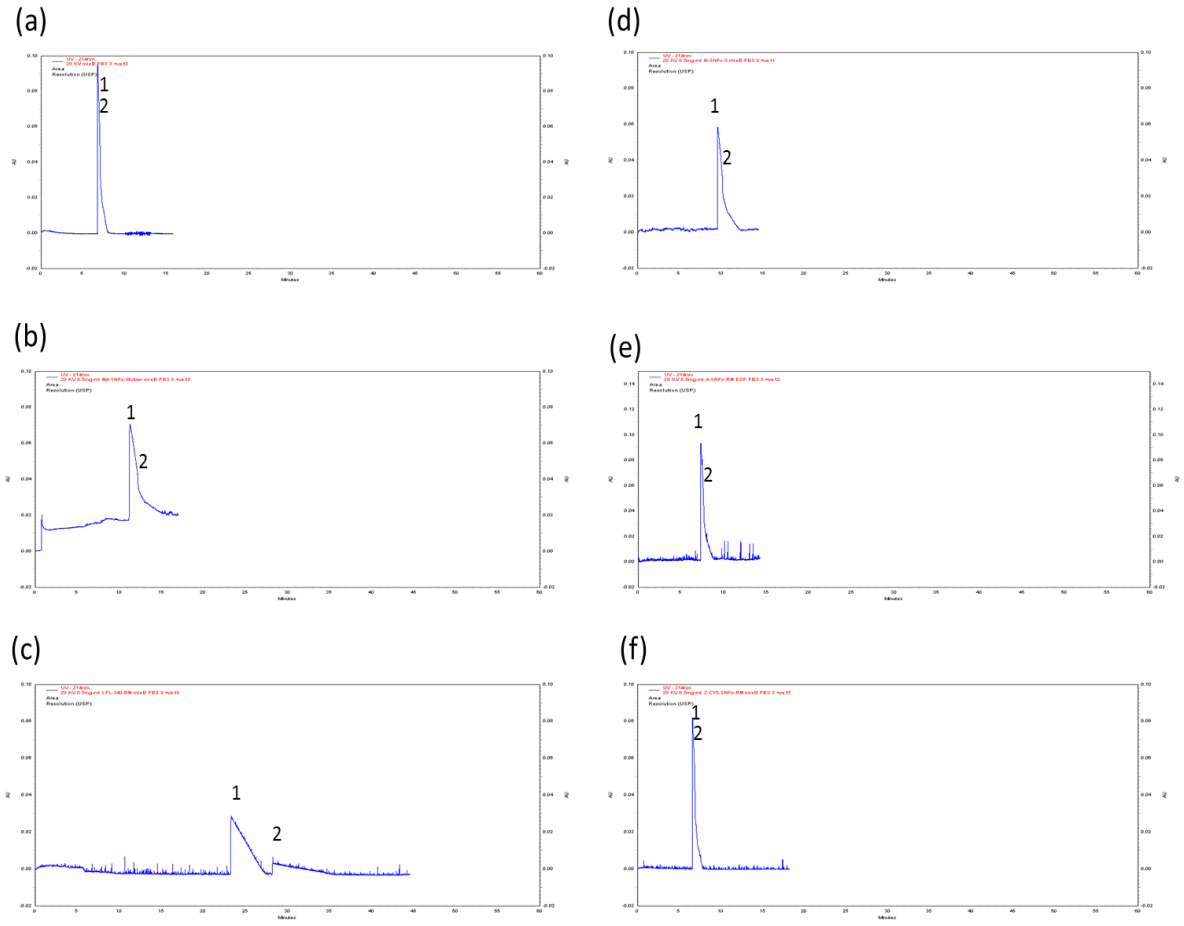

Figure 4.12 Electropherograms obtained from the three acidic drugs in the absence of SNPs (a), in the presence of MA-SNPs (b), LPL-SNPs (c), L-SNPs (d), GLU-SNPs (e), and CYS-SNPs (f). Experimental conditions: buffer, 25 mM phosphate buffer (pH 3) with (or without) 0.5 mg/mL SNPs added; applied voltage 20 kV; injection, 1psi for 6 s. The other conditions are the same as for Fig. 4.8.

Table 4.3 Comparison of migration times and resolution using the proposed modified SNPs as PSPs

		VAL	KET	IBU	ATN	PRP
Unmodified capillary	Migration time (min)	14.4	19.5	32.6	7.2	7.6
	Resolution	1.07		1.68	----	
MA-SNPs	Migration time (min)	9.5	11.2	13.0	11.4	13.1
	Resolution	1.43		1.18	-----	
LPL-SNPs	Migration time (min)	8.5	9.5	10.6	23.5	29.1
	Resolution	0.91		1.0	1.55	
L-SNPs	Migration time (min)	14.6	------	25.7	9.6	11.1
	Resolution	10.9			-----	
GLU-SNPs	Migration time (min)	15.1	19.2	15.9	7.4	8.2
	Resolution	-----		0.97	-----	
CYS-SNPs	Migration time (min)	16.8	21.3	24.2	6.7	7.3
	Resolution	0.95		0.78	-----	

4.3.3.2 Effect of pH

Running buffer pH is often important in achieving separations with high resolution in CE [26]. In this investigation, MA-SNPs and LPL-SNPs were used as PSPs and added to the running buffer using a pH ranging from 3 to 8 to evaluate any enhancement in the separation of the selected mixtures of the acidic and basic drugs. It is clear that separation efficiency can be readily tuned by adjusting the running buffer pH. For MA-SNPs (Fig. 4.13) and LPL-SNPs (Fig. 4.14), it was observed that at pH 3 the three acidic analytes were not resolved and at pH 8 only VAL appeared. The pH range of 4 to 6.5 was suitable for the separation of the three acidic analytes within a reasonable time where pH 4 showed the best separation efficiency for the three analytes using both amine-based PSPs as presented in Table 4.3. Regarding the separation of the two basic analytes, MA-SNPs did not show any obvious resolution of the two peaks over the tested pH range (Fig. 4.15) whereas LPL-SNPs at pH 3 showed separation of the two peaks but with poor peak shapes and prolonged migration times, (Fig. 4.16).

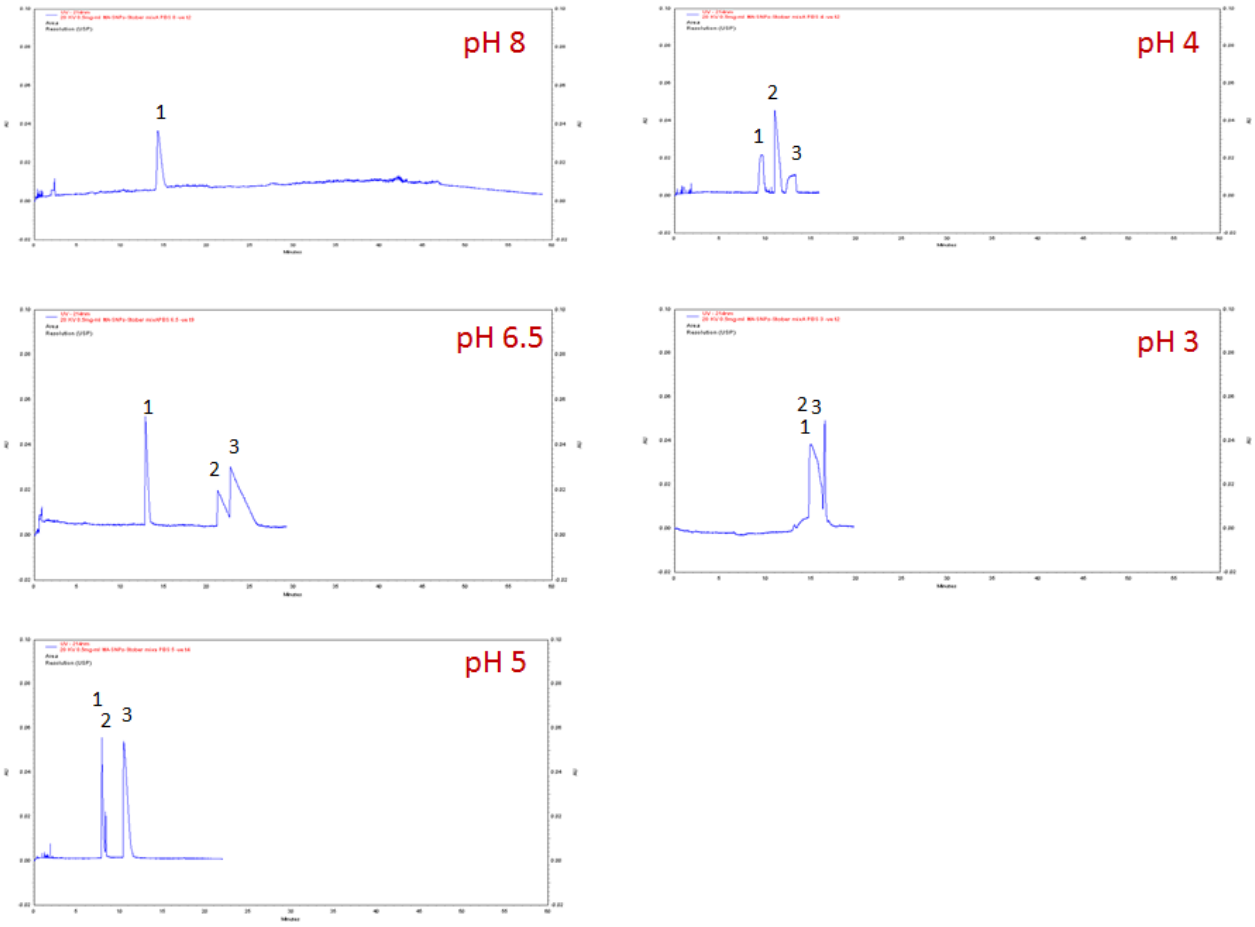

Figure 4.13 The effect of pH on the separation of the three acidic drugs using 0.5 mg/mL MA-SNPs. Experimental conditions: 25 mM phosphate buffer at pH 3, 4, 5, 6.5 or 8. The other conditions are the same as given in Fig. 4.11.

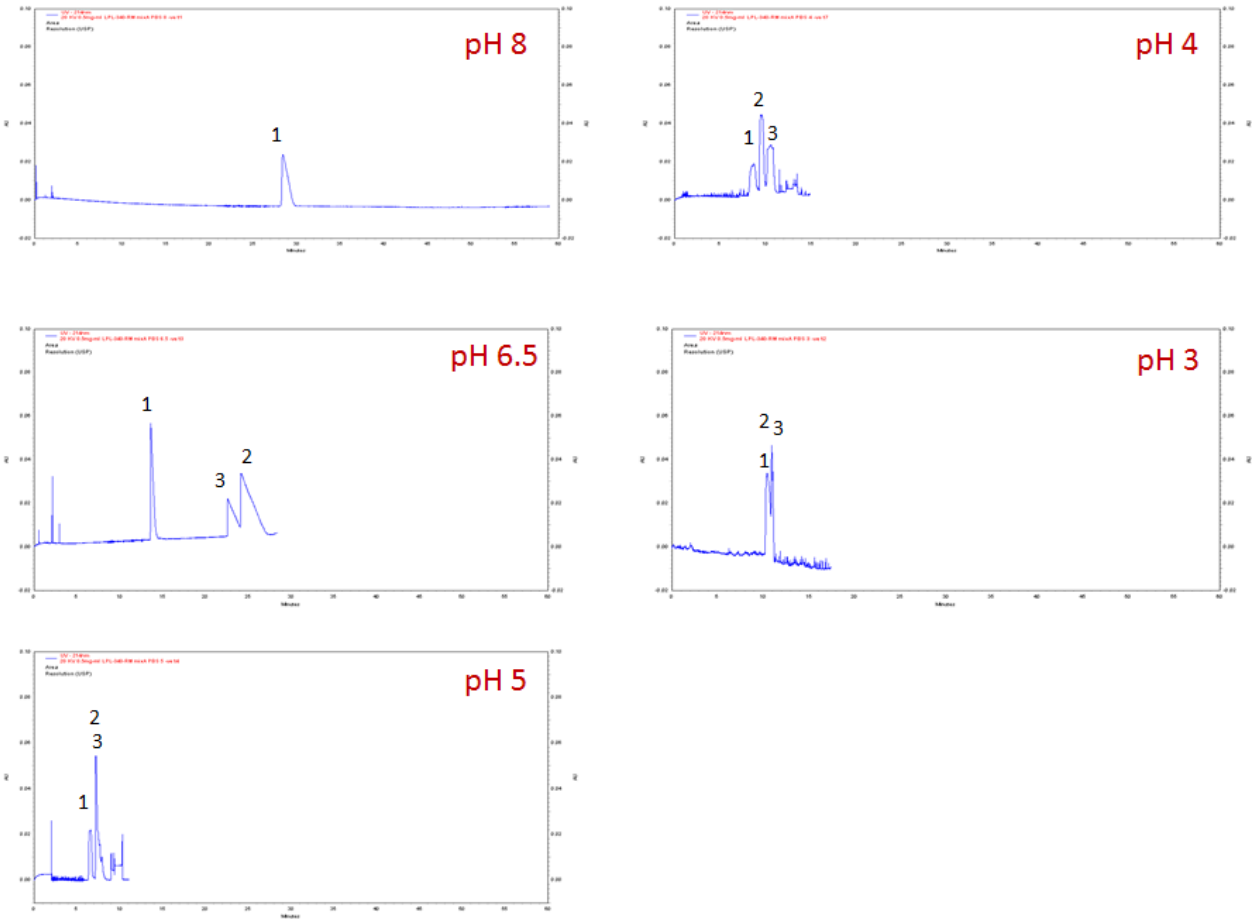

Figure 4.14 The effect of pH on the separation of the three acidic drugs using 0.5 mg/mL LPL-SNPs. Experimental conditions: 25 mM phosphate buffer at pH 3, 4, 5, 6.5 or 8. The other conditions are the same as given in Fig. 4.11.

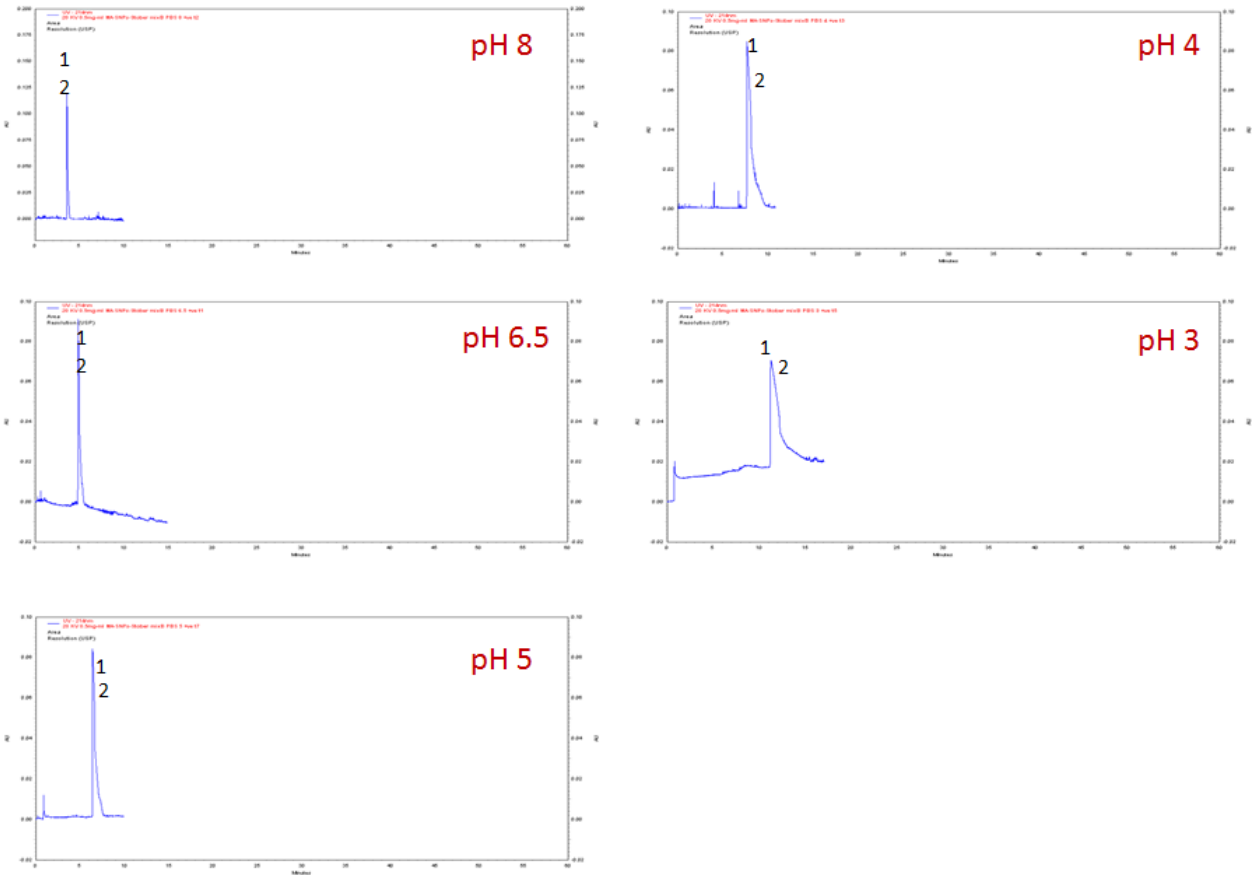

Figure 4.15 The effect of pH on the separation of the two basic drugs using 0.5 mg/mL MA-SNPs. Experimental conditions: 25 mM phosphate buffer at pH 3, 4, 5, 6.5 or 8. The other conditions are the same as given in Fig. 4.12.

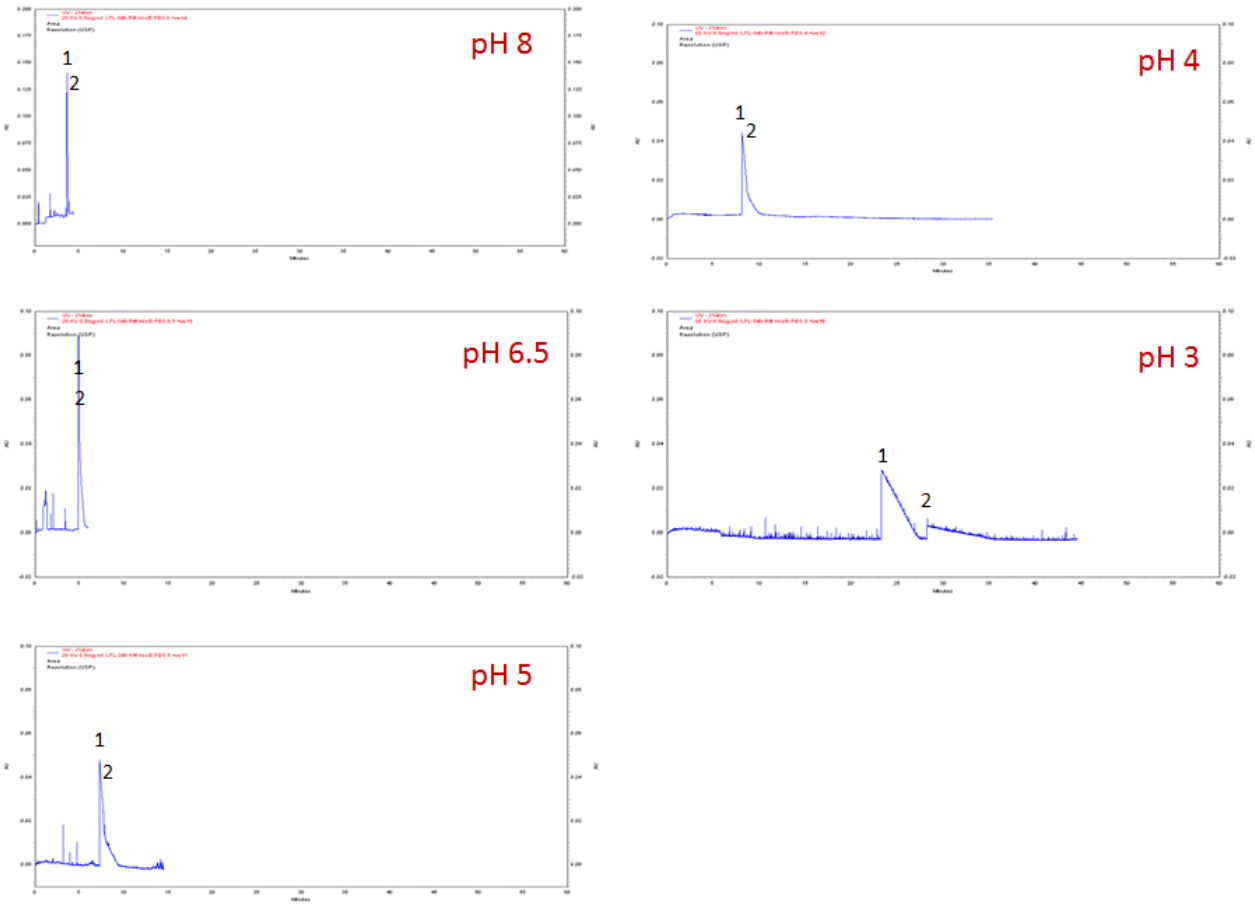

Figure 4.16 The effect of pH on the separation of the two basic drugs using 0.5 mg/mL MA-SNPs. Experimental conditions: 25 mM phosphate buffer at pH 3, 4, 5, 6.5 or 8. The other conditions are the same as given in Fig. 4.12.

4.3.3.3 Effect of applied voltage and SNPs concentration

In order to enhance the peak shapes, optimize the separation efficiency, and shorten the run time while separating PRP and ATN using LPL-SNPs as PSPs, the effect of the applied voltage was investigated. As can be observed in Fig. 4.17, increasing the voltage to +25 KV did not show a significant enhancement in the separation efficiency of the two basic analytes. On the other hand, the effect of changing the concentration of LPL-SNPs on the separation of the

selected analytes was also investigated. As shown in Fig. 4.18, decreasing the concentration of LPL-SNPs from 0.5 mg/mL to 0.2 mg/mL decreased the resolution and the migration times in the case of the basic drugs and increased the migration times with a better resolution and poor peak shapes in the case of the acidic drugs.

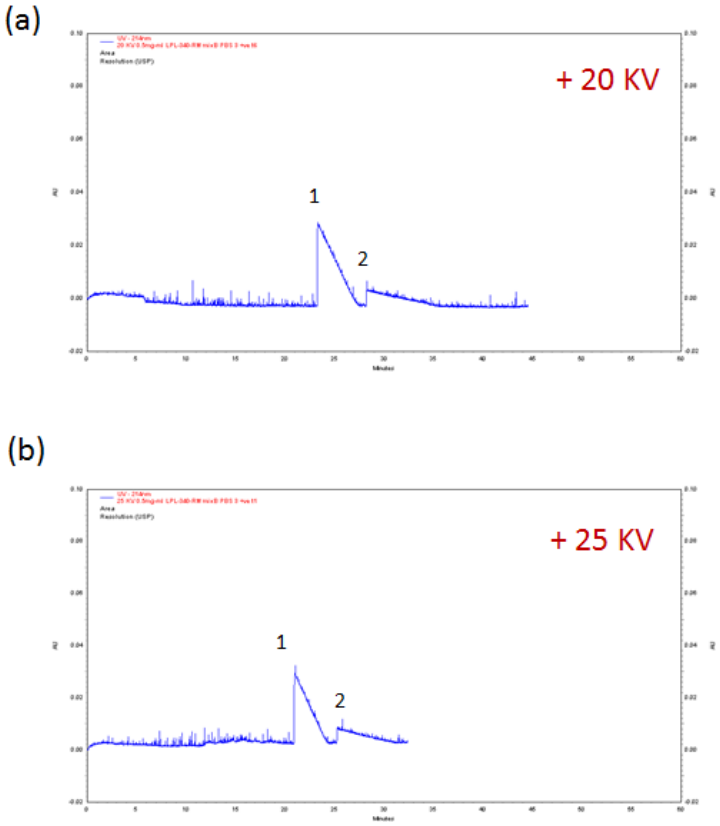

Figure 4.17 The effect of voltage on the separation of the two basic drugs without SNPs. Experimental conditions: 25 mM phosphate buffer at pH 3. The other conditions are the same as given in Fig. 4.12.

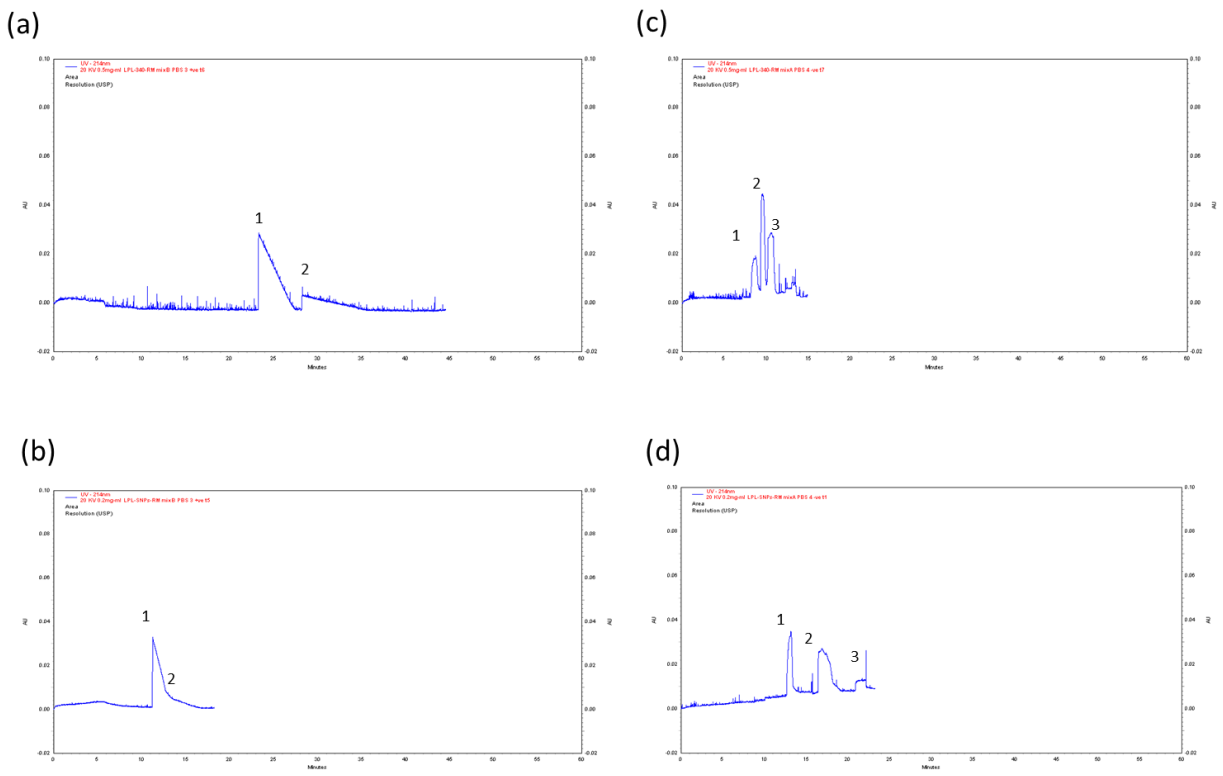

Figure 4.18 The effect of LPL-SNPs concentration on the separation of the two basic drugs using 0.5 mg/mL LPL-SNPs (a) and 0.2 mg/mL LPL-SNPs (b), and on the three acidic analytes using 0.5 mg/mL LPL-SNPs (c) and 0.2 mg/mL LPL-SNPs (d). The other conditions are the same as given in Fig. 4.11 and 4.12.

4.4 Conclusions

Five functionalized-SNPs were successfully prepared by using Stöber or reverse microemulsion methods. Under optimum experimental conditions, the obtained functionalized SNPs were tested as PSPs which can be used to enhance the electrophoretic separation of challenging mixtures of acidic or basic drugs. Four of these modifications were based on amino acids to form suitable conjugate moieties to be copolymerized and grafted on the surface of SNPs and render them different charges and ionization patterns based on the nature of the added functional groups and the pH of the used background electrolyte. Furthermore, the electrophoretic properties of bare SNPs and the functionalized SNPs, determined by their different surface properties, were systematically investigated. The effects of running buffer pH, applied voltage and concentrations of the PSPs on separation efficiency were also evaluated. It was found that bare SNPs, L-SNPs, CYS-SNPs, and GLU-SNPs did not result in any significant enhancement in the separation of the selected acidic or basic drugs` mixtures. However, MA-SNPs and LPL-SNPs showed obvious enhancement in the separation of the acidic drugs VAL, KET, and IBU in the pH range of 4-6.5 in terms of migration times, peak shapes, and separation efficiency especially at pH 4. The fast and successful separation of the acidic analytes can be attributed to the anodic co-EOF caused by the positive charge of the amino groups on the surface of these modified SNPs at low pH. Regarding PRP and ATN binary mixtures, LPL-SNPs at pH 3 provided the most suitable conditions to resolve these two analytes but with prolonged migration times and poor peak shapes. Finally, the introduced functionalized SNPs could be tested either alone or in combination with other chiral selectors for their ability to enhance the separation of some enantiomeric drug mixtures using the CE technique.

References

1. Gan, X.; Liu, T.; Zhong, J.; Liu, X.; Li, G. Effect of silver nanoparticles on the electron transfer reactivity and the catalytic activity of myoglobin. ChemBioChem 2004, 5 (12), 1686-1691.
2. Cademartiri, L.; Ozin, G. A. Concepts of nanochemistry. Wiley-VCH: Weinheim, 2009
3. Cai, J.-r.; Duan, H.-g.; Wang, T.-h. Imaging techniques and applications of the Au/Ag nanoparticles. Faguang Xuebao 2013, 34 (6), 792-796.
4. Schwarz, M.; Doerfler, A.; Engelhorn, T.; Struffert, T.; Tietze, R.; Janko, C.; Tripal, P.; Cicha, I.; Duerr, S.; Alexiou, C.; Lyer, S. Imaging modalities using magnetic nanoparticles - overview of the developments in recent years. Nanotechnol. Rev. 2013, 2 (4), 381-394.
5. Sardan, M.; Yildirim, A.; Mumcuoglu, D.; Tekinay, A. B.; Guler, M. O. In Noncovalent approach for developing hybrid mesoporous silica nanoparticle-peptide amphiphile system, American Chemical Society: 2015; pp COLL-372.
6. Lai, C.-Y.; Trewyn, B. G.; Jeftinija, D. M.; Jeftinija, K.; Xu, S.; Jeftinija, S.; Lin, V. S. Y. A mesoporous silica nanosphere-based carrier system with chemically removable CdS nanoparticle caps for stimuli-responsive controlled release of neurotransmitters and drug molecules. J. Am. Chem. Soc. 2003, 125 (15), 4451-4459.
7. Nilsson, C.; Nilsson, S. Nanoparticle-based pseudostationary phases in capillary electrochromatography. Electrophoresis 2006, 27 (1), 76-83.
8. Goettlicher, B.; Baechmann, K. Application of particles as pseudo-stationary phases in electrokinetic chromatography. J. Chromatogr. A 1997, 780 (1 + 2), 63-73.
9. Nilsson, C.; Harwigsson, I.; Becker, K.; Kutter, J. P.; Birnbaum, S.; Nilsson, S. Nanoparticle-based capillary electroseparation of proteins in polymer capillaries under

physiological conditions. Electrophoresis 2010, 31 (3), 459-464.

10. Fanali, S.; Catarcini, P.; Blaschke, G.; Chankvetadze, B. Enantioseparations by capillary electrochromatography. Electrophoresis 2001, 22 (15), 3131-3151.
11. Wang, Y.; Baeyens, W. R. G.; Huang, C.; Fei, G.; He, L.; Ouyang, J. Enhanced separation of seven quinolones by capillary electrophoresis with silica nanoparticles as additive. Talanta 2009, 77 (5), 1667-1674.
12. Gupta, A. K.; Gupta, M. Synthesis and surface engineering of iron oxide nanoparticles for biomedical applications. Biomaterials 2005, 26 (18), 3995-4021.
13. Bachmann, K.; Gottlicher, B. New particles as pseudostationary phase for electrokinetic chromatography. Chroma 1997, 45, 249-254.
14. Neiman, B.; Grushka, E.; Lev, O. Use of gold nanoparticles to enhance capillary electrophoresis. Anal. Chem. 2001, 73 (21), 5220-5227.
15. Ding, G.; Da, Z.; Yuan, R.; Bao, J. J. Reversed-phase and weak anion-exchange mixed-mode silica-based monolithic column for capillary electrochromatography. Electrophoresis 2006, 27 (17), 3363-3372.
16. Zhanga, J. L. B.; Zhenga, C.; Changb, M. Chemical Engineering Journal 2014, 256, 93-100.
17. Stöber, W.; Fink, A.; Bohn, E. Controlled growth of monodisperse silica spheres in the micron size range. Journal of Colloid and Interface Science 1968, 26 (1), 62-69.
18. Bagwe, R. P.; Yang, C.; Hilliard, L. R.; Tan, W. Optimization of Dye-Doped Silica Nanoparticles Prepared Using a Reverse Microemulsion Method. Langmuir 2004, 20 (19), 8336-8342.
19. Shahabi, S.; Treccani, L.; Rezwan, K. A comparative study of three different synthesis

routes for hydrophilic fluorophore-doped silica nanoparticles. Journal of Nanoparticle Research 2016, 18 (1), 28.

20. Costa, C. A. R.; Leite, C. A. P.; Galembeck, F. Size Dependence of Stober Silica Nanoparticle Microchemistry. J. Phys. Chem. B 2003, 107 (20), 4747-4755.
21. Kim, K.-M.; Kim, H. M.; Lee, W.-J.; Lee, C.-W.; Kim, T.-i.; Lee, J.-K.; Jeong, J.; Paek, S.-M.; Oh, J.-M. Surface treatment of silica nanoparticles for stable and charge-controlled colloidal silica. International Journal of Nanomedicine 2014, 9 (Suppl 2), 29-40.
22. Li, H.; Ding, G. S.; Chen, J.; Tang, A. N. Amphiphilic silica nanoparticles as pseudostationary phase for capillary electrophoresis separation. Journal of chromatography. A 2010, 1217 (47), 7448-54.

5 FLUORESCENTLY LABELED SILICA NANOPARTICLES FOR SOME FORENSIC AND BIO-RELATED APPLICATIONS

5.1 Introduction

Silica nanoparticles (SNPs) have proven to be useful in many applications in the areas of chemistry, forensics, nanomedicine and related technologies. Combining the properties of SNPs and fluorescent dyes that can serve as chemical probes is relatively easy by synthesizing fluorophore-encapsulated core-shell silica nanoparticles (FLSNPs), a process that results in the fluorescent dye covalently or non-covalently attached to the structure of the silica matrix. Moreover, this platform can enhance both the brightness and photostability of the dyes, compared to the free dye [1].

Several approaches have been reported for the encapsulation of organic fluorophores into SNPs [2, 3]. To meet certain applications` requirements, FLSNPs must possess high quantum yield, good photostability, size uniformity as well as minimized dye leakage. Synthesis of FLSNPs is usually carried out through two sol–gel methods: the Stöber method [4] and the water in oil reverse microemulsion (WORM) method [5]. The particles prepared by Stöber methods usually are not uniform. To overcome these shortcomings, WORM method is preferred as it results in SNPs with better monodispersity. However, a high amount of surfactants is needed in the synthesis process which necessitates extensive subsequent cleaning steps [6]. Recently, an approach via an amino acid-catalyzed seeds regrowth technique (ACSRT) using L-arginine as a catalyst to prepare nanoparticles of tunable sizes as well as minimized dye leakage without covalent copolymerization has been developed [7]. The new technique can overcome the limitations of the other two methods by obtaining less polydisperse SNPs without the use of surfactants.

The formation mechanism of SNPs affects the rate of dye leaching. Toshiyuki Yokoi et al. [8], reported that silica nanoparticles were synthesized under weakly basic conditions where the basic amino acid, L-arginine was used as a catalyst. The pH of the reaction medium during the seeds formation step is about 9-10 in the basic amino acids based approach whereas the hydrolysis reaction of TEOS in the other methods is conducted under much more basic conditions (pH 12-13). Moreover, a slight change in the pH was observed in the ACSRT system. This is probably due to consumption of the hydroxyl species as well as the formation of a large number of weakly acidic silanol groups. The presence of arginine with a buffering action might cause the slight reduction in the pH during the synthesis to achieve a slow hydrolysis of TEOS which allows particle growth through complete hydrolysis. Thus, the FLSNPs synthesized with the amino acid approach are less vulnerable to dissolution and dye leakage [8, 9].

5.2 A Comparative Study of Fluorescein Isothiocyanate-Encapsulated Silica Nanoparticles Prepared in Seven Different Routes for Developing Fingerprints

Preparation of fluorescein isothiocyanate (FITC)-encapsulated silica nanoparticles (F-SNPs) with seven different approaches to be used as developing agents for fingerprints detection is presented in this report. In this study, the suitability of each synthesis route toward incorporation of the selected fluorophore into silica matrix and its efficiency in fingerprints detection were systematically studied. The composition of the particles was designed to examine the hydrophobic and/or ionic interactions between the silicate backbone and both of the fluorescent reporter molecule and the fingerprint residues. F-SNPs were prepared using two conventional approaches; Stöber method and water in oil reverse microemulsion (WORM) method. The alkoxysilane precursor, tetraethoxyorthosilicate (TEOS) and its binary mixtures with phenyltriethoxysilane (PTEOS) or 3-aminopropyl triethoxysilane (APTES) have been used in preparing the F-SNPs to study the effect of nanoparticles composition on fingerprints development. In addition, FITC was conjugated with APTES so it can be covalently bonded to the silica matrix and to be compared with the non-covalently FITC-doped SNPs. Moreover, the enhancement effect of introducing polyvinylpyrrolidone (PVP) onto the surface of the less hydrophobic F-SNPs on fingerprints detection was also investigated. The mean diameters of the F-SNPs were between 4.1±0.6 and 110.4±31.1 nm as shown by TEM size analysis for the nanoparticles prepared by WORM and Stöber methods, respectively. The obtained results clearly highlight the advantages of using a mixture of TEOS and PTEOS alkoxysilane precursors in preparing F-SNPs with remarkable encapsulation efficiency and clear detection of fingerprints due to the efficient embedding of the fluorophore inside the silica network even without

conjugation. It was also observed that both Stöber and WORM methods gave comparable results and that PVP coated particles did not show any significant enhancement in fingerprints visualization. This systematic investigation can be followed to determine the appropriate preparation route of silica nanoparticles loaded with any other small molecules to be utilized in forensic or biomedical applications.

5.2.1 Introduction

Detection of fingerprints at a crime scene is of great interest in forensic investigation mainly for collecting physical evidences. Fingerprints visualization requires a specific reaction of the developing agent with the fingerprint residue to obtain a clear contrast from the underlying substrate. This residue is a complex mixture of organic compounds such as proteins, amino acids, and lipids and some inorganic substances. Development of fingerprint can be achieved either through a chemical interaction between the reagent and the components found in the fingerprint deposit or via physical adhesion of a developing agent to the sticky fingerprint residue [10, 11].

Various methods such as powder dusting, cyanoacrylate fuming, and ninhydrin have been developed for fingerprint visualization. However, there is still a need for selective and sensitive reagents for fingerprint development. Recently, there have been increased interests in using nanoparticles (NPs) for fingerprints detection due to their unique properties. First, their small particle size enhances detection of fingerprints due to increased resolution because small particles have the ability to adhere with high affinity to the fingerprint residue [12]. Second, the optical properties of fluorescent NPs allow detecting fingerprints with improved overall sensitivity [13]. Finally, surface modification can be achieved by the incorporation of functional groups possessing the potential interactions with certain components in the fingerprint residue,

and thus increase the selectivity. Leggett et al. reported the use of antibody-functionalized gold NPs to detect specifically cotinine, a metabolite of nicotine, only present in fingerprints left by smokers [14]. Many types of NPs such as gold NPs [15], quantum dots [16, 17], nanostructured powders [18], and silica nanoparticles (SNPs) [19-21], have been used as developing agents for fingerprints. Despite all advantages of nanoparticles for fingerprint detection, there are still concerns regarding their toxicity, cost, and laborious procedures. SNPs are a favorable candidate for fingerprints detection due to their great surface-to-volume ratio, biocompatibility and high photochemical stability [19]. Furthermore, modification of SNPs surface can be easily achieved by introducing several types of silicate monomer to target various compounds in the fingerprint residue. For example, amphiphilic SNPs were synthetized and used as a developing agent where the hydrophobic and hydrophilic nature of the used monomers made the surface of these particles sensitive to the amino acids present in the fingerprint residue [20]. Moreover, fluorophores such as organic dye molecules can be incorporated within the silica matrix during the synthesis process, providing superior optical properties and low background interference as presented in Theaker et al. work where they developed hydrophobic silica micro- and NPs encapsulating fluorescent dyes as developing agents for fingerprints detection [21].

Synthesis of SNPs is typically carried out through two commonly used sol–gel methods: the Stöber method [4] and the water in oil reverse microemulsion (WORM) method [5]. The modified Stöber process is used in synthesizing silica colloids by means of hydrolysis and condensation of the organosilicate monomers such as tetraethyl orthosilicate (TEOS), 3-aminopropyl triethoxysilane (APTES) and phenyltriethoxysilane (PTEOS) in alcoholic alkaline solutions (pH 11–12) where ammonia acts as a catalyst. On the other hand, the NPs prepared by WORM show less polydispersity with better control of particle size allowed [5, 22]. However, a

high amount of surfactants and co-surfactants are needed in the synthesis process making tedious subsequent washing steps necessary [23]. Regardless of the synthesis route, several approaches have been suggested for coupling of organic fluorophores into the SNPs platform [2, 3]. The simplest approach is the non-covalent encapsulation of dyes into the silica matrix. Nevertheless, the absence of a stable covalent attachment between the fluorophores and the silica matrix implies that the dye molecules can leak out of the NPs over time, resulting in decrease in the brightness of the NPs, increase in the background signal and exposition of the fluorophores to the surrounding environment making them less suitable for fingerprints detection [24]. On the contrary, the dye leakage can be effectively avoided by covalent dye encapsulation. The covalent incorporation of dyes into silica can be achieved by using an amine-containing organosilane as the crosslinker such as APTES which can form a covalent binding between its amine group and cyanate of the dye leading to the formation of thiourea linkage [25]. It is obvious that the covalent bonding approach is the best method for incorporation of a dye into SNPs. However, the dye should have the necessary functional groups towards modification and conjugation with the silicate precursors. This concept might increase considerably the difficulty of dye selection and pre-modification.

To the best of our knowledge, most of the reports dealing with the application of fluorescent SNPs in fingerprints development concentrated on the incorporation of fluorophores into the colloidal silica spheres and on the nature of these fluorophores [26-28]. Nevertheless, very few studies have been carried out that focus on the core and surface properties of the NPs used for fluorophore encapsulation and their effects on the efficiency of fingerprints detection in a systematic manner. It was suggested that for effective dye doping and fingerprints visualization, mixtures of TEOS and PTEOS have to be used in synthesizing the NPs, hence it was concluded

that analogous hydrophobic and electrostatic interactions occur within these hydrophobic NPs between compatible groups within the fluorescein isothiocyanate (FITC) dye molecules or any other dye of a related structure and the silica matrix [21]. Moreover, it was reported that the dye is not subject to photo-bleaching under exposure to high intensity UV illumination. Hence, these NPs can be utilized as agents for developing fingerprints, including aged prints where the residues mainly consist of hydrophobic endogenous chemicals secreted by the donor, due to the hydrophobic nature of some of the proposed FITC-encapsulated silica nanoparticles (F-SNPs) [21]. It should also be noted that as the proportion of PTEOS increases, the hydrophobicity of the resulting sol–gel also increases [29].

In this study, a systematic investigation of several factors that may influence the efficiency of developing fingerprints is presented. These factors include (i) method of SNPs preparation, (ii) the method of fluorophore encapsulation into the NPs matrix, and (iii) nature of the used organosilicate precursors and (iv) surface modification of the dye encapsulated SNPs using adhesive agents such as polyvinylpyrrolidone (PVP) and its enhancing effect on the binding affinity to fingerprints. In order to study these factors, F-SNPs were prepared using seven different approaches and tested as developing agents for some forensic applications such as fingerprints detection.

5.2.2 Experimental

5.2.2.1 Materials and reagents

All the chemicals used were of Analytical Reagent grade, and the solvents were of HPLC grade. All the following chemicals were produced by Sigma-Aldrich, MO, USA: fluorescein isothiocyanate (FITC) (isomer I, 90%), 1-hexanol (anhydrous, ≥99%), 3-aminopropyl triethoxysilane (APTES) (≥98%), tetraethyl orthosilicate (TEOS) (99.99% trace metal basis),

sodium hydroxide (pellets, 97+%, A.C.S. reagent), cyclohexane (anhydrous, 99.5%), Ethanol (99.7%), and Triton™ X-100 (laboratory grade). Fisher Scientific, Fair Lawn, NJ, produced ammonium hydroxide solution (28%). Phenyltriethoxysilane (PTEOS) was supplied by Chem-Impex Int`l Inc., IL, USA whereas polyvinylpyrrolidone (PVP) was supplied by Alfa Aesar, MA, USA.

5.2.2.2 Pre-modification of FITC

In order to covalently incorporate FITC in the silica matrix, it was modified by inducing a reaction between the isothiocyanate group of FITC and the amine group of APTES and forming a thiourea linkage. A known amount of FITC was added to 1-hexanol to make a 1.0 mM solution. 10 molar equivalents of APTES were added and allowed to stir for 24 h in a round-bottom flask to get the FITC conjugated with APTES (FCA), (Scheme 5.2.1). The reagents are air sensitive and the reaction needs to be completed in a closed container in the dark.

5.2.2.3 Preparation of F-SNPs

To obtain F-SNPs with narrow size distribution patterns, the amounts of all reagents for each preparation method were adjusted carefully in preliminary experiments. Seven synthesis routes are schematically illustrated in Scheme 5.2.1.

5.2.2.3.1 Preparation of FITC doped (non-covalently) into the TEOS/PTEOS-based SNPs (FDTPS)

FDTPS were prepared using the Stöber method where 0.30 mL 10 mM solution of FITC in ethanol was transferred into a 25 mL round flask containing 2.7 mL ethanol and mixed with 0.25 mL PTEOS. 0.20 mL ammonium hydroxide was added to the resulting solution to start the hydrolysis of the alkoxysilane precursor. The solution was stirred at low speed for 24 hours at room temperature. 0.5 mL TEOS and 0.25 mL PTEOS, dissolved in 5.0 mL ethanol were added

to the hydrolyzed solution and further reacted with 0.10 mL ammonium hydroxide solution via the Stöber process. The reaction was carried out for an hour at 0°C with continuous sonication and frequent vortexing then stirred for another 24 hours at room temperature. The formed particles were centrifuged and washed 3 times with a solution composed of ethanol and DI water (1:1, *v/v*), then the residue was left to dry completely.

5.2.2.3.2 Preparation of FITC three covalently bonded-SNPs (FCTS, FCTPS, and FCTAS)

FCTS, FCTPS, and FCTAS were also prepared by the Stöber method where 0.50 mL of the FCA conjugate solution were dissolved in 20.0 mL ethanol, followed by the sequential addition of the proper volume of the alkoxysilane precursor(s), 1.60 mL DI H_2O, and 1.60 mL ammonium hydroxide solution. 1.00 mL TEOS was used in the case of FCTS preparation while 0.5 mL TEOS and 0.5 mL PTEOS were used in the case of FCTPS preparation. Similarly, 0.5 mL TEOS and 0.5 mL APTES were used in the case of FCTAS. The mixture was stirred at 400 rpm for 24 hours at room temperature. The formed particles were centrifuged and washed 3 times with ethanol and water, then the residue was left to dry completely, (Scheme 5.2.1).

5.2.2.3.3 Preparation of FITC covalently encapsulated SNPs using WORM method (FCTPS-RM)

The micelles were prepared using 15.0 mL cyclohexane, 2.60 mL 1-hexanol, 3.55 mL Triton™ X-100, and 1.13 mL DI H_2O which were stirred for 10 min to generate the microemulsion. After time elapsed, 0.50 mL of the FCA conjugate solution was slowly added to the microemulsion and stirred for 30 min at 120 rpm. Finally, 0.50 mL TEOS, 0.50 mL PTEOS, and 0.12 mL ammonium hydroxide were added and the solution was stirred for 24 h. Afterward, 5.0 mL acetone were added and the NPs were collected by centrifugation and washed 5 times

with absolute ethanol and two times with water to remove any unreacted chemicals and free dye conjugates, (Scheme 5.2.1).

5.2.2.3.4 Surface Modification of F-SNPs with PVP

60 mg PVP were dissolved in a solution containing 30 mg of either FCTS or FCTAS in 5.0 mL ethanol, and the mixture was stirred for 24 hours at room temperature and then centrifuged for 20 min at 3800 rpm. The precipitate was re-dispersed in ethanol, and the dispersion was centrifuged again then the residue was left to dry completely to obtain the corresponding PVP coated F-SNPs, FCTS-PVP and FCTAS-PVP, respectively (Scheme 5.2.1).

5.2.2.4 Instruments and particles characterization

0.1 mg/mL F-SNPs suspensions dispersed in ethanol were subjected to particle size determination analysis using a Malvern Mastersizer (Malvern Instruments Ltd., Malvern, UK. Polydispersity index (PDI), and standard deviation were obtained from three independent measurements of the dispersions of NPs. Zeta potential of NPs dispersions in ethanol was also measured. Transmission electron microscopy micrographs were conducted by the Zeiss LEO 912AB (Zeiss, Thornwood, NY). NPs separation required an Allegra 64R Centrifuge (Beckman Coulter Inc., Brea, CA). A SympHonly (SB20) pH-meter (Thermo Orion, MA, USA) was used for pH adjustment. Nano pure water was prepared using a Barnstead NANO pure DIamond Analytical ultrapure water system (Fischer Scientific, NJ, USA). All fluorescence spectra were performed on ISS K2 multifrequency cross-correlation phase and modulation fluorimeter (ISS™ Focus and Discover, Champaign, IL, USA), equipped with a 300W xenon arc lamp. A 1.0 cm disposable plastic was used for all fluorescence measurements. To investigate the fluorescence properties of the F-SNPs, they were dispersed in a 1:1 (v/v) water/ethanol solvent and their emission spectra were recorded.

5.2.2.5 Use of F-SNPs as developing agents for fingerprints:

Fingerprints were collected from a 26-year-old male donor and then developed after 24 hours of deposition. Fingerprints were obtained by requesting the donor to rub his finger with his nose immediately prior to fingerprints deposition. The donor was instructed not to wash his hands within the last two hours. Fingerprints were deposited onto glass microscope slides (Fisher Scientific, Fair Lawn, NJ) which were used as received. A specific concentration of 5.0 mg/mL suspensions for each of the F-SNPs in a solvent composed of 1:1 (v/v) DI water: ethanol were prepared, then the they were sonicated for 10 min to ensure sufficient particles dispersion. About 0.5-1.0 mL of the suspension was pipetted onto the sample using a transfer pipette. After 5 minutes, the excess solution was removed, and the sample was gently washed with a mixture of 1:1 (v/v) DI water: ethanol. After that the developed fingerprint sample was left to dry at room temperature. The photographs were recorded with luminescence mode using the forensic light source (FLS), Mini-CrimeScope 400 MCS-400 (Spex Forensics, Edison, NJ) at excitation wavelength of 445 nm and crime scene search (CSS) settings. The fingerprint image was photographed using a digital camera (Nikon D3300) with a 520 nm long-pass filter. The sample was placed on a black surface to enhance the contrast of fingerprint image during illumination and taking pictures.

5.2.3 Results and discussion

To achieve stable incorporation of small molecules such as dyes, either covalent copolymerization of the dye conjugate or strong non-covalent binding interactions between the added dye molecules and the backbone of the cross-linked silicate matrix is needed. These interactions are likely to arise from hydrophobic and hydrophilic groups in the dye molecules and the silicate backbone. To identify the factors leading to stable incorporation of the

fluorogenic molecules into the SNPs and efficient visualization of fingerprints, seven different routes for preparing F-SNPs have been examined in this report. The produced SNPs have embedded within them either FITC or its conjugate with APTES, FCA. Two of the most commonly used sol-gel methods for SNPs preparation namely Stöber method and WORM method were used. Moreover, covalent encapsulation of the FCA dye conjugate versus encapsulation of the FITC dye itself non-covalently into the SNPs has been examined. In addition, three organosilicate monomers namely TEOS, PTEOS, APTES and their binary combinations were used to prepare the NPs. Finally, the adhesive agent, PVP was introduced onto the surface of the less hydrophobic F-SNPs to investigate the enhancement effect on the binding affinity of PVP-coated F-SNPs towards fingerprints residue.

5.2.3.1 Particle characterization

The physical nature and dimensions of the particles were derived from the DLS and TEM scans for FCTPS and FCTPS-RM, (Fig. 5.2.1). The NPs are composed of discrete monodispersed spherical particles with an average diameter of 110.4±31.1 and 4.1±0.6 for the NPs prepared by WORM and Stöber methods, respectively. The NP diameter obtained from TEM images, the mean hydrodynamic particle sizes by DLS, PDI, and zeta potential values are summarized in Table 5.2.1.

TEM micrographs showed that the labeled F-SNPs prepared by WORM method had a spherical shape and a narrow size distribution of 4.1±0.6 which was confirmed by the DLS measurements. On the other hand, NPs prepared by Stöber method had a relatively larger diameter of about 110.4±31.1 with lower control on the monodispersity of the size and shape. The zeta potentials of FCTPS and SCTPS-RM in ethanol were ranging from -12.8 to -26.7 mV, respectively, Table 5.2.1.

Table 5.2.1 Diameter determined by TEM and DLS, polydispersity index (PDI), zeta potential of 0.1 mg/ml labeled SNPs in ethanol

F-SNPs	Diameter (TEM) (nm)	Diameter (DLS) (nm)	PDI	Zeta potential (mV)
FCTPS	110.4 ± 31.1	605.7 ± 131.5	0.48	-26.7 ± 14.3
FCTPS-RM	4.1 ± 0.6	5.3 ± 0.4	1.00	-12.8 ± 14.2

5.2.3.2 Preparation method of the F-SNPs

Two different F-SNPs, FCTPS and FCTPS-RM, were prepared to be used in this investigation. Both of them were prepared using a mixture of TEOS and PTEOS alkoxysilane precursors [21]. FCTPS were prepared using the Stöber method [4] whereas FCTPS-RM were prepared using the WORM method [5]. The Stöber method has the advantages of simplicity besides avoiding using surfactants which requires extensive cleaning steps. However, controlling the particle size is easily achieved using the WORM method, as nanoreactors of water droplets in the oil phase define the particles dimension [28]. As expected, WORM method resulted in NPs with smaller size of about 4.1±0.6 nm and better monodispersity in comparison with the Stöber method as can be revealed from the SEM and DLS measurements. Due to the simplicity and cost effectiveness of the Stöber method, it was chosen as the method of F-SNPs preparation to investigate the other factors affecting fingerprints visualization.

5.2.3.3 Covalent versus non-covalent fluorophore encapsulation into the SNPs matrix

Two different F-SNPs, FDTPS and FCTPS, were prepared to be used in this investigation. Both of them were prepared using the Stöber method with equal volumes of TEOS

and PTEOS alkoxysilane precursors [21]. FITC (logP 5.03) was non-covalently doped into a hydrophobic core composed of PTEOS (logP 3.25) then entrapped in a shell composed of TEOS (LogP 1.68) and PTEOS in the case of FDTPS. The composition of the core and the shell of FDTPS allowed stable non-covalent encapsulation of the hydrophobic FITC dye molecules with minimal leakage under the used experimental conditions. For FCTPS, APTES was used for crosslinking the FITC dye molecules with the silica matrix, where the binding between cyanate groups of the dye and amine groups of APTES results in the formation of thiourea linkage [30]. The formed FITC conjugate with APTES, FCA, was covalently copolymerized into the SNPs to form FCTPS. Investigation of the emission spectra of these NPs, confirmed the successful encapsulation of the hydrophobic FITC dye, (Fig 5.2.2). The fluorescence maximum for all the NPs is within the same range of the pure dye. Different patterns were observed due to the differences in the composition of the NPs.

It is reported that the incorporation yield of non-covalently bound fluorophores is poor, as it is only based on physical adsorption forces [31]. Nevertheless, non-covalent incorporation of FITC was made suitable using the hydrophobic alkoxysilane precursor, PTEOS, and this observation is consistent with other reports [6, 21, 32, 33]. It was also noted that the intensity of FDTPS fluorescence increased as the proportion of PTEOS in the initial monomer mixture increased [21]. A ratio of 1:1 (v/v) was used thereafter in all incorporation experiments. However, the dye is prone to leaking from FDTPS under exposure to the used solvent for longer time so the more stable FCTPS was found to be more suitable for developing fingerprints.

5.2.3.4 Type of the alkoxysilane precursor(s)

Three different organosilicate monomers have been used in this investigation, namely TEOS (logP 1.68), PTEOS (logP 3.25), and APTES (logP -1.83) to incorporate FCA covalently

into the silica platform. It is hypothesized that the planar aromatic phenyl groups of PTEOS would form hydrophobic interactions with the planar rings of FITC and that negatively charged Si–O groups present in the alkoxysilane precursors would form strong interaction with the polar functional groups of FITC, and thus producing a highly fluorescent and stable complex on encapsulation can be obtained [7]. Nevertheless, the nature of organosilicate monomers will not have a significant effect on the dye loading and its leaking from the NPs as the dye was covalently bonded into the silica matrix to form highly stable F-SNPs. Thus, the nature of the organosilicate monomers is expected to influence mainly the binding affinity to the fingerprints residue as it will be discussed in details in the following section.

5.2.3.5 Use of dye-encapsulated SNPs suspensions as developing agents for fingerprints

To investigate the binding affinity of F-SNPs to fingerprints, suspensions of these particles were applied on a glass substrate as shown in Fig 5.2.3. The nature of the precursor plays an important role in fingerprint detection. When the binary mixture of TEOS and PTEOS used in three different preparation routes of F-SNPs namely FCTPS, FCTPS-RM, and FDTPS, clear luminescent fingerprint ridges were obtained for the three F-SNPs suspensions at CSS setting of the FLS viewed through a 520 nm long pass filter as shown in Fingers 3a, b, and c (first row). The surface of NPs has been decorated with PTEOS which increases the hydrophobic interaction between the phenyl group of PTEOS and the sebaceous secretion in the fingerprint residue resulting in enhanced binding and detection of fingerprints. Despite the differences in the preparation methods, the efficiency of these hydrophobic NPs as developing agents able to produce clear luminescent fingerprints with high contrast was observed and attributed to the PTEOS-modified hydrophobic surface. However, a more distinct definition in fingerprint detection was noticed using another setting of FLS at excitation wavelength of 445 nm viewed

through the same filter as shown in Fig. 5.2.3a, b, and c (second row). Fingerprints developed with FDTPS appeared luminescent with clear ridge pattern. The luminescence intensity of fingerprints decreased with FCTPS-RM and FCTPS, and the latter appeared more as dotted marks. It was found that CSS setting of the crimescope was the best choice for fingerprints visualization. When TEOS was used solely for the preparation of FCTS, weak luminescence and poor contrast were obtained as shown in Fig. 5.2.3d in both settings of the FLS. Therefore, using these particles as developing agents for fingerprint detection is not practical. On the other hand, the binary mixture of TEOS and APTES used in preparing FCTAS resulted in highly luminescent ridges with obvious background noise as shown in Fig. 5.2.3e using both CSS and 445 nm settings. The observed background noise could be due to undesirable interactions between the polar APTES with the glass substrate. The presence of amine group in APTES promotes interaction with any compounds bearing carboxyl groups in fingerprint residue to produce amide linkage. The formation of this linkage was confirmed by the work of Moret et al. in understanding the mechanism of fingerprint development using SNPs [34].

Friction ridge features of a fingerprint have been classified into three levels of detail [35]. First- level detail describes the overall ridge pattern such as fingerprint orientation and ridge flow direction. The general information obtained from the first-level detail are not decisive. Thus, it cannot be used for personal identification. Second-level detail involves ridge formations and pattern minutiae such as ridge ending, bifurcation, and dots. Third-level detail includes the morphology of a ridge such as width, shape, and pores. Both second and third- level details enable identification and fingerprint matching due to the unique individual features. The typical features of second-level detail of fingerprint friction ridge of FCTPS, FCTPS-RM, and FDTPS

are shown in Fig. 5.2.4. Such features including bifurcations and ridge endings were slightly clear in fingerprints developed by FCTPS-RM, and FDTPS compared with FCTPS.

5.2.3.6 Surface modification of fluorescent SNPs with PVP

In order to enhance the fingerprints detection, the less hydrophobic FCTS and FCTAS were coated with the adhesive agent, PVP to improve their binding affinity to the hydrophobic components present in the fingerprint residue. PVP has been used as adhesive agent or binder in pharmaceutical industry because of its binding affinity to polar and nonpolar molecules contributed to intrinsic amphiphilic property of PVP [36, 37]. Thus, compared to uncoated NPs, their PVP-modified counterparts, FCTS-PVP and FCTAS-PVP should show much higher contrast fingerprints images on glass because of their high binding affinity [12]. Fingerprints detection using PVP-coated SNPs as fluorescent labeling markers should be well-defined in terms of finger ridge details without background staining, resulting in a good definition of enhanced detection. However, it was observed that the PVP-coated SNPs did not result in any enhanced visualization as shown in Fig. 5.2.3f and g.

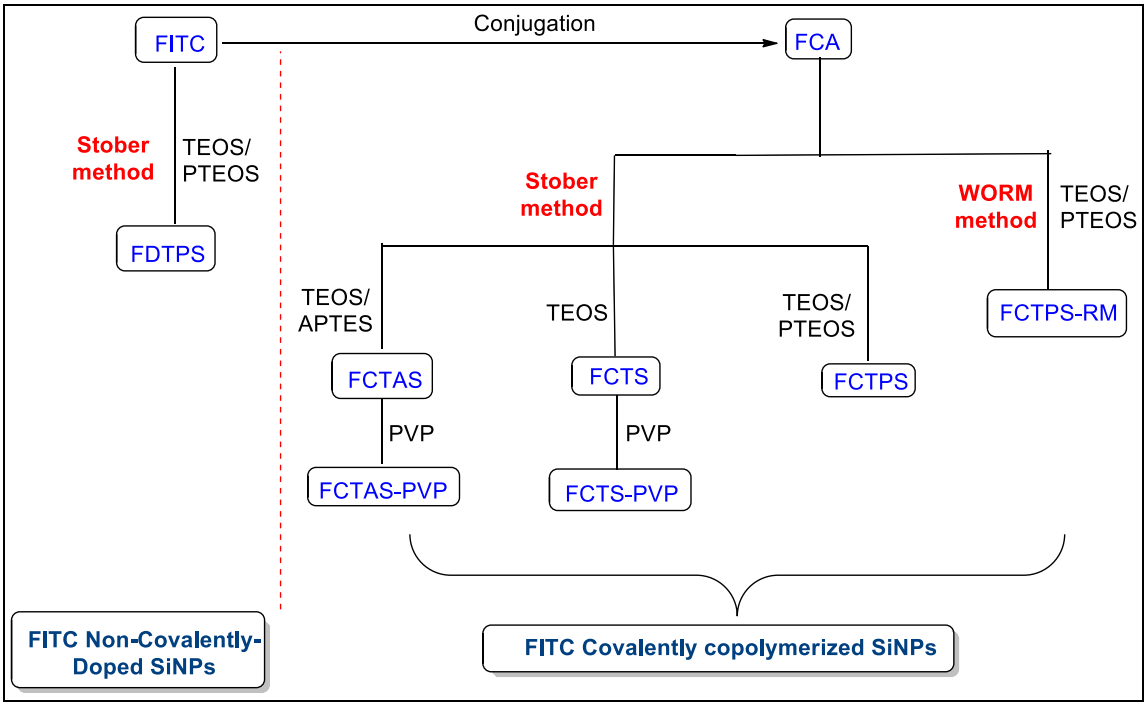

Scheme 5.2.1 Preparation routes for F-SNPs

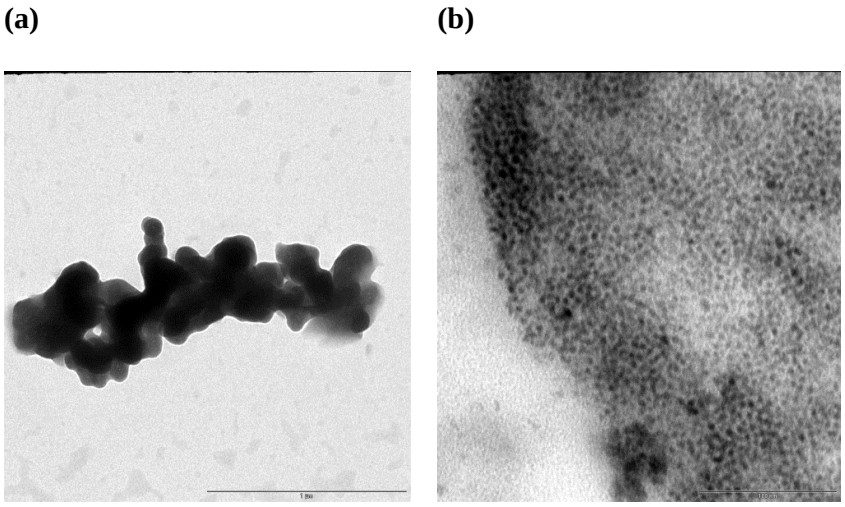

Figure 5.2.1 TEM micrographs of (a) FCTPS and (b) FCTPS-RM

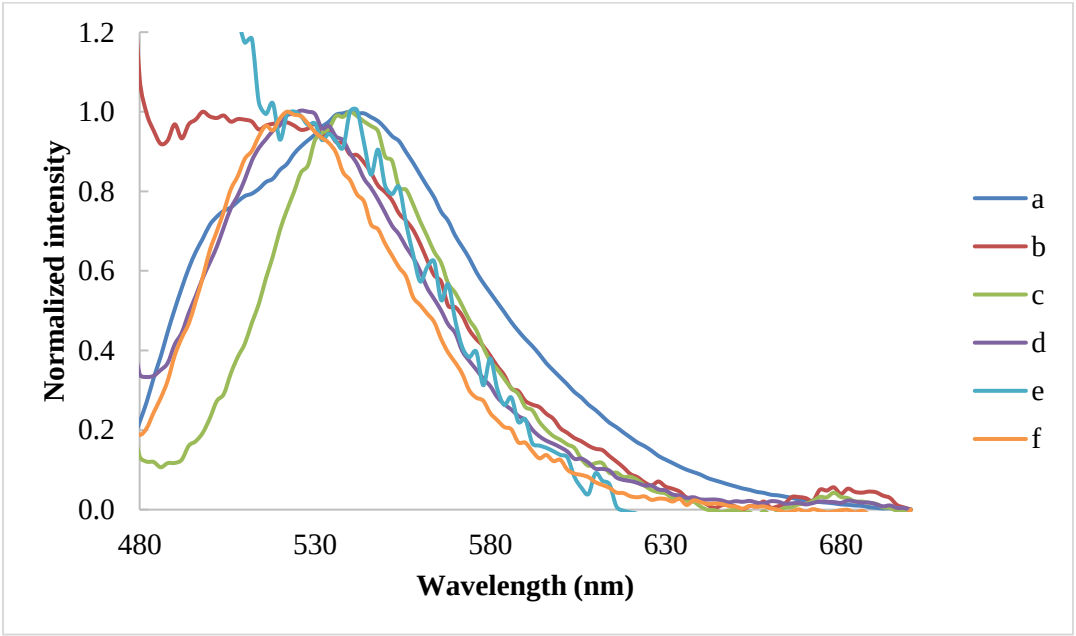

Figure 5.2.2 Normalized emission spectra of (a) FITC (b) FCTPS, (c) FCTPS-RM, (d) FDTPS, (e) FCTS, and (f) FCTAS in water: ethanol (1:1, v/v) at excitation wavelength of 455 nm

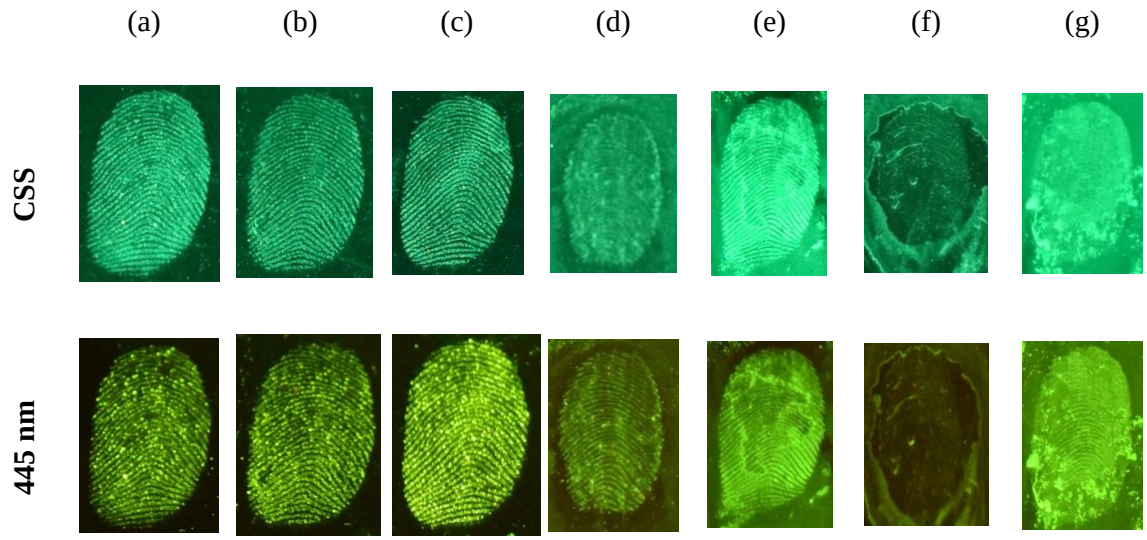

Figure 5.2.3 Fluorescence images of the fingerprints developed using 5.0 mg/mL F-SNPs suspensions in water: ethanol (1:1, v/v) of (a) FCTPS, (b) FCTPS-RM, (c) FDTPS, (d) FCTS, (e) FCTAS, (f) FCTS-PVP, and (g) FCTAS-PVP at different FLS settings

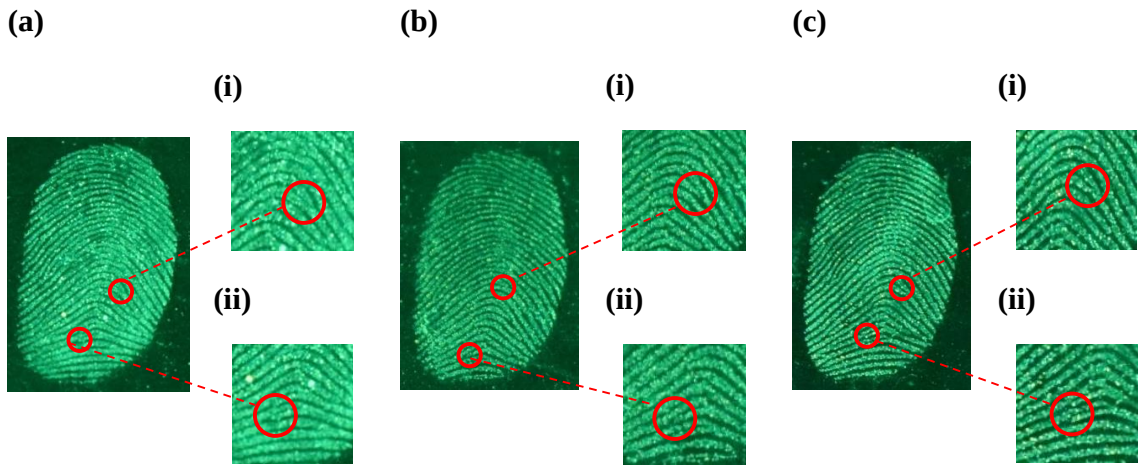

Figure 5.2.4 Fluorescence images of fingerprints of (a) FCTPS, (b) FCTPS-RM, and (c) FDTPS, at CSS setting of FLS, showing second-level detail of fingerprint friction ridge (i) bifurcation and (ii) ridge ending

5.3 Preparation of Fluorescently Labeled Silica Nanoparticles Using an Amino Acid-catalyzed Seeds Regrowth Technique: Application to Latent Fingerprints Detection and Hemocompatibility Studies

Journal of Colloid and Interface Science (2018) 512: 801–811

DOI 10.1016/j.jcis.2017.10.062

The efficiency of an amino acid catalyzed seed regrowth technique (ACSRT) in synthesizing twelve fluorescently labeled core-shell silica nanoparticles (FLSNPs) with tunable sizes, tailored hydrophobicity, low polydispersity as well as high labeling efficiency and minimized dye leakage using different organosilicate monomers and fluorophores have been systematically investigated in this report. The utilization of some of these FLSNPs in some applications that are facilitated by hydrophobicity such as developing and visualizing latent fingerprints (LFPs) on different surfaces was also investigated. The non-specific binding affinity of the developed nanoparticles to human serum albumin (HSA) and immunoglobulin G (IgG) has also been studied. Fluorescein, fluorescein isothiocyanate and its more hydrophilic butenamine derivative (WA6) have been used in this study. Also, the alkoxysilane precursor, tetraethoxyorthosilicate (TEOS) and its binary mixture with phenyltriethoxysilane (PTEOS) or 3-aminopropyl triethoxysilane (APTES) have been used in preparing the FLSNPs with tailored compositions for the core and shell of the nanoparticles. The mean diameters of the PTEOS-coated FLSNPs were between 33.4±5.9 and 42.2±10.8 nm as shown by the SEM measurements. The obtained results highlight the advantages of having a hydrophobic surface along with proper selection of the monomers forming the core to match the properties of the fluorescent reporters

for clear detection of LFPs even using dyes of low hydrophobicity such as fluorescein and WA6. Furthermore, some of the developed FLSNPs were compared with bare silica nanoparticles in terms of nonspecific protein adsorption and hemolysis. The obtained results proved that the selected FLSNPs had a superior hemocompatibility in comparison with bare silica nanoparticles. These FLSNPs could also be used in some bio-related and diagnostic studies such as immunoassays and cell imaging purposes.

5.3.1 Introduction

Using APTES-based organosilane chemistry is the common approach to achieve proper dye encapsulation via Stöber and WORM methods. Shakiba Shahabi et al. [6] reported that the poor incorporation efficiency of non-covalently bound fluorophores could be enhanced using ACSRT [31]. The synthesis pathway of ACSRT eliminates the need for covalent crosslinking step such as APTES-conjugation of dyes. Furthermore, enhanced dye stability and a higher labeling efficiency can be obtained with ACSRT, even without using APTES. The use of L-arginine as a catalyst also induces a stable crosslinking of some dyes into the silica matrix through a thiourea linkage [6, 38].

In this report, the synthesis of twelve fluorophore-encapsulated SNPs with well-controllable size and tunable hydrophobicity for the core and shell of the particles based on the ACSRT is presented, (Fig. 5.3.1, Table 5.3.1). Besides L-arginine, water, and the proper organosilicate precursors, the fluorophore molecules were introduced in the nucleation step, to form the fluorescent silica. The water-soluble organic fluorophore, fluorescein, or its more hydrophobic derivative, fluorescein isothiocyanate (FITC) or the more hydrophilic butenamine derivative of FITC (WA6) were directly incorporated into the seeds without covalent binding. The structure formulae of the three dyes are presented in Fig. 5.3.1.

Based on Shakiba Shahabi et al., work [6], particle size can be adjusted by controlling the reaction parameters and the proportion of seeds and organosilicate precursors in the regrowth step. The obtained fluorescent SNPs were characterized using scanning electron microscopy (SEM), dynamic light scattering (DLS), and fluorescence spectrometry. In addition, the labeling efficiency, dye leakage and colloidal stability were evaluated. The utilization of these particles in some hydrophobicity-based detection applications such as developing latent fingerprints (LFPs) [39] was systematically investigated. Furthermore, the suitability of these FLSNPs for biological studies was assessed by testing their non-specific binding to plasma proteins and by assessing their hemocompatibility. SNPs have been successfully used in such applications because of their unique advantages. Firstly, excellent physicochemical stability and cost-effective fabrication. Secondly, SNPs have tunable structural properties such as particle shape, particle sizes, pore structures, pore volumes, specific surface areas, hydrophobicity and so on. Thirdly, efficient loading of a wide range of hydrophilic or hydrophobic organic molecules such as organic dyes. Fourthly, SNPs are not toxic with great biocompatibility and biodegradability. Finally, facile multi-functionalization on the abundant -Si-OH, where their surfaces can be modified to satisfy the required purpose [39, 40].

The developed hydrophobic FLSNPs can be used for LFPs detection which is useful for personal identification in forensic investigations. The common form of fingerprint evidence left at the scenes of crime is LFPs, which is generally invisible to the naked eyes. Therefore, it needs to be developed to enable its visualization [10]. This can be achieved by obtaining an obvious contrast between the secretion residues of the LFPs pattern and the underlying substrates [41]. Many micro- or nanometer-sized particles with various compositions, such as gold nanoparticles, semiconductor quantum dots, magnetic particles, rare earth nanomaterials, silica particles,

composites, have been exploited as the developing agents using the powdering method [19]. Among various compositions, the hydrophobic SNPs, which were doped with dyes, metals, metal oxides or carbon, were used in developing clear LFPs [42].

Some reports concentrated on the incorporation of fluorophores into the colloidal silica spheres and on the nature of these fluorophores [26-28]. Nevertheless, very few studies have been carried out that focus on the nature of the SNPs core and shell composition used for dye encapsulation and their effects on the efficiency of LFPs detection in a systematic manner. Theaker et al reported that for effective dye doping mixtures of TEOS and PTEOS have to be used in synthesizing the SNPs, hence it was concluded that analogous hydrophobic and electrostatic interactions occur within these hydrophobic SNPs between compatible groups within the fluorescein isothiocyanate (FITC) dye molecules or any other dye of a related structure and the silica matrix [39]. Moreover, it was found that this dye was not subjected to photo-bleaching under exposure to high intensity UV illumination. Hence, these FLSNPs can be utilized as agents for developing LFPs, including aged prints where the residues mainly consist of hydrophobic endogenous chemicals secreted by the donor, due to their hydrophobic nature [39]. It should also be noted that as the proportion of PTEOS increases, the hydrophobicity of the resulting sol–gel also increases [29].

To the best of our knowledge, this is the first report that describes the synthesis of fluorescent SNPs based on a basic amino acid-catalyzed approach for developing LFPs using different combinations of hydrophilic and hydrophobic organosilicate precursors for modifying the core and shell of the SNPs. Moreover, the efficiency of embedding three fluorescent reporters with different LogP values in the core of theses SNPs has also been investigated. It was attempted in this study to enhance the loading efficiency of the used dyes and decrease their

leakage from the silica matrix just through non-covalent interactions between the dye and the alkoxysilane molecules in the core of the SNPs as well as encapsulating the dye molecules insides a shell with the suitable composition. Also, this is the first time to systematically study the effect of organosilane precursors on the size and colloidal stability of the ACSRT-made silica nanoparticles. Moreover, the scalable synthesis of silica nanoparticles from ultra-small size (13.9 nm) to large size (hundreds nm) with varying the nature of the core and shell compositions can provide a great benefit to study the effect of these factors, which have been considered to play a major role in the interaction with different surfaces, in vivo pharmacokinetics, and other bio-relevant issues.

On the other hand, it is reported that bare SNPs exhibit a noticeable hemolytic behavior, besides, their nonspecific binding to human serum albumin (HSA) and immunoglobulin G (IgG) [43]. In this report, some of the proposed hydrophobic FLSNPs were compared with bare silica nanoparticles in terms of nonspecific protein adsorption and percentage of hemolysis.

Different requirements should characterize those SNPs to achieve the desired properties. Therefore, hydrophobicity, labeling efficiency, dye leakage, monodispersity, colloidal stability as well as hemocompatibility of the synthesized FLSNPs were carefully considered.

5.3.2 Experimental

5.3.2.1 Materials and reagents

All the chemicals used were of Analytical Reagent grade, and the solvents were of HPLC grade. All the following chemicals were produced by Sigma-Aldrich, MO, USA: fluorescein isothiocyanate (FITC) (isomer I, 90%), 1-heptanol (anhydrous, ≥99%), 3-aminopropyl triethoxysilane (APTES) (≥98%), tetraethyl orthosilicate (TEOS) (99.99% trace metal basis), sodium hydroxide (pellets, 97+%, A.C.S. reagent), cyclohexane (anhydrous, 99.5%), albumin

from human serum (>96%), purified human immunoglobulin G (IgG), sodium phosphate, dibasic (98+%), potassium phosphate monobasic (>95%), hydrochloric acid (37%), and Triton™ X-100 (laboratory grade). Fisher Scientific, Fair Lawn, NJ, produced ammonium hydroxide solution (28%) and sodium chloride crystals (certified A.C.S). Phenyltriethoxysilane (PTEOS) was supplied by Chem-Impex Int`l Inc., IL, USA. Ethanol (200 proof) was obtained from Decon labs Inc (King of Prussia, PA USA) while KCl was obtained from J.T.Backer Inc. (NJ, USA). 3-Buten-1-amine (97%) was purchased from Alfa Aesar (MA, USA).

5.3.2.2 Pre-modification of WA6

1-(but-3-en-1-yl)-3-(3',6'-dihydroxy-3-oxo-4a',9a'-dihydro-3H-spiro[isobenzofuran-1,9'-xanthen]-5-yl)thiourea (WA6) was prepared by inducing a reaction between the isothiocyanate groups in FITC with the amine group of 3-butene-1-amine. 0.22 mmole of FITC was added to 0.32 mmole of 3-butene-1-amine and refluxed for 24 h in a round-bottom containing 2 mL ethanol, (Scheme 5.3.1). The residue was filtered and washed several times with methanol and then dried under reduced pressure to obtain the pure form.

5.3.2.3 Synthesis of FLSNPs using ACSRT

All FLSNPs were synthesized by slightly modifying previous methods [6, 7].

5.3.2.3.1 Preparation of labeled seeds

One mmole L-arginine was dissolved in 16.9 ml DI H_2O and stirred thoroughly at room temperature. Afterward, 0.02 mmoles of the corresponding fluorescent dye dissolved in 500 µL ethanol was added to the L-arginine solution. The mixture was stirred for 10 min and then heated up to 70 °C, before the addition of 0.001 mmoles of TEOS. In the case of using a binary mixture of the organosilicate monomer, 0.0005 mmoles from each monomer were used instead. The mixture was stirred for 24 h at 70 °C in an oil bath. Finally, the dispersion containing the labeled

seeds was used as stock for the regrowth step. The synthesis was carried out in the dark to minimize photo-bleaching of the fluorescent dye.

5.3.2.3.2 Regrowth of labeled seeds

4.47 mmole L-arginine were dissolved in 1 mL water and 4 mL ethanol. Subsequently, 1 mL of the labeled seeds was added to the L-arginine solution. The mixture was stirred for 10 min before heating up to 70 °C. Thereafter, 1 mL of TEOS was added. In the case of using a binary mixture of the organosilicate monomer, 0.5 mL from each monomer was used instead. The suspension was then stirred at 70 °C for 24 h in the dark. Twelve different types of FLSNPs with different sizes were prepared only by varying the fluorophore and/or the organosilicate precursor (Table 5.3.1), while the other parameters were kept constant. Then, the particles were collected by centrifugation, washed with ethanol and water twice and left to dry at 60°C. A different set of the SNPs namely; T-T, T-TP, TP-TP, TA-T, and TA-TP, was prepared for colloidal stability and characterization studies according to the same procedure without labeling with any fluorophores in the seeds preparation step. The effect of the amount of L-arginine on the size of the silica nanoparticles was investigated by varying the concentration of the amino acid catalyst in the regrowth step to be 0.0, 1.0, and 4.47 mmoles in the prepared particles; T-T-0, T-T-1, and T-T, respectively.

5.3.2.4. Instruments and particle characterization

0.2 mg/mL FLSNPs suspensions dispersed in ethanol were subjected to particle size determination analysis using a Malvern Mastersizer (Malvern Instruments Ltd., Malvern, UK. Polydispersity index (PDI), and standard deviation were obtained from three independent measurements of the dispersions of SNPs. Zeta potential of particles dispersions in ethanol and water were also measured. Scanning electron microscopy micrographs were conducted by the

Tescan Vega3 LMU scanning electron microscope (TESCAN, Kohoutovice, Czech Republic) and Denton Desk II sputter coated with a gold target (Denton Vacuum, NJ, USA). Nanoparticle separation required an Allegra 64R Centrifuge (Beckman Coulter Inc., Brea, CA). A SympHonly (SB20) pH-meter (Thermo Orion, MA, USA) was used for pH adjustment. Nano pure water was prepared using a Barnstead NANO pure DIamond Analytical ultrapure water system (Fischer Scientific, NJ, USA). All fluorescence spectra were performed on ISS K2 multifrequency cross-correlation phase and modulation fluorimeter (ISS™ Focus and Discover, Champaign, IL, USA), equipped with a 300W xenon arc lamp. A 1.0 cm disposable plastic was used for all fluorescence measurements. The nuclear magnetic resonance spectra were obtained using high quality Kontes NMR tubes (Kimble Chase, Vineland, NJ) rated to 500 MHz and were recorded on a Bruker Avance 400 MHz spectrometer interfaced to a PC using Topspin 3.1. High-resolution accurate mass spectra were obtained at the Georgia State University Mass Spectrometry Facility using a Waters Q-TOF micro (ESI-Q-TOF) mass spectrometer or utilizing a Waters Micromass LCT TOF ES+ Premier mass spectrometer.

5.3.2.5 Solvatochromic effect

The solvatochromic effect was studied by measuring the emission spectra of 5 mg/mL WA6-TA-T as well as the free WA6 dye (3.3×10^{-7} M) in different solvents including water, ethanol, and 0.1 M HCl using the ISS K2 fluorimeter.

5.3.2.6 Labeling efficiencies and dye leakage studies for the prepared FLSNPs

Labeling efficiencies are the fraction of added dye molecules actually incorporated in the SNPs [44] by comparing the fluorescence intensities of the remained free dyes with standard samples. For the dye leakage study, seven of the FLSNPs, sets of three samples of 22.5 mg for each type of the FLSNPs dispersed by sonication in 3 mL of a dispersant composed of ethanol

and water mixture (1:1, v/v) or (1:9, v/v) were prepared. After measuring the initial fluorescence, the samples were kept in the dark at room temperature. After 1 hour, the SNPs were centrifuged at 3200 rpm for 5 min. The supernatant was discarded, and the pellet of FLSNPs was resuspended in the corresponding dispersant. Then, the fluorescence signal of the FLSNPs suspensions was measured. This procedure was repeated with a different set of samples after 24 hours using a solvent composed of ethanol and water with a ratio of (1:9, v/v) [45].

5.3.2.7 LFPs detection using FLSNPs

Two methods for applying the resulting particles to latent prints were used; one used an aqueous suspension which consisted of discrete nanoparticles, and the second used the nanoparticles powder for dusting the LFPs. Fingerprints were collected from the same donor, a 26-year-old male and then developed after 24 hours of deposition. Fingerprints were obtained by requesting the donor firstly; to wash his hands thoroughly with the soap then rub his finger with his nose immediately prior to fingerprints deposition onto the tested surfaces. The photographs were recorded with luminescence mode using the forensic light source (FLS), Mini-CrimeScope 400 MCS-400 (Spex Forensics, Edison, NJ, USA) at excitation wavelength of 445 nm or crime scene search (CSS) settings. The fingerprint image was photographed using a digital camera (Nikon D3300) with a 540 nm long-pass filter. The sample was placed on a black surface to enhance the contrast of fingerprint image during illumination and taking pictures.

5.3.2.7.1 Use of FLSNPs suspensions as developing agents for LFPs

The particle suspension method was carried out with the glass slides substrates only as follows: a specific concentration of 2.5 mg/mL suspensions for each of the twelve FLSNPs in 9:1 (v/v) DI water: ethanol dispersant was prepared as the working suspension, then they were sonicated for 10 min to ensure sufficient particles dispersion. About 0.5-1.0 mL of the

suspension was pipetted onto the sample using a transfer pipette. After 5 minutes, the excess solution was removed, and the sample was gently washed with a mixture of 9:1 (v/v) DI water: ethanol. After that, the developed fingerprint sample was left to dry at room temperature.

5.3.2.7.2 Use of FLSNPs powders as developing agents for LFPs on various substrates

Five different substrate surfaces were tested in this investigation, namely; glass slide, petri dish (polystyrene), aluminum foil, common white paper, and the white area of paper currency. F-TA-TP was selected as representative hydrophobic FLSNPs in this investigation. The powder method was performed as follows: a commercial Lightning Powder Zephyr Fiberglass Fingerprint Brush was used to pick up some F-TA-TP powder, and then carefully applied to the surface of LFPs with a light brushing action. The excess powder was removed by using a hair dryer for 90 seconds.

5.3.2.8 Protein adsorption

WA6-T-T particles were selected as a representative for FLSNPs without surface hydrophobization whereas WA6-T-TP particles were selected as representative hydrophobic FLSNPs in this investigation to be compared with bare SNPs in terms of non-specific protein binding. HSA and IgG were used in this investigation where 1.5 mL of 10 mg/mL of IgG solution and 72 mg of HSA were dissolved in 10 and 18 mL pure water to get a 1.5 and 4.0 mg/mL stock solutions, respectively. WA6-T-T, WA6-T-TP and bare SNPs were dispersed in 10 mM isotonic PBS (pH = 7.4) buffer with a concentration of 5 mg/mL. Then 2 mL of each of the SNPs suspension were mixed with 2 mL of the corresponding protein solution and shook at 37 °C for 6 h at 100 rpm in the incubator. Finally, the mixture was centrifuged and the supernatant was measured using a UV spectrophotometer, the adsorbed protein was presented as adsorption efficiency (AE(wt.%)) and calculated. The absorption efficiency was calculated using the

following formula: AE (wt.%) = (Ci−Cf)/Cn × 100% Ci and Cf represents the initial and final protein concentration in the solution, respectively, Cn represent the concentration of the nanoparticles [46].

5.3.2.9 Hemolysis study

A hematology-3, sample hem-02, American proficiency institute (manufactured by Streck, LaVista, NE, USA) was used in this study. Red blood cells (RBCs) were isolated from a 2-mL sample by centrifugation for 10 min, and washed three times with sterile isotonic PBS solution. Following the last wash, RBCs were diluted 1:5 in sterile isotonic PBS solution. The RBCs suspension from the diluted sample (0.4 mL) was added into 1.2 mL of nanoparticles isotonic PBS suspension to reach a final concentration of 2 mg/mL. Bare SNPs, WA6-T-T, WA6-T-TP, WA6-TP-TP, WA6-TA-T, and WA6-TA-TP were used. The RBCs incubated with pure water and isotonic PBS solution were set as positive and negative controls, separately. The mixtures were shaken before being incubated for 1.5 h at 37 °C. Finally; the mixtures were centrifuged for 10 min, then the absorbance of the clear upper solutions at 538 nm were recorded by a UV spectrophotometer.

5.3.3 Results and discussion

5.3.3.1 Preparation method of the FLSNPs and labeling efficiency

The labeling efficiency and photophysical properties of FLSNPs intrinsically depend on the applied synthesis method. In this investigation, an amino acid-catalyzed seed regrowth method was used for the synthesis of twelve FLSNPs and tested for efficient control on the core and shell composition of the SNPs in order to achieve proper non-covalent embedding of the fluorescent reporters. The Stöber method has the advantages of simplicity besides avoiding using surfactants which requires extensive washing steps whereas controlling the particle size is easily

achieved using the WORM method, as nanoreactors of water droplets in the oil phase define the particles dimension [28]. Unlike the conventional methods such as Stöber [4] and WORM [5], ACSRT permits the synthesis of fluorescent SNPs in a water-based system, without the use of any surfactants or co-surfactants. By this approach, additional linkers for covalent coupling of the fluorophore to silica matrix were omitted, while a remarkable doping efficiency was achieved, Table 5.3.1 [7]. L-arginine was applied as a catalyst while the dye molecules were incorporated into the particle nuclei formed by hydrolysis and recondensation of three different organosilane monomers, namely; TEOS (logP 1.68), PTEOS (logP 3.25) and APTES (logP -1.83). Particle regrowth was achieved in the second stage due to the polymerization of either TEOS or its binary mixture with the more hydrophobic organosilicate precursor, PTEOS, or the polar oeganosilicate precursor, APTES, Table 5.3.1. Fluorescein (logP 3.4), Fluorescein isothiocyanate (logP 4.8) and WA6 (logP -1.1) have been used in this study. The logP of the novel WA6 dye was determined using the shake flask method based on the distribution between equal volumes of chloroform and water. Twelve different FLSNPs were prepared with tailored compositions for the core and the shell of the SNPs. From the results presented in Table 5.3.1, it was found that using TEOS as the sole organosilane precursor in the core and shell of F-T-T, FITC-T-T and WA6-T-T resulted in poor labeling efficiency of 15.8, 8.0, and 16.3 %, respectively, due to absence of efficient non-covalent interactions between the used dyes and the silica matrix. However, a labeling efficiency of 37.4% was obtained in the case of WA6-TA-T due to strong hydrogen bonding between the amino groups in APTES and the thiourea and hydroxyl groups in WA6. On the other hand, in case of F-T-TP and F-TP-TP, the incorporation of the hydrophobic PTEOS either in the shell only or both in the core and in the shell resulted in intermediate labeling efficiency of 44.9 and 52.6%, respectively, which can be attributed to the reasonable interactions between fluorescein

and the core as well as the successful encapsulation of the dye inside the hydrophobic silica shell. For F-TA-TP and WA6-TA-TP, the use of a mixture of TEOS and the polar APTES in the core of the SNPs allowed proper embedding of fluorescein and WA6 dye molecules with high labelling efficiency of 79.2% and 78.4%, respectively, through strong non-covalent interactions which were then entrapped by a hydrophobic shell composed of a mixture of TEOS and the hydrophobic PTEOS. Furthermore, FITC-T-TP should higher labeling efficiency than FITC-TP-TP of 74.5 and 53.6%, respectively. This can be attributed to the use of L-arginine that induces the stable incorporation of FITC into the TEOS based silica matrix in the core of FITC-T-TP. As the thiocyanate groups of FITC are reactive that they can bind to the amine groups of L-arginine forming a stable thiourea linkage. It is suggested that L-arginine, used as the catalyst in ACSRT, also plays a crosslinking role to bind the dye molecules to the silica matrix [6]. Finally, WA6-T-TP and WA6-TP-TP showed satisfactory labeling efficiencies of 63.9 and 72.4%, respectively which highlights the virtue of using a hydrophobic shell in achieving a successful encapsulation of dye molecules even the ones of low lipophilicity such as WA6 and fluorescein. It is worth noting that, APTES was not used for encapsulating FITC to avoid any interferences in the obtained labeling efficiency results as APTES can form a covalent thiourea linkage with FITC [38].

5.3.3.2 Particle characterization

The synthesized FLSNPs were characterized via different methods prior to the application to LFPs detection and hemocompatibility studies. The physical nature and dimensions of the particles were derived from the SEM scans and DLS for WA6-T-T, WA6-T-TP, WA6-TP-TP, WA6-TA-T and WA6-TA-TP, (Fig. 5.3.2, Table 5.3.2). Also, the mean hydrodynamic particle sizes and PDI measurements in deionized water by DLS for the used three

unlabeled seeds T, TP, and TP as well as for the unlabeled particles; T-T, T-TP, TP-TP, TA-T, and TA-TP were summarized in Table 5.3.3.

SEM micrographs showed that the labeled FLSNPs prepared using PTEOS had a smaller diameter and narrow size distribution in comparison with WA6-T-T and WA6-TA-T which were prepared under the same conditions, Table 5.3.2. The hydrophobic SNPs were composed of discrete monodispersed globular particles with an average diameter (SEM) of 33.4.6±5.9, 42.2±10.8, and 39.8±3.0 nm, for WA6-T-TP, WA6-TP-TP, and WA6-TA-TP, respectively, whereas the WA6-T-T and WA6-TA-T had an average diameter (SEM) of 1511.0±354.8 and 1428.26±116.3, respectively. The bigger size of the particles that don`t have PTEOS in their shell composition may be attributed to the higher rate of hydrolysis and recondensation of TEOS in comparison with PTEOS.

The hydrodynamic diameters for the seeds; T, TP, and TA as well as for the SNPs; T-T, T-T-1, T-TP, TP-TP, TA-T, and TA-TP were characterized using DLS, Table 5.3.3. The obtained hydrodynamic size data for the seeds and for the core-shell nanoparticles reflect the size of the regrowth shell which proved to be dependent on the nature of the used organosilane precursors and on the amount of the L-arginine catalyst in the regrowth step. When TEOS was used solely in the regrowth step, bigger particles was obtained.

The effect of the amount of L-arginine on the size of the prepared unmodified silica nanoparticles was investigated by varying the concentration of the amino acid catalyst in the regrowth step to be 0.0, 1.0, and 4.47 mmoles. As a control, no silica product was obtained at x=0, likely because of the lack of catalysis for the hydrolysis of TEOS followed by condensation of the resultant products. The DLS hydrodynamic diameter measurements with the composition of arginine varied are shown in Table 5.3.3. When the concentration of the basic amino acid was

decreased from 4.47 mmoles in the case of T-T to 1.0 mmoles in the case of T-T-1, the hydrodynamic dimeter decreased.

The zeta potential measurements for five unlabeled SNPs; T-T, T-TP, TP-TP, TA-T, and TA-TP were presented in Table 5.3.3 and Fig. 5.3.3. The obtained results showed that zeta potentials of the PTEOS-modified particles, T-TP, TP-TP and TA-TP, were less negative than the unmodified particles.

5.3.3.4 Dye leakage

The leakage of fluorescein, FITC and WA6 dye molecules from SNPs was also examined in this report. Fig. 5.3.4a shows the changes in fluorescence intensities from nine FLSNPs kept for 1 hour at room temperature in two different solvents composed of ethanol and water in the ratio of (1:1, v/v) or (1:9, v/v). The obtained results clearly highlight the advantage of using a lower ratio of ethanol to avoid a significant dye leakage as hydrophobicity of the dye plays an important role in this process. In Fig. 5.3.4b, the experiment was repeated for the seven FLSNPs in a solvent composed of ethanol and water in the ratio of (1:9, v/v) for 24 hours.

The obtained results show the virtue of using the polar APTES in the core of WA6-TA-T and F-TA-TP in achieving a stable non-covalent encapsulation of WA6 and fluorescein with only 21% and 33% decrease in fluorescence intensity after 1 hour in comparison with 72% decrease for WA6-TP-TP and F-T-TP and 69% for F-TP-TP, respectively. For FITC-T-TP and FITC-TP-TP, decreases of 45% and 43%, respectively, were obtained after 1 hour indicating the importance of having a core with a hydrophobic nature in minimizing the leakage of the relatively hydrophobic FITC dye molecules. On the other hands, WA6-TA-TP and WA6-T-TP showed average leakage results with decreases of 54% and 47% after an hour, respectively.

It is worth noting that using 10% ethanol in water was necessary to help the dispersion of the FLSNPs for the LFPs detection application. Moreover, it can be concluded that using the hydrophilic dye molecules in this study, WA6 and fluorescein along with keeping a nonhydrophobic composition for the core are extremely important in minimizing the dye leakage under the prescribed experimental conditions for developing LFPs using the pipetting method which is just a 20 min process.

5.3.3.5 Solvatochromic effect

Solvatochromic characteristics were studied for WA6-TA-T, which showed minimal dye leakage (Fig. 5.3.4), and compared to WA6 free dye by measuring their fluorescent spectra in three different solvents namely water, ethanol and 0.1M HCl, (Fig. 5.3.5 a&b). The normalized absorbance spectra of WA6-TA-T and the free dye were measured in water and ethanol, (Fig. 5.3.5 c &d). Free WA6 showed different fluorescence behaviors in the selected solvents, (Fig. 5.3.5a, Fig. 5.3.6).

This solvatochromic shift indicated the changes in the excited state energies of WA6 depending on solvents polarity [47]. According to previous reports [6, 48], the response profiles of SNPs prepared by Stöber and WORM show obvious solvent-dependent characteristics. This suggests that dye molecules are randomly localized near the SNP surface. As a consequence, the solvatochromic characteristics of these SNPs are the outcome of the behaviors of dye molecules with inhomogeneous localizations which can be minimized by using the ACSRT due to the protective architecture of silica in these FLSNPs [6]. A dense localization of fluorophores in the seeds can be reached before they get completely covered with silica in the regrowth step using ACSRT.

It was observed that WA6 showed no fluorescence at all in 0.1M HCl due to protonation of the carboxylic group in the presence of an acidic medium, (Fig. 5.3.5a). However, when the dye molecules were properly embedded in the seeds of WA6-TA-T, the fluorescence was retained, (Fig. 5.3.5b). Also, the normalized fluorescence spectra of the free WA6 dye in ethanol and water showed obvious stokes shift of about 18 nm (Fig. 5.3.5c) which was minimized to less than 9 nm in the case of WA6-TA-T, (Fig. 5.3.5d). These observations confirm that the incorporated dye molecules are inside the silica matrix and can be shielded effectively from the outside exposure featuring a higher photo-stability.

5.3.3.6 LFPs detection using FLSNPs

Two methods; dusting and SNPs suspensions pipetting were investigated to develop the resultant LFPs.

5.3.3.6.1 Use of FLSNPs suspensions as developing agents for LFPs

To investigate the binding affinity of FLSNPs to LFPs, suspensions of these particles were applied on a glass substrate as shown in Fig. 5.3.7 and Fig. 5.3.8. The nature of the precursors in the shell of the SNPs plays an important role in fingerprint detection. Also, the photographs for the developed fingerprints using white light source were presented in Fig. 5.3.9.

When a binary mixture of TEOS and PTEOS used in eight different FLSNPs, clear luminescent fingerprint ridges were obtained using CSS setting of the FLS viewed through a 540 nm long pass filter. The surface of the FLSNPs has been decorated with PTEOS which increases the hydrophobic interaction between the phenyl group of PTEOS and the sebaceous secretion in the fingerprint residue resulting in enhanced binding and detection of fingerprints. Despite the differences in hydrophobicity in the used fluorescent reporter, the efficiency of these

hydrophobic FLNPs as developing agents able to produce clear luminescent fingerprints with high contrast was observed and attributed to the PTEOS-modified hydrophobic surface.

When the surface was not coated with PTEOS in the case of F-T-T, FITC-T-T, WA6-T-T and WA6-TA-T, weak luminescence and poor contrast were obtained as shown in Fig. 5.3.8 a&e and Fig. 5.3.7a&e, respectively. Therefore, using these particles as developing agents for fingerprint detection is not practical.

Friction ridge features of a fingerprint have been classified into three levels of detail [35]. First- level detail describes the overall ridge pattern such as fingerprint orientation and ridge flow direction. The general information obtained from the first-level detail are not decisive. Thus, it cannot be used for personal identification. Second-level detail involves ridge formations and pattern minutiae such as ridge ending, bifurcation, and dots. Third-level detail includes the morphology of a ridge such as width, shape, and pores. Both second and third- level details enable identification and fingerprint matching due to the unique individual features.

The typical features of second-level detail of fingerprint friction ridge developed using WA6-TP-TP are shown in Fig. 5.3.7c, where well-defined ridges of fingerprint were observed displaying the sweat pores of the fingerprint, which is the typical feature of tertiary structure of fingerprint.

5.3.3.6.2 Use of FLSNPs powders as developing agents for LFPs on various substrates

The colloidal particle suspension method is not very suitable to be used in actual crime scenes due to its tedious procedure and low efficiency [19]. Subsequently, powder method was examined using F-TA-TP as developing agents to test the contrast and selectivity in LFPs detection. Five different substrate surfaces were tested in this investigation, namely; glass slide,

petri dish (polystyrene), aluminum foil, common white paper, and the white area of currency paper and the results are presented in Fig. 5.3.10 (CSS) and Fig. 5.3.11 (CSS and white light).

As shown in Fig. 5.3.10 and Fig. 5.3.12, F-TA-TP as developing agents can realize the LFPs development on the surface of nonporous substrates such as glass slides (Fig. 5.3.10a), common transparent polystyrene petri-dish (Fig. 5.3.10b), regular aluminum foil (Fig. 5.3.10c) as well as a porous surface such regular white papers (Fig. 5.3.10d). No clear contrast was obtained when F-TA-TP was tried to detect the details of LFPs on the surface of currency paper, (Fig. 5.3.10e). However, the margins of the LFPs and some details can still be observed.

5.3.3.7 Colloidal Stability

The aqueous dispersion stability of five SNPs namely; T-T, T-TP, TP-TP, TA-T, and TA-TP, has been investigated over seven days. 0.5 mg/mL suspensions in deionized water from each SNPs type were used in this study. As shown in Fig. 5.3.13a&b, the five SNPs showed good suspension stability for 1 and 3 hours, respectively. After two days (Fig. 5.3.13c) and seven days (Fig. 5.3.13d), only the hydrophobic NPs; T-TP, TP-TP, and TA-TP remained as one phase showing a good colloidal stability whereas T-T and TA-T, which were not modified with PTEOS, started to show phase separation. Moreover, the DLS measurements of the hydrodynamic diameter of the PTEOS-modified SNPs did not show any significant increase in size after seven days whereas T-T and TA-T showed an obvious increase in size, Table 5.3.3. These results suggest the potential of using these hydrophobic NPs at low concentrations for bio-related applications [49].

5.3.3.8 Protein adsorption

The adsorption of proteins to surfaces involves electrostatic interactions and Van der Waals binding forces [50]. Therefore proteins tend to adsorb more strongly to nonpolar than to

polar, and to charged than to neutral substrates [51]. Bare unmodified SNPs with rich surface silanol groups possess negatively charged surface potential is expected to show nonspecific binding to HSA and IgG. Hence, in this study, WA6-T-T (-34.1 ± 8.1 mV) with comparable charge to bare SNPs (Table 5.3.3) and WA6-T-TP (-26.1 ± 7.5 mV) with the surface coated with PTEOS of a lower charge were tested for reducing nonspecific protein adsorption. To evaluate the efficiency of this modification in minimizing nonspecific protein adsorption, the amount of HSA or IgG adsorbed on the surface of WA6-T-T, WA6-T-TP and bare SNPs were quantified. The adsorption efficiency (%) of HSA decreased from 2.64 wt.% for bare SNPs to 0.0 wt.% for WA6-T-T and WA6-T-TP whereas for IgG it dropped from 7.55 wt.% of bare SNPs to 1.36% and 3.77% wt.% for WA6-T-T and WA6-T-TP, respectively (Fig. 5.3.14). These results indicate the reduced non-specific protein binding of the tested FLSNPs and promising potential for biological applications.

5.3.3.9 Hemolysis study

In-vivo applications of bare SNPs for drug delivery are highly limited by their nonnegligible hemolytic effect [46] which is caused by the generation of reactive oxygen species induced by the surface of silica, denaturation of membrane proteins, and the high binding affinity of the tetra-alkyl ammonium groups that are abundant in the membranes of RBCs for the silanol groups [52]. To assess the effect of surface modification and hydrophobization on the hemocompatibility of FLSNPs, hemolytic effect of samples to RBCs was investigated. Five SNPs with different composition namely, WA6-T-T, WA6-T-TP, WA6-TP-TP, WA6-TA-T, and WA6-TA-TP were compared with the same concentration of unmodified bare SNPs in this study. In addition, to quantify the extent of hemolysis, concentration of hemoglobin released in the

supernatant was measured by UV absorbance of the supernatant at 538 nm. As shown in Fig. 5.3.15.

In the chosen concentration 2 mg/mL, none of the selected FLSNPs suspension showed obvious hemolysis after 1.5 h in comparison with the bare SNPs, which caused a hemolysis of 14.02%, where the three hydrophobic FLSNPs WA6-T-TP, WA6-TP-TP and WA6-TA-TP resulted in very low hemolysis of 1.29, 1.02, and 1.13%, respectively. Also, WA6-T-T and WA6-TA-T resulted in a low hemolysis of 2.06 and 1.61%, respectively. The obtained results indicated that increasing the surface hydrophobicity of the FLSNPs resulted in very good hemocompatibility at concentrations up to 2mg/mL. For FLSNPs modified with PTEOS, the interactions between the exposed silanol groups and the membrane surface of RBCs are minimized, thereby reducing hemolytic effects.

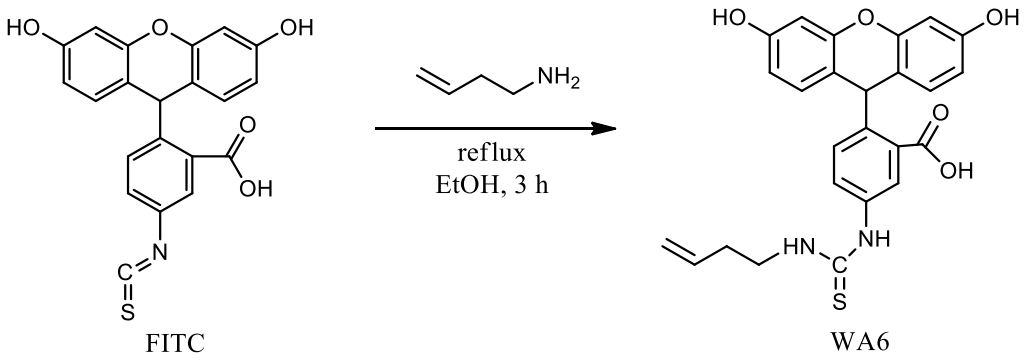

Scheme 5.3.1 Synthesis of WA6

Table 5.3.1 Used fluorophores and composition for the core and shell of the labeled SNPs and their labeling efficiencies

FLSNPs	Fluorophore	Core composition	Shell composition	Labelling efficiencies (%)
F-T-T	Fluorescein	TEOS	TEOS	15.8
F-T-TP	Fluorescein	TEOS	TEOS + PTEOS	44.9
F-TP-TP	Fluorescein	TEOS + PTEOS	TEOS + PTEOS	77.6
F-TA-TP	Fluorescein	TEOS + APTES	TEOS + PTEOS	79.2
FITC-T-T	FITC	TEOS	TEOS	8.0
FITC-T-TP	FITC	TEOS	TEOS + PTEOS	74.5
FITC-TP-TP	FITC	TEOS + PTEOS	TEOS + PTEOS	53.6
WA6-T-T	WA6	TEOS	TEOS	16.3
WA6-T-TP	WA6	TEOS	TEOS + PTEOS	63.9
WA6-TP-TP	WA6	TEOS + PTEOS	TEOS + PTEOS	72.4
WA6-TA-T	WA6	TEOS + APTES	TEOS	37.4
WA6-TA-TP	WA6	TEOS + APTES	TEOS + PTEOS	78.4

Table 5.3.2 Diameter determined by TEM and DLS, polydispersity index (PDI), zeta potential of 0.1 mg/ml labeled SNPs in ethanol

FLSNPs	Diameter (SEM) (nm)	Diameter (DLS) (nm)	PDI
WA6-T-T	1511.0 ± 354.8*	1096.0 ± 40.9	0.999
WA6-T-TP	33.4 ± 5.9*	217.1 ± 34.9	0.903
WA6-TP-TP	42.2 ± 10.8*	138.2 ± 11.4	0.774
WA6-TA-T	1428.26 ± 116.3*	994.2 ± 177.2	0.449
WA6-TA-TP	39.8 ± 9.4*	196.6± 28.5	0.724

* SD where n=21

Table 5.3.3 Diameter determined by DLS, polydispersity index (PDI), zeta potential of 0.1 mg/ml unlabeled SNPs in water

	FLSNPs	Diameter (DLS) (nm)	PDI	Zeta potential (mV)
	T seeds	13.1 ± 2.3	0.317	
	TP seeds	219.5 ± 68.4	0.557	
	TA seeds	396.1 ± 55.5	1.000	
Fresh samples	**T-T**	911.9 ± 177.6	0.672	-34.1 ± 8.1
	T-TP	385.2 ± 146.6	0.328	-26.1 ± 7.5
	TP-TP	471.8 ± 280.6	0.291	-28.6 ± 6.0
	TA-T	1051 ± 373.6	0.365	-21.9 ± 6.6
	TA-TP	465.1 ± 284.5	0.363	-24.2 ± 8.2
	T-T-1	178.8 ± 49.7	0.473	
After seven days	**T-T**	1239.0 ± 341.7	0.278	
	T-TP	333.3 ± 135.4	0.281	
	TP-TP	392.3 ± 178.7	0.375	
	TA-T	1438.0 ± 546.3	0.233	
	TA-TP	343.2 ± 155.3	0.430	

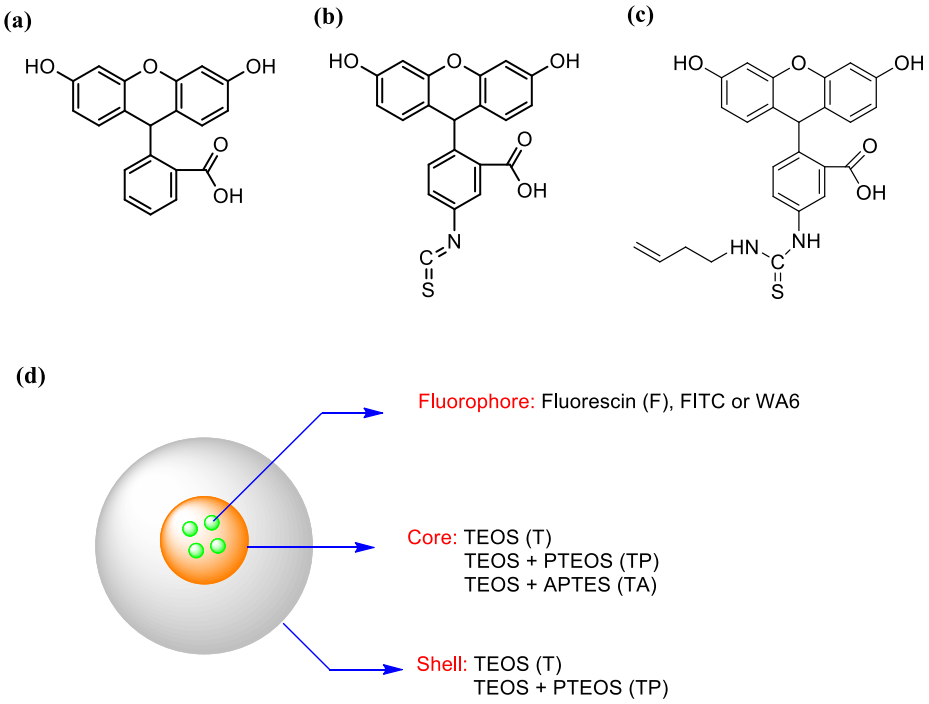

Figure 5.3.1 The structure formulae for (a) fluorescein, (b) FITC, and (c) WA6 as well as (d) illustration of core and shell composition of the proposed FLSNP

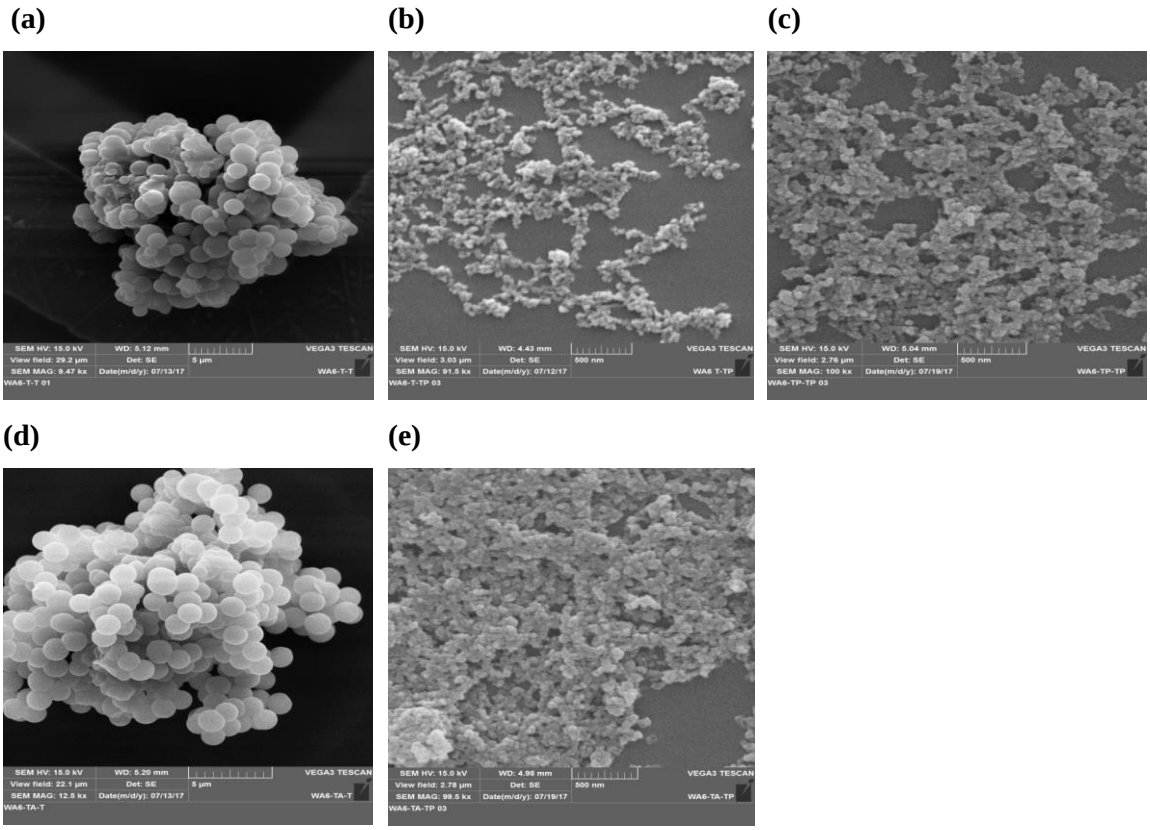

Figure 5.3.2 SEM micrographs of (a) WA6-T-T, (b) WA6-T-TP, (c) WA6-TP-TP, WA6-TA-T and (e) WA6-TA-TP

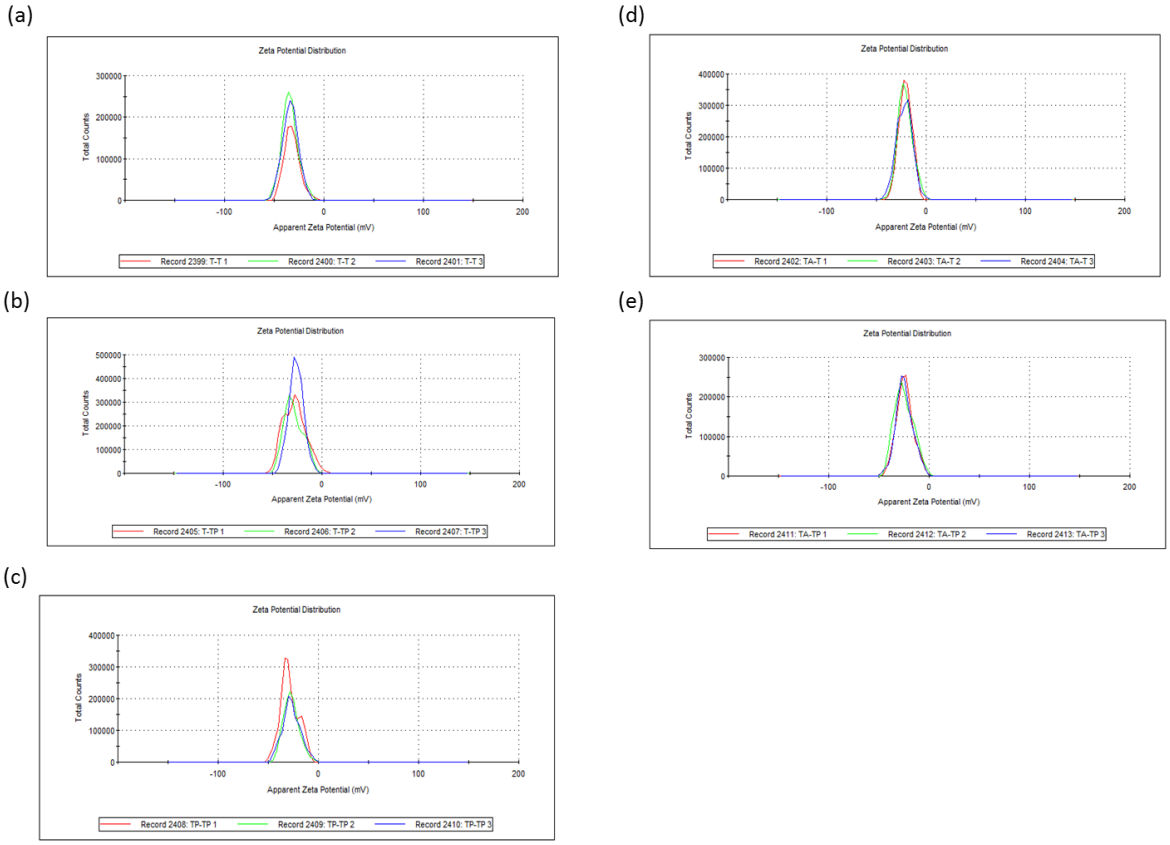

Figure 5.3.3 Zeta potential measurements of 0.1 mg/ml SNPs dispersions in deionized water; (a) T-T, (b) T-TP, (c) TP-TP, (d) TA-T, and (e) TA-TP

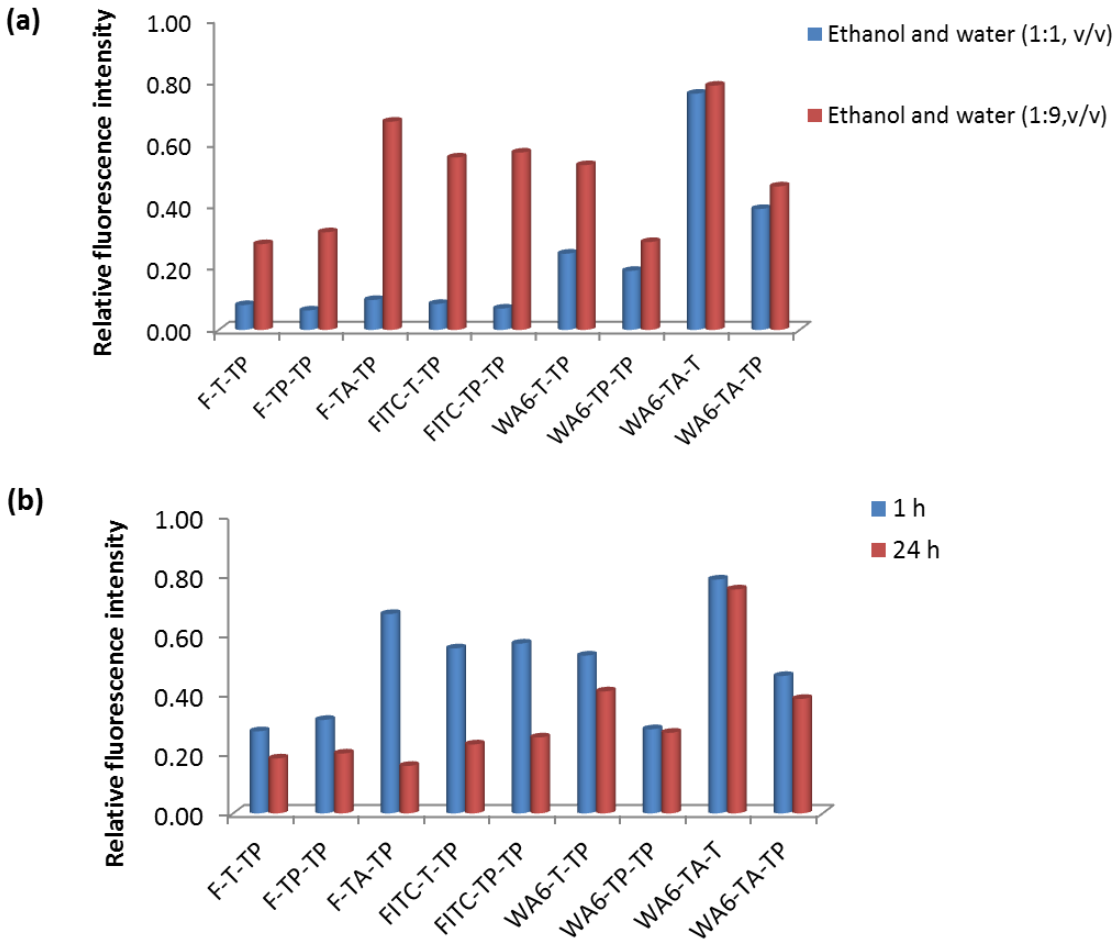

Figure 5.3.4 Dye leakage from nine of the FLSNPs. Fluorescence intensity change of 7.5 mg/mL FLSNPs kept at room temperature in dark at λex of 485 nm (a) after 1 hour in a solvent composed of ethanol and water in the ratio of (1:1, v/v) or (1:9, v/v), (b) after 24 hours in a solvent composed of ethanol and water (1:9, v/v)

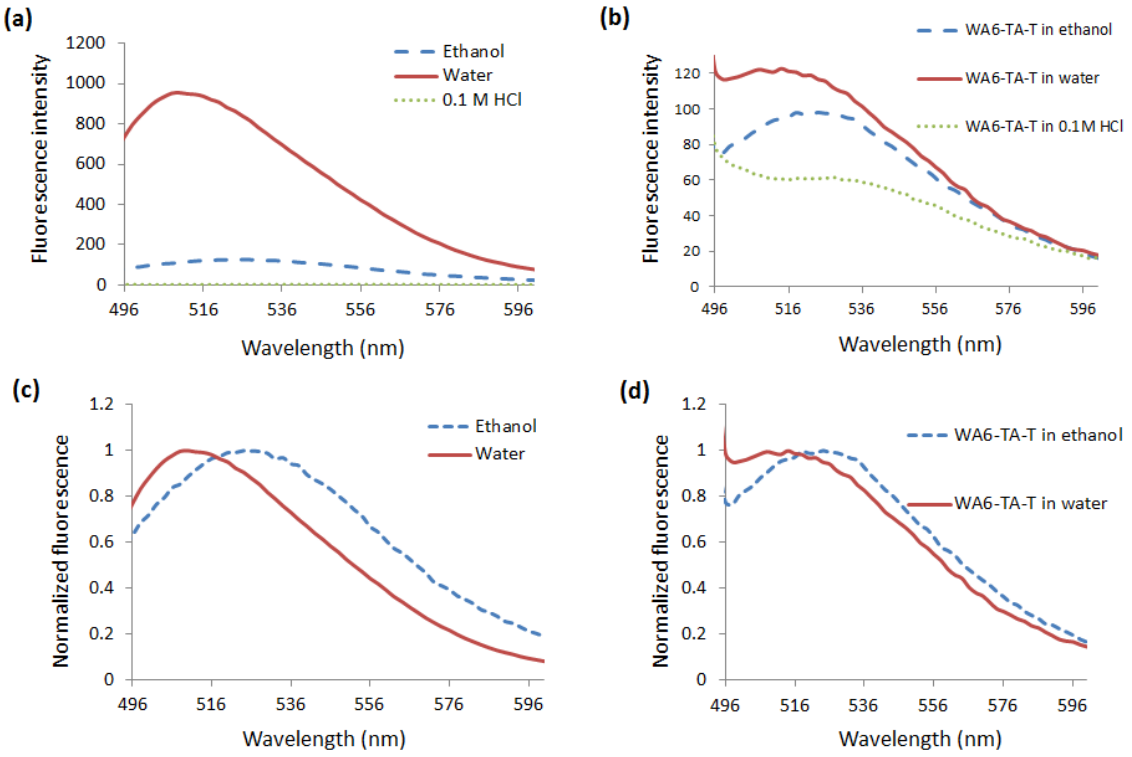

Figure 5.3.5 Fluorescence spectra for (a) free WA6 dye (b) WA6-TA-T in water, ethanol and 0.1 M HCl and the normalized fluorescence spectra for (c) free WA6 dye (d) WA6-TA-T in water and ethanol, indicating the solvatochromic behavior

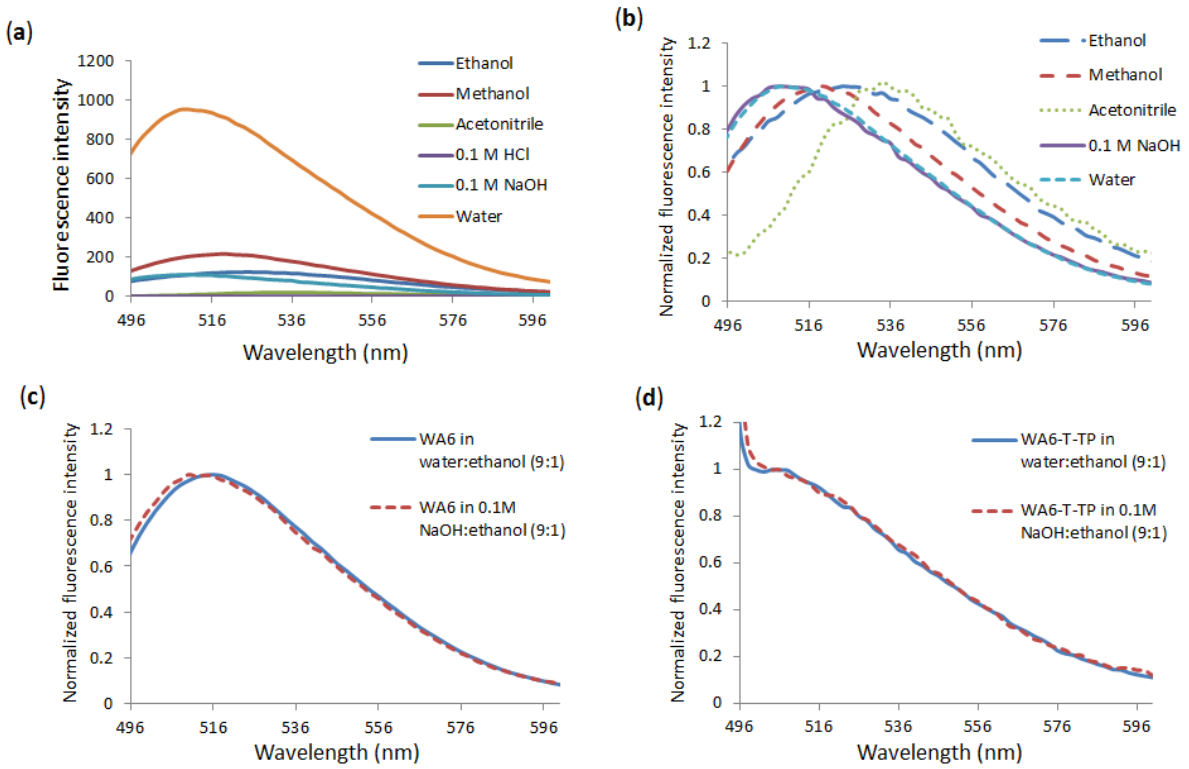

Figure 5.3.6 Fluorescence spectra for (a) free WA6 dye in water, ethanol, methanol, acetonitrile, 0.1 M HCl, and 0.1 M NaOH (b) normalized fluorescence spectra for free WA6 dye in water, ethanol, methanol, acetonitrile and 0.1 M NaOH (c) normalized fluorescence spectra for free WA6 dye in water: ethanol (9:1, v/v) and 0.1M NaOH: ethanol (9:1, v/v), and (d)) normalized fluorescence spectra for WA6-T-TP dye in water: ethanol (9:1, v/v) and 0.1M NaOH: ethanol (9:1, v/v), indicating solvatochromic behavior

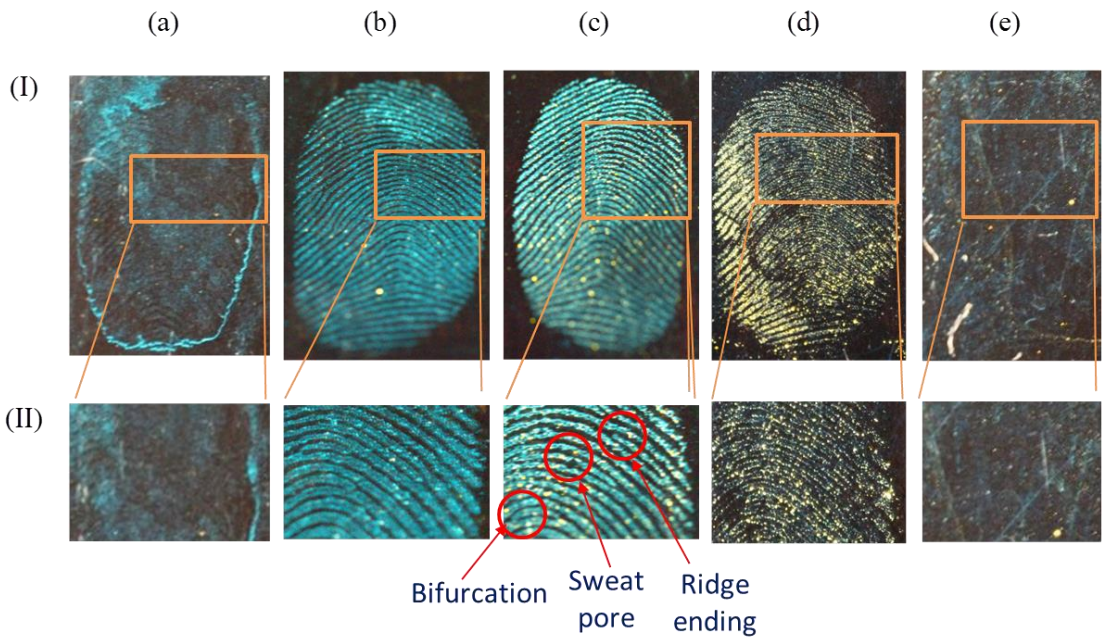

Figure 5.3.7 Fluorescence images of the fingerprints on glass slides developed using 2.5 mg/mL FLSNPs suspensions in water: ethanol (9:1, v/v) of (a) WA6-T-T, (b) WA6-T-TP, (c) WA6-TP-TP, (d) WA6-TA-TP, and (e) WA6-TA-T at CSS FLS setting and emission filter of 540 nm, (II) is the magnified part in (I)

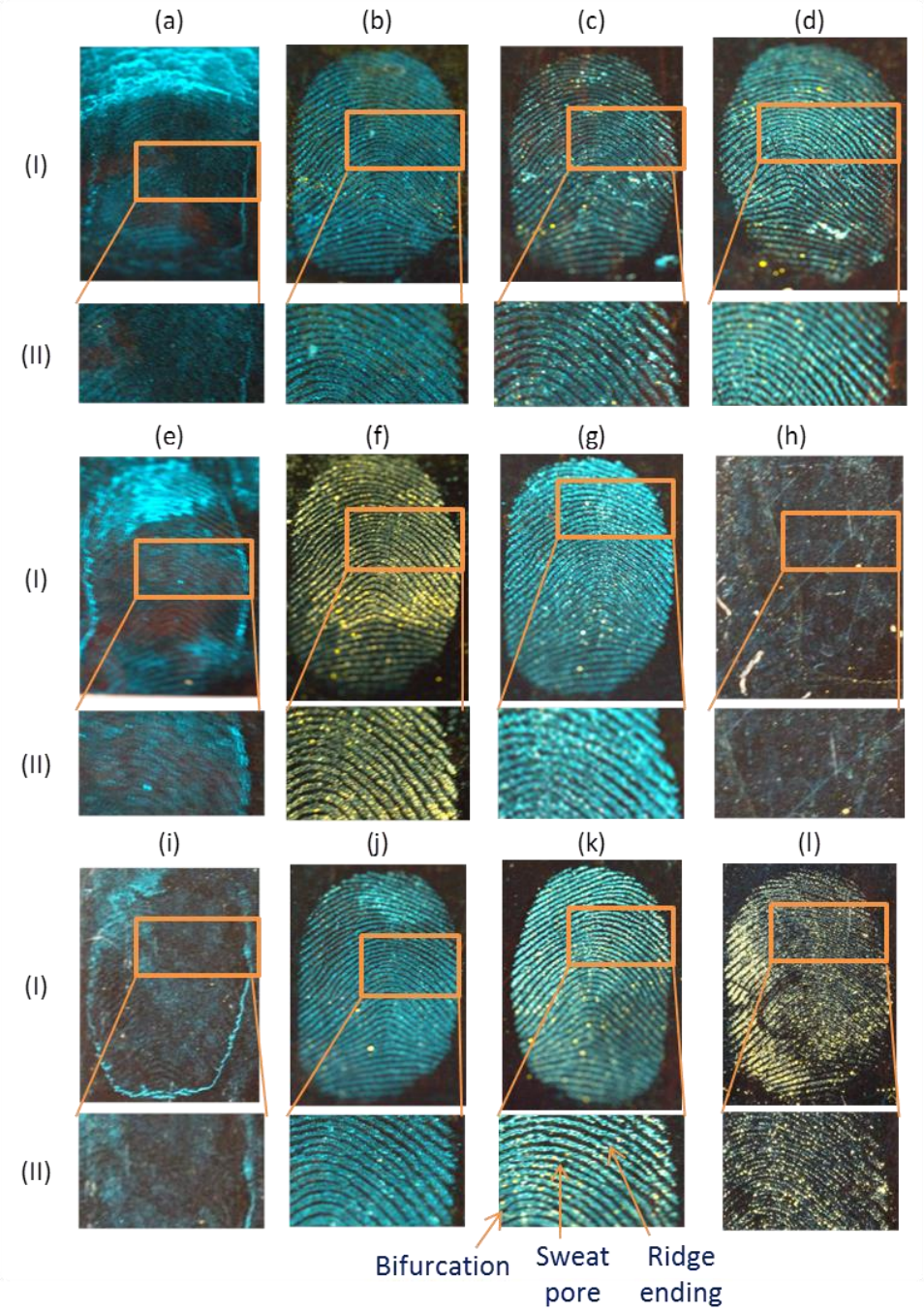

Figure 5.3.8 Fluorescence images of the fingerprints on glass slides developed using 2.5 mg/mL FLSNPs suspensions in water: ethanol (9:1, v/v) of (a) F-T-T, (b) F-T-TP, (c) F-TP-TP, (d) F-TA-TP, (e) FITC-T-T, (f) FITC-T-TP, (g) FITC-TP-TP, (h) WA6-TA-T, (i) WA6-T-T, (j) WA6-T-TP, (k) WA6-TP-TP, and (l) WA6-TA-TP at CSS FLS setting and emission filter of 540 nm, (II) is the magnified part in (I)

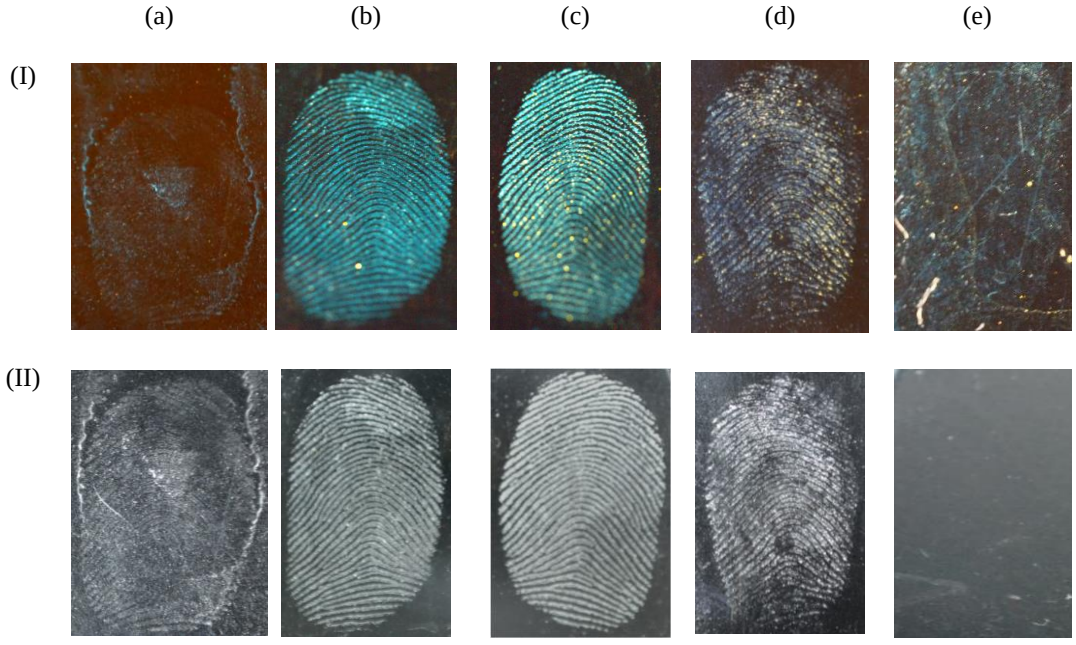

Figure 5.3.9 Images of the fingerprints on glass slides developed using 2.5 mg/mL FLSNPs suspensions in water: ethanol (9:1, v/v) for (a) WA6-T-T, (b) WA6-T-TP, (c) WA6-TP-TP, (d) WA6-TA-TP, and (e) WA6-TA-T at (I) CSS FLS setting and emission filter of 540 nm, and (II) white light source

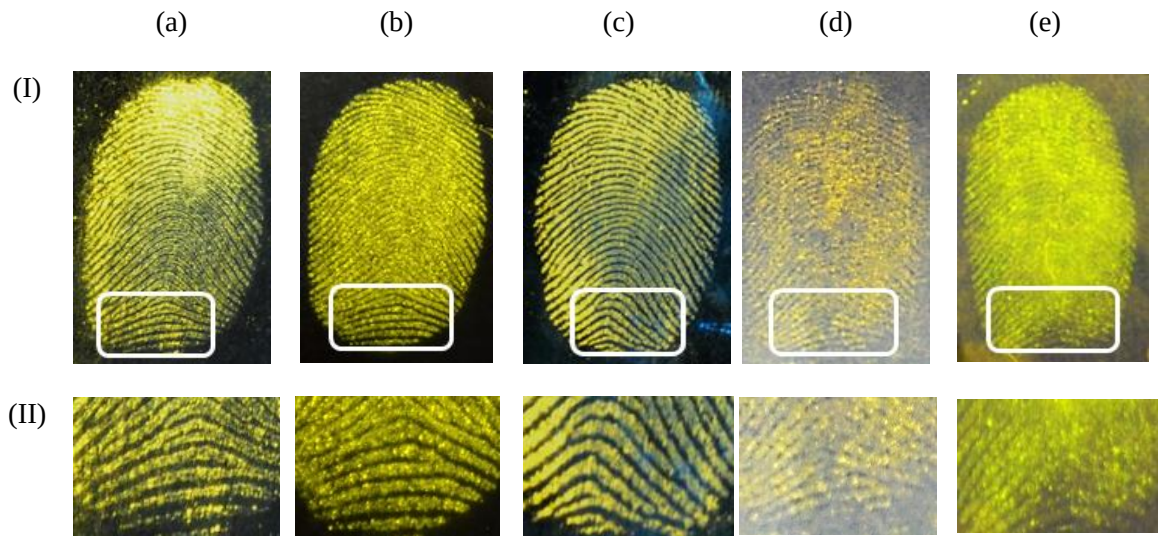

Figure 5.3.10 Photographs LFPs developed with F-TA-TP powder on different substrates: (a) glass slide, (b) petri dish (polystyrene), (c) aluminum foil, (d) common white paper, and (e) the white area of currency paper, (II) is the magnified part in (I)

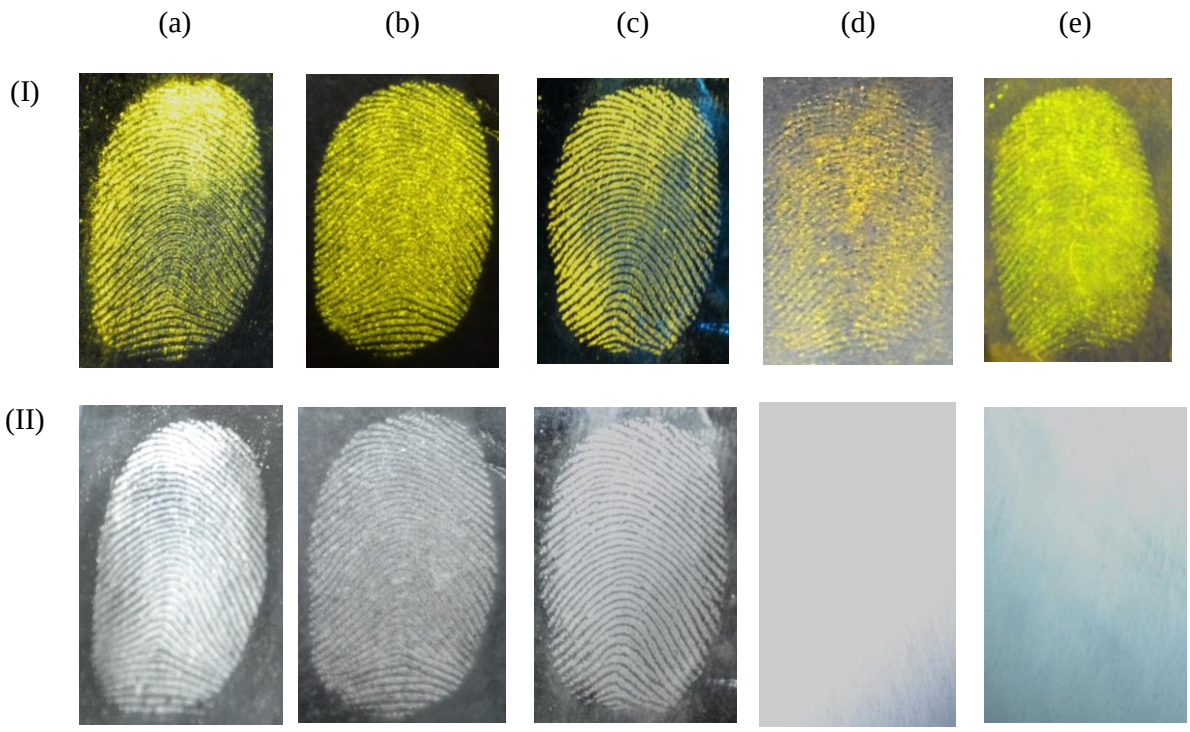

Figure 5.3.11 Photographs LFPs developed with F-TA-TP powder on different substrates: (a) glass slide, (b) petri dish (polystyrene), (c) aluminum foil, (d) common white paper, and (e) the white area of currency paper using (I) CSS FLS setting and emission filter of 540 nm, and (II) white light source

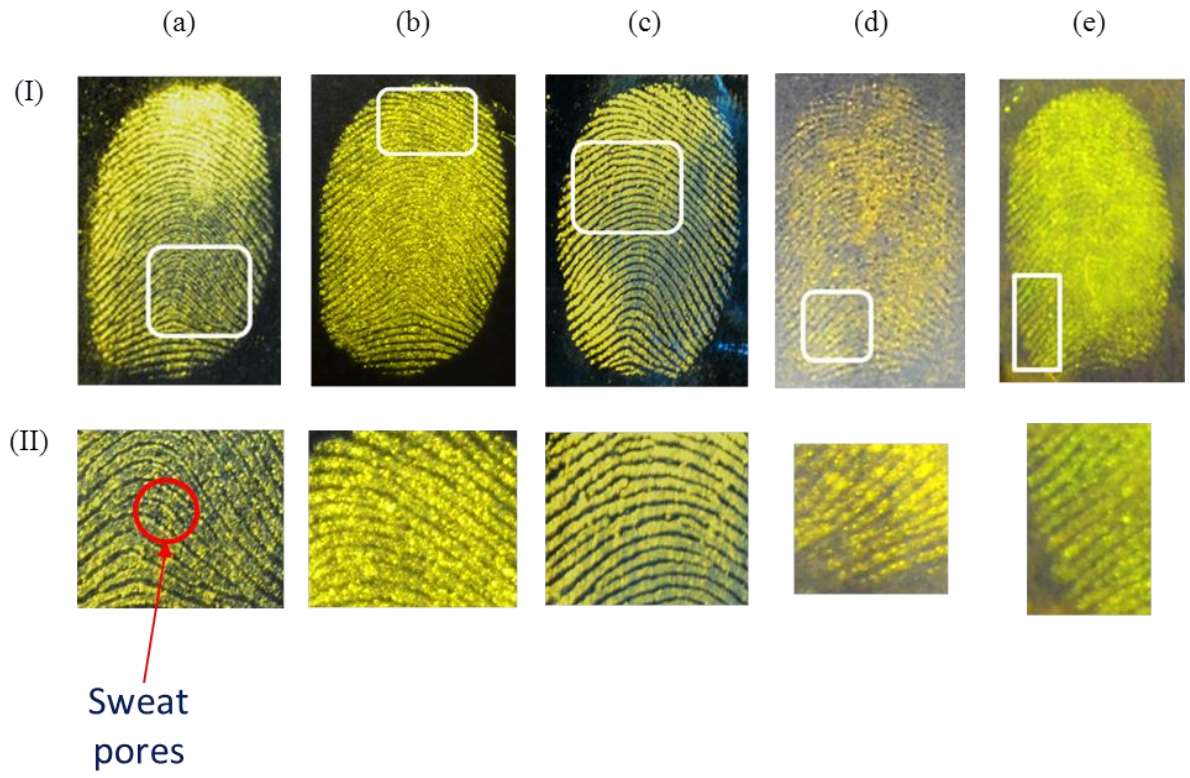

Figure 5.3.12 Photographs LFPs developed with F-TA-TP powder on different substrates: (a) glass slide, (b) polystyrene, (c) Aluminum foil, (d) common white paper, and (e) the white area of money paper, (II) is the magnified part in (I)

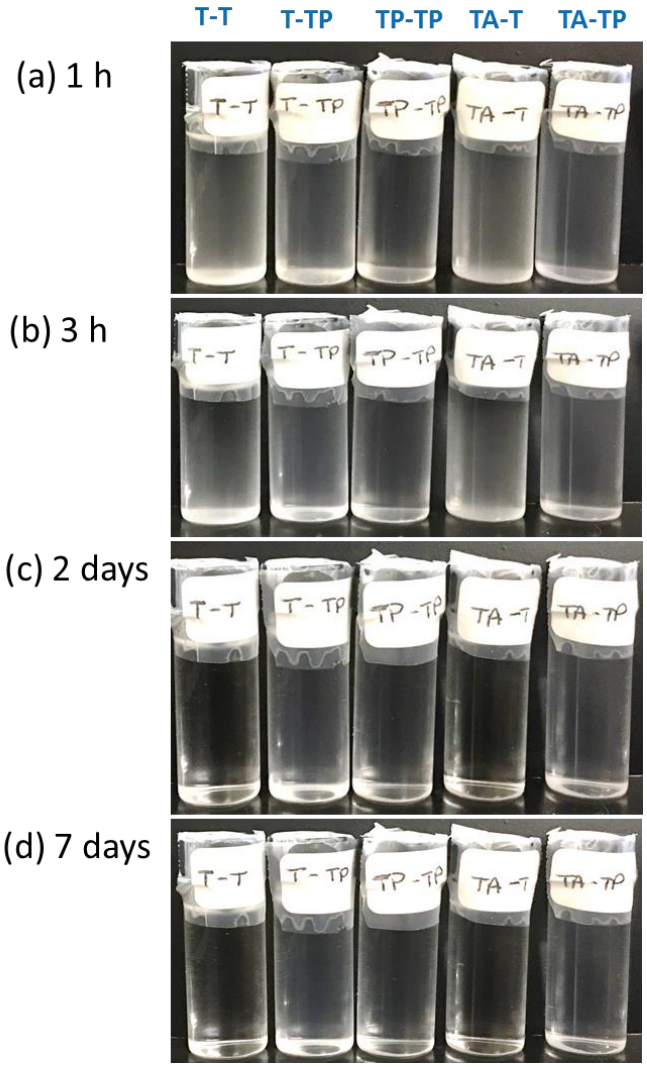

Figure 5.3.13 Photographs of sealed vials that show the phase behavior of 0.5 mg/ml SNPs dispersions in deionized water at (a) 1 h, (b) 3 h, (c) 2 days, and (d) 7 days

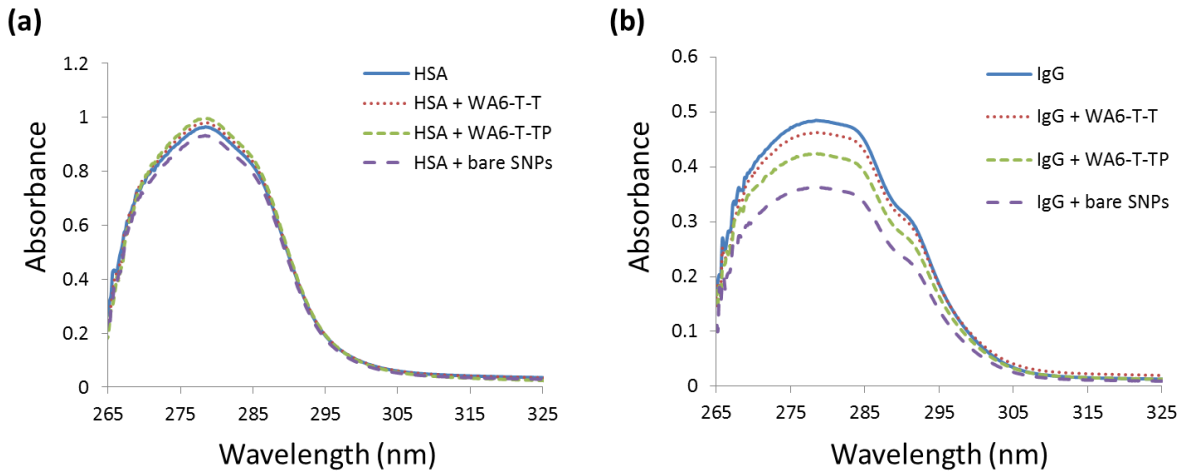

Figure 5.3.14 UV–Vis absorbance of (a) HSA and (b) IgG solutions after interaction with WA6-T-T, WA6-T-TP and bare SNPs suspensions

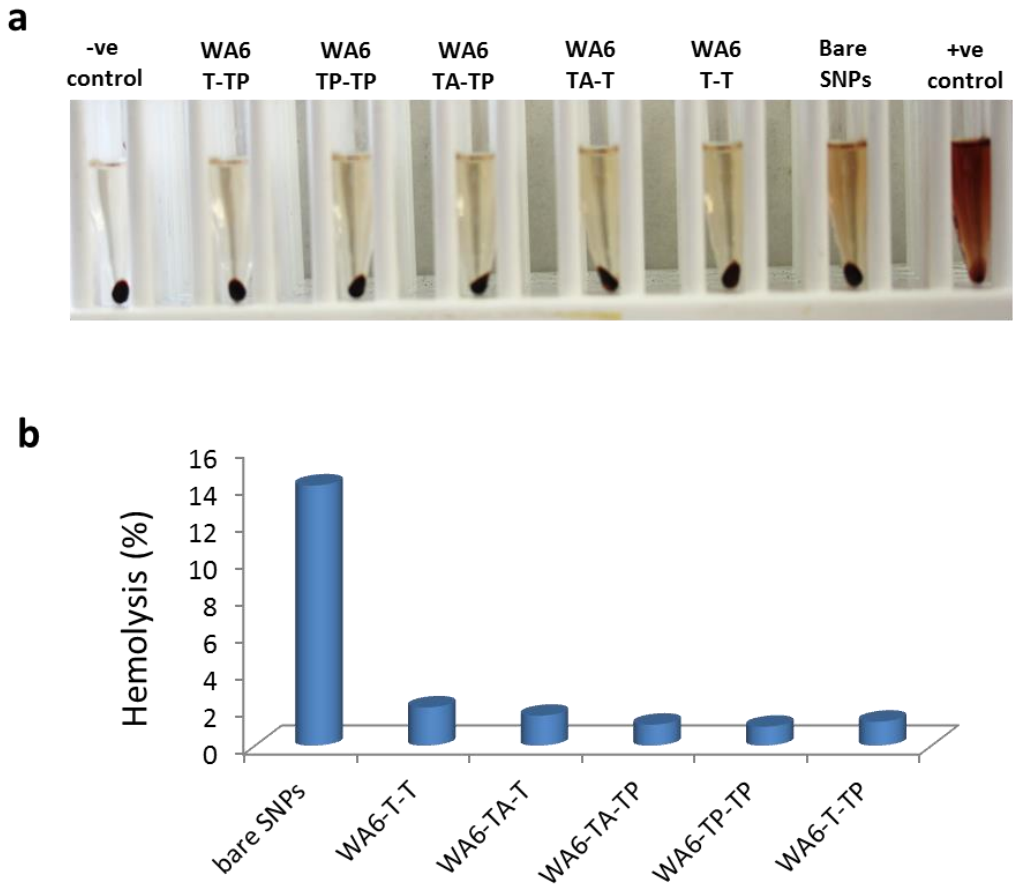

Figure 5.3.15 Hemolysis test results after 1.5 h incubation with 2mg/mL from each of bare SNPs, WA6-T-T, WA6-T-TP, WA6-TP-TP, WA6-TA-T, and WA6-TA-TP suspensions: (a) optical images and (b) relative hemolysis (%) from measuring the UV absorbance at 538 nm

5.4 Conclusions

Uniform F-SNPs with a small particle size with diameters in the range of 4.1-110.4 nm were fabricated using seven different routes and characterized by DLS and SEM and spectrofluorometric measurements in section 5.2. In this study, a systematic investigation of several factors affecting the efficiency of developing fingerprints was carried out. FITC as a representative dye was loaded into the NPs matrix in order to increase the contrast of the developed fingerprints while the nanometer-sized particles improve the resolution of the developed fingerprints. It was found that the most important factor affecting this application was the hydrophobic nature of the F-SNPs. This can be obtained by using a mixture of TEOS and PTEOS alkoxyilane precursors during the formation of the NPs. This allowed proper loading of the used hydrophobic fluorophore and at the same time increased the binding affinity to hydrophobic components of the fingerprints. The obtained results indicated that the developed NPs are effective in fingerprint detection when the surface is modified with functional groups have the potential to react particularly with the most abundant components present in the fingerprint residue and not with the substrate. Therefore, FCTPS, FCTPS-RM, and FDTPS are considered good fingerprints developing agents as they developed clear luminescent fingerprints with good contrast. Both Stöber and WORM methods can be used for F-SNPs synthesis. However, Stöber method is simpler and more cost-effective. Moreover, FITC can be non-covalently or covalently encapsulated after being conjugated with APTES into the silica matrix with efficient fingerprints detection results obtained. However, the FCA covalently bonded-SNPs are more stable and show no dye leakage. In addition, although the less hydrophobic F-SNPs were coated on the surface with PVP to increase the binding affinity to fingerprints, they did not result in any enhancement effect on fingerprints development. Thus, these systematic

investigations demonstrate the features that the dye-encapsulated NPs should hold in order to be utilized as reliable developing agents for fingerprints forensic applications. This insight may be applied to the preparation of a range of stable dye covalently or non-covalently loaded-NPs. In addition, a major understanding of these factors will provide the elemental basis for the effective utilization of similar dye-encapsulated NPs in other fields such as nanomedicine, tissue imaging, drug delivery and theranostics.

On the basis of the previously reported basic amino acids-catalyzed approaches for preparing silica nanoparticles [6-8], the work presented in section 5.3 has demonstrated that the dye encapsulation efficiency and other photophysical properties of the FLSNPs intrinsically depend on the applied synthesis route and on the composition of the core-shell structures. In this study, an amino acid-catalyzed seed regrowth method was used for the synthesis of twelve FLSNPs with controllable size and tunable hydrophobicity for both the core and shell of the SNPs. The mean diameters of the hydrophobic FLSNPs were between 33.4±5.9 and 42.2±10.8 nm as shown by the SEM measurements. The obtained results clearly highlight the advantages of surface hydrophobization for clear visualization of LFPs, broadly similar to what was observed from reported doped hydrophobic SNPs [39]. With maximizing the non-covalent interactions between the core of the SNPs and dye molecules, as in the case of F-TA-TP, even dyes of low hydrophobicity such as fluorescein and WA6 were used successfully in developing LFPs. Moreover, high dye encapsulation efficiency, high fluorescence intensity, enhanced stability against dye leaking were obtained, for example, WA6-TA-T, where the composition of both the core and the shell of the FLSNPs was made suitable for achieving strong non-covalent interactions with the dye molecules. Furthermore, the selected FLSNPs had superior hemocompatibility in comparison with bare silica nanoparticles in terms of minimizing the non-

specific binding with plasma proteins and decreasing the hemolysis rates. On the other hand, dyes with alkene side chain such as WA6 have the potential to be covalently copolymerized into the silica matrix in order to achieve higher stability instead of the commonly used APTES-conjugation route, a feature similar to those reported about several other silane-modified organic dye molecules [53]. Moreover, it is reported that the globular and less ordered hydrophobic materials have lower hemolytic effects compared with the ordered structures which match the obtained hemocompatibility results presented in this work [54].

Finally, the modified hydrophobic nanoparticles developed here have a great potential to impact many bio-related and diagnostic applications such as immunoassays and cell imaging purposes [54].

References

1. Burns, A.; Ow, H.; Wiesner, U. Fluorescent core-shell silica nanoparticles: towards "Lab on a Particle" architectures for nanobiotechnology. Chem. Soc. Rev. 2006, 35 (11), 1028-1042.
2. Liang, J.; Xue, Z.; Xu, J.; Li, J.; Zhang, H.; Yang, W. Highly efficient incorporation of amino-reactive dyes into silica particles by a multi-step approach. Colloids and Surfaces A: Physicochemical and Engineering Aspects 2013, 426, 33-38.
3. Rampazzo, E.; Bonacchi, S.; Juris, R.; Montalti, M.; Genovese, D.; Zaccheroni, N.; Prodi, L.; Rambaldi, D. C.; Zattoni, A.; Reschiglian, P. Energy transfer from silica core-surfactant shell nanoparticles to hosted molecular fluorophores. The journal of physical chemistry. B 2010, 114 (45), 14605-13.
4. Stöber, W.; Fink, A.; Bohn, E. Controlled growth of monodisperse silica spheres in the micron size range. Journal of Colloid and Interface Science 1968, 26 (1), 62-69.
5. Bagwe, R. P.; Yang, C.; Hilliard, L. R.; Tan, W. Optimization of Dye-Doped Silica Nanoparticles Prepared Using a Reverse Microemulsion Method. Langmuir 2004, 20 (19), 8336-8342.
6. Shahabi, S.; Treccani, L.; Rezwan, K. A comparative study of three different synthesis routes for hydrophilic fluorophore-doped silica nanoparticles. Journal of Nanoparticle Research 2016, 18 (1), 28.
7. Shahabi, S.; Treccani, L.; Rezwan, K. Amino acid-catalyzed seed regrowth synthesis of photostable high fluorescent silica nanoparticles with tunable sizes for intracellular studies. Journal of Nanoparticle Research 2015, 17 (6), 270.

8. Yokoi, T. Syntheses and Applications of Well-ordered Porous Silicas by Using Anionic Surfactants and Basic Amino Acids. Journal of the Japan Petroleum Institute 2012, 55 (1), 13-26.
9. Fouilloux, S.; Taché, O.; Spalla, O.; Thill, A. Nucleation of Silica Nanoparticles Measured in Situ during Controlled Supersaturation Increase. Restructuring toward a Monodisperse Nonspherical Shape. Langmuir 2011, 27 (20), 12304-12311.
10. Champod, C.; Lennard, C.; Margot, P.; Stoilovic, M. Fingerprints and Other Ridge Skin Impressions. CRC Press: Boca Raton, 2004.
11. Becue, A.; Moret, S.; Champod, C.; Margot, P. Use of stains to detect fingermarks. Biotechnic & Histochemistry 2011, 86 (3), 140-160.
12. Kim, Y. J.; Jung, H. S.; Lim, J.; Ryu, S. J.; Lee, J. K. Rapid Imaging of Latent Fingerprints Using Biocompatible Fluorescent Silica Nanoparticles. Langmuir 2016, 32 (32), 8077-8083.
13. Moret, S.; Becue, A.; Champod, C. Functionalised silicon oxide nanoparticles for fingermark detection. Forensic Science International 2016, 259, 10-18.
14. Leggett, R.; Lee-Smith, E. E.; Jickells, S. M.; Russell, D. A. "Intelligent" fingerprinting: Simultaneous identification of drug metabolites and individuals by using antibody-functionalized nanoparticles. Angew. Chem.-Int. Edit. 2007, 46 (22), 4100-4103.
15. Gao, D.; Li, F.; Song, J.; Xu, X.; Zhang, Q.; Niu, L. One step to detect the latent fingermarks with gold nanoparticles. Talanta 2009, 80 (2), 479-483.
16. Cai, K.; Yang, R.; Wang, Y.; Yu, X.; Liu, J. Super fast detection of latent fingerprints with water soluble CdTe quantum dots. Forensic Science International 2013, 226 (1–3), 240-243.

17. Liu, J.; Shi, Z.; Yu, Y.; Yang, R.; Zuo, S. Water-soluble multicolored fluorescent CdTe quantum dots: Synthesis and application for fingerprint developing. Journal of Colloid and Interface Science 2010, 342 (2), 278-282.

18. Mi, C.; McBean, K.; Ping, N.; McDonagh, A.; Maynard, P.; Lennard, C.; Roux, C. An evaluation of nanostructured zinc oxide as a fluorescent powder for fingerprint detection. Journal of Materials Science 2008, 43 (2), 732.

19. Zhang, M.; Ou, Y.; Du, X.; Li, X.; Huang, H.; Wen, Y.; Zhang, X. Systematic study of dye loaded small mesoporous silica nanoparticles for detecting latent fingerprints on various substrates. Journal of Porous Materials 2017, 24 (1), 13-20.

20. Huang, W.; Li, X. J.; Wang, H. F.; Xu, X. J.; Liu, H.; Wang, G. Q. Synthesis of Amphiphilic Silica Nanoparticles for Latent Fingerprint Detection. Anal. Lett. 2015, 48 (9), 1524-1535.

21. Theaker, B. J.; Hudson, K. E.; Rowell, F. J. Doped hydrophobic silica nano- and micro-particles as novel agents for developing latent fingerprints. Forensic Science International 2008, 174, 26-34.

22. Gao, F.; Tang, L.; Dai, L.; Wang, L. A fluorescence ratiometric nano-pH sensor based on dual-fluorophore-doped silica nanoparticles. Spectrochimica Acta Part A: Molecular and Biomolecular Spectroscopy 2007, 67 (2), 517-521.

23. Finnie, K. S.; Bartlett, J. R.; Barbé, C. J. A.; Kong, L. Formation of Silica Nanoparticles in Microemulsions. Langmuir 2007, 23 (6), 3017-3024.

24. Santra, S.; Zhang, P.; Wang, K.; Tapec, R.; Tan, W. Conjugation of Biomolecules with Luminophore-Doped Silica Nanoparticles for Photostable Biomarkers. Analytical Chemistry 2001, 73 (20), 4988-4993.

25. van Blaaderen, A.; Vrij, A. Synthesis and Characterization of Monodisperse Colloidal Organo-silica Spheres. Journal of Colloid and Interface Science 1993, 156 (1), 1-18.

26. Lian, W.; Litherland, S. A.; Badrane, H.; Tan, W.; Wu, D.; Baker, H. V.; Gulig, P. A.; Lim, D. V.; Jin, S. Ultrasensitive detection of biomolecules with fluorescent dye-doped nanoparticles. Analytical biochemistry 2004, 334 (1), 135-44.

27. Santra, S.; Wang, K.; Tapec, R.; Tan, W. Development of novel dye-doped silica nanoparticles for biomarker application. Journal of biomedical optics 2001, 6 (2), 160-6.

28. Auger, A.; Samuel, J.; Poncelet, O.; Raccurt, O. A comparative study of non-covalent encapsulation methods for organic dyes into silica nanoparticles. Nanoscale Res Lett 2011, 6 (1), 328.

29. Tapec, R.; Zhao, X. J.; Tan, W. Development of organic dye-doped silica nanoparticles for bioanalysis and biosensors. Journal of nanoscience and nanotechnology 2002, 2 (3-4), 405-9.

30. Van Blaaderen, A.; Vrij, A. Synthesis and characterization of colloidal dispersions of fluorescent, monodisperse silica spheres. Langmuir 1992, 8 (12), 2921-2931.

31. Ethiraj, A. S.; Hebalkar, N.; Kharrazi, S.; Urban, J.; Sainkar, S. R.; Kulkarni, S. K. Photoluminescent core-shell particles of organic dye in silica. Journal of Luminescence 2005, 114 (1), 15-23.

32. Canton, G.; Riccò, R.; Marinello, F.; Carmignato, S.; Enrichi, F. Modified Stöber synthesis of highly luminescent dye-doped silica nanoparticles. Journal of Nanoparticle Research 2011, 13 (9), 4349-4356.

33. Gao, X.; He, J.; Deng, L.; Cao, H. Synthesis and characterization of functionalized rhodamine B-doped silica nanoparticles. Optical Materials 2009, 31 (11), 1715-1719.

34. Moret, S.; Becue, A.; Champod, C. Nanoparticles for fingermark detection: an insight into the reaction mechanism. Nanotechnology 2014, 25 (42), 10.

35. Vanderkolk, J. R. Examination Process. In The Fingerprint Sourcebook., Holder, E. H.; Robinson, L. O.; Laub, J. H., Eds. Washington, DC : U.S. Dept. of Justice, Office of Justice Programs, National Institute of Justice, [2011]: 2011.

36. Lee, J. Intrinsic adhesion properties of poly(vinyl pyrrolidone) to pharmaceutical materials: humidity effect. Macromolecular bioscience 2005, 5 (11), 1085-93.

37. Benahmed, A.; Ranger, M.; Leroux, J. C. Novel polymeric micelles based on the amphiphilic diblock copolymer poly(N-vinyl-2-pyrrolidone)-block-poly(D,L-lactide). Pharmaceutical Research 2001, 18 (3), 323-328.

38. Wacker, J. B.; Lignos, I.; Parashar, V. K.; Gijs, M. A. M. Controlled synthesis of fluorescent silica nanoparticles inside microfluidic droplets. Lab on a Chip 2012, 12 (17), 3111-3116.

39. Theaker, B. J.; Hudson, K. E.; Rowell, F. J. Doped hydrophobic silica nano- and micro-particles as novel agents for developing latent fingerprints. Forensic Science International 2008, 174 (1), 26-34.

40. De, M.; Ghosh, P. S.; Rotello, V. M. Applications of Nanoparticles in Biology. Advanced Materials 2008, 20 (22), 4225-4241.

41. Becue, A.; Moret, S.; Champod, C.; Margot, P. Use of stains to detect fingermarks. Biotechnic & histochemistry : official publication of the Biological Stain Commission 2011, 86 (3), 140-60.

42. Benton, M.; Rowell, F.; Sundar, L.; Jan, M. Direct detection of nicotine and cotinine in dusted latent fingermarks of smokers by using hydrophobic silica particles and MS. Surface and Interface Analysis 2010, 42 (5), 378-385.

43. Pirollo, K. F.; Chang, E. H. Does a targeting ligand influence nanoparticle tumor localization or uptake? Trends in biotechnology 2008, 26 (10), 552-8.

44. Imhof, A.; Megens, M.; Engelberts, J. J.; de Lang, D. T. N.; Sprik, R.; Vos, W. L. Spectroscopy of Fluorescein (FITC) Dyed Colloidal Silica Spheres. The Journal of Physical Chemistry B 1999, 103 (9), 1408-1415.

45. Quan, B.; Choi, K.; Kim, Y. H.; Kang, K. W.; Chung, D. S. Near infrared dye indocyanine green doped silica nanoparticles for biological imaging. Talanta 2012, 99, 387-93.

46. Zhou, G.; Li, L.; Xing, J.; Cai, J.; Chen, J.; Liu, P.; Gu, N.; Ji, M. Layer-by-layer construction of lipid bilayer on mesoporous silica nanoparticle to improve its water suspensibility and hemocompatibility. Journal of Sol-Gel Science and Technology 2017, 82 (2), 490-499.

47. Blechinger, J.; Herrmann, R.; Kiener, D.; García-García, F. J.; Scheu, C.; Reller, A.; Bräuchle, C. Perylene-Labeled Silica Nanoparticles: Synthesis and Characterization of Three Novel Silica Nanoparticle Species for Live-Cell Imaging. Small (Weinheim an der Bergstrasse, Germany) 2010, 6 (21), 2427-2435.

48. Alberto, G.; Caputo, G.; Viscardi, G.; Coluccia, S.; Martra, G. Molecular Engineering of Hybrid Dye–Silica Fluorescent Nanoparticles: Influence of the Dye Structure on the Distribution of Fluorophores and Consequent Photoemission Brightness. Chemistry of Materials 2012, 24 (14), 2792-2801.

49. Ujiie, H.; Shimojima, A.; Kuroda, K. Synthesis of colloidal Janus nanoparticles by asymmetric capping of mesoporous silica with phenylsilsesquioxane. Chemical Communications 2015, 51 (15), 3211-3214.

50. Kurrat, R.; Prenosil, J. E.; Ramsden, J. J. Kinetics of Human and Bovine Serum Albumin Adsorption at Silica–Titania Surfaces. Journal of Colloid and Interface Science 1997, 185 (1), 1-8.

51. Rabe, M.; Verdes, D.; Seeger, S. Understanding protein adsorption phenomena at solid surfaces. Advances in Colloid and Interface Science 2011, 162 (1), 87-106.

52. Slowing, I. I.; Wu, C.-W.; Vivero-Escoto, J. L.; Lin, V. S. Y. Mesoporous Silica Nanoparticles for Reducing Hemolytic Activity Towards Mammalian Red Blood Cells. Small (Weinheim an der Bergstrasse, Germany) 2009, 5 (1), 57-62.

53. Kim, Y.-J.; Jung, H.-S.; Lim, J.; Ryu, S.-J.; Lee, J.-K. Rapid Imaging of Latent Fingerprints Using Biocompatible Fluorescent Silica Nanoparticles. Langmuir 2016, 32 (32), 8077-8083.

54. Paula, A. J.; Montoro, L. A.; Filho, A. G. S.; Alves, O. L. Towards long-term colloidal stability of silica-based nanocarriers for hydrophobic molecules: beyond the Stober method. Chemical Communications 2012, 48 (4), 591-593.

APPENDIX

^{1}H NMR, and HRMS Spectra

a-

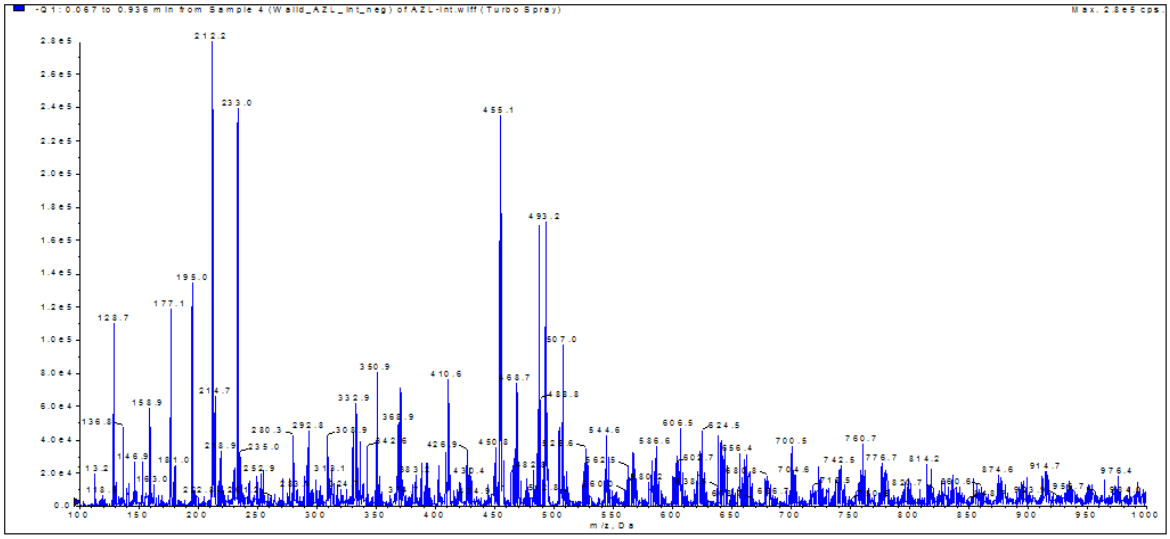

b-

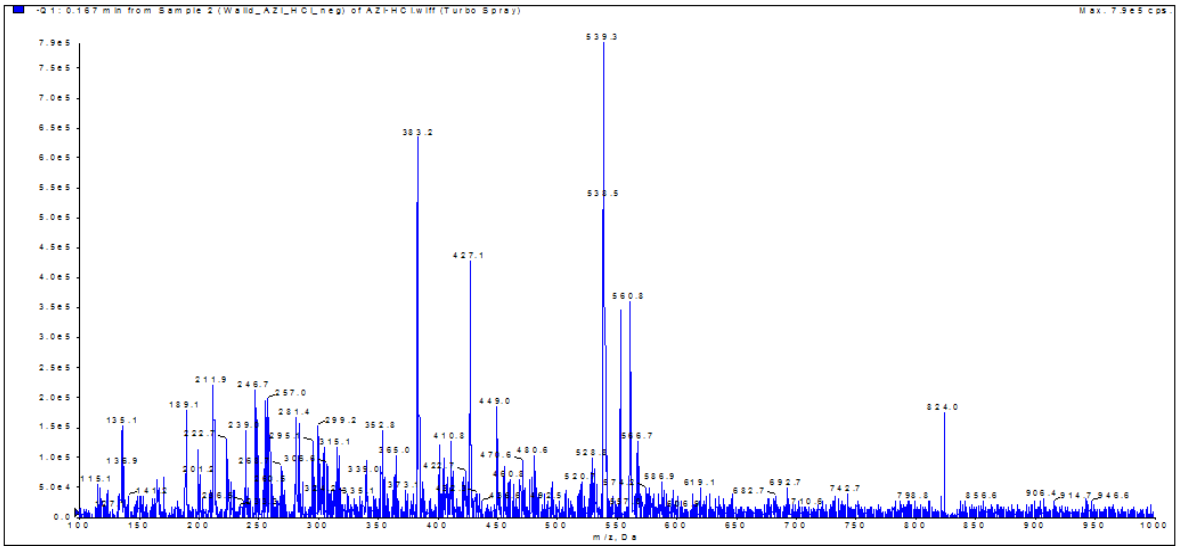

LC-MS ion chromatograms for (a) intact AZL (b) acid induced degradation products of AZL.

a-

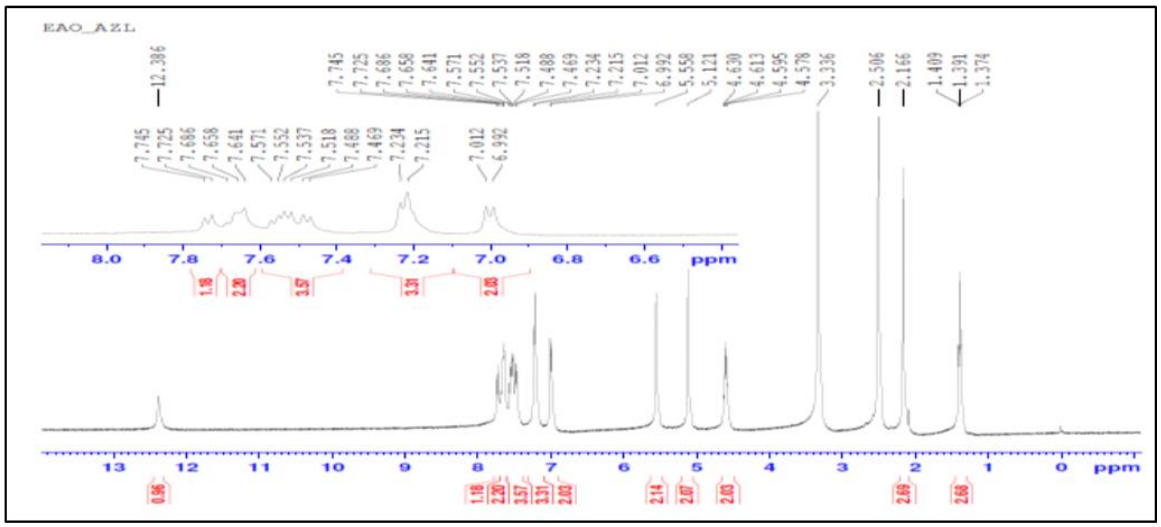

b-

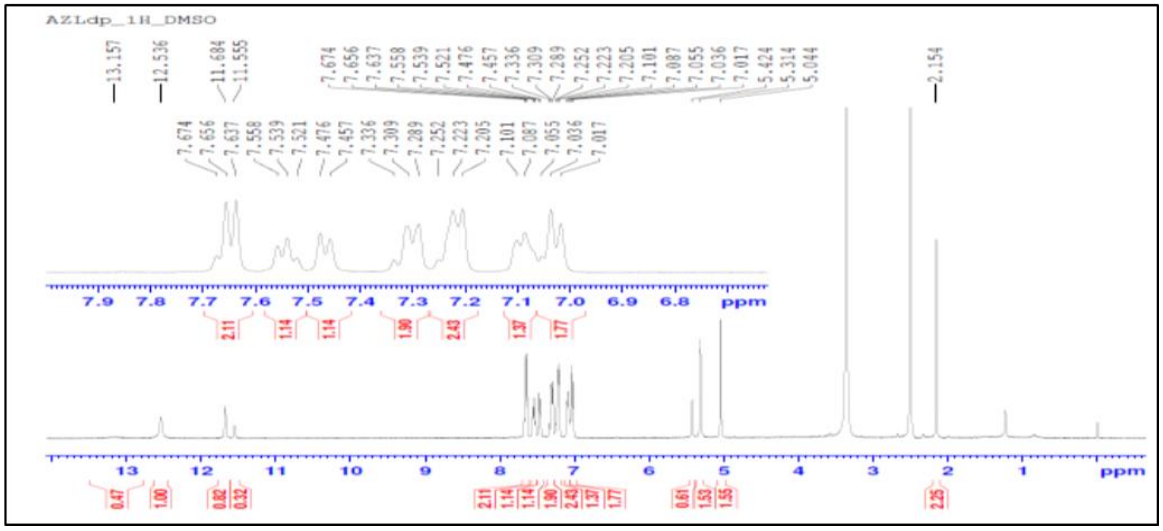

[1]HNMR spectra (400 MHz, DMSO-d6) for (a) intact AZL (b) acid induced degradation products of AZL.

a-

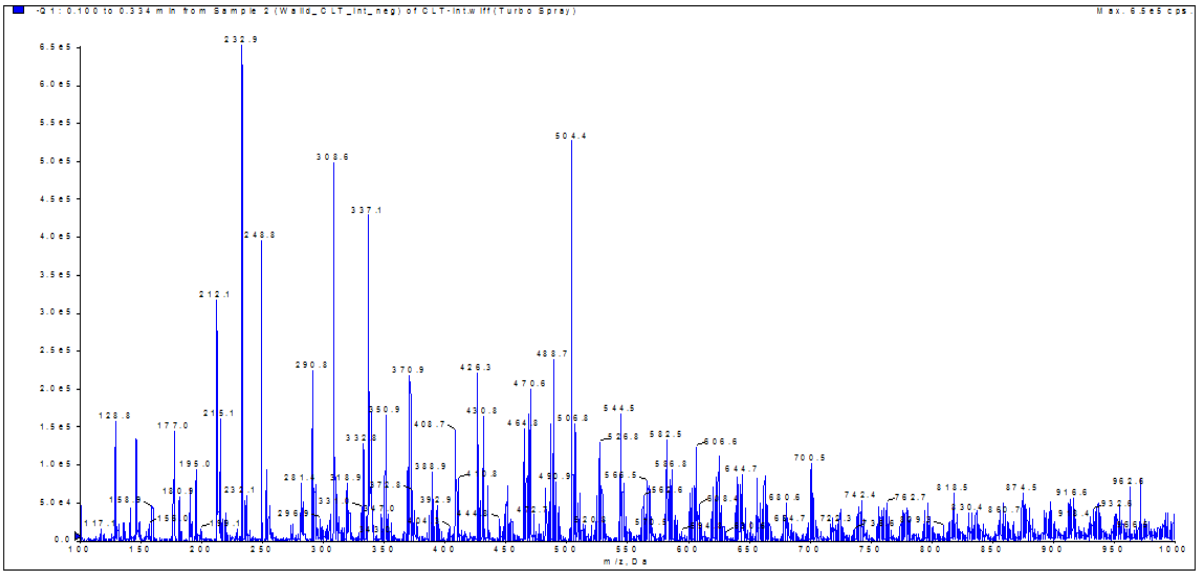

b-

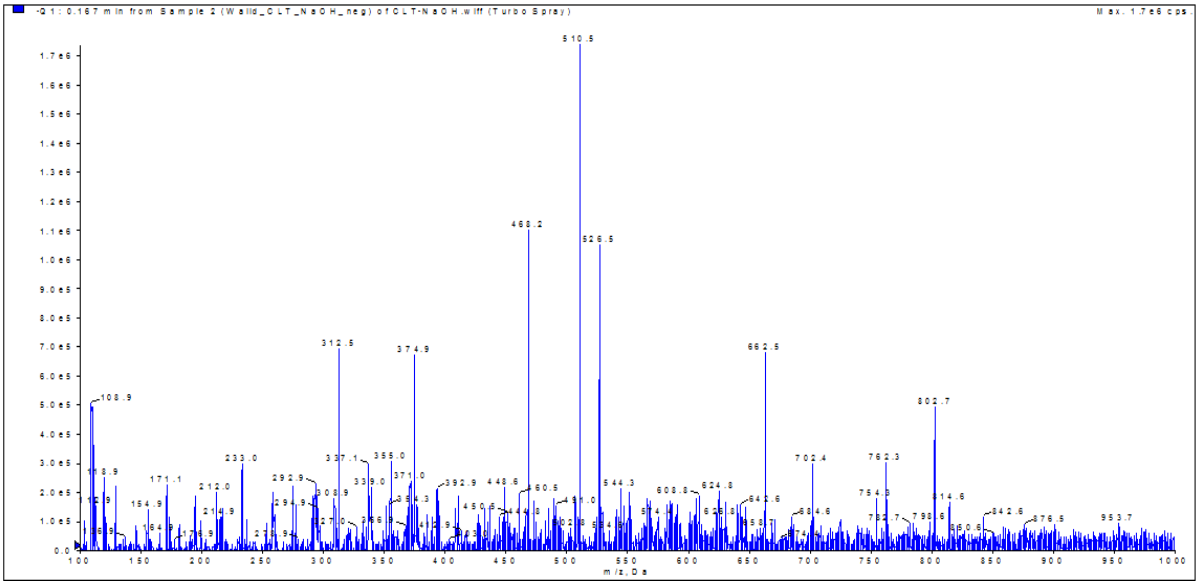

LC-MS ion chromatograms for (a) intact CLT and (b) alkaline induced degradation products of CLT.

a-

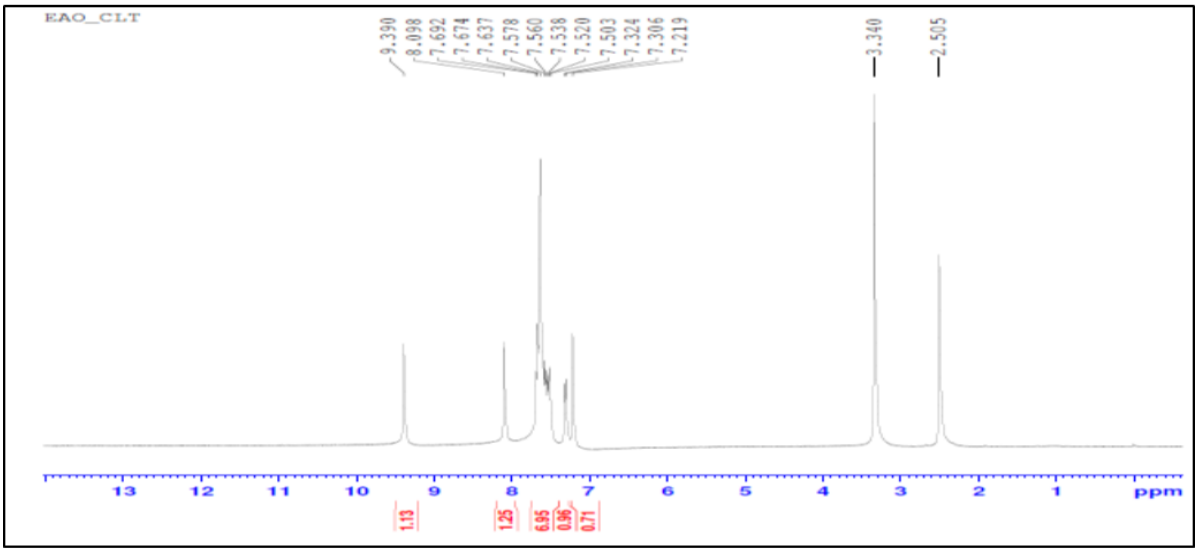

b-

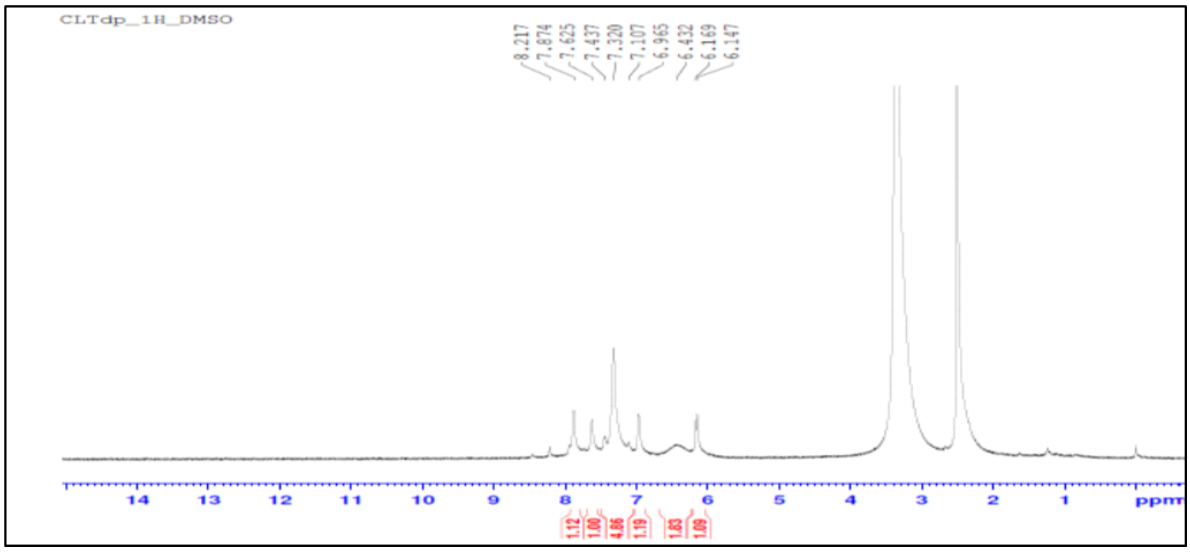

[1]HNMR spectra (400 MHz, DMSO-d6) for (a) intact CLT (b) alkaline induced degradation products of CLT.

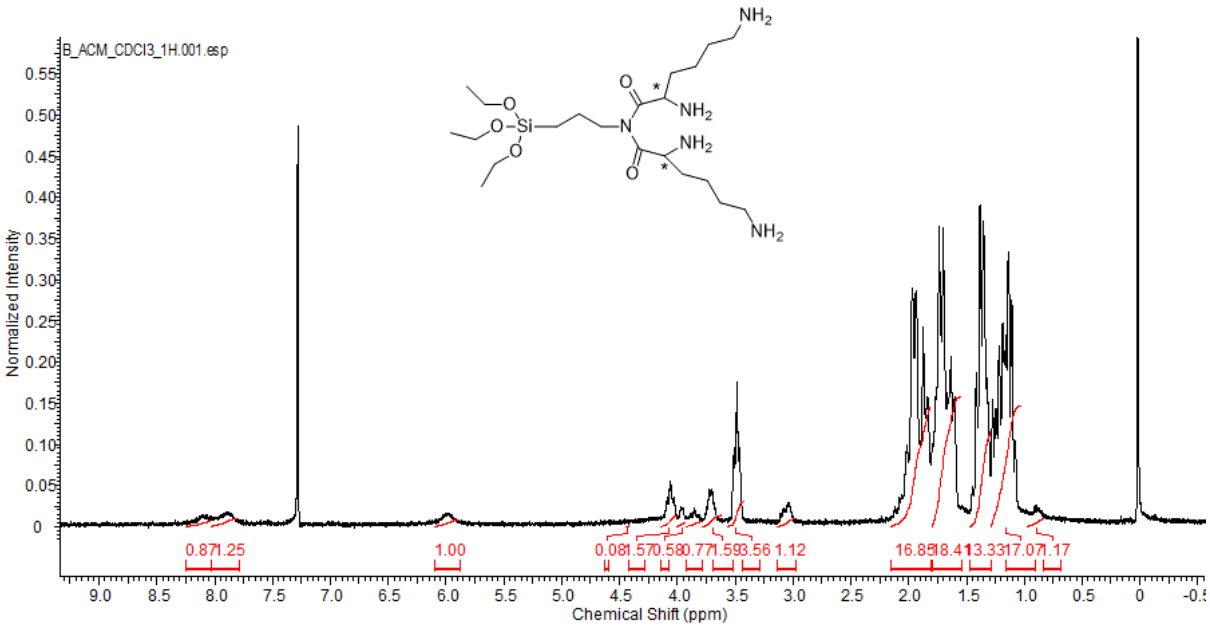

^{1}H NMR spectrum ((400 MHz, $CDCl_3$) for L-ACM

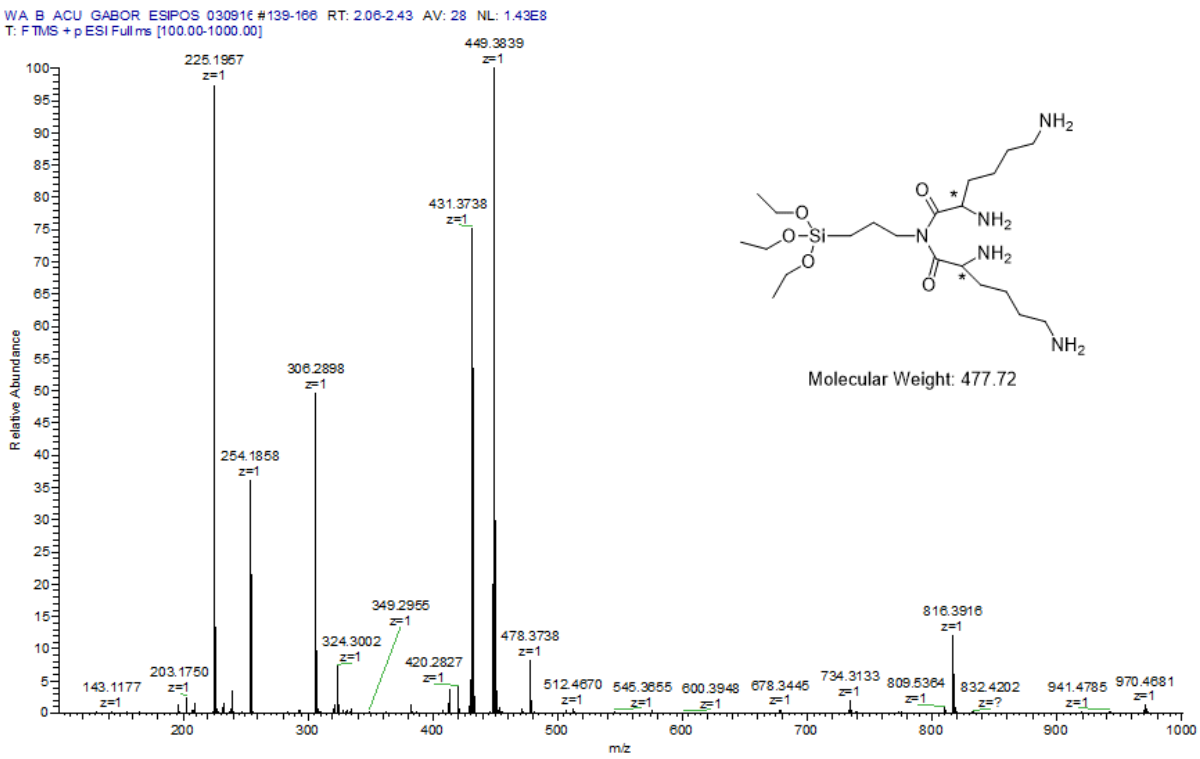
WA B ACU GABOR ESIPOS 030916 #139-166 RT: 2.06-2.43 AV: 28 NL: 1.43E8
T: FTMS + p ESI Full ms [100.00-1000.00]
Relative Abundance
m/z
225.1957 z=1
449.3839 z=1
431.3738 z=1
306.2898 z=1
254.1858 z=1
349.2955 z=1
324.3002 z=1
478.3738 z=1
420.2827 z=1
203.1750 z=1
143.1177 z=1
512.4670 z=1
545.3655 z=1
600.3948 z=1
678.3445 z=1
734.3133 z=1
809.5364 z=1
816.3916 z=1
832.4202 z=?
941.4785 z=1
970.4681 z=1
NH2
NH2
NH2
Molecular Weight: 477.72

MS for L-ACM

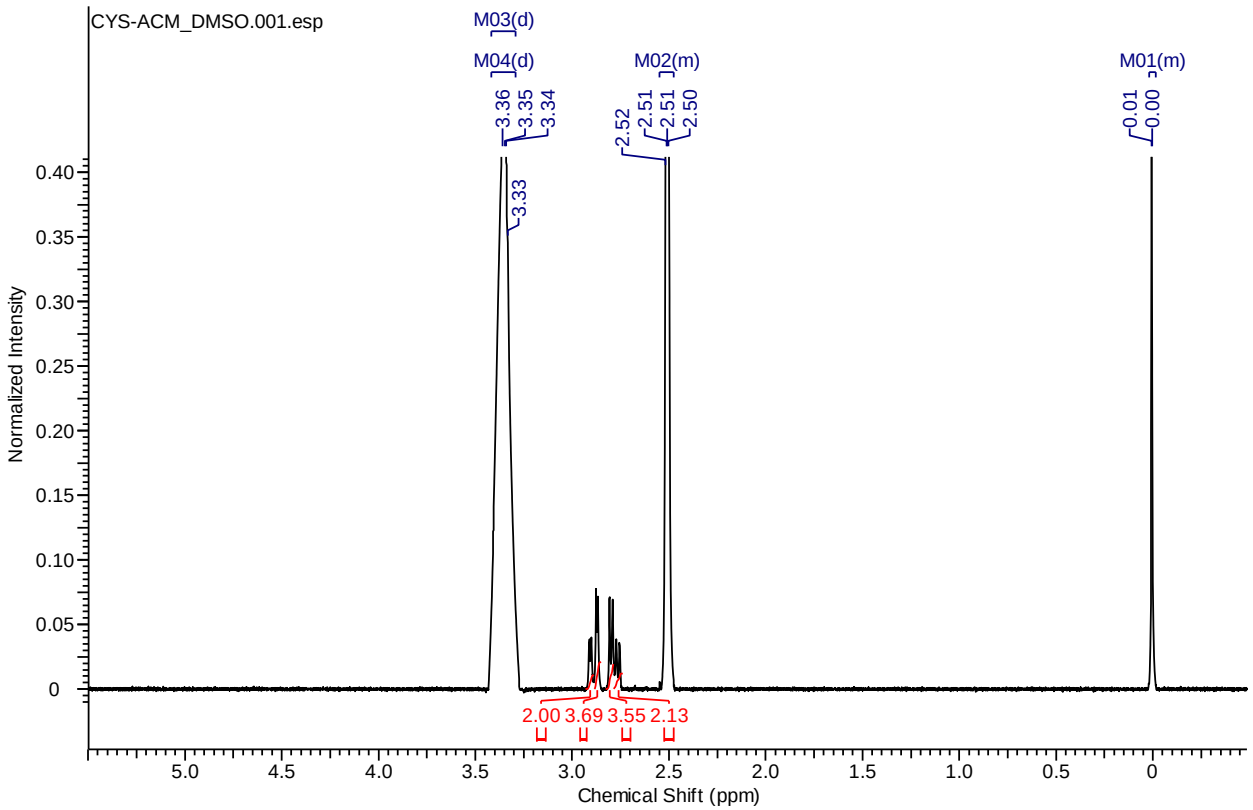

^{1}H NMR spectrum for CYS-ACM in DMSO-d6 using a 400 MHz Bruker instrument

(a)

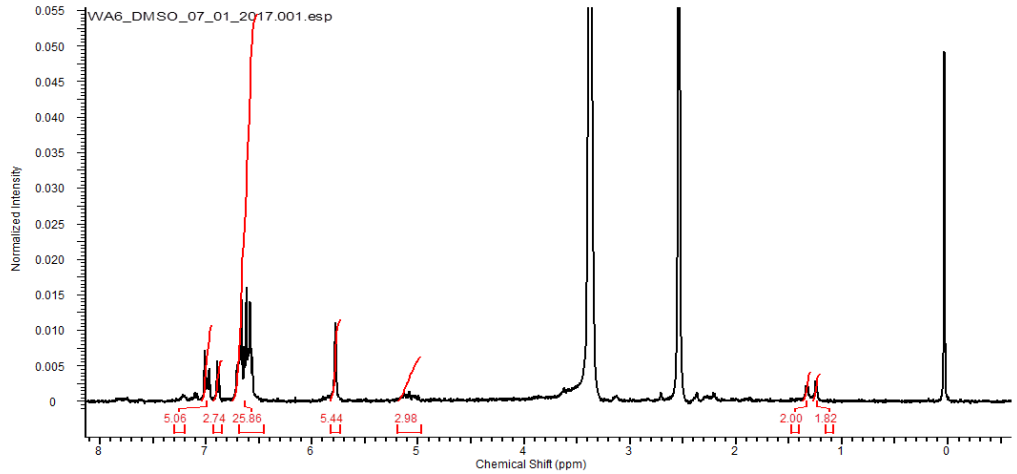

(b)

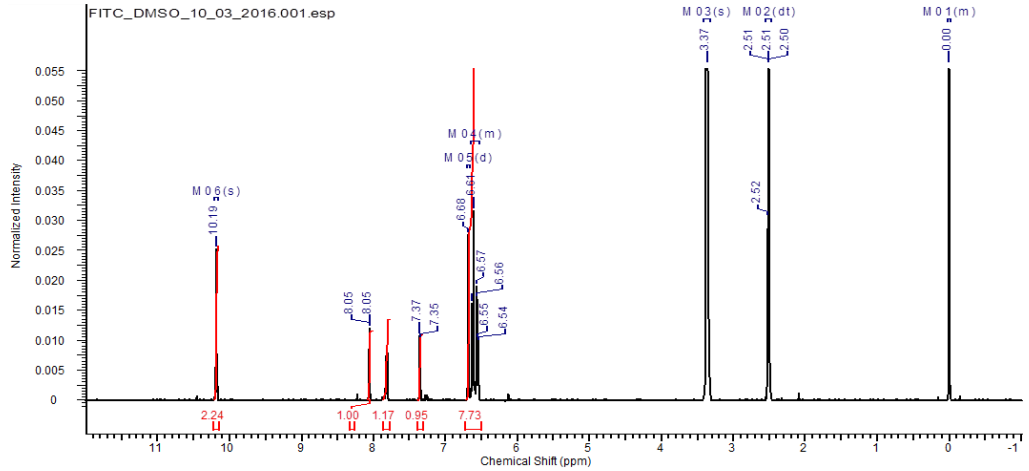

The [1]H NMR spectra for (a) WA6 and (b) FITC in DMSO-d6 using a 400 MHz Bruker instrument. 1H NMR δ 1.22 (t, 2H), 1.35 (q, 2H), 5.1 (m, 1H), 5.77 (t, 2H), 6.55 (m, 9H), 6.87 (t, 1H), 6.95 (m, 2H) and 10.12 (s, 1H). 77% yield